# Sex Differences in the Control of Adipose Tissue Function

Kasiphak Kaikaew

# Sex Differences in the Control of Adipose Tissue Function

Sekseverschillen in regulatie van vetweefselfunctie

**Thesis**

to obtain the degree of Doctor from the
Erasmus University Rotterdam
by command of the
rector magnificus

Prof.dr. R.C.M.E. Engels

and in accordance with the decision of the Doctorate Board.

The public defense shall be held on
Wednesday 11 March 2020 at 13:30 hrs

by

## Kasiphak Kaikaew

born in Kanchanaburi, Thailand

**Erasmus University Rotterdam**

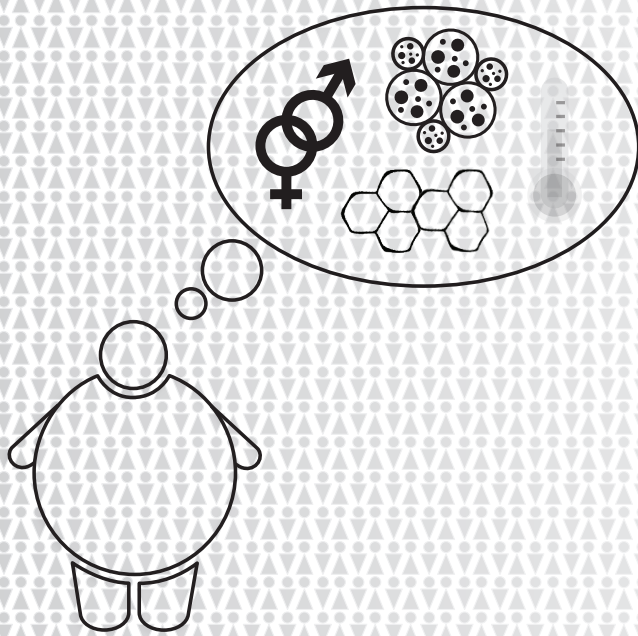## Doctoral Committee

**Promotor:**        Prof.dr. A.J. van der Lelij

**Other members:**  Prof.dr. O.C. Meijer
Prof.dr. P.M. van Hagen
Prof.dr. E.F.C. van Rossum

**Co-promotors:**  Dr.ir. J.A. Visser
Dr. A. Grefhorst

**Table of contents**

# Chapter 1A

## General Introduction

## Sex Difference in Adipose Tissue Biology: Gonadal and Adrenal Steroid Perspectives

*Manuscript in preparation*

1

**1**

## 1. Introduction

Excessive or abnormal fat accumulation in the body causes overweight and obesity. The latest report by the World Health Organization revealed that the prevalence of obesity worldwide has almost tripled from 1975 to 2016 and that 39% of adults were overweight and 13% or over 650 million were obese in 2016 (1). Obesity is a risk for many noncommunicable diseases such as insulin resistance and type 2 diabetes mellitus, cardiovascular diseases, hypertension, and also some types of cancer (1,2). Studies have demonstrated that chronic obesity leads to adipose tissue dysfunction and systemic low-grade inflammation. Intriguingly, this obesity-induced inflammation likely causes disrupted energy homeostasis, resulting in insulin resistance and other metabolic diseases, such as cardiovascular diseases and hypertension (1,3)

Although women in most ethnic groups have a higher prevalence of obesity than men, women in their reproductive age have a lower incidence of metabolic diseases than men. This sex difference is attenuated after women become postmenopausal (4-7). The relatively higher metabolic risk of men and postmenopausal women is correlated with the distribution of adipose tissue to the visceral part of the body, called visceral obesity. In other words, the subcutaneous fat accumulation pattern of premenopausal women is associated with a lower metabolic risk (8,9). Hence, it is important to study the mechanisms that contribute to the sexual dimorphism in adipose tissue biology since it may lead to a better sex-specific treatment option for combating this obesity pandemic. Moreover, insight about how the sex differences in adipose tissue distribution is regulated might reveal novel treatment modalities to combat obesity and the associated metabolic complications.

Differences in gonadal and adrenal steroid levels and responses to those steroids play an important role in the sexually dimorphic pathophysiology of obesity and metabolic diseases. It is evident that males are more prone to metabolic consequences of chronic stress than females (10,11). As a response to stress, glucocorticoid (GC) is synthesized and secreted under the control of the hypothalamic-pituitary-adrenal (HPA) axis (12). The hypothalamus and the anterior pituitary also regulate the sex steroid synthesis of the gonads, termed the hypothalamic-pituitary-gonadal (HPG) axis (13,14). The HPA and HPG axes are interconnected at many levels which could partly account for the sex difference in metabolic alterations. For example, sex steroids interfere with the negative feedback of the HPA axis and with the expression and function of the GC receptor (GR) (11). On the other hand, administration of corticosterone in female mice to reach maximal concentrations that occur in response to stress suppressed estradiol-induced LH secretion and completely blocked the ovarian

cycle (15). Activation of the HPA axis in male rats by repeated immersion in cold water (chronic stress) gradually reduced serum testosterone levels and disrupted spermatogenesis (16).

Other mechanisms could also contribute to sex difference in obesity and adipose tissue metabolism, such as epigenetic modifications, e.g. DNA methylation, histone modifications, small single-stranded non-coding RNA [microRNA (miRNA)] interference; the presence of sex chromosomes (X- and Y-chromosomes in males, only X-chromosomes in females); and perinatal and pubertal development of the brain, known as the organizational effect of sex steroids (5,17,18). However, these topics are outside the focus of this chapter that will focus on the effects of sex steroids after puberty, the principal difference between males and females at reproductive age. The majority of studies in humans and rodents on the effects of sex steroids on metabolism and energy homeostasis have focused on the effects of estrogens and androgens in both sexes (19,20). The contribution of progesterone, another female sex hormone crucial for the luteal phase of the reproductive cycle and during pregnancy, to sex differences in energy metabolism has barely been investigated.

This chapter will provide an overview of sex differences in adipose tissue function and distribution, and the roles of gonadal and adrenal steroids therein. In addition, this chapter will touch upon the mechanisms by which gonadal and adrenal steroid hormones affect adipose tissue function and distribution in various clinical conditions associated with disturbances in gonadal and adrenal steroids.

## 2. Adipose tissue function, characteristics, and distribution

For a long time, adipose tissue had been considered only a passive organ for storing excess calories as triglycerides (TGs) and providing energy-rich substrates to the body when needed. However, it is currently known that adipose tissue is not merely a passive bystander, but secretes a plethora of bioactive products, termed adipokines, which regulate whole-body homeostasis and reflect its adaptation in physiological and pathological states (21). This section will discuss the types and distribution of adipose tissue as well as its metabolic and secretory functions, with a focus on sex differences in these properties. Other auxiliary functions of adipose tissue, which will not be discussed in detail, include cushioning mechanical stress such as in palms, buttocks, and soles, and providing thermal insulation for the body since thermal conductivity of adipose tissue is only about 40–50% of that of lean tissues (22).

**1**

## 2.1 Types and distribution of adipose tissues

Adipose tissue has traditionally been categorized into two types which serve opposite roles: lipid-storing white adipose tissue (WAT) and thermogenic lipid-burning brown adipose tissue (BAT). Many studies have demonstrated a high degree of plasticity in adipose tissues. WAT can become brown-like by, for example, chronic exposure to cold or sustained adrenergic stimulation. This process is called browning and the resulting adipose tissue is called beige (or brite [brown-in-white]) adipose tissue (23,24). In contrast, BAT can be 'whitened' by multiple factors, e.g. acclimation to chronic warm temperatures and β-adrenergic signaling impairment (25).

To store excess energy in WAT, adipose tissue can expand in size (enlargement of existing adipocytes, called hypertrophy) and/or increase cell number (forming new adipocytes from the resident progenitor cells, called hyperplasia). Hypertrophic expansion is considered detrimental since the enlarged adipocytes reach a limit of oxygen diffusion, resulting in hypoxia, inflammation, fibrosis, adipose tissue dysfunction, and subsequently insulin resistance (26-29). Hyperplastic expansion is considered a healthy adaptation and occurs together with proper angiogenesis – formation of new vasculature to supply the growing adipocytes (21,30). Adipogenesis and angiogenesis are reciprocally regulated by peroxisome proliferator-activated receptor-γ (PPARγ) and vascular endothelial growth factor (VEGF). Reducing PPARγ activity by a dominant-negative PPARγ results in reduced preadipocyte differentiation and inhibits angiogenesis and an immunologic inhibition of VEGF blocks vessel formation and inhibits adipocyte differentiation (31), showing that these two processes are reciprocally regulated.

Concerning body fat distribution, WAT can generally be divided into two anatomical depots: subcutaneous depots, e.g. abdominal subcutaneous and gluteofemoral depots for humans or anterior (axillary) and posterior (inguinal) subcutaneous depots for rodents; and visceral depots, e.g. omental, mesenteric, gonadal, and retroperitoneal depots (32,33). Depot difference in WAT expansion is evident in rodent and human studies. In mice fed a high-fat diet (HFD), subcutaneous WAT expands more significantly by hyperplasia while visceral WAT shows a greater hypertrophic expansion. Indeed, adipose progenitor cells, responsible for adipogenesis, are more abundant in the subcutaneous depot than the visceral depot of mice (34). Likewise, adipocyte progenitor cells isolated from a subcutaneous depot of mice differentiated better by a standard *in vitro* culture protocol and express higher levels of pro-adipogenic genes and lower levels of anti-adipogenic genes than cells isolated from a murine visceral depot (35).
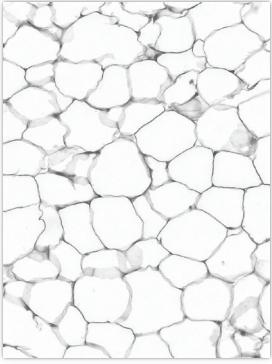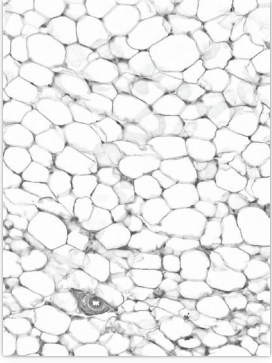
Also in humans, obese subjects have more preadipocytes in their abdominal subcutaneous WAT than in their omental visceral WAT. Isolated preadipocytes from the subcutaneous depot also differentiated more efficiently into mature adipocytes and expressed higher levels of adipogenic transcription factors than those isolated from the visceral depot (36,37). In morbidly obese subjects [body mass index (BMI) > 40 kg/m$^2$], the amount of visceral fat in insulin-resistant individuals is negatively correlated with insulin sensitivity: insulin-resistant obese subjects have significantly higher waist circumference and visceral fat accumulation than insulin-sensitive obese persons (27). Overall, visceral fat accumulation is associated with an increased risk of metabolic complications of obesity and clinical practice guidelines support measurement of waist circumference (a reasonable proxy for visceral obesity) as an indicator for the risk to develop metabolic diseases (38-41). A brief summary of adipose tissue expansion and its adaptive mechanisms is presented in **Table 1**. Of note, some characteristics will be discussed in following sections of this chapter.

### 2.1.1 Sex difference in adipose tissue distribution

Throughout life, women typically have a higher percentage of body fat than men at an equivalent BMI (42-44). Body composition also shows many sex-dependent characteristics including regional distribution. Women tend to accumulate body fat around hips and thighs, called a gynoid or pear-shaped pattern, whereas men accumulate fat around the abdomen, termed an android or apple-shaped pattern (8,9,44). Subsequently, women and female rodents have relatively more subcutaneous WAT and less visceral WAT than age-matched men and male rodents (19,45-47). One of the possible mechanisms accounting for this sex difference is that women have a higher activity of lipoprotein lipase (LPL) in subcutaneous WAT than men (48). LPL is the enzyme involved in hydrolysis of TGs to yield fatty acids that can be taken up by adipocytes. Upon uptake, the fatty acids will be re-esterified with glycerol into TGs and stored in the adipocyte (see section 2.3 for more detail). The sex-dependent pattern of fat distribution is apparent after pubertal development, indicating a role of sex steroids in fat accumulation (49). Moreover, this sex-dependent fat accumulation diminishes at an older age; in other words, women gain more visceral fat, and thus their body fat distribution becomes android-like, after menopause (50,51).

Inflammation in adipose tissues typically precedes systemic metabolic inflammation and occurs when proper adipogenesis is limited (52). This is especially the case in visceral depots, the predominant fat depot of males. A mouse study demonstrated that female mice had a higher ratio of adipose progenitor cells to adipocytes in gonadal and inguinal WATs than male mice (53).

**1**

**Table 1** WAT expansion and relevant characteristics

| Characteristics | Mode of WAT Expansion | |
| --- | --- | --- |
| | **Hypertrophy** | **Hyperplasia** |
| Adipocyte adaptation | Increased cell size/volume | Increased cell number |
| Adipose depot size | Enlarged | Enlarged |
| Storage type | Metabolically detrimental | Metabolically healthy |
| Main anatomical sites | Visceral depots | Subcutaneous depots |
| Histological appearance (similar magnification) | | |
| Blood flow | Relatively insufficient | Sufficient due to angiogenesis |
| Hypoxic/necrotic adipocytes | Present | Absent or minimal |
| Major immune cell infiltration | Pro-inflammatory cells | Anti-inflammatory cells |
| Inflammatory cytokine secretion | High | Low |
| Adiponectin production | Highly decreased | Increased |
| Leptin production | Highly increased | Relatively decreased |
| Adiponectin/leptin ratio | Low | High |
| Response to insulin | Insulin resistant | Insulin sensitive |

Fed a HFD for 14 weeks, males expanded the gonadal depot only by hypertrophic expansion accompanied by an accumulation of macrophages and other immune cells, whereas females expanded the gonadal depots by both hyperplasia and hypertrophy. This difference coincided with more weight gain and a worse metabolic profile in males than in females after the HFD challenge (53). Other studies also confirmed that females had less intra-abdominal fat accumulation than males although both sexes consumed an equal amount of HFD. These sex-differential effects were absent when the female sex steroids were depleted by ovariectomy. Treatment with 17β-estradiol (E2) in the HFD-fed ovariectomized mice restored the visceral deposition to the amount of non-ovariectomized females.In addition, gonadal adipocytes were larger in males and ovariectomized females than in non-ovariectomized females and E2-treated ovariectomized females, suggesting protective properties of E2 on hypertrophic expansion (54, 55). Another study in male and female mice demonstrated that an obesogenic (high-fat and high-sugar) diet resulted in greater diet-induced obesity, higher mesenteric fat accumulation, and a worse metabolic profile in males. Intriguingly, E2 treatment feminized and attenuated the diet-induced disturbances of male mice (56). Altogether, these data in humans and rodents suggest direct effects of sex steroids on adipose tissues, which will be discussed in more detail in section 3.

## 2.2 Adipogenic programming

Adipogenesis is a complex process in which multipotent mesenchymal stem cells commit to the adipogenic lineage after which these preadipocytes differentiate into lipid-containing mature adipocytes (**Figure 1**). White adipocytes and classical brown adipocytes (as found in interscapular BAT depots in rodents and human infants) are derived from different progenitor lineages. Brown adipocytes and skeletal myoblasts arise from the paired box 7 (Pax7)- and myogenic factor 5 (Myf5)-expressing progenitors. The transcriptional regulator PR domain-containing 16 (Prdm16) controls the differentiation towards brown adipocytes, whereas myogenic factors, i.e. Myf5 and the myogenic differentiation (MyoD), repress Prdm16 and promote myoblast differentiation (57,58). White and beige adipocytes are derived from Pax7- and Myf5-negative progenitors, but activation of the transcription factor early B-cell factor 2 (Ebf2) commits the progenitor cells to a beige adipocyte lineage. Of note, *Prdm16* is an Ebf2-target gene and brown adipocytes also express Ebf2 (59). On the contrary, the transcriptional regulator zinc finger protein (Zfp423) is critical for white preadipocyte commitment since Zfp423 can bind and repress Ebf2 transcriptional activity, allowing preadipocytes to differentiate to white adipocytes (60).

**1**
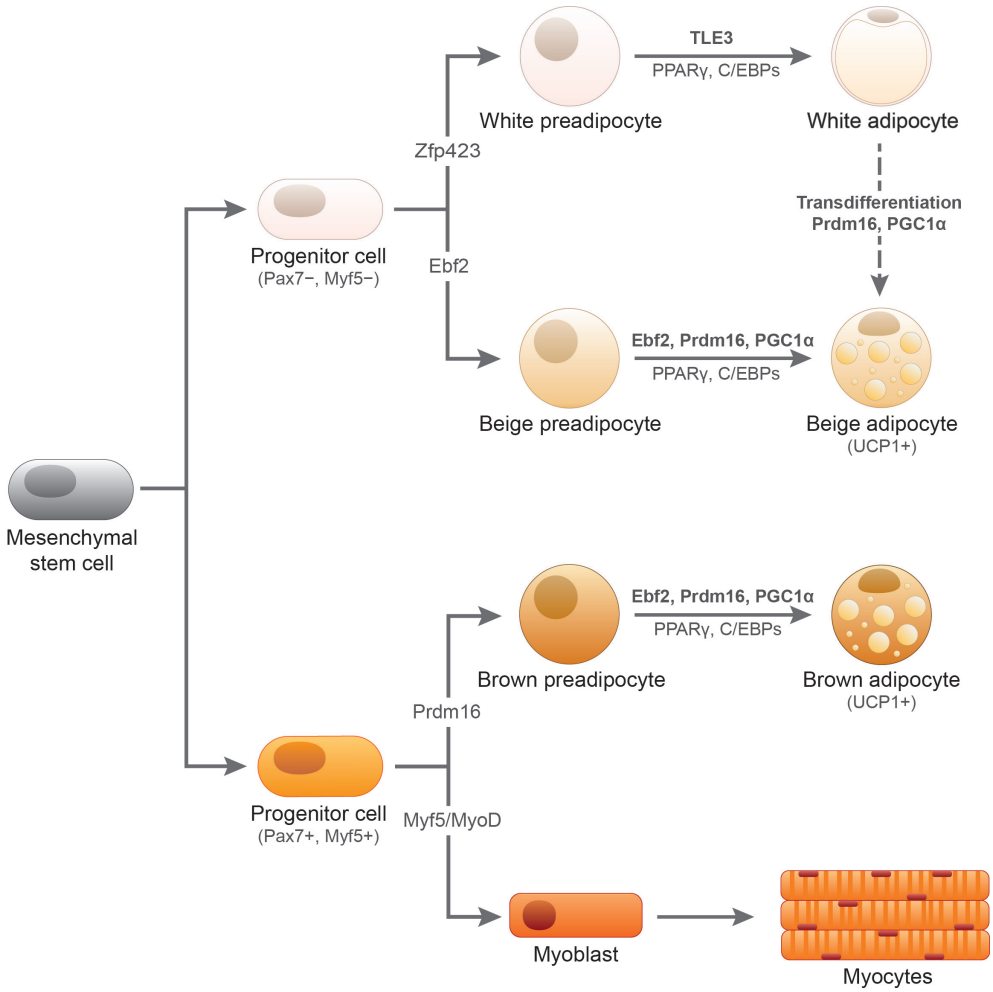


**Figure 1** Adipogenesis and progenitor lineage

Classical white and brown adipocytes are derived from different progenitors. Adipogenic programming is modulated by distinct transcription factors, listed by the arrows in the diagram.

The general program of differentiation into mature lipid-containing adipocytes is regulated by the transcription factor PPARγ (the master regulator of adipogenesis) and the transcription co-activators CCAAT/enhancer-binding protein α and β (C/EBPα and C/EBPβ) (61). White preadipocyte differentiation is promoted by the transducin-like enhancer of split 3 (TLE3), whereas beige and brown preadipocyte differentiation is promoted by Prdm16 (62). During differentiation, committed preadipocytes arrest in growth, accumulate lipids, and form functional insulin-responsive mature adipocytes. Early differentiated adipocytes express PPARγ, C/EBPα or C/EBPβ, fatty acid binding protein 4 (FABP4, also known as adipocyte protein 2 [aP2]), and the insulin-responsive glucose transporter 4 (GLUT4) (30). Continuous activation of PPARγ promotes terminal differentiation by inducing a variety of differentiation-dependent target genes. Mature adipocytes then express the genes important for adipose tissue function, such as LPL, adipose triglyceride lipase (ATGL), hormone-sensitive lipase (HSL), perilipin, adiponectin, and leptin, as well as all of the early differentiation markers (30,63).

The key regulator important for brown and beige adipocyte differentiation is the transcriptional coactivator protein PPARγ coactivator 1α (PGC1α). PGC1α co-activates PPARγ and other transcriptional factors to initiate a broad program of mitochondrial biogenesis, including the induction of expression of the gene encoding the thermogenic uncoupling protein 1 (UCP1), a protein in the inner mitochondrial membrane that allows protons to leak independently of ATP synthesis and dissipate energy of substrate oxidation as heat, a unique function of brown and beige adipocytes (64,65). The thermogenic function of BAT is discussed in more detail in section 2.5. Upon prolonged cold exposure or β-adrenergic stimulation, white adipocytes can also transdifferentiate into beige adipocytes by upregulating Prdm16 and PGC1α (61,66), and thereby having a beneficial contribution to energy metabolism.

### 2.3 Lipid metabolism in adipose tissue

As an energy reservoir in postprandial or positive energy balance conditions, WAT depots store excess nutrient calories as TG by uptake of fatty acids from plasma or *de novo* lipogenesis. In prolonged fasting or high energy demand conditions, on the other hand, white adipocytes lipolyze the stored TGs to supply fatty acids and glycerol as energy substrates to the circulation to be used by other tissues (67). The balance in lipid storage and breakdown determines adipose tissue mass. Principle enzymes and substrates for lipid metabolism in white adipocytes are illustrated in **Figure 2**.
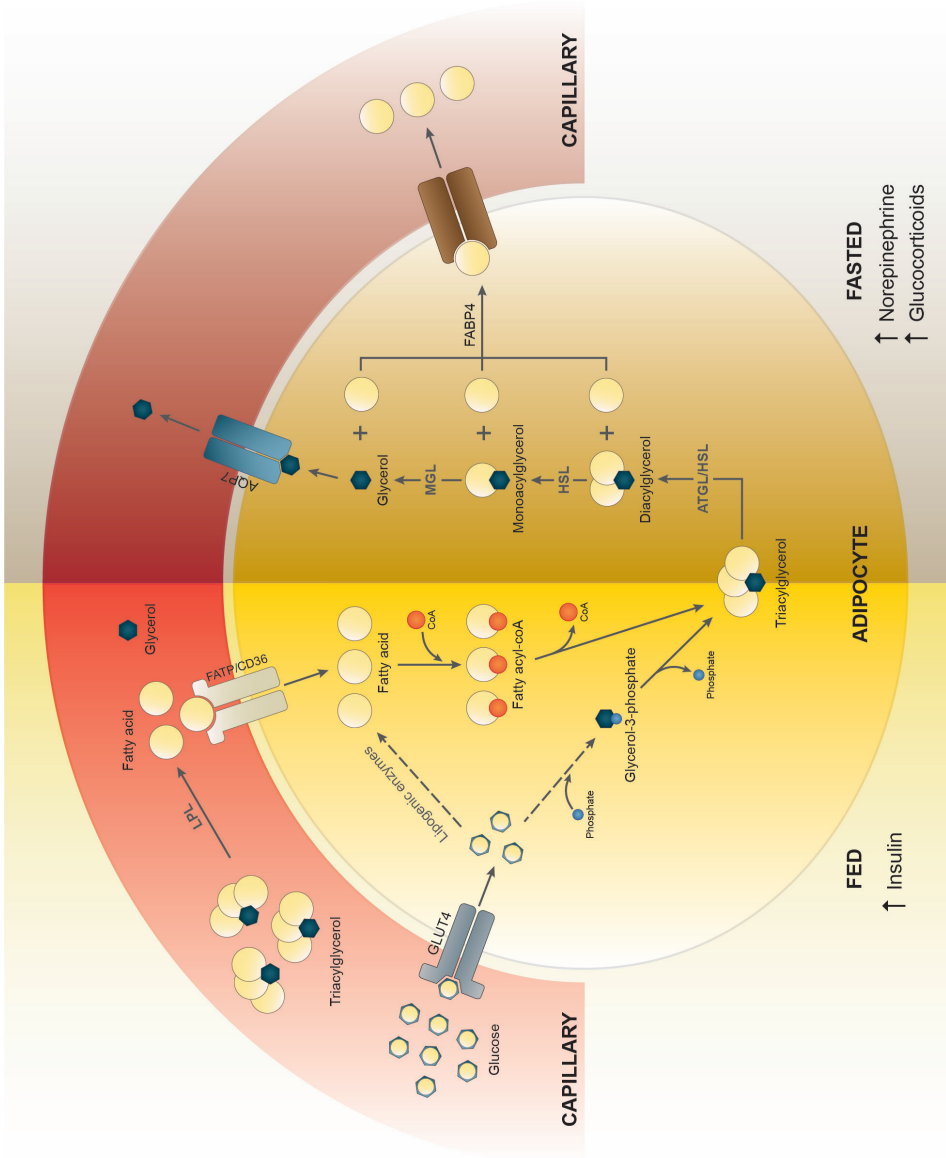
**1**



**Figure 2** Lipid metabolism in white adipocytes

During physiological substrate-rich conditions, e.g. after meals, an increase in plasma insulin levels not only promotes glucose uptake but also stimulates fatty acid uptake and lipogenesis in white adipocytes (68). For the uptake, adipocytes obtain fatty acids from two TG-rich lipoproteins, namely chylomicrons (enterocyte-derived lipoproteins that transport exogenous [dietary] fats) and very low-density lipoproteins (VLDL, endogenous lipoproteins secreted by the liver). The fatty acids are hydrolyzed from the TG-rich lipoproteins by LPL after which they can be taken up through fatty acid transport proteins (FATP) or fatty acid translocase (FAT, also known as CD36). In the adipocytes, these fatty acids are activated to fatty acyl-CoAs and sequentially esterified with glycerol-3-phosphate to form TGs that are subsequently packed and stored in lipid droplets (67-69).

*De novo* lipogenesis contributes only marginally to the TG content of adipocytes. This pathway is less active in adipocytes than in the liver and is less important in humans than in rodents (68,70). An increase in intracellular substrate concentrations, for example by insulin stimulation, stimulates *de novo* lipogenesis in adipocytes by inducing the transcription factors carbohydrate response element-binding protein (ChREBP) and sterol regulatory element-binding protein 1c (SREBP1c), which subsequently induce many lipogenic genes such as those that encode for acetyl-CoA carboxylase 1 (ACC1), fatty acid synthase (FASN), and stearoyl-CoA desaturase 1 (SCD1) (71-73).

When the body lacks energy, e.g. upon prolonged fasting, or requires extra metabolic supplies, e.g. during exercise, lipolysis in adipocytes is induced. In this process that involves multiple lipases, a complete breakdown of one molecule of TG generates three fatty acid molecules and one molecule of glycerol as substrates for direct utilization in other tissues or for gluconeogenesis in the liver. The first fatty acid is cleaved from TG by ATGL or, to a minor extent, by HSL. The remaining diacylglycerol is hydrolyzed into monoacylglycerol and a second fatty acid by HSL. Monoacylglycerol lipase (MGL) cleaves the remaining monoacylglycerol into a third fatty acid and glycerol (67,74). Likely various transporters such as FABP4 facilitate the export of fatty acids, while aquaporin 7 (AQP7) facilitates the transport of glycerol out of adipocytes (75,76).

At basal conditions, proteins such as perilipins coat the surface of lipid droplets preventing them from lipase action (67,77). When lipolysis is required, systemic cues such as the sympathetic nervous system and the HPA axis can regulate lipase activities in many ways. The sympathetic outflow products catecholamines bind to β-adrenergic receptors and initiate signaling cascades to inactivate the protecting effect of perilipins and promote the translocation of HSL to the lipid droplets. GCs, produced in response to activation of the HPA axis, promote lipolysis in adipocytes by inducing the transcription of the lipolytic enzymes ATGL and HSL (67,74,77,78).

**2.4 Secretory function of adipose tissue**

Besides the well-known function as an energy reservoir, adipocytes produce and secrete various adipokines that function as autocrine, paracrine, and endocrine signaling molecules. Various systemic functions of adipokines are known, such as regulation of systemic energy homeostasis, endothelial function, insulin sensitivity, and inflammation. More than 600 adipokines have been discovered, including adiponectin, adipsin, apelin, bone morphogenetic protein 4 (BMP4), BMP7, dipeptidyl peptidase 4 (DPP4), fibroblast growth factor 21 (FGF21), interleukin-1β (IL-1β), IL-6, leptin, lipocalin 2, omentin, resistin [for rodents], retinol binding protein 4 (RBP4), tumor necrosis factor α (TNFα), and visfatin (79-81). Leptin and adiponectin are the two most studied adipokines which regulate feeding behavior and whole-body insulin sensitivity and will therefore be discussed in more detail below.

**2.4.1 Leptin**

Leptin was the first identified adipokine in 1994 (82), but its physiological roles had already been known since 1950, when an autosomal inherited mutation was identified in an obese mouse strain (83). This mutation, and later the gene, was originally called obese (*ob*). Another gene mutation, which turned out to encode the leptin receptor, was identified in 1966 in an obese and early-onset diabetic (*db*) mouse strain (84). The leptin-deficient *ob/ob* mice and the leptin receptor-deficient *db/db* mice are among the most used animal models of obesity and metabolic diseases since the shared phenotypes of these two models include profound obesity, hyperphagia, reduced energy expenditure, hyperglycemia and hyperinsulinemia (which leads to insulin resistance or diabetes depending on age and strain), and hyperlipidemia (85).

Leptin is a 167-amino acid protein produced mainly in adipose tissues, with WAT producing significantly more leptin than BAT. *Lep* mRNA expression is however detected in many other tissues as well, including skeletal muscles, stomach, placenta, and ovaries (86). Under healthy physiological conditions, excess nutrient calories promote an expansion of adipose tissues which induces leptin production and secretion. Thus plasma leptin concentrations reflect energy status and total fat mass. Leptin binds to the leptin receptors on neurons in various brain regions, including energy-control centers in the hypothalamus. Here, leptin promotes satiety signals to reduce food intake and accelerate energy expenditure in peripheral tissues through sympathetic nervous system activation. In addition, leptin also regulates lipid metabolism in WAT since sympathetic activation induces lipolysis and reduces *de novo* lipogenesis. While plasma leptin concentrations are positively correlated with the total amount of body fat, the leptin-induced inhibition of food intake is blunted in many obese subjects, indicating that obesity may reflect a leptin-resistant state (87-90).

### 2.4.2 Adiponectin

Adiponectin, a 247-amino acid adipokine that has a higher plasma level (μg/mL) than other conventional factors, e.g. insulin and leptin (ng/mL), was discovered in the mid 90's by many research groups giving this protein different names: Acrp30 (adipocyte complement-related protein of 30 kDa), AdipoQ, apM1 (adipocyte most abundant gene transcript 1), and GBP28 (gelatin-binding protein of 28 kDa) (91-94). Adiponectin is generally accepted as an adipocyte-specific marker produced by BAT and WAT (95,96). However, *Adipoq* mRNA expression has been detected beyond adipose tissue depots under some specific conditions, e.g. lipopolysaccharide-induced muscle inflammation (97,98).

Adiponectin displays many metabolically favorable effects and circulating adiponectin concentrations decline with increasing BMI, increasing waist circumference, and insulin resistance (89,99,100). Within morbidly obese individuals (BMI > 40 kg/m$^2$), the insulin-resistant group exhibits lower serum adiponectin levels than the insulin-sensitive group. Thus, lower circulating adiponectin concentration together with adipose tissue inflammation appears a good predictor of insulin resistance (27). Adiponectin is also associated with an hyperplastic expansion of adipose tissue (99). Since plasma leptin concentrations increase and adiponectin concentrations decrease in obese subjects, the adiponectin/leptin ratio is considered a reliable indicator for assessing subclinical insulin resistance, metabolic disorders, and adipocyte dysfunction (95,99,101,102).

Another unique characteristic of secreted adiponectin is that it circulates in higher-order complex forms: the high-molecular-weight (HMW) form consisting of 12–18 adiponectin molecules; the low-molecular-weight (LMW) hexamer form; and the trimer form. Distribution of adiponectin complexes contributes to distinct biological effects and HMW adiponectin is considered the active form of this adipokine. As a result, the HMW/total adiponectin ratio is considered another predictor for insulin sensitivity (103,104).

### 2.4.3 Extragonadal steroid synthesis

In addition to adipokines, WAT depots are an important source of extra-gonadal estrogen biosynthesis, through aromatization of intracellular androgens by the enzyme aromatase (CYP19A1) (105). Aromatase can convert testosterone (the main circulating male sex hormone) to E2 (the main circulating female sex hormone), or androstenedione (a weak androgen) to estrone (a weak estrogen). The aromatization of androgens in adipose tissues contributes substantially to circulating estrogen levels, especially in obese men and postmenopausal women (106,107). Moreover, aromatization might contribute to local effects of sex

**1**

steroids on adipose tissue. An imbalance in the testosterone/E2 ratio in obese men causes metabolic syndrome and hypogonadism, which will be discussed further in section 3.3.

GCs (cortisol for humans or corticosterone for rodents) can be converted from their inactive 11-keto steroid precursors (cortisone or 11-dehydrocorticosterone, respectively) by the reductase activity of the enzyme 11β-hydroxysteroid dehydrogenase type 1 (11β-HSD1) in adipose tissues. The active GCs act locally to promote preadipocyte differentiation, adipocyte hypertrophic expansion, and hence adipose tissue and systemic insulin resistance, rather than contributing to an increase in circulating GC levels (108). Interestingly, 11β-HSD1 reductase activity is higher in preadipocytes from visceral depots than in those from subcutaneous depots of male mice, supporting a role of local activation of GCs in visceral obesity (109).

### 2.5 Thermogenic function of BAT

BAT is a thermogenic organ that dissipates nutrient energy as heat through its classical mitochondrial protein UCP1. It was originally recognized that BAT was present and actively functioning only in human infants, small mammals, and hibernating animals to maintain body temperature without thermogenic shivering of skeletal muscles. Likewise, the concept has been that BAT in humans regresses within the first years of life, resulting in an absence of BAT in adults (110). Although the existence of activated BAT in healthy adults had been suggested in the positron emission tomography/computed tomography (PET/CT) imaging since 2002 (111), direct evidence of cold-activated glucose uptake in BAT together with UCP1-immunoreactive brown adipocytes was confirmed in 2009 (112-115). After the rediscovery of active BAT in adults, BAT has gained much attention from researchers as activating BAT is suggested a promising tool to combat the obesity pandemic.

Under physiological conditions, exposure to low ambient temperatures stimulates cutaneous thermoreceptors to transmit sensory signals to the thermocenter preoptic area of the hypothalamus. Subsequently, the hypothalamic network provides signals to stimulate the sympathetic premotor neurons that hence activate 1) cutaneous vasoconstriction (to reduce heat loss), 2) non-shivering thermogenesis in BAT, and 3) shivering in skeletal muscles (116). In humans, repeated exposure to cold (cold acclimation), e.g. 2 hours/day and 5 days/week for 4 weeks, increases BAT mass and the oxidative capacity of BAT. Furthermore, the prevalence of BAT detected by PET/CT imaging is higher during winter than other seasons and negatively correlates with outdoor temperatures (117,118).

Cold exposure induces sympathetic nerves in BAT to secrete norepineph-rine that stimulates BAT thermogenesis through β-adrenergic receptors (β-ADR). Although all three types of β-ADRs ($β_1$, $β_2$, and $β_3$) are expressed in human and murine BAT, to date only treatment with $β_3$-ADR agonists, but not with non-specific β-ADR agonists, has resulted in increased BAT activity, suggesting that $β_3$-ADR mediates BAT thermogenesis (119-121). A single dose of propranolol (a competitive non-selective β-ADR antagonist) given to patients with a strong BAT activity signal in PET/CT imaging suppressed BAT activity in most cases (122,123). Since propranolol binds $β_1$- and $β_2$-ADRs with high affinity but has a lower binding affinity for $β_3$-ADR (124), the suppression of BAT activity after administration of propranolol may indicate less specificity in β-ADR subtypes regulating human BAT activity.

The acute adrenergic response of BAT enhances lipolysis through the activation of ATGL and HSL, and the fatty acids released in this process stimulate UCP1 activity (125). In addition, cold exposure stimulates the uptake of glucose and fatty acids in BAT, resulting in a decrease in circulating glucose levels and also reductions in plasma free fatty acid and TG concentrations (126). After the fatty acids are imported into brown adipocytes, they are most likely first esterified into TG and incorporated into lipid droplets after which they are hydrolyzed to be metabolized for uncoupling thermogenesis (126). This was confirmed by the presence of significantly defective BAT thermogenesis in ATGL-deficient mice upon an acute cold exposure (127), underscoring the need of intracellular TG. **Figure 3** illustrates the current hypothesis on lipid metabolism in brown adipocytes for UCP1 thermogenesis.

Interestingly, not only the transcription of genes and activation of enzymes involved in substrate turnover are upregulated, UCP1 transcription and protein abundance in BAT are also increased upon cold exposure, called adaptive thermogenesis (**Figure 3**) (126,128-130). Prolonged cold exposure also induces browning of inguinal WAT in mice, with subsequent upregulation of *Ucp1* mRNA and protein expression (59,66,128). This inducible browning process was observed in all WAT depots, but was much more pronounced in subcutaneous depots than in visceral depots (131).

## 2.5.1 Sex difference in BAT abundance and function

In general, research has revealed that women and female rodents have a greater BAT mass and/or higher prevalence of metabolically active BAT and have greater inducible browning of their WAT depots than men and male rodents (132,133). A retrospective study determining the prevalence of BAT by PET/CT imaging found that BAT was detectable in 328 out of 4,842 (6.8%)
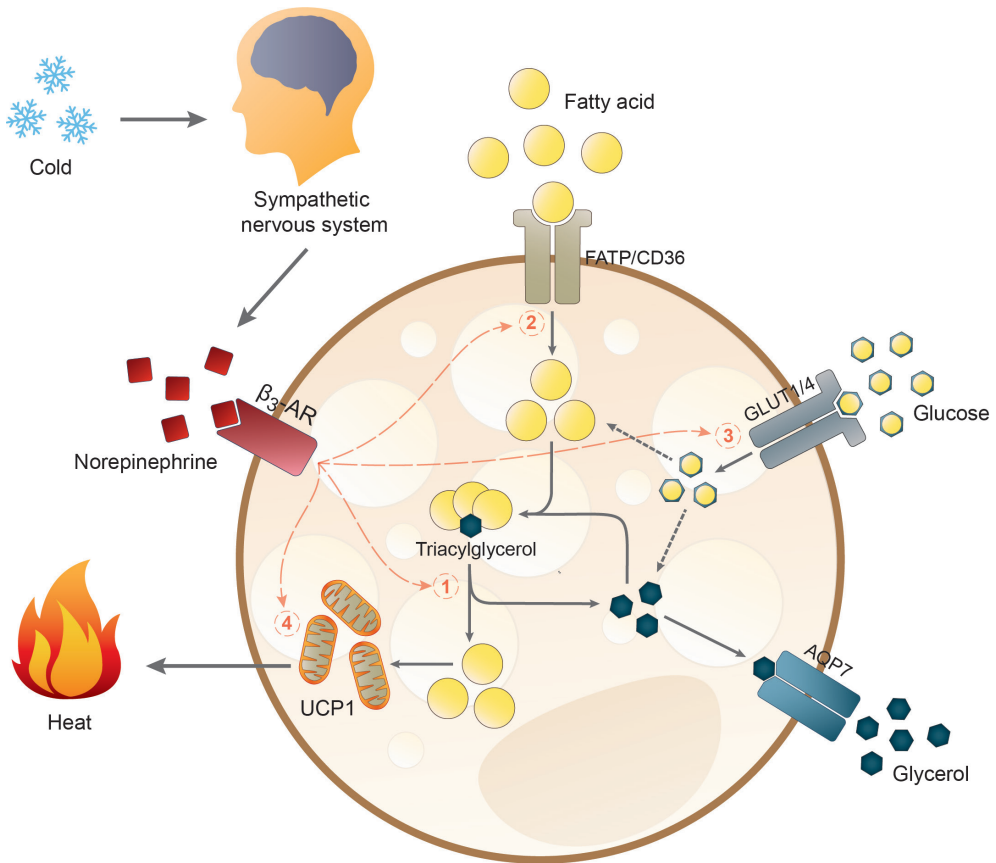
**Figure 3** Activation of BAT thermogenesis and lipid metabolism in brown adipocytes

Acute thermogenic responses by $\beta_3$-adrenergic stimulation include activation of (1) intracellular lipolysis, (2) fatty acid uptake, and (3) glucose uptake. Altogether, these processes increase intracellular free fatty acid availability for mitochondrial UCP1 thermogenesis. Prolonged cold exposure also induces adaptive thermogenesis by (4) upregulating *Ucp1* mRNA expression.

participants and significant determinants for BAT activity included, besides low outdoor temperatures (seasonal variation), young age, low-to-normal BMI, absence of diabetes, and female sex (118). Of note, the influence of sex on BAT prevalence declined with age (118). Also in rodents, female rats have a higher BAT mass (relative to body mass), higher total and mitochondrial protein content in BAT with larger mitochondria with more cristae, and higher BAT UCP1 protein expression than male rats under normal housing conditions at 22°C and *ad libitum* fed with chow diet (134,135). Circulating sex steroids are likely one of the most important regulators of BAT differentiation and activity (136). In cultured brown adipocytes isolated from BAT of mice or rats, treatment with E2 or progesterone stimulated while testosterone inhibited mitochondrial biogenesis signaling and brown adipocyte differentiation (137,138).

Under caloric restriction conditions (e.g. 60% caloric intake of the *ad libitum* fed animals for 100 days), female rats showed a greater deactivation of BAT thermogenesis to reduce energy expenditure than male rats, and hence females are better able to protect other metabolically active organs, advantageous for survival in food-limited conditions, than males (139). When fed a HFD for 8 weeks, female rats maintained a higher expression of proteins involved in thermogenesis (e.g. UCP1, PGC1α) and fat oxidation, and a lower expression of proteins involved in fat synthesis (e.g. FASN, ACC1) in BAT than male rats, again suggestive for increased protective adaptations of female BAT, also under energy-excess conditions (140). Another study, in which rats had been exposed to a high-fat, high-sugar diet for 100 days followed by a chow diet for 70 days, confirmed that female rats had a higher BAT mass (relative to body mass), higher total and mitochondrial protein in BAT, higher *Ucp1* and *Adrb3* ($\beta_3$-ADR) mRNA expression, and a greater weight loss during the chow diet state than male rats. This study confirms a higher functional capacity of BAT in females during an overweight state (134).

## 3. Effects of sex and stress steroids on adipose tissues

This section will review the effects of sex- and stress-steroids on the distribution and function of adipose tissues. Such effects have mainly been addressed by administration of the biological hormones or their agonists/antagonists to humans and rodents, as wells as *ex vivo* treatment of adipose tissue-derived cells and stable adipocyte cell lines. Also, the removal of the sex steroid producing gonads (gonadectomy) and animals deficient in specific steroid receptors are commonly used methods and models to study the role of sex steroids. A brief summary of the effects of sex- and stress-steroids on adipose tissues is presented in **Table 2** and will be discussed in more detail below.

**1**

**Table 2** Sex- and stress-steroid actions in fat distribution and adipokine production

| Properties | Estrogens | Progestogens | Androgens | Glucocorticoids |
|---|---|---|---|---|
| Major circulating hormone | E2 | Progesterone | Testosterone | Cortisol (humans) or corticosterone (rodents) |
| Main functioning nuclear receptor in adipose tissue | ERα | PR | AR and ERα (for testosterone-derived E2) | GR |
| Other receptors expressed in adipose tissue | ERβ, GPER | PAQR, PGRMC | – | MR |
| Fat distribution and adipogenesis | Promote subcutaneous fat and reduce visceral fat deposition | For males: no data For females: likely promote fat accumulation, but effects on fat distribution remain controversial | For males: reduce fat mass in both visceral and subcutaneous depots (for eugonadism) For females: promote visceral fat and reduce subcutaneous fat deposition | Promote visceral fat and reduce subcutaneous fat deposition Crucial for initial steps of adipogenesis |
| Leptin production | Stimulate | Controversial | Inhibit | Stimulate |
| Adiponectin production | Likely inhibit, but increased adiponectin/ leptin ratio | Controversial | Inhibit | Controversial |
| Whole-body insulin sensitivity | Increase | For males: no data For females: likely decrease | For males: likely increase (for eugonadism) For females: decrease | Decrease |

Abbreviations: AR, androgen receptor; E2, 17β-estradiol; ER, estrogen receptor; GPER, G protein-coupled ER; GR, glucocorticoid receptor; MR, mineralocorticoid receptor; PAQR, progestin and adipoQ receptor; PGRMC, PR membrane component; PR, progesterone receptor.

### 3.1 Estrogens

Estrogens are female sex hormones, the effects of which at target organs are classically mediated by the nuclear estrogen receptors (ERs): ERα and ERβ. Upon binding to ER, the estrogen-ER complex interacts with estrogen response elements and other transcription factors, and hence stimulates or inhibits target gene expression (19). Estrogens can also bind to membrane-associated ERs, such as the G protein-coupled ER (GPER, formerly known as GPR30), and initiate rapid non-genomic actions (141). In premenopausal women, E2 is the main circulating estrogen produced by ovaries during the menstrual cycle.

Estrogen deficiency after menopause is associated with many metabolic risks, such as obesity, metabolic syndrome, type 2 diabetes mellitus, and cardiovascular diseases. Postmenopausal estrogen therapy has beneficial effects against these metabolic risks. However, individualized treatment formula, route of administration, dosage, and duration should be considered because thrombo-embolism, a major harmful consequence of the hormone treatment, needs to be monitored and evaluated (19,142,143). Estrogens also regulate energy homeostasis via the central nervous system, mainly through activation of ERα in many brain regions, which is beyond the scope of this chapter. The net central effect of estrogens is towards a negative energy balance by inhibiting feeding behavior and promoting energy expenditure through sympathetic nervous system activation, and hence BAT thermogenesis [see for a comprehensive review (144)].

Concerning adipose tissue expansion and distribution, estrogens promote the subcutaneous gluteofemoral or gynoid/pear-shaped fat distribution, which is associated with low metabolic risks. Postmenopausal women shift towards the visceral or central/android/apple-shaped fat distribution and increase their body weight and fat mass. Hormone replacement therapy in early postmenopausal women counteracts weight gain, prevents the central fat distribution, and increases gluteofemoral fat accumulation (145,146). Interestingly, administration of E2, in combination with an antiandrogen, for gender-affirming hormone therapy in transwomen (male-to-female transgender persons) resulted in a marked increase in subcutaneous fat deposition at the abdominal area, hip, and thigh, but only a slight increase in visceral fat deposition (147).

Studies in rodents also confirm this effect of estrogens on fat distribution. Female rats have more subcutaneous fat and less visceral fat than male rats. Ovariectomy increased visceral fat deposition in females and E2 treatment of ovariectomized females reversed the fat distribution to that of ovary-intact females. In addition, E2 treatment of castrated males also increased the subcutaneous fat percentage (148). Male and female mice with estrogen deficiency such

**1**

as aromatase knockout (ArKO) mice, which cannot synthesize endogenous estrogens due to targeted disruption of the aromatase gene, had heavier gonadal and infrarenal fat pads than their wild-type (WT) littermates. E2 replacement in female ArKO mice restored the fat pad mass to those of WT animals (149).

To study whether ERα or ERβ is involved in the effects of estrogens on adipose tissues, studies with ERα knockout (ERαKO) male and female mice showed that these animals had an increased WAT mass, especially the gonadal WAT (150). Studies comparing ERαKO, ERβ knockout (ERβKO), and double ERs knockout (ERαβKO) mice showed that ERαKO and ERαβKO, but not ERβKO females had increased overall fat mass and circulating leptin levels. In addition, treatment of ovariectomized females with E2 resulted in a reduction in gonadal fat mass in WT and ERβKO, but not in ERαKO or ERαβKO mice (151,152). Adipocyte-specific deletion of ERα led to visceral obesity and adipose tissue inflammation in both sexes of mice, but more severe metabolic disturbances were observed in male mice (153). These animal studies underscore that the fat-reducing effect of estrogens is mediated through ERα, which is in accordance with a finding in humans that adipose tissues of obese women had lower ERα mRNA levels than those of non-obese women (154).

Recent studies revealed that GPER may also regulate adipose tissue function and expansion, but the findings are still contradictory and warrant further studies. One study found that female but not male GPER knockout (GPERKO) mice were protected from HFD-induced obesity without significant changes in food intake and energy expenditure. GPER deficiency did not affect the metabolic phenotypes of chow-fed male and female mice (155). In contrast, another study found that chow-fed GPERKO males had increased visceral and subcutaneous fat mass, elevated circulating proinflammatory cytokine levels, and reduced adiponectin levels, without changes in food consumption or physical activity (156).

Regarding adipokine production, plasma adiponectin levels are in general higher in women than in men (157). Postmenopausal women, nevertheless, have higher circulating total and HMW adiponectin levels than premenopausal women (158,159). Total and HMW adiponectin concentrations were negatively correlated with E2 levels and insulin resistance status (158). Although estrogen status alone cannot fully explain adiponectin levels in all mentioned conditions, a higher adiponectin level remains a significant determinant for lower risk of insulin resistance in postmenopausal women, confirming the anti-diabetic effect of adiponectin (159). Gender-affirming hormone therapy in transwomen not only increased total fat mass but also serum leptin and adiponectin concentrations (160,161). In addition, *in vitro* stimulation of WAT explants or isolated adipocytes from subcutaneous WAT of women confirmed a direct stimulatory effect of E2 on leptin secretion and on *LEP* mRNA expression (162). Likewise,

E2 directly reduced adiponectin production and secretion in cultured 3T3-L1 adipocytes (163).

Also female mice have higher plasma adiponectin levels, greater HMW/total adiponectin ratio, and better insulin sensitivity than male mice (104,163). Ovariectomy increases while E2 treatment in ovariectomized mice decreases plasma adiponectin levels (163). Another study found that E2 treatment reduced body weight and abdominal fat mass and attenuated insulin resistance of female mice with HFD-induced obesity. Circulating leptin levels were elevated while adiponectin levels were unchanged by HFD, yet E2 treatment reduced the circulating levels of both leptin and adiponectin. Most likely, this is mediated through a different mechanism since E2 treatment did not affect *Adipoq* mRNA expression in WAT of the HFD-fed females while it reduced *Lep* mRNA expression (164).

The finding that E2-treated obese mice had improved insulin sensitivity but decreased circulating adiponectin levels is contradictory to a general observation that adiponectin levels decline in obese and insulin-resistant state, whereas leptin levels increase proportionally to fat mass and correlate with insulin resistance (81). Another study in ovariectomized mice found that E2 treatment reduced fat mass, adipocyte size, and serum leptin and adiponectin levels, but increased the adiponectin/leptin ratio which was in parallel with an improved glucose tolerance (165). This discrepancy in adiponectin levels and insulin sensitivity in each estrogen condition is likely caused by physiological adaptations of adipose tissue, modes of adipose tissue expansion, or alterations of circulating adiponectin isoforms, which require further investigation to draw a firm conclusion.

### 3.2 Progestogens

Progestogens are steroid hormones synthesized in ovaries, adrenal glands, and the placenta. Progesterone, the natural endogenous progestogen, is essential for the development of female reproductive organs in the luteal phase of female reproductive cycle, when it prepares the endometrium for possible implantation of a fertilized egg, and for maintenance of pregnancy. The classical signaling pathway of progestogens is through binding to the nuclear progesterone receptors (PRs), subsequently interacting with progesterone response elements, and initiating transcription of PR target genes. In addition, progestogens can also signal through non-classical pathways by binding to other receptors, e.g. membrane-associated receptors (mPRs), which belong to the progestin and adipoQ receptor (PAQR) family, and the PR membrane component (PGRMC) 1 and 2 (166). Furthermore, progesterone can be converted into the neuroactive metabolite allopregnanolone which acts through the membrane-associated GABA type A (GABA$_A$) receptor (166).

Clinical observations propose a lipogenic effect of progestogens. A longitudinal study in pregnant women found that weight gain during pregnancy was positively correlated with plasma progesterone levels but not with E2 levels or amount of dietary intake (167). Women using depot-medroxyprogesterone acetate (DMPA), a progestogen-only injectable contraceptive, gained more weight than women without hormonal contraceptives. This weight gain was contributed to an increase in fat mass with a more central distribution (168). Of note, although DMPA has the highest affinity to PR, it can also bind to GR and AR albeit with low affinity, and thus DMPA also has some androgenic and glucocorticoid effects (169). Furthermore, progestogen-only contraceptive users usually have elevated plasma insulin concentrations after a glucose challenge, suggesting progestogen-induced insulin resistance (170).

Progesterone administration to rats had no effect on body weight and fat mass of male rats, but led to increased body weight and inguinal fat mass in female rats without affecting the intra-abdominal fat mass. Activity and mRNA expression of lipogenic enzymes were also upregulated in the inguinal WAT of female rats (171,172). An *in vitro* progesterone treatment of rat adipocytes, obtained from parametrial fat pads of females, confirmed the lipogenic effects of progesterone since it dose-dependently upregulated *Srebp1c* and *Fasn* mRNA expression (173). However, an *in vitro* study using cultured adipocytes isolated from subcutaneous and omental WATs of women, showed inconsistent effects of progesterone on adipocyte differentiation and lipid accumulation (174).

Concerning adipokine production, progesterone administration in rats resulted in upregulated *Lep* mRNA but downregulated *Adipoq* mRNA expression in inguinal WAT of females. The effect of progesterone on the adipokine mRNA expression was abolished when mifepristone (RU486, a potent PR and GR antagonist) was co-administered, suggesting a PR-regulated mechanism. Of interest, progesterone did not alter *Lep* and *Adipoq* mRNA expression in retroperitoneal WAT of females or in inguinal, epididymal, and retroperitoneal WATs of males, and did not affect circulating levels of leptin and adiponectin in both sexes (171). However, prolonged treatment with progesterone increased adiponectin production but did not affect leptin production in 3T3-L1 adipocytes (175). Hence, these depot- and sex-specific effects of progesterone on adipokine production warrant further investigation, especially since this female sex steroid is less well studied than the other major hormone, E2.

### 3.3 Androgens

Androgens are male sex hormones which are not only required for male reproductive system development and secondary male sex characteristics, but are also involved in energy/metabolic homeostasis. Testosterone is the main

circulating androgen for adult men and male rodents, synthesized in testes. At target organs, testosterone can be converted to E2 by the enzyme aromatase, e.g. in WAT, or to the more potent androgen derivative dihydrotestosterone (DHT) by the enzyme 5α-reductase in, for example, male reproductive organs, hair follicles, liver, and many brain regions. Principal actions of testosterone and DHT are mediated by the androgen receptor (AR). Apart from the gonads, adrenal glands also produce androgen precursors, so-called adrenal androgens, i.e. dehydroepiandrosterone (DHEA), DHEA sulfate, and androstenedione, which are found in plasma of both sexes after the adrenarche, i.e. maturation of adrenal steroidogenesis (20,176).

Male hypogonadism, i.e., men with low testosterone levels, is associated with visceral obesity, metabolic syndrome, and an increased incidence of type 2 diabetes mellitus (177,178). Testosterone replacement therapy for male hypogonadism reduces fat mass and improves the metabolic profile (177). In contrast, androgen deprivation therapy (so-called chemical castration) for patients with prostate cancer leads to increases in body weight, total fat mass, and insulin resistance (179,180). The mentioned studies suggest that androgen deficiency in men contributes to obesity and the metabolic syndrome. On the other hand, obesity itself is also considered a cause of male hypogonadism since leptin and obesity-induced proinflammatory cytokines have been shown to suppress the HPG axis and testicular testosterone production (181). Nutritional intervention for weight reduction or bariatric surgery (surgical treatment for severely obese patients) leads to increased plasma testosterone concentrations (182). Therefore, it should be concluded that obesity and testosterone deficiency are bidirectionally regulated.

Regarding fat distribution, testosterone treatment as a gender-affirming hormonal therapy for transmen (female-to-male transgender persons) resulted in a reduced subcutaneous fat deposition and a slight increase in visceral fat accumulation, resembling the male fat distribution pattern (147). In healthy men, testosterone administration dose-dependently affects total fat mass. Low serum testosterone concentrations increase fat mass while supra-physiological concentrations reduce fat mass, but the changes in fat mass are evenly distributed between the visceral and subcutaneous depots (183). In men with hypogonadism, treatment with testosterone alone or in combination with finasteride (a 5α-reductase inhibitor for blocking peripheral conversion of testosterone to DHT) both resulted in an increase in lean body mass; decreases in waist circumference and total fat mass; improvement of physical performance; and decreased levels of leptin, insulin, inflammatory markers, and plasma lipid concentrations (184,185). These studies suggest a beneficial effect of testosterone on the metabolic profile in men, including a decrease in visceral adiposity.

However, a study in abdominally obese men found that testosterone decreased whereas DHT increased visceral fat mass, while subcutaneous fat mass was unaffected by either treatment. Testosterone but not DHT increased glucose disposal under fixed hyperinsulinemic conditions, decreased fasting plasma glucose levels, and improved plasma lipid profiles, suggesting a complex mechanism rather than only a direct activation of AR (186). These studies are suggestive for (local) effects of E2 because DHT cannot be converted into E2 whereas testosterone can. Indeed, testosterone treatment to hypogonadal men led to increased plasma concentrations of both testosterone and E2. Moreover, this treatment restored the reduced mRNA expression of *AR*, *ERα*, and *CYP19A1* in adipose tissue of hypogonadal men to those in eugonadal men (187). Importantly, an elegant study in healthy men revealed that the fat mass reducing effect of testosterone disappeared when an aromatase inhibitor was co-administered with testosterone. This co-administration resulted in a greater total fat mass than at baseline. In other words, estrogen deficiency may in fact be the main cause of increased body fat in hypogonadal and obese men (188). These studies illustrate the complex hormonal regulation of adipose tissue function and a potential estrogenic effect of testosterone through ERα in male adipose tissues.

Studies in male mice demonstrate some contradictory effects of castration on fat masses. For example, one study showed that castration led to an increased gonadal fat mass (189), whereas other studies showed no significant effect of castration on retroperitoneal, gonadal, and subcutaneous fat masses (47,190). Surprisingly, specific activation of AR by DHT and combined treatment of testosterone and an aromatase inhibitor in castrated mice resulted in an increased retroperitoneal fat mass, but neither testosterone treatment alone nor E2 treatment negatively affected the fat mass (190). However, the AR knockout (ARKO) mouse model revealed that ARKO males have increased fat mass, elevated serum leptin levels, and reduced physical activity, but the effects on insulin sensitivity, leptin sensitivity, adiponectin levels, and food intake were inconsistent (191-193). A possible explanation of the inconsistent phenotypes is the markedly reduced testosterone level and thus aromatase-synthesized E2 in ARKO mice because AR is crucial for testicular testosterone production and ARKO males had atrophic testes. In fact, male mice with adipose-specific AR deficiency showed normal body weight and adiposity with unaffected serum testosterone and E2 levels, but an increase in intra-adipose E2 levels and hyperleptinemia, yet without leptin resistance. The increased leptin production is likely E2-driven (194).

Concerning adipokine synthesis, androgen deprivation in healthy men induced by gonadotropin-releasing hormone (GnRH) antagonist treatment led

to elevated plasma leptin and adiponectin concentrations, whereas testosterone administration suppressed the plasma concentrations of both adipokines (195). Likewise, testosterone treatment in transmen also resulted in reduced serum concentrations of leptin and adiponectin (160,161). *In vitro* stimulation of WAT explants or isolated adipocytes from subcutaneous WAT of men confirmed that DHT inhibited *LEP* mRNA expression and decreased leptin secretion. Moreover, the inhibitory effect of DHT on leptin synthesis was attenuated upon cotreatment with an AR antagonist, suggesting an AR-mediated mechanism (162). In male mice, castration resulted in elevated levels of total and HMW adiponectin, whereas testosterone treatment in castrated males reduced the circulating adiponectin levels. In addition, testosterone or DHT treatment in cultured adipocytes confirmed a direct inhibitory effect of testosterone on adiponectin secretion (196,197).

In contrast to men, hyperandrogenism in women, e.g. women with polycystic ovary syndrome (PCOS), is associated with increased total fat mass and insulin resistance, but without a difference in regional fat distribution compared to BMI-matched female controls (198). Another study however showed that women with PCOS had increased visceral fat accumulation and decreased insulin sensitivity, features which were also observed in normal-weight PCOS subjects (199). Interestingly, recent studies revealed that the reduced insulin sensitivity of PCOS women was associated with low serum adiponectin levels, hypertrophic morphology of adipocytes, and an increased waist/hip ratio, but not with androgen excess (200,201). Also in mice, continuous administration of DHT in prepubertal females resulted in a disturbed metabolic phenotype that included increased body weight, enlarged adipocytes in gonadal and inguinal WAT depots, impaired glucose tolerance, elevated leptin levels, and reduced adiponectin levels (202). Intriguingly, female mice with global loss of AR signaling were protected against the ovarian and metabolic consequences of DHT treatment, indicating that AR-mediated androgen actions are crucial for the pathogenesis of PCOS in the rodent DHT model (203).

### 3.4 Glucocorticoids

GCs are synthesized in adrenal glands under the control of the HPA axis, as a crucial stress response mechanism. GCs regulate energy substrate metabolism in many aspects, namely by inducing hepatic gluconeogenesis, reducing glucose uptake in skeletal muscles and adipose tissues, promoting lipolysis in adipose tissues, inhibiting insulin secretion from pancreatic β cells, and stimulating glucagon secretion from pancreatic α cells (204). Endogenous GC synthesis is different among mammal species. Due to a lack of the steroidogenic enzyme CYP17A1 (functioning as 17α-hydroxylase or 17,20-lyase) in adrenal

**1**

glands of mice and rats, corticosterone is the main endogenous GC for rodents, whereas cortisol is the main endogenous GC for humans (12,205). At target tissues, GCs bind the GR or the mineralocorticoid receptor (MR), depending on their expression profile and function in each target tissue.

Synthetic GCs, such as dexamethasone, prednisolone, and hydrocortisone, are commonly prescribed medications due to their immunosuppressive properties. Weight gain is one of the most common side effects of synthetic GCs with a prevalence of 70% based on a self-reported population-based study, or at a hazard ratio of 2.4 based on an outpatient rheumatology clinic study (206,207). In patients with Cushing syndrome (clinical manifestation of pathological hypercortisolism), overweight/obesity is the most prevalent phenotype, present in 57–100% of patients, with a preferential pattern towards visceral rather than subcutaneous fat accumulation (208). The GC-induced visceral obesity can be explained by several mechanisms, especially with respect to the effects of GCs on WAT. First, *GR* mRNA expression levels and the binding capacity for GC in WAT homogenates are higher in omental tissues than in abdominal subcutaneous tissues (48,209). Second, intra-adipose cortisol levels are higher in omental WAT than in subcutaneous WAT, independent of serum cortisol level. This can be explained by an increased turnover rate and local generation of GC in adipose tissues, controlled by the 11β-HSD enzymes (209,210). The reductase 11β-HSD1 activates cortisone to cortisol, whereas the hydrogenase 11β-HSD2 deactivates cortisol to cortisone. Both enzymes are present and functioning in WAT, but only the reductase activity and *HSD11B1* mRNA expression are positively correlated with adipocyte size and total fat mass. Actually, GC treatment indirectly promotes the reductase activity by providing the cofactor NADPH for 11β-HSD1 activity in adipocytes from omental depots only. Direct effects on *HSD11B1* mRNA expression or 11β-HSD1 protein levels, however, remain inconclusive (209,210). Third, LPL activity was higher while norepinephrine-induced lipolysis was lower in abdominal WAT of Cushing patients than in those of non-Cushing obese subjects, suggesting GC-induced lipid accumulation in the visceral depot. Of note, lipogenic and lipolytic activities in femoral WAT of Cushing patients were unaffected (211).

Concerning direct effects of GCs on lipid metabolism, dexamethasone (a potent GR agonist with a very weak binding to the MR) treatment of rat adipocytes directly stimulated lipolysis in a dose-dependent manner and this effect was abolished by RU486 (a potent GR and PR antagonist). Likewise, dexamethasone treatment of rats resulted in increased plasma levels of glycerol and free fatty acids, confirming the lipolytic effect of GCs. Epididymal fat of dexamethasone-treated mice also showed higher lipolytic activity and greater levels of HSL and ATGL mRNA expression and protein content (212). An *in*

*vitro* stimulation of 3T3-L1 adipocytes with corticosterone confirmed the direct lipolytic effect of GCs and the GC-induced basal lipolysis in adipocytes that had been chronically exposed to GCs (213).

However, the direct lipolytic effect of GCs alone cannot explain the increase in visceral fat accumulation in Cushing patients. Indeed, GCs have another crucial function in adipose tissues, namely promoting adipogenesis. Corticosterone treatment in rats showed that corticosterone increased in fat mass and number of adipocytes in the visceral depot but not the subcutaneous depot, indicating depot-dependent adipogenic recruitment (213). Of interest, among many compounds used in a standard cocktail for 3T3-L1 adipocyte differentiation, dexamethasone is the most crucial compound in the initial stage of differentiation, as without it adipogenesis is not induced (214). Likewise, in human preadipocytes obtained from abdominal subcutaneous adipose tissues of healthy subjects, knockdown of GR by small interfering RNA (siRNA) completely blocked the adipogenic action of cortisol, whereas knockdown of MR did not affect the differentiation (215). Hence, all studies suggest that GR plays a more important role than MR for the adipogenic action of GCs.

Regarding adipokine production, plasma leptin levels were elevated in patients with Cushing syndrome compared to non-obese subjects or obese subjects without endocrine diseases. Curative resection of adrenal tumors reduced plasma leptin levels while a dexamethasone challenge in healthy individuals increased plasma leptin levels (216). Cortisol treatment of cultured human adipocytes also resulted in increased *LEP* mRNA expression and leptin secretion. A siRNA knockdown of the gene encoding GR but not MR reduced the stimulatory effect of cortisol on leptin production, showing that GR is also the receptor involved in the stimulatory effect of GCs on leptin production (215). Likewise, dexamethasone treatment in cultured rat adipocytes also led to an upregulated *Lep* mRNA expression (217).

The effects of GCs on adiponectin are different. Non-obese Cushing patients had a lower plasma adiponectin concentration than non-obese control subjects, but obese Cushing patients had the same low level of plasma adiponectin concentration as the obese control subjects. Hydrocortisone injection in healthy individuals confirmed the inhibitory effect of GCs on adiponectin production (218). Also in cultured human subcutaneous adipocytes, dexamethasone directly suppressed adiponectin secretion (219). In contrast, another study found that cortisol treatment of cultured human adipocytes isolated from abdominal subcutaneous depots induced *ADIPOQ* mRNA expression and adiponectin secretion. Knockdown of GR by siRNA reduced the stimulatory effect of cortisol on adiponectin production, whereas knockdown of MR had no effect (215). The contradictory effect of GC on adiponectin production warrant further studies.

**1**

The HPA axis has been shown to exhibit sexually dimorphic regulation and activity. For example, many stress-induced psychiatric disorders, such as depressive and anxiety disorders, are more prevalent and severe in women than in men (220). Also in rodent studies, female rats have higher baseline levels and higher stress-induced levels of corticosterone and adrenocorticotropic hormone (ACTH; the pituitary hormone that stimulates the adrenal glands to synthesize and secrete GCs) than male rats (221,222). However, there are only a limited number of studies addressing sex differences in GC-induced alterations in adipose tissue function. In male mice, cotreatment of corticosterone and DHT potentiated, whereas cotreatment of corticosterone and the AR-antagonist enzalutamide attenuated GR responses in WAT (223). Another recent study showed that the GC-induced obesity and hypertrophic expansion of visceral fat depots in ovariectomized rats were attenuated by E2 treatment (224). Further studies are required to elucidate if the GC-induced metabolic derangements, including effects on adipose tissues, are sex-dependent.

## 4. Conclusion

Males and females display differences in adipose tissue distribution and functions that contribute to differences in the risk to develop obesity and obesity-related comorbidities. Differences in sex steroid hormone levels contribute significantly to these differences. However, studies in human and animal models also revealed that sex steroids have sex-dependent effects on adipose tissues. Recent studies showing that sex steroid hormone levels influence the metabolic effects of glucocorticoids, underline the need for more studies to gain a full understanding of the molecular mechanisms regulating these sex-dependent effects. Additional studies are also needed since sex-dependent effects of sex steroids and glucocorticoids have largely been overlooked with respect to their clinical implications, for instance, sex differences in the effects of pharmacological GCs. Better understanding of sex-dependent regulation of adipose tissues will facilitate the development of novel sex-specific therapeutic strategies to combat the obesity pandemic.

## References

1. World Health Organization. Obesity and overweight - Fact sheets. 2018; https://www.who.int/en/news-room/fact-sheets/detail/obesity-and-overweight. Accessed 13 June, 2019.
2. Pearson-Stuttard J, Zhou B, Kontis V, Bentham J, Gunter MJ, Ezzati M. Worldwide burden of cancer attributable to diabetes and high body-mass index: a comparative risk assessment. Lancet Diabetes Endocrinol. 2018;**6**(6):e6-e15.
3. Saltiel AR, Olefsky JM. Inflammatory mechanisms linking obesity and metabolic disease. *J Clin Invest*. 2017;**127**(1):1-4.
4. Hales CM, Carroll MD, Fryar CD, Ogden CL. Prevalence of Obesity Among Adults and Youth: United States, 2015-2016. *NCHS Data Brief*. 2017(288):1-8.

5.  Arnold AP, Cassis LA, Eghbali M, Reue K, Sandberg K. Sex Hormones and Sex Chromosomes Cause Sex Differences in the Development of Cardiovascular Diseases. *Arterioscler Thromb Vasc Biol.* 2017;**37**(5):746-756.

6.  Perez-Lopez FR, Larrad-Mur L, Kallen A, Chedraui P, Taylor HS. Gender differences in cardiovascular disease: hormonal and biochemical influences. *Reprod Sci.* 2010;**17**(6):511-531.

7.  Yang Y, Kozloski M. Sex differences in age trajectories of physiological dysregulation: inflammation, metabolic syndrome, and allostatic load. *J Gerontol A Biol Sci Med Sci.* 2011;**66**(5):493-500.

8.  Palmer BF, Clegg DJ. The sexual dimorphism of obesity. *Mol Cell Endocrinol.* 2015;**402**:113-119.

9.  Karastergiou K, Smith SR, Greenberg AS, Fried SK. Sex differences in human adipose tissues - the biology of pear shape. *Biol Sex Differ.* 2012;**3**(1):13.

10. Pasquali R. The hypothalamic-pituitary-adrenal axis and sex hormones in chronic stress and obesity: pathophysiological and clinical aspects. *Ann N Y Acad Sci.* 2012;**1264**:20-35.

11. Bourke CH, Harrell CS, Neigh GN. Stress-induced sex differences: adaptations mediated by the glucocorticoid receptor. *Horm Behav.* 2012;**62**(3):210-218.

12. Pihlajoki M, Heikinheimo M, Wilson DB. Regulation of Adrenal Steroidogenesis. In: Levine AC, ed. *Adrenal Disorders.* Cham: Humana Press; 2018:15-66.

13. Jin JM, Yang WX. Molecular regulation of hypothalamus-pituitary-gonads axis in males. *Gene.* 2014;**551**(1):15-25.

14. Christensen A, Bentley GE, Cabrera R, Ortega HH, Perfito N, Wu TJ, Micevych P. Hormonal regulation of female reproduction. *Horm Metab Res.* 2012;**44**(8):587-591.

15. Luo E, Stephens SB, Chaing S, Munaganuru N, Kauffman AS, Breen KM. Corticosterone Blocks Ovarian Cyclicity and the LH Surge via Decreased Kisspeptin Neuron Activation in Female Mice. *Endocrinology.* 2016;**157**(3):1187-1199.

16. Juarez-Rojas L, Vigueras-Villasenor RM, Casillas F, Retana-Marquez S. Gradual decrease in spermatogenesis caused by chronic stress. *Acta Histochem.* 2017;**119**(3):284-291.

17. Mauvais-Jarvis F. Sex differences in metabolic homeostasis, diabetes, and obesity. *Biol Sex Differ.* 2015;**6**:14.

18. Kasinska MA, Drzewoski J, Sliwinska A. Epigenetic modifications in adipose tissue - relation to obesity and diabetes. *Arch Med Sci.* 2016;**12**(6):1293-1301.

19. Mauvais-Jarvis F, Clegg DJ, Hevener AL. The role of estrogens in control of energy balance and glucose homeostasis. *Endocr Rev.* 2013;**34**(3):309-338.

20. Navarro G, Allard C, Xu W, Mauvais-Jarvis F. The role of androgens in metabolism, obesity, and diabetes in males and females. *Obesity (Silver Spring).* 2015;**23**(4):713-719.

21. Kloting N, Bluher M. Adipocyte dysfunction, inflammation and metabolic syndrome. *Rev Endocr Metab Disord.* 2014;**15**(4):277-287.

22. Speakman JR. Chapter 26 - Obesity and thermoregulation. In: Romanovsky AA, ed. *Handbook of Clinical Neurology.* Vol 156: Elsevier; 2018:431-443.

23. Young P, Arch JR, Ashwell M. Brown adipose tissue in the parametrial fat pad of the mouse. *FEBS Lett.* 1984;**167**(1):10-14.

24. Frontini A, Vitali A, Perugini J, Murano I, Romiti C, Ricquier D, Guerrieri M, Cinti S. White-to-brown transdifferentiation of omental adipocytes in patients affected by pheochromocytoma. *Biochim Biophys Acta.* 2013;**1831**(5):950-959.

25. Kotzbeck P, Giordano A, Mondini E, Murano I, Severi I, Venema W, Cecchini MP, et al. Brown adipose tissue whitening leads to brown adipocyte death and adipose tissue inflammation. *J Lipid Res.* 2018;**59**(5):784-794.

26. Halberg N, Khan T, Trujillo ME, Wernstedt-Asterholm I, Attie AD, Sherwani S, Wang ZV, et al. Hypoxia-inducible factor 1alpha induces fibrosis and insulin resistance in white adipose tissue. *Mol Cell Biol.* 2009;**29**(16):4467-4483.

27. Kloting N, Fasshauer M, Dietrich A, Kovacs P, Schon MR, Kern M, Stumvoll M, Bluher M. Insulin-sensitive obesity. *Am J Physiol Endocrinol Metab.* 2010;**299**(3):E506-515.

28. Lundgren M, Svensson M, Lindmark S, Renstrom F, Ruge T, Eriksson JW. Fat cell enlargement is an independent marker of insulin resistance and 'hyperleptinaemia'. *Diabetologia.* 2007;**50**(3):625-633.

29. Salans LB, Knittle JL, Hirsch J. The role of adipose cell size and adipose tissue insulin sensitivity in the carbohydrate intolerance of human obesity. *J Clin Invest.* 1968;**47**(1):153-165.

30. Ghaben AL, Scherer PE. Adipogenesis and metabolic health. *Nat Rev Mol Cell Biol.* 2019;**20**(4):242-258.

**1**

31. Fukumura D, Ushiyama A, Duda DG, Xu L, Tam J, Krishna V, Chatterjee K, Garkavtsev I, Jain RK. Paracrine regulation of angiogenesis and adipocyte differentiation during in vivo adipogenesis. *Circ Res.* 2003;**93**(9):e88-97.

32. Chusyd DE, Wang D, Huffman DM, Nagy TR. Relationships between Rodent White Adipose Fat Pads and Human White Adipose Fat Depots. *Front Nutr.* 2016;**3**:10.

33. Guglielmi V, Sbraccia P. Obesity phenotypes: depot-differences in adipose tissue and their clinical implications. *Eat Weight Disord.* 2018;**23**(1):3-14.

34. Joe AW, Yi L, Even Y, Vogl AW, Rossi FM. Depot-specific differences in adipogenic progenitor abundance and proliferative response to high-fat diet. *Stem Cells.* 2009;**27**(10):2563-2570.

35. Macotela Y, Emanuelli B, Mori MA, Gesta S, Schulz TJ, Tseng YH, Kahn CR. Intrinsic differences in adipocyte precursor cells from different white fat depots. *Diabetes.* 2012;**61**(7):1691-1699.

36. Tchkonia T, Tchoukalova YD, Giorgadze N, Pirtskhalava T, Karagiannides I, Forse RA, Koo A, et al. Abundance of two human preadipocyte subtypes with distinct capacities for replication, adipogenesis, and apoptosis varies among fat depots. *Am J Physiol Endocrinol Metab.* 2005;**288**(1):E267-277.

37. Tchkonia T, Giorgadze N, Pirtskhalava T, Tchoukalova Y, Karagiannides I, Forse RA, DePonte M, et al. Fat depot origin affects adipogenesis in primary cultured and cloned human preadipocytes. *Am J Physiol Regul Integr Comp Physiol.* 2002;**282**(5):R1286-1296.

38. Durrer Schutz D, Busetto L, Dicker D, Farpour-Lambert N, Pryke R, Toplak H, Widmer D, Yumuk V, Schutz Y. European Practical and Patient-Centred Guidelines for Adult Obesity Management in Primary Care. *Obes Facts.* 2019;**12**(1):40-66.

39. Garvey WT, Mechanick JI, Brett EM, Garber AJ, Hurley DL, Jastreboff AM, Nadolsky K, Pessah-Pollack R, Plodkowski R, Reviewers of the AACEOCPG. American Association of Clinical Endocrinologists and American College of Endocrinology Comprehensive Clinical Practice Guidelines for Medical Care of Patients with Obesity. *Endocr Pract.* 2016;**22 Suppl 3**:1-203.

40. Arnett DK, Blumenthal RS, Albert MA, Buroker AB, Goldberger ZD, Hahn EJ, Himmelfarb CD, et al. 2019 ACC/AHA Guideline on the Primary Prevention of Cardiovascular Disease. *Circulation.* 2019:CIR0000000000000678.

41. Rosenzweig JL, Bakris GL, Berglund LF, Hivert MF, Horton ES, Kalyani RR, Murad MH, Verges BL. Primary Prevention of ASCVD and T2DM in Patients at Metabolic Risk: An Endocrine Society* Clinical Practice Guideline. *J Clin Endocrinol Metab.* 2019.

42. Gallagher D, Visser M, Sepulveda D, Pierson RN, Harris T, Heymsfield SB. How useful is body mass index for comparison of body fatness across age, sex, and ethnic groups? *Am J Epidemiol.* 1996;**143**(3):228-239.

43. Kuk JL, Lee S, Heymsfield SB, Ross R. Waist circumference and abdominal adipose tissue distribution: influence of age and sex. *Am J Clin Nutr.* 2005;**81**(6):1330-1334.

44. Wells JC. Sexual dimorphism of body composition. *Best Pract Res Clin Endocrinol Metab.* 2007;**21**(3):415-430.

45. Kautzky-Willer A, Harreiter J, Pacini G. Sex and Gender Differences in Risk, Pathophysiology and Complications of Type 2 Diabetes Mellitus. *Endocr Rev.* 2016;**37**(3):278-316.

46. Demerath EW, Sun SS, Rogers N, Lee M, Reed D, Choh AC, Couch W, et al. Anatomical patterning of visceral adipose tissue: race, sex, and age variation. *Obesity (Silver Spring).* 2007;**15**(12):2984-2993.

47. Macotela Y, Boucher J, Tran TT, Kahn CR. Sex and depot differences in adipocyte insulin sensitivity and glucose metabolism. *Diabetes.* 2009;**58**(4):803-812.

48. Pedersen SB, Jonler M, Richelsen B. Characterization of regional and gender differences in glucocorticoid receptors and lipoprotein lipase activity in human adipose tissue. *J Clin Endocrinol Metab.* 1994;**78**(6):1354-1359.

49. Taylor RW, Grant AM, Williams SM, Goulding A. Sex differences in regional body fat distribution from pre- to postpuberty. *Obesity (Silver Spring).* 2010;**18**(7):1410-1416.

50. Camhi SM, Bray GA, Bouchard C, Greenway FL, Johnson WD, Newton RL, Ravussin E, Ryan DH, Smith SR, Katzmarzyk PT. The relationship of waist circumference and BMI to visceral, subcutaneous, and total body fat: sex and race differences. *Obesity (Silver Spring).* 2011;**19**(2):402-408.

51. Svendsen OL, Hassager C, Christiansen C. Age- and menopause-associated variations in body composition and fat distribution in healthy women as measured by dual-energy X-ray absorptiometry. *Metabolism.* 1995;**44**(3):369-373.

52. Chang E, Varghese M, Singer K. Gender and Sex Differences in Adipose Tissue. *Curr Diab Rep.* 2018;**18**(9):69.

53. Wu Y, Lee MJ, Ido Y, Fried SK. High-fat diet-induced obesity regulates MMP3 to modulate depot- and sex-dependent adipose expansion in C57BL/6J mice. *Am J Physiol Endocrinol Metab.* 2017;**312**(1):E58-E71.

54. Stubbins RE, Holcomb VB, Hong J, Nunez NP. Estrogen modulates abdominal adiposity and protects female mice from obesity and impaired glucose tolerance. *Eur J Nutr.* 2012;**51**(7):861-870.

55. Litwak SA, Wilson JL, Chen W, Garcia-Rudaz C, Khaksari M, Cowley MA, Enriori PJ. Estradiol prevents fat accumulation and overcomes leptin resistance in female high-fat diet mice. *Endocrinology.* 2014;**155**(11):4447-4460.

56. Dakin RS, Walker BR, Seckl JR, Hadoke PW, Drake AJ. Estrogens protect male mice from obesity complications and influence glucocorticoid metabolism. *Int J Obes (Lond).* 2015;**39**(10):1539-1547.

57. Seale P, Bjork B, Yang W, Kajimura S, Chin S, Kuang S, Scime A, et al. PRDM16 controls a brown fat/skeletal muscle switch. *Nature.* 2008;**454**(7207):961-967.

58. An Y, Wang G, Diao Y, Long Y, Fu X, Weng M, Zhou L, et al. A Molecular Switch Regulating Cell Fate Choice between Muscle Progenitor Cells and Brown Adipocytes. *Dev Cell.* 2017;**41**(4):382-391 e385.

59. Wang W, Kissig M, Rajakumari S, Huang L, Lim HW, Won KJ, Seale P. Ebf2 is a selective marker of brown and beige adipogenic precursor cells. *Proc Natl Acad Sci U S A.* 2014;**111**(40):14466-14471.

60. Shao M, Ishibashi J, Kusminski CM, Wang QA, Hepler C, Vishvanath L, MacPherson KA, et al. Zfp423 Maintains White Adipocyte Identity through Suppression of the Beige Cell Thermogenic Gene Program. *Cell Metab.* 2016;**23**(6):1167-1184.

61. Cristancho AG, Lazar MA. Forming functional fat: a growing understanding of adipocyte differentiation. *Nat Rev Mol Cell Biol.* 2011;**12**(11):722-734.

62. Villanueva CJ, Vergnes L, Wang J, Drew BG, Hong C, Tu Y, Hu Y, et al. Adipose subtype-selective recruitment of TLE3 or Prdm16 by PPARgamma specifies lipid storage versus thermogenic gene programs. *Cell Metab.* 2013;**17**(3):423-435.

63. Rosen ED, Spiegelman BM. What we talk about when we talk about fat. *Cell.* 2014;**156**(1-2):20-44.

64. Seale P. Transcriptional Regulatory Circuits Controlling Brown Fat Development and Activation. *Diabetes.* 2015;**64**(7):2369-2375.

65. Tontonoz P, Spiegelman BM. Fat and beyond: the diverse biology of PPARgamma. *Annu Rev Biochem.* 2008;**77**:289-312.

66. Barbatelli G, Murano I, Madsen L, Hao Q, Jimenez M, Kristiansen K, Giacobino JP, De Matteis R, Cinti S. The emergence of cold-induced brown adipocytes in mouse white fat depots is determined predominantly by white to brown adipocyte transdifferentiation. *Am J Physiol Endocrinol Metab.* 2010;**298**(6):E1244-1253.

67. Lafontan M. Advances in adipose tissue metabolism. *Int J Obes (Lond).* 2008;**32 Suppl 7**:S39-51.

68. Luo L, Liu M. Adipose tissue in control of metabolism. *J Endocrinol.* 2016;**231**(3):R77-R99.

69. Marcelin G, Chua S, Jr. Contributions of adipocyte lipid metabolism to body fat content and implications for the treatment of obesity. *Curr Opin Pharmacol.* 2010;**10**(5):588-593.

70. Letexier D, Pinteur C, Large V, Frering V, Beylot M. Comparison of the expression and activity of the lipogenic pathway in human and rat adipose tissue. *J Lipid Res.* 2003;**44**(11):2127-2134.

71. Herman MA, Peroni OD, Villoria J, Schon MR, Abumrad NA, Bluher M, Klein S, Kahn BB. A novel ChREBP isoform in adipose tissue regulates systemic glucose metabolism. *Nature.* 2012;**484**(7394):333-338.

72. Ferre P, Foufelle F. SREBP-1c transcription factor and lipid homeostasis: clinical perspective. *Horm Res.* 2007;**68**(2):72-82.

73. Crewe C, Zhu Y, Paschoal VA, Joffin N, Ghaben AL, Gordillo R, Oh DY, Liang G, Horton JD, Scherer PE. SREBP-regulated adipocyte lipogenesis is dependent on substrate availability and redox modulation of mTORC1. *JCI Insight.* 2019;**5**.

74. Peckett AJ, Wright DC, Riddell MC. The effects of glucocorticoids on adipose tissue lipid metabolism. *Metabolism.* 2011;**60**(11):1500-1510.

75. Lebeck J. Metabolic impact of the glycerol channels AQP7 and AQP9 in adipose tissue and liver. *J Mol Endocrinol.* 2014;**52**(2):R165-178.

**1**

76. Furuhashi M, Saitoh S, Shimamoto K, Miura T. Fatty Acid-Binding Protein 4 (FABP4): Pathophysiological Insights and Potent Clinical Biomarker of Metabolic and Cardiovascular Diseases. *Clin Med Insights Cardiol.* 2014;**8**(Suppl 3):23-33.

77. Sztalryd C, Brasaemle DL. The perilipin family of lipid droplet proteins: Gatekeepers of intracellular lipolysis. *Biochim Biophys Acta Mol Cell Biol Lipids.* 2017;**1862**(10 Pt B):1221-1232.

78. Lee RA, Harris CA, Wang JC. Glucocorticoid Receptor and Adipocyte Biology. *Nucl Receptor Res.* 2018;**5**.

79. Bluher M. Adipose tissue dysfunction contributes to obesity related metabolic diseases. *Best Pract Res Clin Endocrinol Metab.* 2013;**27**(2):163-177.

80. Bluher M, Mantzoros CS. From leptin to other adipokines in health and disease: facts and expectations at the beginning of the 21st century. *Metabolism.* 2015;**64**(1):131-145.

81. Fasshauer M, Bluher M. Adipokines in health and disease. *Trends Pharmacol Sci.* 2015;**36**(7):461-470.

82. Zhang Y, Proenca R, Maffei M, Barone M, Leopold L, Friedman JM. Positional cloning of the mouse obese gene and its human homologue. *Nature.* 1994;**372**(6505):425-432.

83. Ingalls AM, Dickie MM, Snell GD. Obese, a new mutation in the house mouse. *J Hered.* 1950;**41**(12):317-318.

84. Hummel KP, Dickie MM, Coleman DL. Diabetes, a new mutation in the mouse. *Science.* 1966;**153**(3740):1127-1128.

85. Kennedy AJ, Ellacott KL, King VL, Hasty AH. Mouse models of the metabolic syndrome. *Dis Model Mech.* 2010;**3**(3-4):156-166.

86. Margetic S, Gazzola C, Pegg GG, Hill RA. Leptin: a review of its peripheral actions and interactions. *Int J Obes Relat Metab Disord.* 2002;**26**(11):1407-1433.

87. Park HK, Ahima RS. Physiology of leptin: energy homeostasis, neuroendocrine function and metabolism. *Metabolism.* 2015;**64**(1):24-34.

88. Kelesidis T, Kelesidis I, Chou S, Mantzoros CS. Narrative review: the role of leptin in human physiology: emerging clinical applications. *Ann Intern Med.* 2010;**152**(2):93-100.

89. Stern JH, Rutkowski JM, Scherer PE. Adiponectin, Leptin, and Fatty Acids in the Maintenance of Metabolic Homeostasis through Adipose Tissue Crosstalk. *Cell Metab.* 2016;**23**(5):770-784.

90. Pan WW, Myers MG, Jr. Leptin and the maintenance of elevated body weight. *Nat Rev Neurosci.* 2018;**19**(2):95-105.

91. Scherer PE, Williams S, Fogliano M, Baldini G, Lodish HF. A novel serum protein similar to C1q, produced exclusively in adipocytes. *J Biol Chem.* 1995;**270**(45):26746-26749.

92. Hu E, Liang P, Spiegelman BM. AdipoQ is a novel adipose-specific gene dysregulated in obesity. *J Biol Chem.* 1996;**271**(18):10697-10703.

93. Maeda K, Okubo K, Shimomura I, Funahashi T, Matsuzawa Y, Matsubara K. cDNA cloning and expression of a novel adipose specific collagen-like factor, apM1 (AdiPose Most abundant Gene transcript 1). *Biochem Biophys Res Commun.* 1996;**221**(2):286-289.

94. Nakano Y, Tobe T, Choi-Miura NH, Mazda T, Tomita M. Isolation and characterization of GBP28, a novel gelatin-binding protein purified from human plasma. *J Biochem.* 1996;**120**(4):803-812.

95. Zhang Y, Matheny M, Zolotukhin S, Tumer N, Scarpace PJ. Regulation of adiponectin and leptin gene expression in white and brown adipose tissues: influence of beta3-adrenergic agonists, retinoic acid, leptin and fasting. *Biochim Biophys Acta.* 2002;**1584**(2-3):115-122.

96. Fujimoto N, Matsuo N, Sumiyoshi H, Yamaguchi K, Saikawa T, Yoshimatsu H, Yoshioka H. Adiponectin is expressed in the brown adipose tissue and surrounding immature tissues in mouse embryos. *Biochim Biophys Acta.* 2005;**1731**(1):1-12.

97. Delaigle AM, Jonas JC, Bauche IB, Cornu O, Brichard SM. Induction of adiponectin in skeletal muscle by inflammatory cytokines: in vivo and in vitro studies. *Endocrinology.* 2004;**145**(12):5589-5597.

98. Jasinski-Bergner S, Buttner M, Quandt D, Seliger B, Kielstein H. Adiponectin and Its Receptors Are Differentially Expressed in Human Tissues and Cell Lines of Distinct Origin. *Obes Facts.* 2017;**10**(6):569-583.

99. Choe SS, Huh JY, Hwang IJ, Kim JI, Kim JB. Adipose Tissue Remodeling: Its Role in Energy Metabolism and Metabolic Disorders. *Front Endocrinol (Lausanne).* 2016;**7**:30.

100. Ryo M, Nakamura T, Kihara S, Kumada M, Shibazaki S, Takahashi M, Nagai M, Matsuzawa Y, Funahashi T. Adiponectin as a biomarker of the metabolic syndrome. *Circ J.* 2004;**68**(11):975-981.

101. Lopez-Jaramillo P, Gomez-Arbelaez D, Lopez-Lopez J, Lopez-Lopez C, Martinez-Ortega J, Gomez-Rodriguez A, Triana-Cubillos S. The role of leptin/adiponectin ratio in metabolic syndrome and diabetes. *Horm Mol Biol Clin Investig*. 2014;**18**(1):37-45.

102. Fruhbeck G, Catalan V, Rodriguez A, Gomez-Ambrosi J. Adiponectin-leptin ratio: A promising index to estimate adipose tissue dysfunction. Relation with obesity-associated cardiometabolic risk. *Adipocyte*. 2018;**7**(1):57-62.

103. Schraw T, Wang ZV, Halberg N, Hawkins M, Scherer PE. Plasma adiponectin complexes have distinct biochemical characteristics. *Endocrinology*. 2008;**149**(5):2270-2282.

104. Pajvani UB, Hawkins M, Combs TP, Rajala MW, Doebber T, Berger JP, Wagner JA, et al. Complex distribution, not absolute amount of adiponectin, correlates with thiazolidinedione-mediated improvement in insulin sensitivity. *J Biol Chem*. 2004;**279**(13):12152-12162.

105. Bernasochi GB, Bell JR, Simpson ER, Delbridge LMD, Boon WC. Impact of Estrogens on the Regulation of White, Beige, and Brown Adipose Tissue Depots. *Compr Physiol*. 2019;**9**(2):457-475.

106. Belanger C, Hould FS, Lebel S, Biron S, Brochu G, Tchernof A. Omental and subcutaneous adipose tissue steroid levels in obese men. *Steroids*. 2006;**71**(8):674-682.

107. Kinoshita T, Honma S, Shibata Y, Yamashita K, Watanabe Y, Maekubo H, Okuyama M, Takashima A, Takeshita N. An innovative LC-MS/MS-based method for determining CYP 17 and CYP 19 activity in the adipose tissue of pre- and postmenopausal and ovariectomized women using 13C-labeled steroid substrates. *J Clin Endocrinol Metab*. 2014;**99**(4):1339-1347.

108. Morton NM. Obesity and corticosteroids: 11beta-hydroxysteroid type 1 as a cause and therapeutic target in metabolic disease. *Mol Cell Endocrinol*. 2010;**316**(2):154-164.

109. De Sousa Peixoto RA, Turban S, Battle JH, Chapman KE, Seckl JR, Morton NM. Preadipocyte 11beta-hydroxysteroid dehydrogenase type 1 is a keto-reductase and contributes to diet-induced visceral obesity in vivo. *Endocrinology*. 2008;**149**(4):1861-1868.

110. Nedergaard J, Bengtsson T, Cannon B. Unexpected evidence for active brown adipose tissue in adult humans. *Am J Physiol Endocrinol Metab*. 2007;**293**(2):E444-452.

111. Hany TF, Gharehpapagh E, Kamel EM, Buck A, Himms-Hagen J, von Schulthess GK. Brown adipose tissue: a factor to consider in symmetrical tracer uptake in the neck and upper chest region. *Eur J Nucl Med Mol Imaging*. 2002;**29**(10):1393-1398.

112. van Marken Lichtenbelt WD, Vanhommerig JW, Smulders NM, Drossaerts JM, Kemerink GJ, Bouvy ND, Schrauwen P, Teule GJ. Cold-activated brown adipose tissue in healthy men. *N Engl J Med*. 2009;**360**(15):1500-1508.

113. Virtanen KA, Lidell ME, Orava J, Heglind M, Westergren R, Niemi T, Taittonen M, et al. Functional brown adipose tissue in healthy adults. *N Engl J Med*. 2009;**360**(15):1518-1525.

114. Cypess AM, Lehman S, Williams G, Tal I, Rodman D, Goldfine AB, Kuo FC, et al. Identification and importance of brown adipose tissue in adult humans. *N Engl J Med*. 2009;**360**(15):1509-1517.

115. Zingaretti MC, Crosta F, Vitali A, Guerrieri M, Frontini A, Cannon B, Nedergaard J, Cinti S. The presence of UCP1 demonstrates that metabolically active adipose tissue in the neck of adult humans truly represents brown adipose tissue. *FASEB J*. 2009;**23**(9):3113-3120.

116. Morrison SF. Central neural control of thermoregulation and brown adipose tissue. *Auton Neurosci*. 2016;**196**:14-24.

117. Blondin DP, Labbe SM, Tingelstad HC, Noll C, Kunach M, Phoenix S, Guerin B, et al. Increased brown adipose tissue oxidative capacity in cold-acclimated humans. *J Clin Endocrinol Metab*. 2014;**99**(3):E438-446.

118. Ouellet V, Routhier-Labadie A, Bellemare W, Lakhal-Chaieb L, Turcotte E, Carpentier AC, Richard D. Outdoor temperature, age, sex, body mass index, and diabetic status determine the prevalence, mass, and glucose-uptake activity of 18F-FDG-detected BAT in humans. *J Clin Endocrinol Metab*. 2011;**96**(1):192-199.

119. Cannon B, Nedergaard J. Metabolic consequences of the presence or absence of the thermogenic capacity of brown adipose tissue in mice (and probably in humans). *Int J Obes (Lond)*. 2010;**34 Suppl 1**:S7-16.

120. Cypess AM, Weiner LS, Roberts-Toler C, Franquet Elia E, Kessler SH, Kahn PA, English J, et al. Activation of human brown adipose tissue by a beta3-adrenergic receptor agonist. *Cell Metab*. 2015;**21**(1):33-38.

121. Vosselman MJ, van der Lans AA, Brans B, Wierts R, van Baak MA, Schrauwen P, van Marken Lichtenbelt WD. Systemic beta-adrenergic stimulation of thermogenesis is not accompanied by brown adipose tissue activity in humans. *Diabetes*. 2012;**61**(12):3106-3113.

**1**

122. Agrawal A, Nair N, Baghel NS. A novel approach for reduction of brown fat uptake on FDG PET. *Br J Radiol.* 2009;**82**(980):626-631.

123. Soderlund V, Larsson SA, Jacobsson H. Reduction of FDG uptake in brown adipose tissue in clinical patients by a single dose of propranolol. *Eur J Nucl Med Mol Imaging.* 2007;**34**(7):1018-1022.

124. Louis SN, Nero TL, Iakovidis D, Jackman GP, Louis WJ. LK 204-545, a highly selective beta1-adrenoceptor antagonist at human beta-adrenoceptors. *Eur J Pharmacol.* 1999;**367**(2-3):431-435.

125. Li Y, Fromme T, Schweizer S, Schottl T, Klingenspor M. Taking control over intracellular fatty acid levels is essential for the analysis of thermogenic function in cultured primary brown and brite/beige adipocytes. *EMBO Rep.* 2014;**15**(10):1069-1076.

126. Labbe SM, Caron A, Bakan I, Laplante M, Carpentier AC, Lecomte R, Richard D. In vivo measurement of energy substrate contribution to cold-induced brown adipose tissue thermogenesis. *FASEB J.* 2015;**29**(5):2046-2058.

127. Haemmerle G, Lass A, Zimmermann R, Gorkiewicz G, Meyer C, Rozman J, Heldmaier G, et al. Defective lipolysis and altered energy metabolism in mice lacking adipose triglyceride lipase. *Science.* 2006;**312**(5774):734-737.

128. Kalinovich AV, de Jong JM, Cannon B, Nedergaard J. UCP1 in adipose tissues: two steps to full browning. *Biochimie.* 2017;**134**:127-137.

129. Evans BA, Merlin J, Bengtsson T, Hutchinson DS. Adrenoceptors in white, brown, and brite adipocytes. *Br J Pharmacol.* 2019;**176**(14):2416-2432.

130. Hao Q, Yadav R, Basse AL, Petersen S, Sonne SB, Rasmussen S, Zhu Q, et al. Transcriptome profiling of brown adipose tissue during cold exposure reveals extensive regulation of glucose metabolism. *Am J Physiol Endocrinol Metab.* 2015;**308**(5):E380-392.

131. de Jong JM, Larsson O, Cannon B, Nedergaard J. A stringent validation of mouse adipose tissue identity markers. *Am J Physiol Endocrinol Metab.* 2015;**308**(12):E1085-1105.

132. Law J, Bloor I, Budge H, Symonds ME. The influence of sex steroids on adipose tissue growth and function. *Horm Mol Biol Clin Investig.* 2014;**19**(1):13-24.

133. Kim SN, Jung YS, Kwon HJ, Seong JK, Granneman JG, Lee YH. Sex differences in sympathetic innervation and browning of white adipose tissue of mice. *Biol Sex Differ.* 2016;**7**:67.

134. Rodriguez AM, Quevedo-Coli S, Roca P, Palou A. Sex-dependent dietary obesity, induction of UCPs, and leptin expression in rat adipose tissues. *Obes Res.* 2001;**9**(9):579-588.

135. Rodriguez-Cuenca S, Pujol E, Justo R, Frontera M, Oliver J, Gianotti M, Roca P. Sex-dependent thermogenesis, differences in mitochondrial morphology and function, and adrenergic response in brown adipose tissue. *J Biol Chem.* 2002;**277**(45):42958-42963.

136. Quarta C, Mazza R, Pasquali R, Pagotto U. Role of sex hormones in modulation of brown adipose tissue activity. *J Mol Endocrinol.* 2012;**49**(1):R1-7.

137. Rodriguez AM, Monjo M, Roca P, Palou A. Opposite actions of testosterone and progesterone on UCP1 mRNA expression in cultured brown adipocytes. *Cell Mol Life Sci.* 2002;**59**(10):1714-1723.

138. Rodriguez-Cuenca S, Monjo M, Gianotti M, Proenza AM, Roca P. Expression of mitochondrial biogenesis-signaling factors in brown adipocytes is influenced specifically by 17beta-estradiol, testosterone, and progesterone. *Am J Physiol Endocrinol Metab.* 2007;**292**(1):E340-346.

139. Valle A, Catala-Niell A, Colom B, Garcia-Palmer FJ, Oliver J, Roca P. Sex-related differences in energy balance in response to caloric restriction. *Am J Physiol Endocrinol Metab.* 2005;**289**(1):E15-22.

140. Choi DK, Oh TS, Choi JW, Mukherjee R, Wang X, Liu H, Yun JW. Gender difference in proteome of brown adipose tissues between male and female rats exposed to a high fat diet. *Cell Physiol Biochem.* 2011;**28**(5):933-948.

141. Zimmerman MA, Budish RA, Kashyap S, Lindsey SH. GPER-novel membrane oestrogen receptor. *Clin Sci (Lond).* 2016;**130**(12):1005-1016.

142. Oliver-Williams C, Glisic M, Shahzad S, Brown E, Pellegrino Baena C, Chadni M, Chowdhury R, Franco OH, Muka T. The route of administration, timing, duration and dose of postmenopausal hormone therapy and cardiovascular outcomes in women: a systematic review. *Hum Reprod Update.* 2019;**25**(2):257-271.

143. Bae JM, Yoon BK. The Role of Menopausal Hormone Therapy in Reducing All-cause Mortality in Postmenopausal Women Younger than 60 Years: An Adaptive Meta-analysis. *J Menopausal Med.* 2018;**24**(3):139-142.

144. Xu Y, Lopez M. Central regulation of energy metabolism by estrogens. *Mol Metab.* 2018;**15**:104-115.

145. Gambacciani M, Ciaponi M, Cappagli B, De Simone L, Orlandi R, Genazzani AR. Prospective evaluation of body weight and body fat distribution in early postmenopausal women with and without hormonal replacement therapy. *Maturitas.* 2001;**39**(2):125-132.

146. Haarbo J, Marslew U, Gotfredsen A, Christiansen C. Postmenopausal hormone replacement therapy prevents central distribution of body fat after menopause. *Metabolism.* 1991;**40**(12):1323-1326.

147. Elbers JM, Asscheman H, Seidell JC, Gooren LJ. Effects of sex steroid hormones on regional fat depots as assessed by magnetic resonance imaging in transsexuals. *Am J Physiol.* 1999;**276**(2):E317-325.

148. Clegg DJ, Brown LM, Woods SC, Benoit SC. Gonadal hormones determine sensitivity to central leptin and insulin. *Diabetes.* 2006;**55**(4):978-987.

149. Jones ME, Thorburn AW, Britt KL, Hewitt KN, Wreford NG, Proietto J, Oz OK, et al. Aromatase-deficient (ArKO) mice have a phenotype of increased adiposity. *Proc Natl Acad Sci U S A.* 2000;**97**(23):12735-12740.

150. Heine PA, Taylor JA, Iwamoto GA, Lubahn DB, Cooke PS. Increased adipose tissue in male and female estrogen receptor-alpha knockout mice. *Proc Natl Acad Sci U S A.* 2000;**97**(23):12729-12734.

151. Lindberg MK, Alatalo SL, Halleen JM, Mohan S, Gustafsson JA, Ohlsson C. Estrogen receptor specificity in the regulation of the skeleton in female mice. *J Endocrinol.* 2001;**171**(2):229-236.

152. Lindberg MK, Weihua Z, Andersson N, Moverare S, Gao H, Vidal O, Erlandsson M, et al. Estrogen receptor specificity for the effects of estrogen in ovariectomized mice. *J Endocrinol.* 2002;**174**(2):167-178.

153. Davis KE, M DN, Sun K, W MS, J DB, J AZ, Zeve D, et al. The sexually dimorphic role of adipose and adipocyte estrogen receptors in modulating adipose tissue expansion, inflammation, and fibrosis. *Mol Metab.* 2013;**2**(3):227-242.

154. Nilsson M, Dahlman I, Ryden M, Nordstrom EA, Gustafsson JA, Arner P, Dahlman-Wright K. Oestrogen receptor alpha gene expression levels are reduced in obese compared to normal weight females. *Int J Obes (Lond).* 2007;**31**(6):900-907.

155. Wang A, Luo J, Moore W, Alkhalidy H, Wu L, Zhang J, Zhen W, et al. GPR30 regulates diet-induced adiposity in female mice and adipogenesis in vitro. *Sci Rep.* 2016;**6**:34302.

156. Sharma G, Hu C, Brigman JL, Zhu G, Hathaway HJ, Prossnitz ER. GPER deficiency in male mice results in insulin resistance, dyslipidemia, and a proinflammatory state. *Endocrinology.* 2013;**154**(11):4136-4145.

157. Arita Y, Kihara S, Ouchi N, Takahashi M, Maeda K, Miyagawa J, Hotta K, et al. Paradoxical decrease of an adipose-specific protein, adiponectin, in obesity. *Biochem Biophys Res Commun.* 1999;**257**(1):79-83.

158. Leung KC, Xu A, Craig ME, Martin A, Lam KS, O'Sullivan AJ. Adiponectin isoform distribution in women--relationship to female sex steroids and insulin sensitivity. *Metabolism.* 2009;**58**(2):239-245.

159. Tamakoshi K, Yatsuya H, Wada K, Matsushita K, Otsuka R, Yang PO, Sugiura K, et al. The transition to menopause reinforces adiponectin production and its contribution to improvement of insulin-resistant state. *Clin Endocrinol (Oxf).* 2007;**66**(1):65-71.

160. Auer MK, Ebert T, Pietzner M, Defreyne J, Fuss J, Stalla GK, T'Sjoen G. Effects of Sex Hormone Treatment on the Metabolic Syndrome in Transgender Individuals: Focus on Metabolic Cytokines. *J Clin Endocrinol Metab.* 2018;**103**(2):790-802.

161. Elbers JM, Asscheman H, Seidell JC, Frolich M, Meinders AE, Gooren LJ. Reversal of the sex difference in serum leptin levels upon cross-sex hormone administration in transsexuals. *J Clin Endocrinol Metab.* 1997;**82**(10):3267-3270.

162. Machinal-Quelin F, Dieudonne MN, Pecquery R, Leneveu MC, Giudicelli Y. Direct in vitro effects of androgens and estrogens on ob gene expression and leptin secretion in human adipose tissue. *Endocrine.* 2002;**18**(2):179-184.

163. Combs TP, Berg AH, Rajala MW, Klebanov S, Iyengar P, Jimenez-Chillaron JC, Patti ME, Klein SL, Weinstein RS, Scherer PE. Sexual differentiation, pregnancy, calorie restriction, and aging affect the adipocyte-specific secretory protein adiponectin. *Diabetes.* 2003;**52**(2):268-276.

164. Bryzgalova G, Lundholm L, Portwood N, Gustafsson JA, Khan A, Efendic S, Dahlman-Wright K. Mechanisms of antidiabetogenic and body weight-lowering effects of estrogen in high-fat diet-fed mice. *Am J Physiol Endocrinol Metab.* 2008;**295**(4):E904-912.

165. Kim JH, Meyers MS, Khuder SS, Abdallah SL, Muturi HT, Russo L, Tate CR, et al. Tissue-selective estrogen complexes with bazedoxifene prevent metabolic dysfunction in female mice. *Mol Metab.* 2014;**3**(2):177-190.

166. Garg D, Ng SSM, Baig KM, Driggers P, Segars J. Progesterone-Mediated Non-Classical Signaling. *Trends Endocrinol Metab.* 2017;**28**(9):656-668.

167. Lof M, Hilakivi-Clarke L, Sandin SS, de Assis S, Yu W, Weiderpass E. Dietary fat intake and gestational weight gain in relation to estradiol and progesterone plasma levels during pregnancy: a longitudinal study in Swedish women. *BMC Womens Health.* 2009;**9**:10.

168. Clark MK, Dillon JS, Sowers M, Nichols S. Weight, fat mass, and central distribution of fat increase when women use depot-medroxyprogesterone acetate for contraception. *Int J Obes (Lond).* 2005;**29**(10):1252-1258.

169. Africander D, Verhoog N, Hapgood JP. Molecular mechanisms of steroid receptor-mediated actions by synthetic progestins used in HRT and contraception. *Steroids.* 2011;**76**(7):636-652.

170. Kahn HS, Curtis KM, Marchbanks PA. Effects of injectable or implantable progestin-only contraceptives on insulin-glucose metabolism and diabetes risk. *Diabetes Care.* 2003;**26**(1):216-225.

171. Stelmanska E, Kmiec Z, Swierczynski J. The gender- and fat depot-specific regulation of leptin, resistin and adiponectin genes expression by progesterone in rat. *J Steroid Biochem Mol Biol.* 2012;**132**(1-2):160-167.

172. Stelmanska E, Swierczynski J. Up-regulation of lipogenic enzyme genes expression in inguinal white adipose tissue of female rats by progesterone. *J Steroid Biochem Mol Biol.* 2013;**134**:37-44.

173. Lacasa D, Le Liepvre X, Ferre P, Dugail I. Progesterone stimulates adipocyte determination and differentiation 1/sterol regulatory element-binding protein 1c gene expression. potential mechanism for the lipogenic effect of progesterone in adipose tissue. *J Biol Chem.* 2001;**276**(15):11512-11516.

174. Zhang Y, Nadeau M, Faucher F, Lescelleur O, Biron S, Daris M, Rheaume C, Luu-The V, Tchernof A. Progesterone metabolism in adipose cells. *Mol Cell Endocrinol.* 2009;**298**(1-2):76-83.

175. Pektas M, Kurt AH, Un I, Tiftik RN, Buyukafsar K. Effects of 17beta-estradiol and progesterone on the production of adipokines in differentiating 3T3-L1 adipocytes: Role of Rho-kinase. *Cytokine.* 2015;**72**(2):130-134.

176. Miller WL, Auchus RJ. The molecular biology, biochemistry, and physiology of human steroidogenesis and its disorders. *Endocr Rev.* 2011;**32**(1):81-151.

177. Corona G, Monami M, Rastrelli G, Aversa A, Sforza A, Lenzi A, Forti G, Mannucci E, Maggi M. Type 2 diabetes mellitus and testosterone: a meta-analysis study. *Int J Androl.* 2011;**34**(6 Pt 1):528-540.

178. Wang N, Zhai H, Han B, Li Q, Chen Y, Chen Y, Xia F, Lin D, Lu Y. Visceral fat dysfunction is positively associated with hypogonadism in Chinese men. *Sci Rep.* 2016;**6**:19844.

179. Smith MR, Finkelstein JS, McGovern FJ, Zietman AL, Fallon MA, Schoenfeld DA, Kantoff PW. Changes in body composition during androgen deprivation therapy for prostate cancer. *J Clin Endocrinol Metab.* 2002;**87**(2):599-603.

180. Smith MR, Lee H, Nathan DM. Insulin sensitivity during combined androgen blockade for prostate cancer. *J Clin Endocrinol Metab.* 2006;**91**(4):1305-1308.

181. Grossmann M. Hypogonadism and male obesity: Focus on unresolved questions. *Clin Endocrinol (Oxf).* 2018;**89**(1):11-21.

182. Corona G, Rastrelli G, Monami M, Saad F, Luconi M, Lucchese M, Facchiano E, et al. Body weight loss reverts obesity-associated hypogonadotropic hypogonadism: a systematic review and meta-analysis. *Eur J Endocrinol.* 2013;**168**(6):829-843.

183. Woodhouse LJ, Gupta N, Bhasin M, Singh AB, Ross R, Phillips J, Bhasin S. Dose-dependent effects of testosterone on regional adipose tissue distribution in healthy young men. *J Clin Endocrinol Metab.* 2004;**89**(2):718-726.

184. Kalinchenko SY, Tishova YA, Mskhalaya GJ, Gooren LJ, Giltay EJ, Saad F. Effects of testosterone supplementation on markers of the metabolic syndrome and inflammation in hypogonadal men with the metabolic syndrome: the double-blinded placebo-controlled Moscow study. *Clin Endocrinol (Oxf).* 2010;**73**(5):602-612.

185. Page ST, Amory JK, Bowman FD, Anawalt BD, Matsumoto AM, Bremner WJ, Tenover JL. Exogenous testosterone (T) alone or with finasteride increases physical performance, grip strength, and lean body mass in older men with low serum T. *J Clin Endocrinol Metab.* 2005;**90**(3):1502-1510.

186. Marin P, Holmang S, Gustafsson C, Jonsson L, Kvist H, Elander A, Eldh J, Sjostrom L, Holm G, Bjorntorp P. Androgen treatment of abdominally obese men. *Obes Res.* 1993;**1**(4):245-251.

187. Ghanim H, Dhindsa S, Abuaysheh S, Batra M, Kuhadiya ND, Makdissi A, Chaudhuri A, Dandona P. Diminished androgen and estrogen receptors and aromatase levels in hypogonadal diabetic men: reversal with testosterone. *Eur J Endocrinol.* 2018;**178**(3):277-283.

188. Finkelstein JS, Lee H, Burnett-Bowie SA, Pallais JC, Yu EW, Borges LF, Jones BF, et al. Gonadal steroids and body composition, strength, and sexual function in men. *N Engl J Med.* 2013;**369**(11):1011-1022.

189. Aoki A, Fujitani K, Takagi K, Kimura T, Nagase H, Nakanishi T. Male Hypogonadism Causes Obesity Associated with Impairment of Hepatic Gluconeogenesis in Mice. *Biol Pharm Bull.* 2016;**39**(4):587-592.

190. Moverare-Skrtic S, Venken K, Andersson N, Lindberg MK, Svensson J, Swanson C, Vander-schueren D, Oscarsson J, Gustafsson JA, Ohlsson C. Dihydrotestosterone treatment results in obesity and altered lipid metabolism in orchidectomized mice. *Obesity (Silver Spring).* 2006;**14**(4):662-672.

191. Rana K, Fam BC, Clarke MV, Pang TP, Zajac JD, MacLean HE. Increased adiposity in DNA binding-dependent androgen receptor knockout male mice associated with decreased voluntary activity and not insulin resistance. *Am J Physiol Endocrinol Metab.* 2011;**301**(5):E767-778.

192. Fan W, Yanase T, Nomura M, Okabe T, Goto K, Sato T, Kawano H, Kato S, Nawata H. Androgen receptor null male mice develop late-onset obesity caused by decreased energy expenditure and lipolytic activity but show normal insulin sensitivity with high adiponectin secretion. *Diabetes.* 2005;**54**(4):1000-1008.

193. Lin HY, Xu Q, Yeh S, Wang RS, Sparks JD, Chang C. Insulin and leptin resistance with hyperleptinemia in mice lacking androgen receptor. *Diabetes.* 2005;**54**(6):1717-1725.

194. Yu IC, Lin HY, Liu NC, Wang RS, Sparks JD, Yeh S, Chang C. Hyperleptinemia without obesity in male mice lacking androgen receptor in adipose tissue. *Endocrinology.* 2008;**149**(5):2361-2368.

195. Page ST, Herbst KL, Amory JK, Coviello AD, Anawalt BD, Matsumoto AM, Bremner WJ. Testosterone administration suppresses adiponectin levels in men. *J Androl.* 2005;**26**(1):85-92.

196. Xu A, Chan KW, Hoo RL, Wang Y, Tan KC, Zhang J, Chen B, et al. Testosterone selectively reduces the high molecular weight form of adiponectin by inhibiting its secretion from adipocytes. *J Biol Chem.* 2005;**280**(18):18073-18080.

197. Nishizawa H, Shimomura I, Kishida K, Maeda N, Kuriyama H, Nagaretani H, Matsuda M, et al. Androgens decrease plasma adiponectin, an insulin-sensitizing adipocyte-derived protein. *Diabetes.* 2002;**51**(9):2734-2741.

198. Barber TM, Golding SJ, Alvey C, Wass JA, Karpe F, Franks S, McCarthy MI. Global adiposity rather than abnormal regional fat distribution characterizes women with polycystic ovary syndrome. *J Clin Endocrinol Metab.* 2008;**93**(3):999-1004.

199. Carmina E, Bucchieri S, Esposito A, Del Puente A, Mansueto P, Orio F, Di Fede G, Rini G. Abdominal fat quantity and distribution in women with polycystic ovary syndrome and extent of its relation to insulin resistance. *J Clin Endocrinol Metab.* 2007;**92**(7):2500-2505.

200. Toulis KA, Goulis DG, Farmakiotis D, Georgopoulos NA, Katsikis I, Tarlatzis BC, Papadimas I, Panidis D. Adiponectin levels in women with polycystic ovary syndrome: a systematic review and a meta-analysis. *Hum Reprod Update.* 2009;**15**(3):297-307.

201. Manneras-Holm L, Leonhardt H, Kullberg J, Jennische E, Oden A, Holm G, Hellstrom M, et al. Adipose tissue has aberrant morphology and function in PCOS: enlarged adipocytes and low serum adiponectin, but not circulating sex steroids, are strongly associated with insulin resistance. *J Clin Endocrinol Metab.* 2011;**96**(2):E304-311.

202. van Houten EL, Kramer P, McLuskey A, Karels B, Themmen AP, Visser JA. Reproductive and metabolic phenotype of a mouse model of PCOS. *Endocrinology.* 2012;**153**(6):2861-2869.

203. Caldwell ASL, Edwards MC, Desai R, Jimenez M, Gilchrist RB, Handelsman DJ, Walters KA. Neuroendocrine androgen action is a key extraovarian mediator in the development of polycystic ovary syndrome. *Proc Natl Acad Sci U S A.* 2017;**114**(16):E3334-E3343.

204. Granner DK, Wang JC, Yamamoto KR. Regulatory Actions of Glucocorticoid Hormones: From Organisms to Mechanisms. *Adv Exp Med Biol.* 2015;**872**:3-31.

205. Pihlajoki M, Dorner J, Cochran RS, Heikinheimo M, Wilson DB. Adrenocortical zonation, renewal, and remodeling. *Front Endocrinol (Lausanne).* 2015;**6**:27.

**1**

206. Curtis JR, Westfall AO, Allison J, Bijlsma JW, Freeman A, George V, Kovac SH, Spettell CM, Saag KG. Population-based assessment of adverse events associated with long-term glucocorticoid use. *Arthritis Rheum.* 2006;**55**(3):420-426.

207. Huscher D, Thiele K, Gromnica-Ihle E, Hein G, Demary W, Dreher R, Zink A, Buttgereit F. Dose-related patterns of glucocorticoid-induced side effects. *Ann Rheum Dis.* 2009;**68**(7):1119-1124.

208. Pivonello R, Isidori AM, De Martino MC, Newell-Price J, Biller BM, Colao A. Complications of Cushing's syndrome: state of the art. *Lancet Diabetes Endocrinol.* 2016;**4**(7):611-629.

209. Veilleux A, Laberge PY, Morency J, Noel S, Luu-The V, Tchernof A. Expression of genes related to glucocorticoid action in human subcutaneous and omental adipose tissue. *J Steroid Biochem Mol Biol.* 2010;**122**(1-3):28-34.

210. Lee MJ, Fried SK, Mundt SS, Wang Y, Sullivan S, Stefanni A, Daugherty BL, Hermanowski-Vosatka A. Depot-specific regulation of the conversion of cortisone to cortisol in human adipose tissue. *Obesity (Silver Spring).* 2008;**16**(6):1178-1185.

211. Rebuffe-Scrive M, Krotkiewski M, Elfverson J, Bjorntorp P. Muscle and adipose tissue morphology and metabolism in Cushing's syndrome. *J Clin Endocrinol Metab.* 1988;**67**(6):1122-1128.

212. Xu C, He J, Jiang H, Zu L, Zhai W, Pu S, Xu G. Direct effect of glucocorticoids on lipolysis in adipocytes. *Mol Endocrinol.* 2009;**23**(8):1161-1170.

213. Campbell JE, Peckett AJ, D'Souza A M, Hawke TJ, Riddell MC. Adipogenic and lipolytic effects of chronic glucocorticoid exposure. *Am J Physiol Cell Physiol.* 2011;**300**(1):C198-209.

214. Pantoja C, Huff JT, Yamamoto KR. Glucocorticoid signaling defines a novel commitment state during adipogenesis in vitro. *Mol Biol Cell.* 2008;**19**(10):4032-4041.

215. Lee MJ, Fried SK. The glucocorticoid receptor, not the mineralocorticoid receptor, plays the dominant role in adipogenesis and adipokine production in human adipocytes. *Int J Obes (Lond).* 2014;**38**(9):1228-1233.

216. Masuzaki H, Ogawa Y, Hosoda K, Miyawaki T, Hanaoka I, Hiraoka J, Yasuno A, et al. Glucocorticoid regulation of leptin synthesis and secretion in humans: elevated plasma leptin levels in Cushing's syndrome. *J Clin Endocrinol Metab.* 1997;**82**(8):2542-2547.

217. De Vos P, Lefebvre AM, Shrivo I, Fruchart JC, Auwerx J. Glucocorticoids induce the expression of the leptin gene through a non-classical mechanism of transcriptional activation. *Eur J Biochem.* 1998;**253**(3):619-626.

218. Fallo F, Scarda A, Sonino N, Paoletta A, Boscaro M, Pagano C, Federspil G, Vettor R. Effect of glucocorticoids on adiponectin: a study in healthy subjects and in Cushing's syndrome. *Eur J Endocrinol.* 2004;**150**(3):339-344.

219. Degawa-Yamauchi M, Moss KA, Bovenkerk JE, Shankar SS, Morrison CL, Lelliott CJ, Vidal-Puig A, Jones R, Considine RV. Regulation of adiponectin expression in human adipocytes: effects of adiposity, glucocorticoids, and tumor necrosis factor alpha. *Obes Res.* 2005;**13**(4):662-669.

220. Bangasser DA, Valentino RJ. Sex differences in stress-related psychiatric disorders: neurobiological perspectives. *Front Neuroendocrinol.* 2014;**35**(3):303-319.

221. Kitay JI. Pituitary-Adrenal Function in the Rat after Gonadectomy and Gonadal Hormone Replacement. *Endocrinology.* 1963;**73**:253-260.

222. Seale JV, Wood SA, Atkinson HC, Bate E, Lightman SL, Ingram CD, Jessop DS, Harbuz MS. Gonadectomy reverses the sexually diergic patterns of circadian and stress-induced hypothalamic-pituitary-adrenal axis activity in male and female rats. *J Neuroendocrinol.* 2004;**16**(6):516-524.

223. Spaanderman DCE, Nixon M, Buurstede JC, Sips HC, Schilperoort M, Kuipers EN, Backer EA, et al. Androgens modulate glucocorticoid receptor activity in adipose tissue and liver. *J Endocrinol.* 2019;**240**(1):51-63.

224. de Souza CF, Stopa LRS, Santos GF, Takasumi LCN, Martins AB, Garnica-Siqueira MC, Ferreira RN, et al. Estradiol protects against ovariectomy-induced susceptibility to the anabolic effects of glucocorticoids in rats. *Life Sci.* 2019;**218**:185-196.

**1**
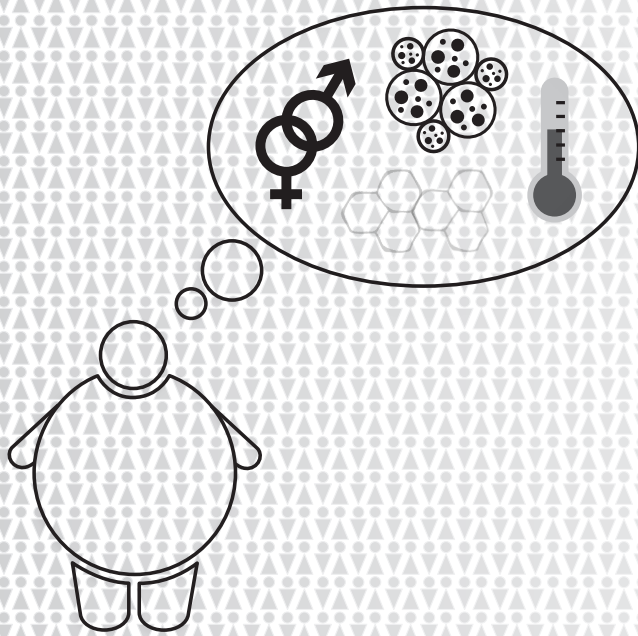
# Chapter 1B

## General Introduction

**Sex Difference in Thermoregulation, a Mechanism beyond Brown Adipose Tissue Activation**

1

**1**

## 1. Introduction

Adipose tissue can be generally categorized into two main types with opposite function: energy-storing white adipose tissue (WAT) and energy-burning brown adipose tissue (BAT), reviewed in chapter 1A. Upon cold stimulation, BAT utilizes energy-rich substrates, mainly fatty acids, to fuel thermogenesis, a mitochondrial process in which the activity of uncoupling protein 1 (UCP1) is pivotal. Upon confirmation of the presence of active BAT in adult humans in 2009 (1-3), BAT has become a "hot organ" for metabolic research. Induced utilization of excess calories through BAT activation is considered a promising strategy for obesity treatment (4). As discussed in chapter 1A, studies in humans and rodents have shown that females generally have a higher BAT prevalence and activity than males (5-7). The thermogenic function of BAT is part of the whole-body thermal homeostasis. This chapter will therefore provide an overview of body temperature regulation and highlight the role of BAT herein. In addition, this chapter will discuss whether thermoregulation is sex-dependently modulated.

## 2. Body temperature regulation

Humans and rodents are endotherms whose core body temperature ($T_c$) is tightly controlled at ~37°C in a narrow range, e.g. 35.4–37.8°C for humans (8). This is because cellular proteins are irreversibly denatured at a $T_c$ above 42°C and cellular reactions slow down at a $T_c$ below the normal range, resulting in, for instance, fatal cardiac failure at $T_c$ ~27°C (9,10). In general, core temperatures, e.g. in the brain and the thoracoabdominal compartment, are usually higher than peripheral temperatures, e.g. skin temperatures ($T_{sk}$) measured at the limbs. Heat is transferred between the core and the periphery via the circulation, which is an important regulator of body thermal homeostasis (10). To achieve optimal thermoregulation, the body integrates three main components for autonomic responses: afferent (input) sensing, central integration, and efferent (output) responses (9,11), see **Figure 1** for a schematic overview.

The skin serves as the principal sensory organ since it contains sensory nerve endings of afferent sensory neurons located in the dorsal root ganglia (DRG) (11). The neuronal receptive endings contain temperature sensors (or thermo-receptors) that belong to the transient receptor potential (TRP) superfamily of cation channels of which the voltage-dependent receptors are affected by different temperatures. Examples of these sensors include the heat-sensitive channel TPRV1, the warm-sensitive channel TRPM2, and the cool-sensitive channel TRPM8 (12,13). Via these sensors, information about the $T_{sk}$ is directed to the thermosensory neurons: first-order neurons in the DRG, second-order neurons in the dorsal horn (DH) of the spinal cord, and third-order neurons in
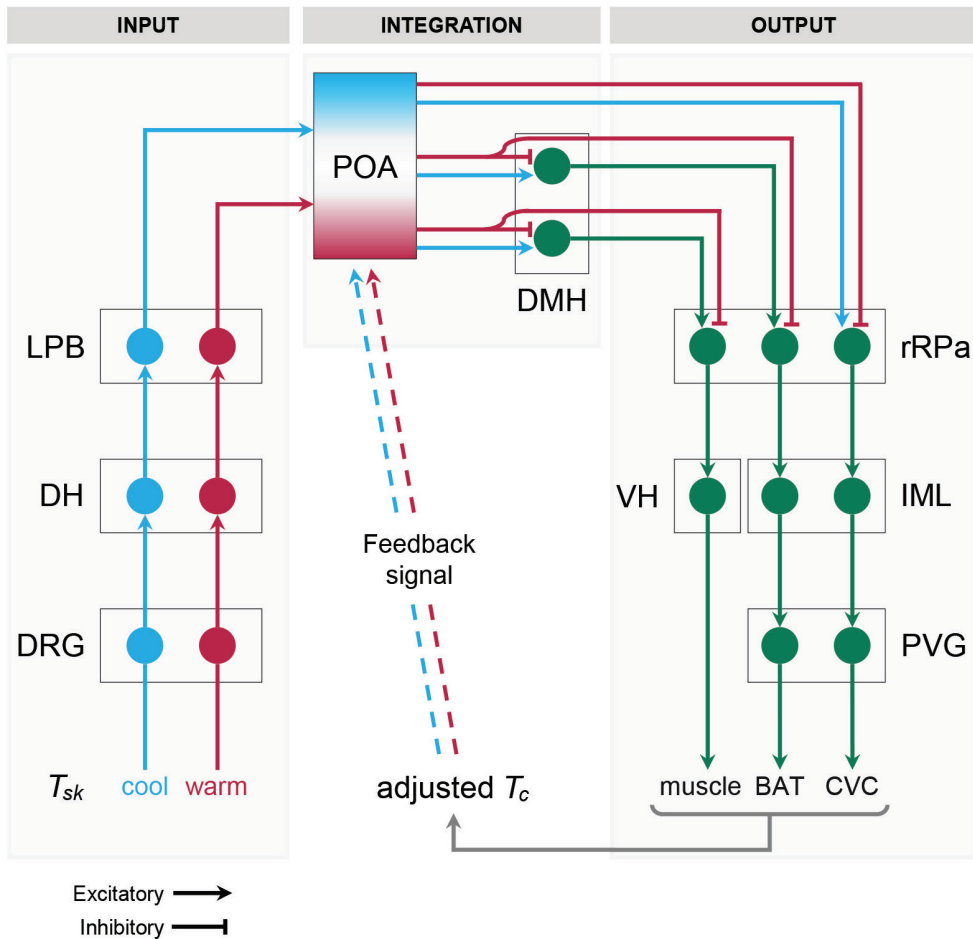
**Figure 1** Overview of autonomic thermoregulation

Abbreviations (from input to output): $T_{sk}$, skin temperature; DRG, dorsal root ganglia; DH, dorsal horn of the spinal cord; LPB, lateral parabrachial nucleus of the pons; POA, preoptic area of the anterior hypothalamus; DMH, dorsomedial hypothalamic nucleus; rRPa, rostral raphe pallidus nucleus in the medulla oblongata; VH, ventral horn; IML, intermediolateral cell column of the spinal cord; PVG, paravertebral ganglia; BAT, brown adipose tissue; CVC, cutaneous vasoconstriction; and $T_c$, core body temperature.

**1**

the lateral parabrachial nucleus (LPB) of the pons. The LPB, in turn, transmits the signal to the preoptic area (POA) of the anterior hypothalamus, the master thermoregulatory sensorimotor integration area (9,11). Of note, warm and cool signals are transmitted through separate populations of afferent neurons that project to distinct populations of neurons in POA to distinguish between warm and cool sensory inputs (14).

The warm-activated neurons and cold-activated neurons in the POA are interconnected to integrate the signals from the LPB, and hence transmit inhibitory or excitatory signals to the dorsomedial hypothalamic nucleus [DMH, the key regulator for body temperature, body weight, and metabolic function (15)] in the posterior hypothalamus and/or to the rostral raphe pallidus nucleus (rRPa) in the medulla oblongata. The DMH contains BAT sympathoexcitatory neurons and shivering promoting neurons, while the rRPa contains cutaneous vasoconstriction (CVC) premotor neurons, BAT sympathetic premotor neurons, and skeletal muscle shivering premotor neurons. In other words, cold exposure leads to excitatory commands to the DMH and the rRPa that stimulate the cold-defensive responses such as a reduction in heat loss by peripheral vasoconstriction and inductions in heat production by skeletal muscle shivering and BAT activation. By contrast, warm exposure inhibits the excitatory commands to the DMH and the rRPa (9,11).

For vasoconstriction and BAT thermogenesis during cold exposure, signals from the premotor neurons in the rRPa are transmitted through the preganglionic neurons in the intermediolateral cell column (IML) of the spinal cord, which synapse onto the postganglionic neurons in the paravertebral ganglia (PVG), and in turn stimulate the effector organs, cutaneous blood vessels or BAT depots. For shivering, the involuntary somatic premotor neurons in the rRPa drive the α- and γ-motoneurons in the ventral horn (VH) of the spinal cord to initiate repeated skeletal muscle contractions (11). Although shivering leads to rapid, maximal heat production during cold stress, it is a more energy-consuming process than BAT activation, even when the cold is rather mild. Hence, shivering thermogenesis is initiated only when the energy-inexpensive vasoconstriction is at its maximum. Non-shivering BAT thermogenesis is enhanced and preferred during habitual/prolonged cold conditions (9,16,17). For example, mice exposed to 4°C for 3 weeks had ~4-fold induction in UCP1 mRNA and protein expression in their BAT, compared to mice housed at 21°C (18). Rats housed at 10°C for 3 weeks also had higher oxidative activity in BAT, as well as a larger BAT depot, indicating a more metabolically active BAT compared to BAT of rats kept at 27°C (19). These rodent findings underscore the importance of non-shivering thermogenesis in BAT for chronic cold-defensive responses.

In contrast, warm exposure leads to peripheral vasodilation for heat dissipation, through inhibition of the sympathetic CVC tone. In hot conditions, warm-activated neurons also activate the sympathetic outflow through sympathetic cholinergic nerves that induce active vasodilation of peripheral vessels and perspiration of eccrine sweat glands, resulting in evaporative heat loss. When the ambient temperature ($T_a$) exceeds $T_c$, evaporative cooling is the only possible mechanism for heat dissipation (9,11,20).

After thermal effectors have responded to external cues, e.g. changes in $T_a$ or $T_{sk}$, temperature sensors in internal organs recheck the adjusted $T_c$, and send a feedback signal to the POA in order to optimize the thermoregulatory circuit (11,21). In fact, only changes in $T_c$ initiate the autonomic thermoregulatory responses and sensory information from $T_c$ contributes more than $T_{sk}$ to the autonomic responses (22). Furthermore, physiological thermoregulatory mechanismsalso involve behavioral adaptations, e.g. changing body posture or clothing [reviewed in (23)], which are beyond the scope of this chapter.

## 3. Sex difference in thermoregulation

Studies in humans and rodents have revealed sex differences in several of the thermoregulatory control mechanisms. A remarkable sex difference is the sex hormone-driven alterations in $T_c$. Women during the luteal phase of the menstrual cycle and women taking hormonal contraceptives have a 0.3–0.5°C higher $T_c$ than men and women during the follicular phase (24,25). Of note, the $T_c$ fluctuation during reproductive cycles is also observed in mice (26). This fluctuation in $T_c$ in females is mediated by progesterone, resulting in decreased firing rates of warm-sensitive neurons and increased firing rates of cold-sensitive neurons in the POA (27). In addition, a study comparing the thermoeffector responses between the early follicular phase and the midluteal phase found that $T_c$ at which women started shivering, sweating, and displaying cutaneous vasodilation were all increased in the luteal phase, confirming the set point altering effects of progesterone (28). Interestingly, estrogen seems to counteract this effect of progesterone on the temperature set point since the $T_c$ of women taking combined estrogen-progestin (a synthetic progesterone) contraceptives was ~0.5°C lower than $T_c$ of women taking progestin-only contraceptives (29).

An important factor for thermoregulation is body composition, an anthropometric feature that is profoundly different between men and women. A higher body surface area (BSA) directly results in a higher rate of heat loss, whereas body mass positively correlates with the rate of heat production and storage. The BSA-to-mass ratio thus dictates the net heat transfer from the body to its surroundings (30,31). With similar adiposity, women generally have a larger

**1**

BSA but a smaller body mass than men, indicating a higher heat loss and a lower heat production capacity compared to men. Therefore, the sex difference in body composition, with women having in general a higher BSA-to-mass ratio than men, suggests that women have a higher basal rate of heat loss than men (30-32). Intriguingly, a recent study found that the BSA-to-mass ratio was almost the sole determinant for heat-dissipating responses during an exercise with matched heat-loss requirements and that women favored dry heat loss (vasodilation) whereas men depended more on evaporative heat loss (sweating) (33).

The thermoeffector responses, e.g., adaptations of cutaneous vessels, sweating, and BAT thermogenesis, have been shown to display a certain degree of sex-dependent regulation. A human study in which the researchers infused warm or cold saline to manipulate $T_c$ while keeping $T_{sk}$ constant found that the average $T_c$ at which women started vasoconstriction, sweating, and shivering were all ~0.3°C higher than the $T_c$ in men (34). However, the inter-threshold range of shifting from vasoconstriction to sweating was ~0.2°C, which was equal in both sexes (34).

Concerning direct effects of sex hormones on vascular tones, 17β-estradiol (E2) directly causes rapid vasodilation by estrogen receptor (ER)-stimulated production of nitric oxide, an endothelium-derived relaxing factor, in vascular walls (35). The effects of progesterone and testosterone on blood vessels have also been studied, but the findings are contradictory. For example, while acute testosterone treatment increased vasodilation, chronic testosterone treatment led to impaired vascular relaxation and augmented vasoconstriction (36,37).

Studies have shown sex differences in sweating. Men had a greater maximal sweat rate than women when they were locally infused with acetylcholine, without a difference in cutaneous blood flow or the number of active sweat glands (38,39). Furthermore, although the acetylcholine-induced sweat rate was increased in physically trained subjects, the sweat rate remained higher in the physically trained men than in trained women (38). The same sex difference was also found when volunteers were exposed to a controlled whole-body heating protocol. Although men had a higher maximal sweat rate than women, the change in $T_c$ and the $T_{sk}$ at which sweating started, as well as cutaneous vasodilation measured by cutaneous vascular conductance, did not differ between the sexes (39).

As reviewed in chapter 1A, BAT is more prevalent and active in females than in males (5-7,40) and studies have demonstrated that the female sex hormones E2 and progesterone stimulate while the male sex hormone testosterone inhibits BAT activities (41,42). In addition, E2 can directly influence the central nervous system through ERα in the ventromedial hypothalamus (VMH),

which subsequently activates the rRPA, resulting in sympathetic nervous system activation, and hence BAT activation (43,44). Female mice lacking ERα in the VMH-specific steroidogenic factor-1 neurons had a reduction in sympathetic outflow activity and impaired BAT thermogenesis, confirming the direct E2-activated BAT thermogenesis in the VMH (45).

## 4. Thermal perception: a matter of sex?

In terms of thermal perception, thermal comfort is not only the sensation of $T_a$, but also a subjective interpretation of an individual how satisfied he/she is with $T_a$. Of interest, research has shown that women are more sensitive to and more often dissatisfied to fluctuations in $T_a$ than men (46-50). In other words, women have a smaller comfort range of $T_a$ than do men, though the findings have not always been statistically significant (50,51). This sex-dependent thermal preference has been nicely demonstrated in mouse studies. For instance, if mice were allowed to choose to reside at either 20, 25, or 30°C, females preferred to spend more time in the 30°C cage and less time in the 20°C cage, compared to males (52,53). One of the possible mechanisms for this sex difference in thermal sensation is the sensitivity of the cool-sensitive TRPM8. Females had higher sensitivity (lower threshold) and greater signal transmission of TRPM8 in the DRG neurons than males. The sex-dependent effects in TRPM8 were lost upon removal of E2 and testosterone from the culture media (54), implicating a role for sex steroids in thermal sensation.

## 5. Conclusion

Optimal control of $T_c$ is achieved by coordination of thermal somato-sensory organs, central integrating centers in the hypothalamus, and thermo-effector organs. Sex differences in thermoregulation are evident in multiple aspects, such as anthropometric characteristics and effects of sex hormones on BAT. However, it is still largely unknown whether sex hormones are involved in the differences in thermal perception. Also, whether the different sensitivities to $T_a$ in males and females are causative for the sex differences in thermoeffector responses requires more dedicated investigations.

## References

1. van Marken Lichtenbelt WD, Vanhommerig JW, Smulders NM, Drossaerts JM, Kemerink GJ, Bouvy ND, Schrauwen P, Teule GJ. Cold-activated brown adipose tissue in healthy men. *N Engl J Med.* 2009;**360**(15):1500-1508.
2. Cypess AM, Lehman S, Williams G, Tal I, Rodman D, Goldfine AB, Kuo FC, et al. Identification and importance of brown adipose tissue in adult humans. *N Engl J Med.* 2009;**360**(15):1509-1517.
3. Virtanen KA, Lidell ME, Orava J, Heglind M, Westergren R, Niemi T, Taittonen M, et al. Functional brown adipose tissue in healthy adults. *N Engl J Med.* 2009;**360**(15):1518-1525.

**1**

4. Virtanen KA. The rediscovery of BAT in adult humans using imaging. *Best Pract Res Clin Endocrinol Metab.* 2016;**30**(4):471-477.

5. Ouellet V, Routhier-Labadie A, Bellemare W, Lakhal-Chaieb L, Turcotte E, Carpentier AC, Richard D. Outdoor temperature, age, sex, body mass index, and diabetic status determine the prevalence, mass, and glucose-uptake activity of 18F-FDG-detected BAT in humans. *J Clin Endocrinol Metab.* 2011;**96**(1):192-199.

6. Rodriguez AM, Quevedo-Coli S, Roca P, Palou A. Sex-dependent dietary obesity, induction of UCPs, and leptin expression in rat adipose tissues. *Obes Res.* 2001;**9**(9):579-588.

7. Law J, Bloor I, Budge H, Symonds ME. The influence of sex steroids on adipose tissue growth and function. *Horm Mol Biol Clin Investig.* 2014;**19**(1):13-24.

8. Sund-Levander M, Forsberg C, Wahren LK. Normal oral, rectal, tympanic and axillary body temperature in adult men and women: a systematic literature review. *Scand J Caring Sci.* 2002;**16**(2):122-128.

9. Tansey EA, Johnson CD. Recent advances in thermoregulation. *Adv Physiol Educ.* 2015;**39**(3):139-148.

10. Kuht J, Farmery AD. Body temperature and its regulation. *Anaesthesia & Intensive Care Medicine.* 2014;**15**(6):273-278.

11. Morrison SF, Nakamura K. Central Mechanisms for Thermoregulation. *Annu Rev Physiol.* 2019;**81**:285-308.

12. Voets T, Droogmans G, Wissenbach U, Janssens A, Flockerzi V, Nilius B. The principle of temperature-dependent gating in cold- and heat-sensitive TRP channels. *Nature.* 2004;**430**(7001):748-754.

13. Tan CH, McNaughton PA. The TRPM2 ion channel is required for sensitivity to warmth. *Nature.* 2016;**536**(7617):460-463.

14. Nakamura K, Morrison SF. A thermosensory pathway mediating heat-defense responses. *Proc Natl Acad Sci U S A.* 2010;**107**(19):8848-8853.

15. Cardinali DP. Third Level: The Hypothalamus. *Autonomic Nervous System.* Cham: Springer; 2018:175-244.

16. Blondin DP, Labbe SM, Phoenix S, Guerin B, Turcotte EE, Richard D, Carpentier AC, Haman F. Contributions of white and brown adipose tissues and skeletal muscles to acute cold-induced metabolic responses in healthy men. *J Physiol.* 2015;**593**(3):701-714.

17. Blondin DP, Labbe SM, Tingelstad HC, Noll C, Kunach M, Phoenix S, Guerin B, et al. Increased brown adipose tissue oxidative capacity in cold-acclimated humans. *J Clin Endocrinol Metab.* 2014;**99**(3):E438-446.

18. Kalinovich AV, de Jong JM, Cannon B, Nedergaard J. UCP1 in adipose tissues: two steps to full browning. *Biochimie.* 2017;**134**:127-137.

19. Labbe SM, Caron A, Bakan I, Laplante M, Carpentier AC, Lecomte R, Richard D. In vivo measurement of energy substrate contribution to cold-induced brown adipose tissue thermogenesis. *FASEB J.* 2015;**29**(5):2046-2058.

20. Johnson JM, Minson CT, Kellogg DL, Jr. Cutaneous vasodilator and vasoconstrictor mechanisms in temperature regulation. *Compr Physiol.* 2014;**4**(1):33-89.

21. Werner J. System properties, feedback control and effector coordination of human temperature regulation. *Eur J Appl Physiol.* 2010;**109**(1):13-25.

22. Frank SM, Raja SN, Bulcao CF, Goldstein DS. Relative contribution of core and cutaneous temperatures to thermal comfort and autonomic responses in humans. *J Appl Physiol (1985).* 1999;**86**(5):1588-1593.

23. Terrien J, Perret M, Aujard F. Behavioral thermoregulation in mammals: a review. *Front Biosci (Landmark Ed).* 2011;**16**:1428-1444.

24. Kattapong KR, Fogg LF, Eastman CI. Effect of Sex, Menstrual Cycle Phase, and Oral Contraceptive Use on Circadian Temperature Rhythms. *Chronobiol Int.* 1995;**12**(4):257-266.

25. Baker FC, Waner JI, Vieira EF, Taylor SR, Driver HS, Mitchell D. Sleep and 24 hour body temperatures: a comparison in young men, naturally cycling women and women taking hormonal contraceptives. *J Physiol.* 2001;**530**(Pt 3):565-574.

26. Sanchez-Alavez M, Alboni S, Conti B. Sex- and age-specific differences in core body temperature of C57Bl/6 mice. *Age (Dordr).* 2011;**33**(1):89-99.

27. Nakayama T, Suzuki M, Ishizuka N. Action of progesterone on preoptic thermosensitive neurones. *Nature.* 1975;**258**(5530):80.

28. Hessemer V, Bruck K. Influence of menstrual cycle on shivering, skin blood flow, and sweating responses measured at night. *J Appl Physiol (1985).* 1985;**59**(6):1902-1910.

29. Stachenfeld NS, Silva C, Keefe DL. Estrogen modifies the temperature effects of progesterone. *J Appl Physiol (1985).* 2000;**88**(5):1643-1649.

30. Anderson GS. Human morphology and temperature regulation. *Int J Biometeorol.* 1999;**43**(3):99-109.

31. Castellani JW, Young AJ. Human physiological responses to cold exposure: Acute responses and acclimatization to prolonged exposure. *Auton Neurosci.* 2016;**196**:63-74.

32. MacAuley D. Exercise physiology: Gender and performance. *Oxford Handbook of Sport and Exercise Medicine.* 2nd ed. Oxford: Oxford University Press; 2012:164-165.

33. Notley SR, Park J, Tagami K, Ohnishi N, Taylor NAS. Variations in body morphology explain sex differences in thermoeffector function during compensable heat stress. *Exp Physiol.* 2017;**102**(5):545-562.

34. Lopez M, Sessler DI, Walter K, Emerick T, Ozaki M. Rate and gender dependence of the sweating, vasoconstriction, and shivering thresholds in humans. *Anesthesiology.* 1994;**80**(4):780-788.

35. Guo X, Razandi M, Pedram A, Kassab G, Levin ER. Estrogen induces vascular wall dilation: mediation through kinase signaling to nitric oxide and estrogen receptors alpha and beta. *J Biol Chem.* 2005;**280**(20):19704-19710.

36. Salerni S, Di Francescomarino S, Cadeddu C, Acquistapace F, Maffei S, Gallina S. The different role of sex hormones on female cardiovascular physiology and function: not only oestrogens. *Eur J Clin Invest.* 2015;**45**(6):634-645.

37. Iliescu R, Reckelhoff JF. Testosterone and vascular reactivity. *Clin Sci (Lond).* 2006;**111**(4):251-252.

38. Inoue Y, Ichinose-Kuwahara T, Funaki C, Ueda H, Tochihara Y, Kondo N. Sex differences in acetylcholine-induced sweating responses due to physical training. *J Physiol Anthropol.* 2014;**33**:13.

39. Gagnon D, Crandall CG, Kenny GP. Sex differences in postsynaptic sweating and cutaneous vasodilation. *J Appl Physiol (1985).* 2013;**114**(3):394-401.

40. Rodriguez-Cuenca S, Pujol E, Justo R, Frontera M, Oliver J, Gianotti M, Roca P. Sex-dependent thermogenesis, differences in mitochondrial morphology and function, and adrenergic response in brown adipose tissue. *J Biol Chem.* 2002;**277**(45):42958-42963.

41. Quarta C, Mazza R, Pasquali R, Pagotto U. Role of sex hormones in modulation of brown adipose tissue activity. *J Mol Endocrinol.* 2012;**49**(1):R1-7.

42. Monjo M, Rodriguez AM, Palou A, Roca P. Direct effects of testosterone, 17 beta-estradiol, and progesterone on adrenergic regulation in cultured brown adipocytes: potential mechanism for gender-dependent thermogenesis. *Endocrinology.* 2003;**144**(11):4923-4930.

43. Martinez de Morentin PB, Gonzalez-Garcia I, Martins L, Lage R, Fernandez-Mallo D, Martinez-Sanchez N, Ruiz-Pino F, et al. Estradiol regulates brown adipose tissue thermogenesis via hypothalamic AMPK. *Cell Metab.* 2014;**20**(1):41-53.

44. Contreras C, Gonzalez F, Ferno J, Dieguez C, Rahmouni K, Nogueiras R, Lopez M. The brain and brown fat. *Ann Med.* 2015;**47**(2):150-168.

45. Xu Y, Nedungadi TP, Zhu L, Sobhani N, Irani BG, Davis KE, Zhang X, et al. Distinct hypothalamic neurons mediate estrogenic effects on energy homeostasis and reproduction. *Cell Metab.* 2011;**14**(4):453-465.

46. Karjalainen S. Gender differences in thermal comfort and use of thermostats in everyday thermal environments. *Build Environ.* 2007;**42**(4):1594-1603.

47. Kim J, de Dear R, Candido C, Zhang H, Arens E. Gender differences in office occupant perception of indoor environmental quality (IEQ). *Build Environ.* 2013;**70**:245-256.

48. Maykot JK, Rupp RF, Ghisi E. Assessment of gender on requirements for thermal comfort in office buildings located in the Brazilian humid subtropical climate. *Energy Build.* 2018;**158**:1170-1183.

49. Schweiker M, Huebner GM, Kingma BRM, Kramer R, Pallubinsky H. Drivers of diversity in human thermal perception - A review for holistic comfort models. *Temperature (Austin).* 2018;**5**(4):308-342.

50. Wang Z, de Dear R, Luo M, Lin B, He Y, Ghahramani A, Zhu Y. Individual difference in thermal comfort: A literature review. *Build Environ.* 2018;**138**:181-193.

51. Fato I, Martellotta F, Chiancarella C. Thermal comfort in the climatic conditions of Southern Italy. *ASHRAE Transactions.* 2004;**110**(2):578-593.

52. Gaskill BN, Rohr SA, Pajor EA, Lucas JR, Garner JP. Some like it hot: Mouse temperature preferences in laboratory housing. *Appl Anim Behav Sci.* 2009;**116**(2-4):279-285.

53. Gaskill BN, Rohr SA, Pajor EA, Lucas JR, Garner JP. Working with what you've got: Changes in thermal preference and behavior in mice with or without nesting material. *J Therm Biol.* 2011;**36**(3):193-199.

54. Kondrats'kyi AP, Kondrats'ka KO, Skryma R, Prevars'ka N, Shuba Ia M. [Gender differences in cold sensitivity: role of hormonal regulation of TRPM8 channel]. *Fiziol Zh.* 2009;**55**(4):91-99.
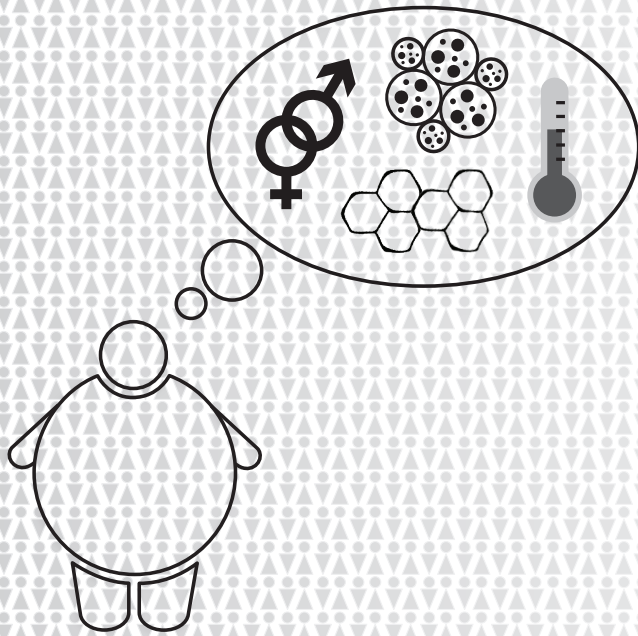
# Chapter 1C

## General Introduction

**Aims and Outline of this Thesis**

1

**1**

Males and females display differences in adipose tissue distribution and function, as well as in thermoregulation, as reviewed in **Chapters 1A** and **1B**. Yet, the mechanisms that underlie this sex dimorphism are not completely understood. So far, most human and rodent studies have studied the role of the sex steroids estrogens and androgens in adipocyte metabolism, proliferation, and function. However, little is known whether other factors, such as glucocorticoids and sensory input, contribute to sex differences in white adipose tissue (WAT) and brown adipose tissue (BAT) function and whether these factors modulate the actions of sex steroids on adipose tissue.

This thesis therefore aims to investigate intrinsic and glucocorticoid-induced sex differences in adipose tissue function. In addition, this thesis aims to unravel the role of sex hormones in thermal perception, as this might be an important factor in controlling sex differences in BAT activity.

**Chapter 2** presents a study on the effects of treatment with high-dose corticosterone (the endogenous rodent glucocorticoid) on whole-body glucose metabolism and adipose tissue adaptation in male and female mice. WAT and BAT are studied by morphological, molecular, and functional approaches. One of the aims of this study was to investigate whether biological sex modulates the adverse metabolic consequences caused by the intensive glucocorticoid treatment.

**Chapter 3** focuses on sex differences in mouse BAT transcriptome with the aim to identify molecular mechanisms that contribute to sex differences in BAT morphology and activity. In addition, the effects of the less studied female sex hormone progesterone on cultured adipocytes were analyzed to gain insight into its regulatory role in BAT activity.

**Chapter 4** demonstrates another aspect of BAT regulation, namely a sensory input for BAT activation. Because exposure to cold (an ambient temperature lower than the thermoneutral zone) is a major driver of BAT thermogenesis for maintaining an optimal body temperature, this study explored whether the thermal preference between young adult male and female mice differs. Since sex hormones are important physiological regulators of the temperature set point in the central nervous system, gonadectomy was performed to study the role of sex steroids herein.

**Chapter 5** is a translational and confirmatory study on the thermal preference in young adult men and women. In this study, the water-filled cooling blanket was used as a body-cooling instrument since this is a common method for studying BAT activity. The temperature at which participants started shivering,

was used as the primary outcome since this is a sensitive and quantitative assessment for evaluating cold perception threshold in humans.

**Chapter 6** provides a general discussion about the findings of the studies presented in this thesis and incorporates some recent updates on interactions between sex and stress hormones influencing adipose tissue function. Finally, conclusions and some future perspectives are provided.

**1**
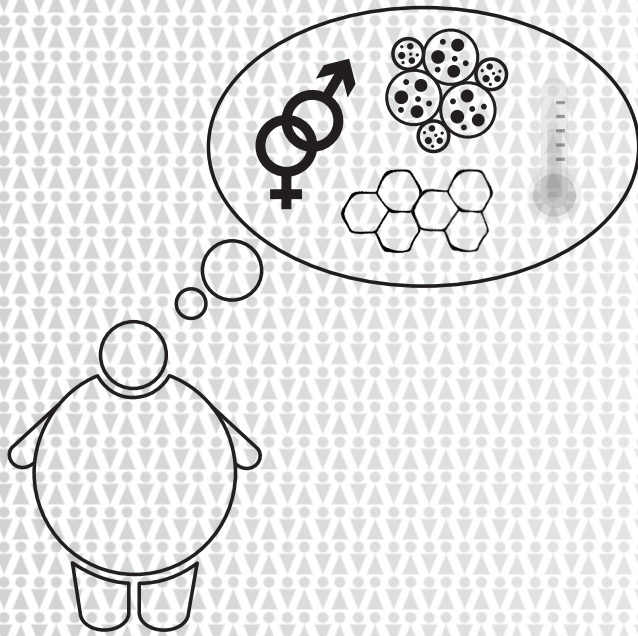
# Chapter 2

# Sex Difference in Corticosterone-Induced Insulin Resistance in Mice

Kasiphak Kaikaew[1,2], Jacobie Steenbergen[1], Theo H. van Dijk[3], Aldo Grefhorst[1,4], Jenny A. Visser[1]

1  Department of Internal Medicine, Erasmus MC, University Medical Center Rotterdam, Rotterdam, the Netherlands

2  Department of Physiology, Faculty of Medicine, Chulalongkorn University, Bangkok, Thailand

3  Department of Laboratory Medicine, University Medical Center Groningen, Groningen, the Netherlands

4  Department of Experimental Vascular Medicine, Amsterdam University Medical Centers, Location AMC, Amsterdam, the Netherlands

2

**2**

## Abstract

Prolonged exposure to glucocorticoids (GCs) causes various metabolic derangements. These include obesity and insulin resistance, as inhibiting glucose utilization in adipose tissues is a major function of GCs. Although adipose tissue distribution and glucose homeostasis are sex-dependently regulated, it has not been evaluated whether GCs affect glucose metabolism and adipose tissue functions in a sex-dependent manner. In this study, high-dose corticosterone (rodent GC) treatment in C57BL/6J mice resulted in nonfasting hyperglycemia in male mice only, whereas both sexes displayed hyperinsulinemia with normal fasting glucose levels, indicative for insulin resistance. Metabolic testing using stable isotope-labeled glucose techniques revealed a sex-specific corticosterone-driven glucose intolerance. Corticosterone treatment increased adipose tissue mass in both sexes, which was reflected by elevated serum leptin levels. However, female mice showed more metabolically protective adaptations of adipose tissues than did male mice, demonstrated by higher serum total and high-molecular-weight adiponectin levels, more hyperplastic morphological changes, and a stronger increase in mRNA expression of adipogenic differentiation markers. Subsequently, *in vitro* studies in 3T3-L1 (white) and T37i (brown) adipocytes suggest that the increased leptin and adiponectin levels were mainly driven by the elevated insulin levels. In summary, this study demonstrates that GC-induced insulin resistance is more severe in male mice than in female mice, which can be partially explained by a sex-dependent adaptation of adipose tissues.

**2**

## Introduction

Glucocorticoids (GCs) are steroid hormones produced by the adrenal gland. External stressors such as infection, trauma, food deprivation, and physical or psychological stress enhance the activity of the hypothalamic-pituitary-adrenal (HPA) axis and trigger the adrenal gland to secrete an endogenous GC: cortisol for humans or corticosterone for rodents (1).

Exogenous synthetic GCs are widely prescribed for a number of autoimmune diseases and allergic reactions due to their immunosuppressive properties (2). However, prolonged exposure to elevated endogenous GCs, such as in Cushing syndrome, or to exogenous GCs leads to various metabolic derangements, such as progressive weight gain, truncal obesity due to expansion of the visceral white adipose tissue (WAT), loss of subcutaneous WAT mass, and development of insulin resistance that might result in diabetes mellitus (2-5). These effects are largely attributable to the role of GC in the control of glucose homeostasis, as they promote hepatic glucose production (gluconeogenesis) and inhibit glucose utilization in WAT and skeletal muscles (1,4).

The HPA axis is controlled in a sexually dimorphic manner: female rodents have higher basal and stress-induced corticosterone levels with a less robust negative feedback on the HPA axis than do males (6,7). The fact that the concentrations of corticosteroid-binding globulin, the glycoprotein that binds 80% of circulating corticosterone, are higher in females than in males likely contributes to this sex difference (6,8). Sex steroid hormones are also involved in the sex-dependent control of the HPA axis (6,7). In adult male rats, castration and estradiol treatment increase responsiveness of the HPA axis to external stressors whereas ovariectomy and androgen replacement in female rats decrease this response (7).

Intriguingly, adipose tissue distribution and function show many sex-dependent characteristics as well. Concerning WAT distribution, females have relatively more subcutaneous WAT and less visceral WAT than do males (9,10). Females also have a relatively higher activity of the metabolically active brown adipose tissue (BAT) and have more brown-like adipocytes in their WAT depots (11,12). Furthermore, glucose metabolism has been shown to differ between males and females, with female mice being more insulin sensitive and glucose tolerant than male mice (13).

Despite these sex differences in HPA axis regulation, adipose tissue distribution, and glucose homeostasis, high-dose GC- or stress-induced adverse effects have only been studied in male rodents (14,15). Whether the metabolic consequences of exposure to high-dose GC differ between males and females is still unknown. To address this knowledge gap, we have studied the effects of

**2**

2-week high-dose corticosterone on whole-body glucose metabolism and adipose tissue function in both male and female C57BL/6J mice.

## Materials and Methods

### Animals, housing conditions, and corticosterone treatment

Eight-week-old C57BL/6J mice (24 males and 24 females) were obtained from Charles River Laboratories (Maastricht, Netherlands). Upon arrival, mice were group housed (three mice per cage) at room temperature (RT; ~22°C) on a 12-hour light/12-hour dark cycle (lights on at 8:00 AM). Chow food pellets (801722 CRM (P), Special Diets Services, Essex, UK) and water were available *ad libitum*. We provided tissue papers (Tork extra soft facial tissue, SCA Hygiene Products, Zeist, Netherlands) as nesting material and woodchips (Lignocel BK 8/15, J. Rettenmaier & Söhne GmbH, Rosenberg, Germany) as bedding material. All experimental procedures were approved by the Animal Ethics Committee at Erasmus MC, Rotterdam, Netherlands.

After 10 to 14 days of acclimatization, a corticosterone pellet [50 mg of corticosterone (Sigma-Aldrich, Zwijndrecht, Netherlands) and 50 mg of cholesterol] or a vehicle pellet (100 mg cholesterol) was implanted subcutaneously at the dorsal region of the neck under isoflurane (Teva Pharmachemie, Haarlem, Netherlands) anesthesia and carprofen (Rimadyl Cattle, Pfizer, Pfizer Animal Health, Capelle aan den IJssel, Netherlands) analgesia. Subsequently, mice were single housed and enrolled in experiment 1 or 2.

### Experiment 1: nonfasting glucose monitoring and endpoint blood and tissue collection

For experiment 1, mice were weighed on day 0 (before pellet implantation) and on days 3, 5, 7, 10, and 12 after pellet implantation at 1:00 PM. At the same time, their nonfasting blood glucose (NFBG) level was determined by tail-tip bleeding using a glucometer and test strips (FreeStyle Freedom Lite, Abbott, Hoofddorp, Netherlands). On day 12, we weighed the food pellets and transferred the mice to a new cage with similar conditions. On day 14 at 8:00 AM, the mice and food pellets were weighed again, the NFBG was measured, and the bedding material was collected for further processing. Next, we transferred the mice to clean cages with similar conditions except for the presence of food pellets. At 1:00 PM (after 5 hours of fasting), the fasting blood glucose (FBG) level was determined and the mice were euthanized by cardiac puncture under isoflurane anesthesia. Thymus involution was confirmed in the corticosterone-treated mice. Blood was stored immediately at 4°C and various tissues (*e.g.*, BAT, WATs,

quadriceps femoris muscle, and liver) were dissected, weighed, and snap-frozen in liquid nitrogen or fixed in 4% paraformaldehyde (PFA) in PBS at RT. The inguinal (also known as posterior subcutaneous) WAT (iWAT) and gonadal WAT (gWAT) depots were cut in half. One half of iWAT was snap-frozen; one half of gWAT was further divided and snap-frozen or fixed as described above. The other half of iWAT and gWAT was washed in PBS and preincubated in DMEM/F12 medium (catalog no. 21331020, Gibco, Life Technologies Europe, Bleiswijk, Netherlands) with 2% fatty acid–free BSA (FF-BSA; catalog no. 03117057001, Roche Diagnostics, Mannheim, Germany) at RT for subsequent *ex vivo* stimulation.

Serum (obtained after an overnight clotting at 4°C) and snap-frozen tissues were stored at −80°C until analyses. After 24-hour fixation in PFA at RT, tissues were stored in 70% ethanol until histological analysis. Feces was collected from the bedding material, air-dried, weighed, crushed, and extracted with ethanol for fecal corticosterone measurement, as described previously (16).

### Experiment 2: intraperitoneal glucose tolerance test

For experiment 2, mice were weighed and their NFBG was determined on days 0 (before pellet implantation), 7, and 14 at 8:00 AM. Next, food pellets were removed and the mice were fasted until 1:00 PM when their FBG was determined and one blood spot (~6 µL) was collected on filter paper (TFN 180 g/m$^2$, Sartorius Stedim Biotech, Göttingen, Germany) for fasting blood insulin (FBI) measurement. Additionally, on day 14 mice were subjected to an intraperitoneal glucose tolerance test (IPGTT). For this, the mice received an IP injection of 2 g/kg glucose [20% glucose solution, which contains 95% D-(+)-glucose (Sigma-Aldrich) and 5% [U-$^{13}$C$_6$]-D-glucose (Cambridge Isotope Laboratories, Andover, MA)]. Blood glucose levels were determined and two blood spots (~3 µL for glucose kinetic analysis and ~6 µL for insulin measurement) were collected on filter paper at 5, 15, 30, 45, 75, and 120 minutes after glucose injection. After the experiment, mice were euthanized by cervical dislocation under isoflurane anesthesia. Blood spots were air-dried for 2 hours and stored at −20°C (for insulin measurement) or at RT (for glucose extraction).

### Insulin stimulation of WAT explants

Pieces of iWAT and gWAT preincubated with 2% FF-BSA in DMEM/F12 (from experiment 1) were cut into small pieces of ~20 mg and incubated in DMEM/F12 medium containing 2% FF-BSA (Roche Diagnostics) with or without 1 µM insulin (Sigma-Aldrich) at 37°C in a humidified incubator with 5% CO$_2$ for 2 hours (refreshed once with fresh solution after 1 hour of incubation).

**2**

Subsequently, tissues were washed twice in cold PBS and stored at −80°C until protein extraction.

### Adipose tissue histology and adipocyte size quantification

PFA-fixed gWAT, anterior subcutaneous (also known as axillary) WAT (aWAT), and BAT were embedded in paraffin. After manually sectioned with a microtome, 8-µm-thick WAT and 5-µm-thick BAT sections were mounted on glass slides and stained with hematoxylin and eosin.

Representative photos from three random sections of gWAT and aWAT from each animal were taken with a digital imaging system (Nikon Eclipse E400 and Nikon Digital Sight DS-L1, Nikon Corporation, Tokyo, Japan). To quantify adipocyte size, we used an automated mode of Adiposoft, a plug-in of Fiji (advanced distribution of ImageJ) software for accurately analyzing number and size of adipocytes (17).

### Circulating hormone and adipokine quantification by ELISA

Serum and fecal concentrations of hormones and adipokines of the mice from experiment 1 were determined according to the manufacturers' protocols. Serum total and high-molecular-weight (HMW) adiponectin levels were measured with a mouse HMW and total adiponectin ELISA kit (18). Serum leptin was measured with a mouse/rat leptin ELISA kit (19). Serum and fecal corticosterone levels were determined with a corticosterone ELISA kit (20).

The insulin concentrations in the blood spots collected in experiment 2 were determined as previously described (21) using a rat insulin ELISA kit (22) with the Mouse Insulin Standard (90020, Crystal Chem, Zaandam, Netherlands). In brief, a completely filled blood spot on filter papers (6-mm diameter) was punched out and eluted in guinea pig anti-insulin in sample diluent overnight at 4°C, followed by the standard procedure of the ELISA kit.

### Derivatization and gas chromatography–mass spectrometry measurements of glucose

Extraction of glucose from the filter paper blood spots, derivatization of the extracted glucose, and gas chromatography–mass spectrometry (GC-MS) measurements of the glucose derivatives were done according to the analytical procedure described before (23). In short, a disk was punched out of the blood spots, glucose was extracted from the disk by incubating it in ethanol/water (10:1 v/v), and glucose was derivatized to its pentaacetate ester. Samples were analyzed by GC-MS (Agilent 5975C inert MSD, Agilent Technologies, Amstelveen,
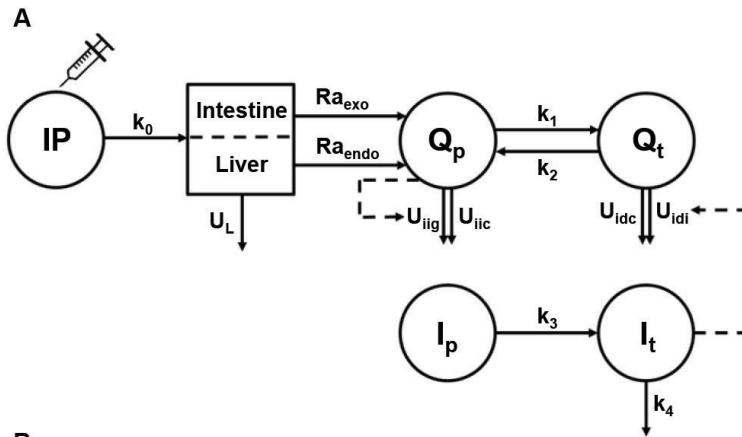
Netherlands) with separation of derivatives on 30-m × 0.25-mm interior diameter (0.25-µm film thickness) capillary columns (ZB-1701, Phenomenex, Utrecht, Netherlands) and with positive-ion chemical ionization with methane. Measured by GC-MS, the fractional isotopomer distribution ($M_0$ to $M_6$) was corrected for the fractional distribution due to natural abundance of $^{13}C$ by multiple linear regression as described by Lee *et al.* (24), to obtain the excess fractional distribution of mass isotopomers ($M_0$ to $M_6$) due to the dilution of administrated [U-$^{13}C_6$]-D-glucose; that is, $M_6$ represents the fractional contribution of the administered tracer and was used in the calculations of blood glucose kinetics.

**Calculation of blood glucose metabolism**

Tracer concentrations were calculated as the product of the blood glucose concentration and the fractional contribution of the tracer at that time point (t): [$^{13}C_6$-glucose]$_t$ = ($M_6$)$_t$·[glucose]$_t$. To determine the effects of the IPGTT on glucose metabolism in mice, we used an adapted minimal model for glucose metabolism after an oral glucose tolerance test (25). This adapted model is presented in **Fig. 1A** and was used in SAAM II software (version 2.3, The Epsilon Group, Charlottesville, VA). To generate sufficient input data for this model, measured data of blood glucose, blood insulin, and tracer concentrations were fitted to the following formula to calculate the concentration (C) of these metabolites at multiple time points (t): $C_t = C_b + C_{(1)_0} \cdot e^{-k_{(1)}t} + C_{(2)_0} \cdot e^{-k_{(2)}t} - C_{(3)_0} \cdot e^{-k_{(3)}t}$, where b indicates the basal value and 0 indicates the estimated value at time point 0. The bioavailability (F) of the bolus was estimated from the tracer curve as follows:

$$F = 1 - \left[ \frac{C_{(3)_0} k_{(1)} k_{(2)}}{C_{(1)_0} k_{(2)} k_{(3)} + C_{(2)_0} k_{(1)} k_{(3)}} \right].$$

The glucose kinetic parameters were calculated using the compartmental model and the relevant equations (26-28), as presented in **Fig. 1**. In this model, $k_1$ and $k_2$ are rate constants for the glucose flux from the accessible plasma pool to the inaccessible tissue pool and *vice versa*, whereas $k_3$ is the rate constant for the insulin flux from the accessible plasma pool to the inaccessible tissue pool, and they are different from the rate constants $k_{(1)}$, $k_{(2)}$, and $k_{(3)}$ used to describe the plasma glucose vs time curve above. We adapted the volume of the accessible glucose pool from literature; that is, 150 mL/kg was suggested by Tissot *et al.* (29) and Gastaldelli *et al.* (30) for humans. The insulin-independent glucose utilization was set to three times the insulin-dependent glucose utilization under basal conditions as was also used for humans (31,32). Furthermore, under basal conditions the independent utilization flux was estimated at 45% of the endogenous glucose production (EGP). The fractional turnover rates ($k_0$ through $k_4$) were estimated within the model.

**2**



**Fig. 1** Compartmental model and formulas used for calculating blood glucose kinetics

**(A)** Kinetic model used to calculate the kinetic parameters of glucose metabolism upon an IPGTT in mice. Upon injection into the IP compartment, the injected glucose passes the liver to contribute to the accessible plasma glucose pool ($Q_p$) and to the inaccessible tissue glucose pool ($Q_t$). Additionally, glucose produced/released by tissues such as the intestine and liver also contribute to $Q_p$. As such, two rates of appearances can be distinguished, namely that of exogenous injected glucose ($Ra_{exo}$) and of endogenous glucose ($Ra_{endo}$). The $Q_p$ is in equilibrium with $Q_t$ via two rate constants ($k_1$ and $k_2$). Disposal of glucose (U) from the $Q_p$ can be divided in insulin-independent glucose-dependent disposal ($U_{iig}$) and insulin-independent constant disposal ($U_{iic}$). Disposal from the $Q_t$ is the sum of insulin-dependent constant disposal ($U_{idc}$) and insulin-dependent disposal ($U_{idi}$). As with glucose, this model also presumes two compartments for insulin, namely the accessible plasma insulin pool ($I_p$) and the inaccessible tissue insulin pool ($I_t$). **(B)** The formulas for assessing glucose metabolism indexes and kinetic parameters. HOMA-IR, an acceptable surrogate index for insulin resistance when applying a mouse-specific constant (26,27), was calculated relative to a median of the vehicle-treated male mice. β-Cell response was estimated as changes in plasma insulin levels relative to changes in glucose levels (28). Subscript b refers to a basal level, subscript 0 refers to an estimated value at time point 0, and $V_g$ indicates the volume of the accessible pool.

**2**

### *In vitro* adipocyte culture

The white preadipocyte cell line 3T3-L1 (33) and the brown preadipocyte cell line T37i [(34); a gift provided by Dr. M. Lombès, Inserm U1185, France] were used to study direct effects of corticosterone and/or insulin on adipocytes. 3T3-L1 preadipocytes were cultured with basal medium [3T3-BM: DMEM 4.5 g/L glucose with L-glutamine and 25 mM HEPES (21063029, Gibco) supplemented with 10% fetal bovine serum (FBS; Gibco) and 100 IU/mL penicillin/100 µg/mL streptomycin (P/S; Gibco)]. Two days after reaching full confluence (differentiation day 0), 3T3-L1 cells were differentiated with differentiation medium 1: 3T3-BM containing 0.5 mM 3-isobutyl-1-methylxanthine, 0.25 µM dexamethasone and 1 µg/mL insulin (all from Sigma-Aldrich). Starting from day 4, cells were maintained in differentiation medium 2 (3T3-BM containing 1 µg/mL insulin) that was refreshed every 2 to 3 days until full differentiation on day 12. T37i preadipocytes were cultured with basal medium [T37i-BM: DMEM/F12 with L-glutamine (21041025, Gibco) supplemented with 10% FBS, P/S, and 20 mM HEPES (Gibco)]. Two days after reaching full confluence (differentiation day 0), T37i cells were differentiated by adding 2 nM triiodothyronine and 20 nM insulin (both from Sigma-Aldrich) to T37i-BM. This medium was refreshed every 2 to 3 days until full differentiation on day 9.

Before corticosterone and insulin stimulation, the differentiating cells were steroid-starved for 24 hours by replacing FBS with dextran-coated charcoal-treated FBS [prepared by incubating 100 mL of FBS twice with 0.1 g of dextran T250 (Pharmacia, Uppsala, Sweden) and 1 g of activated charcoal (C5510, Sigma-Aldrich) for 30 minutes, centrifuged, and sterile-filtered]. Three hours before stimulation, the differentiated cells were starved in starvation medium: DMEM (for 3T3-L1) or DMEM/F12 with 20 mM HEPES (for T37i) supplemented with P/S and 0.2% dextran-coated charcoal-treated FBS. Subsequently, the cells were stimulated for 24 hours in starvation medium containing 1 µL/mL ethanol vehicle control, 1 µM corticosterone, 0.2 µM insulin, or 1 µM corticosterone and 0.2 µM insulin (both from Sigma-Aldrich). After stimulation, the cells were used to determine their glucose uptake or immediately stored at −80°C until RNA isolation or protein extraction. In the latter case, cultured media were also collected, centrifuged, and stored at −20°C for adipokine measurement by ELISA.

### Radioactive glucose uptake

For the glucose uptake studies, the 24-hour corticosterone- and/or insulin-treated cells were washed with PBS and stimulated with 0, 20, or 100 nM insulin in 0.1% FF-BSA (03117057001, Roche Diagnostics) in PBS for 15 minutes. Next, 0.05 µCi of 2-[1-^{14}C]-deoxy-D-glucose (PerkinElmer, Waltham,

**2**

MA) in 0.1% FF-BSA was added to the medium. After an additional 5-minute incubation, the cells were washed twice with cold PBS, lysed with 0.2% SDS solution (Merck, Hohenbrunn, Germany), and protein content in cell lysates was quantified using Advanced protein assay reagent (Cytoskeleton, Denver, CO). Cell lysates were transferred to a scintillation glass vial and homogenized in a scintillation cocktail (Optiphase Hisafe 3, PerkinElmer Health Sciences, Groningen, Netherlands). Radioactivity was detected with a liquid scintillation analyzer (Tri-Carb 2910TR, Packard, PerkinElmer) and reported in counts per minute normalized to protein content.

### Gene expression analysis

RNA was isolated from mouse tissues and cultured cells using the TriPure Isolation Reagent (Roche Diagnostics) according to manufacturer's instructions. Contaminating genomic DNA was removed using RQ1 RNase-Free DNase (Promega Corporation, Madison, WI). Purified RNA was quantified with a NanoDrop 8000 Spectrophotometer (Thermo Fisher Scientific, Wilmington, DE). Reverse transcription was performed using the Transcriptor high-fidelity cDNA synthesis kit (Roche Diagnostics). Quantitative PCR was performed using FastStart Universal SYBR Green Master (Rox) (Roche Diagnostics) with a QuantStudio 7 flex real-time PCR system (Applied Biosystems, Life Technologies, Carlsbad, CA). Expression of the tested genes was normalized to the indicated housekeeping genes using the $2^{-\Delta\Delta CT}$ method. Sequences of the primers for all genes are listed in **Table 1**.

### Protein extraction

Protein was extracted from the insulin-stimulated WAT explants by mincing the tissues with a micropestle in lysis buffer containing 50 mM HEPES, 150 mM NaCl, 10 mM EDTA, 2 mM $Na_3VO_4$, 20 mM NaF, 1% Triton X-100, phosphatase inhibitor (P5726, Sigma-Aldrich), and protease inhibitor (cOmplete, Roche Diagnostics). After centrifugation to remove debris, lysates were collected. For the cultured adipocytes, cells were lysed in the aforementioned lysis buffer and sonicated for 10 seconds. Protein concentrations were quantified relatively to BSA (Sigma-Aldrich) using the Advanced protein assay reagent (Cytoskeleton).

### Western blot analysis

Protein extracts were diluted in Laemmli sample buffer (Bio-Rad Laboratories, Veenendaal, Netherlands) with 50 mM dithiothreitol and denatured at 95°C for 5 minutes. A total of 15 µg of protein was electrophoresed on an

8% acrylamide gel and blotted onto a nitrocellulose membrane. Membranes were blocked in 3% skim milk powder in PBS for 1 hour at RT and incubated overnight at 4°C with an Akt antibody [1:1,000 (35)] or a phosphorylated Akt (Ser473) antibody [1:2,000 (36)] in PBS containing 0.1% Tween 20 and 5% BSA. Next, membranes were washed and incubated for 1 hour at RT with an IRDye 800CW goat anti-rabbit secondary antibody [1:10,000 (37)] in PBS containing 0.1% Tween 20 and 3% skim milk powder. The Akt and phosphorylated Akt immunoreactivities were detected with an Odyssey infrared imaging system (LI-COR, Biotechnology, Bad Homburg, Germany) and were quantified using Image Studio Lite software (version 5.2, LI-COR).

**Table 1** Primer Sequences

| Gene | Forward (5′→3′) | Reverse (5′→3′) |
|------|------------------|------------------|
| *Adamts1* | TGCTCCAAGACATGCGGCTCAG | TGGTACTGGCTGGCTTCACTTCC |
| *Adipoq* | GCACTGGCAAGTTCTACTGCAA | GTAGGTGAAGAGAACGGCCTTGT |
| *Cebpb* | ACGACTTCCTCTCCGACCTCT | CGAGGCTCACGTAACCGTAGT |
| *Chrebpb* | TCTGCAGATCGCGTGGAG | CTTGTCCCGGCATAGCAAC |
| *Fkbp5* | ATTTGATTGCCGAGATGTG | TCTTCACCAGGGCTTTGTC |
| *Foxo1* | CTTCAAGGATAAGGGCGACA | GACAGATTGTGGCGAATTGA |
| *Irs1* | CGATGGCTTCTCAGACGTG | CAGCCCGCTTGTTGATGTTG |
| *Irs2* | GTGGGTTTCCAGAACGGCCT | ATGGGGCTGGTAGCGCTTCA |
| *Klf15* | GCGAGAAGCCCTTTGCCT | GCTTCACACCCGAGTGAGAT |
| *Lep* | ACCCCATTCTGAGTTTGTCC | TCCAGGTCATTGGCTATCTG |
| *Nr3c1* | CCGGGTCCCCAGGTAAAGA | TGTCCGGTAAAATAAGAGGCTTG |
| *Nr3c2* | ATGGAAACCACACGGTGACCT | AGCCTCATCTCCACACACCAAG |
| *Pck1* | ATGTGTGGGCGATGACATT | AACCCGTTTTCTGGGTTGAT |
| *Pcx* | GGGATGCCCACCAGTCACT | CATAGGGCGCAATCTTTTTGA |
| *Pparg* | GAAAGACAACGGACAAATCACC | GGGGGTGATATGTTTGAACTTG |
| *Slc2a1* | GACCCTGCACCTCATTGG | GATGCTCAGATAGGACATCCAAG |
| *Slc2a2* | CCAGTACATTGCGGACTTCCTT | CTTTCCTTTGGTTTCTGGAACTTT |
| *Slc2a4* | GTGACTGGAACACTGGTCCTA | CCAGCCACGTTGCATTGTAG |
| *Tsc22d3* | CAGCAGCCACTCAAACCAGC | ACCACATCCCCTCCAAGCAG |
| *Ucp1* | GGCCTCTACGACTCAGTCCA | TAAGCCGGCTGAGATCTTGT |
| *Actb* | AAGGCCAACCGTGAAAGAT | GTGGTACGACCAGAGGCATAC |
| *B2m* | ATCCAAATGCTGAAGAACGG | CAGTCTCAGTGGGGGTGAAT |
| *Gapdh* | TGTCCGTCGTGGATCTGAC | CCTGCTTCACCACCTTCTTG |
| *Rn18s* | GTAACCCGTTGAACCCCATT | CCATCCAATCGGTAGTAGCG |

**2**

## Statistical Analysis

Data were analyzed and graphs were plotted in GraphPad Prism for Windows (version 6, GraphPad Software, San Diego, CA) and IBM SPSS Statistics for Windows (version 24, IBM Corp., Armonk, NY). Unless otherwise indicated, differences between groups were analyzed by two-way ANOVA with Tukey *post hoc* test when the interaction of factors was significant or with Bonferroni test if the interaction was not significant. $P < 0.05$ was considered statistically significant [abbreviations for $P$ values: $P_C$ for corticosterone treatment, $P_I$ for insulin treatment, and $P_S$ for sex, $P_T$ for time (duration) of treatment]. When analyzing the IPGTT data, the area under the curve (AUC) was calculated normalized to the fasting level of each animal (26,38). Unless specified, data and graphs are shown as mean ± SEM.

## Results

### Corticosterone increases nonfasting glucose concentrations only in male mice

Corticosterone treatment for 2 weeks differentially affected body weight (BW) of male and female mice (experiment 1). The corticosterone-treated male mice were only 1.2 g heavier than vehicle-treated male mice whereas the corticosterone-treated female mice were 3.5 g heavier than vehicle-treated female mice (repeated three-way ANOVA: $P_{S \times C \times T} < 0.001$; **Fig. 2A**). Relative to BW at implantation, the corticosterone-treated female mice gained more weight than did the other three groups ($P_{S \times C} = 0.002$; **Fig. 2B**). While vehicle-treated female mice consumed more food (relative to BW) than did vehicle-treated male mice, corticosterone treatment significantly increased the 24-hour food intake to a comparable amount in both sexes ($P_S < 0.001$, $P_C < 0.001$; **Fig. 2C**). The 24-hour fecal output was higher in female than in male mice, was increased by corticosterone treatment ($P_S < 0.001$, $P_C < 0.001$; **Fig. 2D**), and was positively correlated with food intake ($r = 0.93$, $P < 0.001$; data not shown). Serum corticosterone levels (at time of euthanization) and fecal corticosterone levels (2-day average levels between days 12 and 14 of treatment) were measured and confirmed that corticosterone-treated mice had significantly higher corticosterone levels in serum and feces than did vehicle-treated mice ($P_C < 0.001$; **Fig. 2E** and **2F**). Moreover, the corticosterone-treated male mice tended to have higher corticosterone levels than corticosterone-treated female mice, but levels in vehicle-treated mice were not different between males and females (**Fig. 2E** and **2F**).

Corticosterone treatment differentially affected NFBG of male and female mice. Corticosterone increased NFBG of male mice by approximately twofold whereas it had no effect on NFBG of female mice (repeated three-way ANOVA: $P_{S \times C \times T}$ = 0.02; **Fig. 3A**). Measurement of 5-hour FBG after the 2-week treatment period revealed that female mice had a lower FBG than did male mice, and corticosterone treatment reduced the FBG in both sexes, but more pronounced in female mice ($P_S$ = 0.01, $P_C$ = 0.008; **Fig. 3B**). These data suggest that corticosterone treatment disturbs glucose homeostasis more severely in male than in female mice because only corticosterone-treated male mice presented with an elevated NFBG.
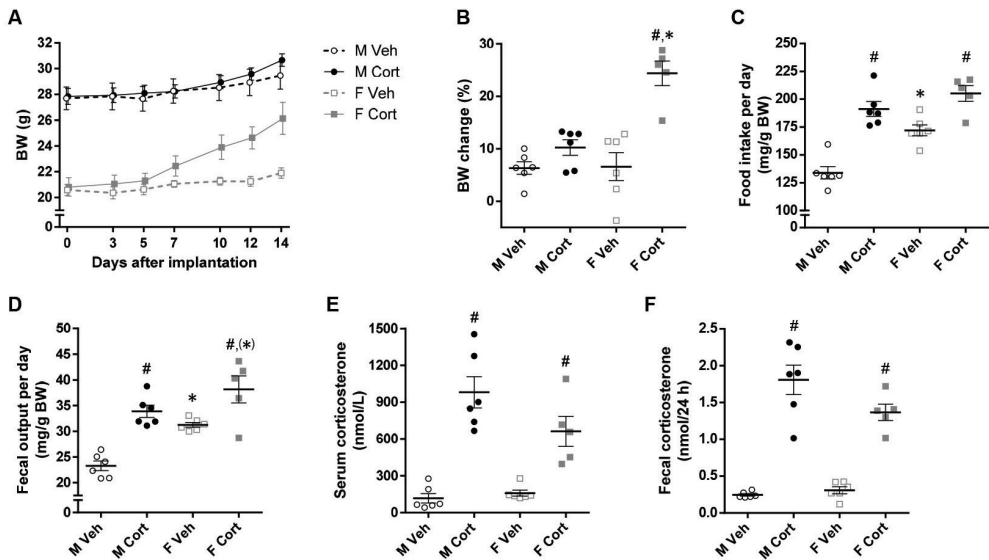


**Fig. 2** Effects of corticosterone treatment on BW and energy balance of mice

**(A)** BW of *ad libitum*-fed mice before (day 0) and after (days 3 to 14) pellet implantation (repeated three-way ANOVA: $P_S$ < 0.001, $P_C$ = 0.11, $P_T$ < 0.001, $P_{S \times C}$ = 0.29, $P_{S \times T}$ = 0.02, $P_{C \times T}$ < 0.001, $P_{S \times C \times T}$ < 0.001). **(B)** BW changes after 2-wk treatment relative to BW before pellet implantation ($P_S$ = 0.002, $P_C$ < 0.001, $P_{S \times C}$ = 0.002). **(C)** Daily food intake and **(D)** fecal production relative to BW, determined during days 12 and 14 of treatment (food intake, $P_S$ < 0.001, $P_C$ < 0.001, $P_{S \times C}$ = 0.06; fecal output, $P_S$ < 0.001, $P_C$ < 0.001, $P_{S \times C}$ = 0.20). **(E)** Serum corticosterone levels (level at time of euthanization: $P_S$ = 0.14, $P_C$ < 0.001, $P_{S \times C}$ = 0.06). **(F)** Fecal corticosterone levels (average level during days 12 to 14: $P_S$ = 0.13, $P_C$ < 0.001, $P_{S \times C}$ = 0.05). Unless stated, statistical significance was determined by two-way ANOVA. * $P$ < 0.05, (*) $P$ < 0.10 (tendency to significance), for sex difference between mice with the same treatment; # $P$ < 0.05, for effect of corticosterone treatment in mice of the same sex, by *post hoc* test.

**2**
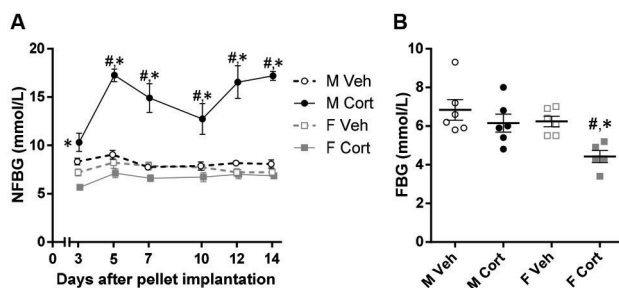


**Fig. 3** Sex-dependent effects of corticosterone treatment on glucose homeostasis

**(A)** NFBG levels during days 3 to 14 of treatment (repeated three-way ANOVA: $P_S < 0.001$, $P_C < 0.001$, $P_T < 0.001$, $P_{S \times C} < 0.001$, $P_{S \times T} = 0.02$, $P_{C \times T} < 0.001$, $P_{S \times C \times T} = 0.02$; two-way ANOVA at each time point: $P_S < 0.05$ every time point, $P_C = 0.69$ for day 3, $P_C < 0.05$ for days 5 to 14, $P_{S \times C} < 0.05$ every time point). **(B)** FBG levels determined on day 14 of treatment ($P_S = 0.01$, $P_C = 0.008$, $P_{S \times C} = 0.19$). Unless stated, statistical significance was determined by two-way ANOVA. * $P < 0.05$, for sex difference between mice with the same treatment; # $P < 0.05$, for effect of corticosterone treatment in mice of the same sex, by *post hoc* test.

## Differential effects of corticosterone on glucose tolerance in male and female mice

To investigate the differential effects of high-dose corticosterone on blood glucose homeostasis in male and female mice in more detail, mice were subjected to an IPGTT on day 14 in the second experiment. Also in this experiment, corticosterone treatment differentially affected BW of male and female mice (data not shown) and increased NFBG only in male mice (NFBG day 14: $P_{S \times C} < 0.001$; **Fig. 4A**). Compared with the vehicle-treated mice of the same sex, corticosterone treatment reduced the 5-hour FBG by 28.1% ± 7.4% in male mice and by 7.6% ± 4.6% in female mice (unpaired *t* test: $P = 0.04$; **Fig. 4A**). FBI was elevated in both sexes after 7 and 14 days of corticosterone treatment, and the effect was more pronounced in male than in female mice ($P_{S \times C} < 0.01$ for both days; **Fig. 4B**). Likewise, corticosterone treatment increased the homeostatic model assessment of insulin resistance (HOMA-IR) values more profoundly in male mice than in female mice ($P_{S \times C} < 0.05$ for both days; **Fig. 4C**). These data underscore that corticosterone-induced insulin resistance is more pronounced in male than in female mice.

After the IP administration of glucose, peak glucose levels of corticosterone-treated male mice were lower than in vehicle-treated males. However, corticosterone-treated male mice showed a delayed glucose clearance, and glucose levels did not return to baseline levels (**Fig. 4D** and **4E**). As a result, baseline-corrected AUC values were slightly but not significantly increased in the corticosterone-treated males ($P_{S \times C} = 0.03$; **Fig. 4F**). In contrast, in corticosterone-treated female mice the blood glucose levels were blunted, resulting in a
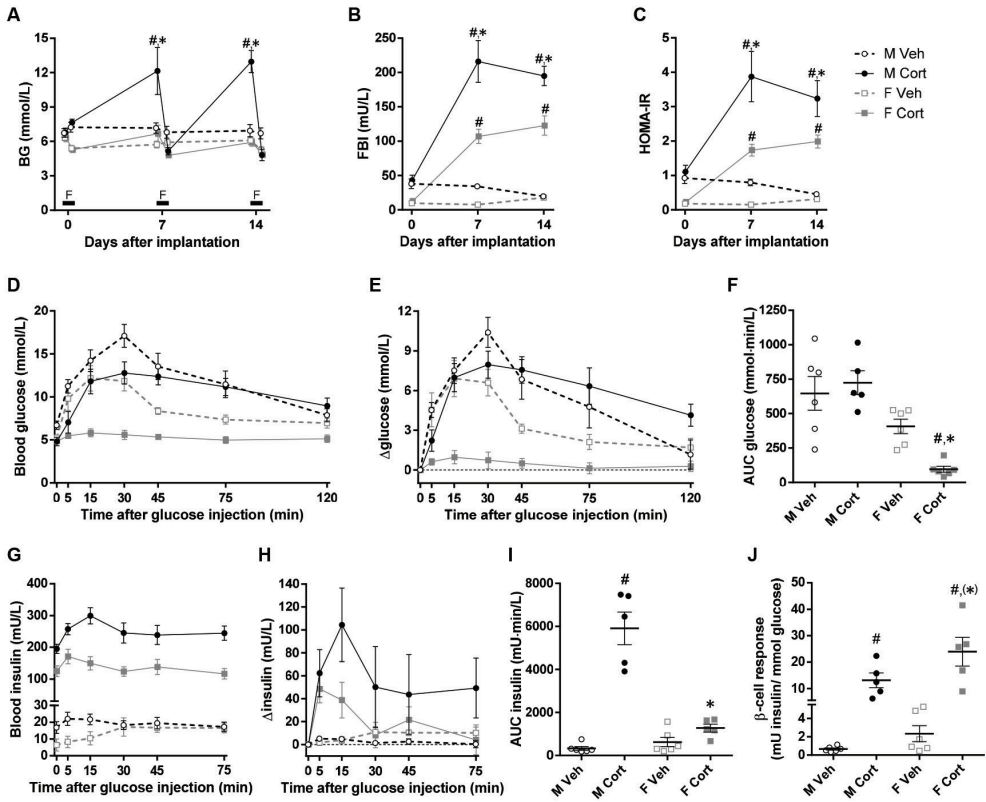
**Fig. 4** Sex-dependent effects of corticosterone treatment on glucose clearance

**(A)** Nonfasting and 5-h FBG levels (NFBG day 7, $P_S$ = 0.003, $P_C$ = 0.008, $P_{S \times C}$ = 0.06; FBG day 7, $P_S$ = 0.22, $P_C$ = 0.01, $P_{S \times C}$ = 0.60; NFBG day 14, $P_S$ < 0.001, $P_C$ < 0.001, $P_{S \times C}$ < 0.001; FBG day 14, $P_S$ = 0.08, $P_C$ = 0.009, $P_{S \times C}$ = 0.07). F indicates the 5-h fasting period on days 0, 7, and 14. **(B)** Five-hour FBI levels and **(C)** HOMA-IR calculated from FBG and insulin levels before (day 0) and after (days 7 and 14) pellet implantation (FBI day 7, $P_S$ < 0.001, $P_C$ < 0.001, $P_{S \times C}$ = 0.009; FBI day 14, $P_S$ = 0.001, $P_C$ < 0.001, $P_{S \times C}$ = 0.002; HOMA-IR day 7, $P_S$ < 0.001, $P_C$ < 0.001, $P_{S \times C}$ = 0.04; HOMA-IR day 14, $P_S$ = 0.01, $P_C$ < 0.001, $P_{S \times C}$ = 0.04). **(D)** Blood glucose levels, **(E)** changes in blood glucose levels over individual baseline values, **(F)** baseline corrected AUCs of glucose levels, **(G)** blood insulin levels, **(H)** changes in blood insulin levels over individual baseline values, and **(I)** baseline corrected AUCs of insulin levels after IP glucose administration in the 2-wk vehicle- or corticosterone-treated mice are shown (AUC glucose levels, $P_S$ < 0.001, $P_C$ = 0.16, $P_{S \times C}$ = 0.03; AUC insulin levels, $P_S$ < 0.001, $P_C$ < 0.001, $P_{S \times C}$ < 0.001). **(J)** β-Cell response to the IPGTT ($P_S$ = 0.04, $P_C$ < 0.001, $P_{S \times C}$ = 0.12). Statistical significance was determined by two-way ANOVA. * $P$ < 0.05, (*) $P$ < 0.10 (tendency to significance), for sex difference between mice with the same treatment; # $P$ < 0.05, for effect of corticosterone treatment in mice of the same sex, by *post hoc* test.

**2**

significantly reduced baseline-corrected AUC value (**Fig. 4D–4F**). Blood insulin levels after IPGTT were markedly different between the groups, mainly due to the elevated baseline FBI upon corticosterone treatment (**Fig. 4G**). Interestingly, the rise in blood insulin levels upon glucose injection was greater in the corticosterone-treated male mice than in the other three groups ($P_{S×C}$ < 0.001; **Fig. 4H** and **4I**). Calculated from the glucose and insulin AUC, the β-cell response was largely increased by corticosterone treatment and was higher in female mice than in male mice ($P_S$ = 0.04, $P_C$ < 0.001; **Fig. 4J**).

Using the enrichment of blood [U-$^{13}$C$_6$]-D-glucose (**Fig. 5A**), the effects of corticosterone treatment on the glucose clearance rate (GCR) and the EGP at baseline (before glucose injection) can be calculated. The GCR was higher in female mice than in male mice, and corticosterone treatment tended to sex-dependently affect GCR, namely a reduction in male and an increase in female mice ($P_{S×C}$ = 0.04; **Fig. 5B**). The EGP was reduced by corticosterone treatment in male but was unaffected in female mice ($P_{S×C}$ = 0.006; **Fig. 5C**). The factors contributing to blood glucose levels after the injected bolus can also be assessed. First, the bioavailability of the injected glucose was reduced by corticosterone treatment, but sex-independently ($P_C$ < 0.001; **Fig. 5D**). Second, detailed analysis of the clearance of the injected glucose revealed that the glucose-mediated flux, the insulin-mediated flux, and the independent flux were in general reduced by corticosterone treatment in both male and female mice (AUC total flux: $P_C$ < 0.001; **Fig. 5E** and **5F**). Interestingly, the percentage contribution of each flux was sex-dependently altered by corticosterone treatment, shifting toward insulin-mediated flux for male mice but toward independent flux for female mice ($P_{S×C}$ < 0.05 for all fluxes; **Fig. 5G**). Finally, the insulin sensitivity index (insulin-mediated glucose clearance) was markedly reduced by corticosterone treatment, and female mice had a greater insulin sensitivity index than did male mice ($P_S$ < 0.001, $P_C$ < 0.001; **Fig. 5H**). This finding once again underscores that corticosterone-induced insulin resistance is more pronounced in male mice than in female mice.

**Sex-differential effects of corticosterone on WAT morphology**

Adipose tissue is one of the glucose-consuming tissues, and we previously reported marked effects of corticosterone treatment on adipose tissue depots in male mice (39). Because the current data suggest that glucose clearance is differentially affected by corticosterone treatment in male and female mice, we next investigated the effects of corticosterone on male and female adipose tissues in more detail. Corticosterone treatment altered many aspects of WAT and BAT morphology and function with some clear differences between male and female
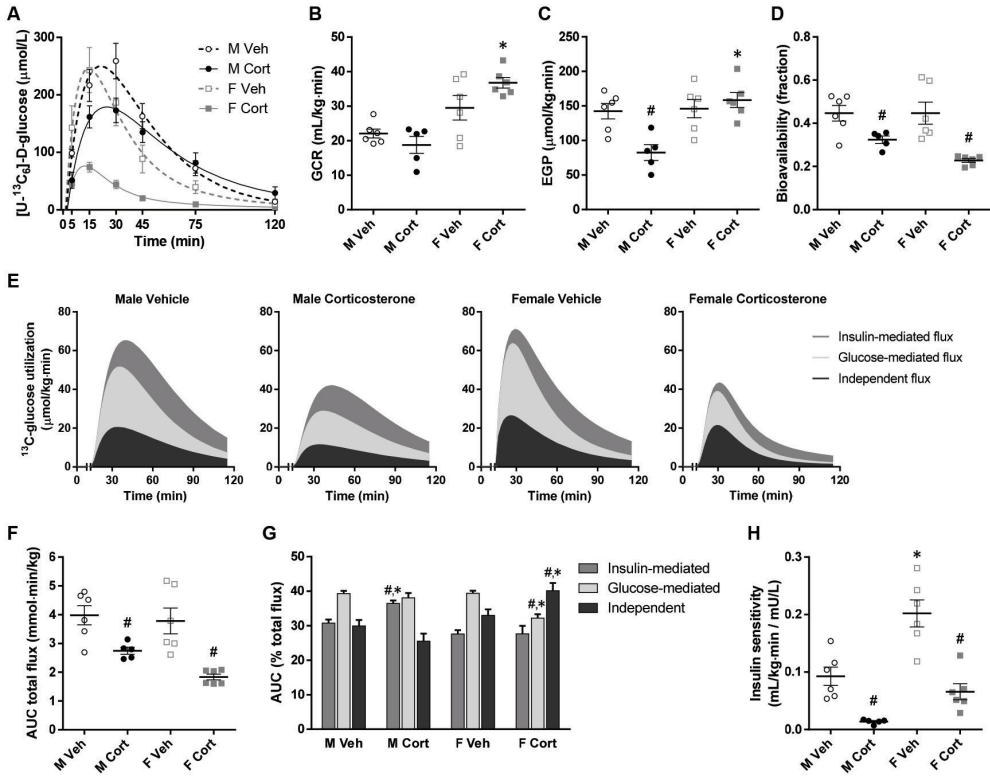
**Fig. 5** Glucose kinetic parameters from stable isotope-labeled glucose analyses

**(A)** Blood [U-$^{13}C_6$]-D-glucose levels with model-fitted line plots after IP stable isotope-labeled glucose administration in the 2-wk vehicle- or corticosterone-treated mice. This plot was used for calculating following glucose kinetic parameters. **(B)** Glucose clearance rate and **(C)** endogenous glucose production at basal state (before glucose administration; GCR, $P_S < 0.001$, $P_C = 0.42$, $P_{S\times C} = 0.04$; EGP, $P_S = 0.003$, $P_C = 0.06$, $P_{S\times C} = 0.006$). **(D)** Bioavailability of the injected glucose in the accessible pool of the minimal mouse model ($P_S = 0.18$, $P_C < 0.001$, $P_{S\times C} = 0.18$). **(E)** Stacked area plots demonstrating utilization of the injected glucose, separated into independent, glucose-mediated, and insulin-mediated fluxes. **(F)** AUCs of total glucose utilization (AUC total flux: $P_S = 0.08$, $P_C < 0.001$, $P_{S\times C} = 0.26$). **(G)** Relative percentages of each glucose utilization flux ($P_{S\times C} < 0.05$ for all fluxes). **(H)** Insulin sensitivity reflecting the clearance of injected glucose by endogenous insulin secretion ($P_S < 0.001$, $P_C < 0.001$, $P_{S\times C} = 0.10$). Statistical significance was determined by two-way ANOVA. $*P < 0.05$, for sex difference between mice with the same treatment; $^\#P < 0.05$, for effect of corticosterone treatment in mice of the same sex, by *post hoc* test.

**2**

mice. The visceral depot gWAT had a substantially greater mass in vehicle-treated male mice than in vehicle-treated female mice. This sex-dependent pattern disappeared after corticosterone treatment as corticosterone-treated male and female mice had a comparable gWAT mass ($P_{S \times C}$ = 0.001; **Fig. 6A**). Two subcutaneous depots, iWAT and aWAT, also gained more mass upon corticosterone treatment, but there was no significant sex difference ($P_C$ < 0.001 for both depots, $P_{S \times C}$ = 0.04 for iWAT; **Fig. 6B** and **6C**). Corticosterone treatment noticeably elevated the total WAT mass (the sum of the aforementioned WAT masses) without a significant sex difference ($P_{S \times C}$ = 0.006; **Fig. 6D**).

Because the mode of WAT expansion (hypertrophy or hyperplasia) can explain WAT functions and adaptations, the histologies of gWAT (**Fig. 6E**) and aWAT (**Fig. 6F**) after corticosterone treatment were studied. Female mice had a remarkably smaller gWAT adipocyte size than did male mice, and corticosterone treatment enlarged gWAT adipocyte size in both sexes ($P_S$ < 0.001, $P_C$ < 0.001; **Fig. 6G**). The cross-sectional area of aWAT adipocytes was also smaller in female mice than in male mice, and corticosterone treatment increased the aWAT adipocyte size in both sexes ($P_S$ = 0.008, $P_C$ < 0.001; **Fig. 6H**).

Corticosterone treatment induces significant changes in gene expression in a partly depot- and sex-dependent manner. The mRNA expression of *Nr3c1* encoding the glucocorticoid receptor (GR) in gWAT was lower in female mice than in male mice, whereas its expression in iWAT was higher in female mice than in male mice. Corticosterone treatment reduced *Nr3c1* mRNA expression in both depots of both sexes (**Table 2**). The mRNA expression of the GR target genes *Fkbp5* and *Tsc22d3* was significantly induced by corticosterone treatment in both depots with a general trend of higher expression in corticosterone-treated male depots than in female depots (**Table 2**). Although corticosterone and sex of the mice did not affect the mRNA expression of *Nr3c2* encoding the mineralocorticoid receptor (MR) in gWAT, its expression in iWAT was strikingly higher in vehicle-treated female mice than male mice. However, this sex-differential pattern in iWAT disappeared upon corticosterone treatment because it reduced *Nr3c2* mRNA expression in female mice only (**Table 2**).

In gWAT, mRNA expression of the adipogenic transcription factors *Cebpb* and *Pparg* was generally elevated by corticosterone treatment in both sexes. In iWAT, expression of both transcription factors tended to be higher in female mice than in male mice (**Table 2**). ADAMTS1, an extracellular protein secreted from mature adipocytes, together with *Adamts1* mRNA expression has been considered a marker of the hyperplastic limitation in WAT because it inhibits the generation of new adipocytes from adipocyte precursor cells (40). In gWAT, female mice had a lower *Adamts1* mRNA expression than did male mice, and corticosterone treatment induced its expression in both sexes. However,

corticosterone treatment induced *Adamts1* mRNA expression by sevenfold in iWAT of male mice but did not significantly affect the expression in female mice (**Table 2**). Of note, *Adamts1* mRNA expression in gWAT was on average 11-fold higher than in iWAT (data not shown).
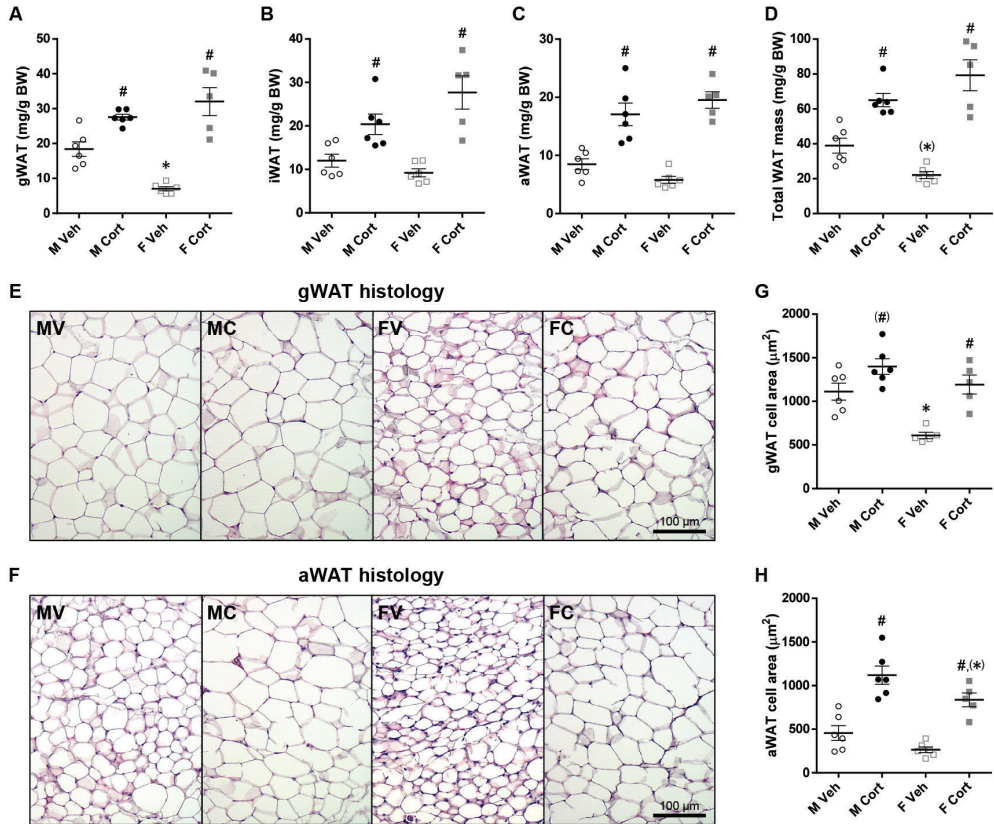


**Fig. 6** Sex differences in WAT mass and morphology upon corticosterone treatment

**(A–D)** gWAT, iWAT, aWAT, and total WAT mass relative to BW of the 2-wk vehicle- or corticosterone-treated mice (gWAT, $P_S$ = 0.12, $P_C$ < 0.001, $P_{S\times C}$ = 0.001; iWAT, $P_S$ = 0.33, $P_C$ < 0.001, $P_{S\times C}$ = 0.04; aWAT, $P_S$ = 0.93, $P_C$ < 0.001, $P_{S\times C}$ = 0.07; total WAT mass, $P_S$ = 0.80, $P_C$ < 0.001, $P_{S\times C}$ = 0.006). **(E** and **F)** Hematoxylin and eosin–stained gWAT and aWAT. Experimental group abbreviations: FC, female corticosterone; FV, female vehicle; MC, male corticosterone; MV, male vehicle. Scale bar, 100 µm. **(G** and **H)** gWAT and aWAT adipocyte sizes (gWAT, $P_S$ < 0.001, $P_C$ < 0.001, $P_{S\times C}$ = 0.12; aWAT, $P_S$ = 0.008, $P_C$ < 0.001, $P_{S\times C}$ = 0.58). Statistical significance was determined by two-way ANOVA. * $P$ < 0.05, (*) $P$ < 0.10 (tendency to significance), for sex difference between mice with the same treatment; # $P$ < 0.05, (#) $P$ < 0.10 (tendency to significance), for effect of corticosterone treatment in mice of the same sex, by *post hoc* test.

**2**

**Table 2** mRNA Expression in gWAT and iWAT

| Genes | gWAT | | | | | iWAT | | | | |
|---|---|---|---|---|---|---|---|---|---|---|
| | Sig. | M Veh | M Cort | F Veh | F Cort | Sig. | M Veh | M Cort | F Veh | F Cort |
| GR, MR, and GR-target genes | | | | | | | | | | |
| Nr3c1 | S,C | 1.00±0.16 | 0.46±0.04# | 0.58±0.08* | 0.34±0.04 | S,C,× | 1.00±0.06 | 0.67±0.04# | 1.78±0.13* | 0.41±0.05#,* |
| Fkbp5 | S,C,× | 1.00±0.28 | 6.90±0.81# | 0.38±0.02 | 3.57±0.84#,* | S,C,× | 1.00±0.26 | 10.46±1.49# | 2.58±0.83 | 3.53±0.81* |
| Tsc22d3 | C | 1.00±0.33 | 6.31±0.34# | 0.59±0.11 | 5.82±1.05# | C,× | 1.00±0.34 | 6.39±0.57# | 1.51±0.32 | 4.53±0.34#,* |
| Nr3c2 | – | 1.00±0.32 | 0.51±0.12 | 0.62±0.08 | 0.72±0.19 | S,C,× | 1.00±0.06 | 0.80±0.26 | 6.83±2.76* | 0.85±0.25# |
| Adipogenic differentiation markers | | | | | | | | | | |
| Cebpb | C | 1.00±0.12 | 3.78±0.86# | 0.90±0.16 | 2.61±0.43(#) | C | 1.00±0.18 | 1.76±0.13# | 1.41±0.32 | 2.13±0.28(#) |
| Pparg | (C) | 1.00±0.23 | 1.46±0.16 | 1.10±0.21 | 1.65±0.36 | (S) | 1.00±0.26 | 1.12±0.08 | 1.51±0.34 | 1.50±0.23 |
| Adamts1 | S,C | 1.00±0.10 | 2.48±0.23# | 0.40±0.07* | 0.81±0.11#,* | C,× | 1.00±0.26 | 7.17±0.84# | 3.06±0.80(*) | 4.02±0.71* |
| Adipokine production | | | | | | | | | | |
| Lep | S,C,× | 1.00±0.01 | 24.19±4.55# | 0.22±0.01* | 9.63±1.24#,* | C,× | 1.00±0.37 | 9.45±1.39# | 1.97±0.69 | 5.83±0.83# |
| Adipoq | C | 1.00±0.16 | 0.68±0.07 | 1.09±0.15 | 0.58±0.11# | (S),C | 1.00±0.20 | 0.57±0.09 | 1.93±0.52(*) | 0.90±0.26(#) |
| Glucose transport | | | | | | | | | | |
| Irs1 | – | 1.00±0.12 | 0.67±0.14 | 1.24±0.18 | 1.11±0.46 | C | 1.00±0.21 | 0.33±0.10# | 1.04±0.35 | 0.42±0.12(#) |
| Slc2a1 | S,(C) | 1.00±0.31 | 1.30±0.19 | 0.31±0.06 | 0.88±0.25 | C | 1.00±0.41 | 0.29±0.04# | 0.97±0.14 | 0.51±0.12 |
| Slc2a4 | C | 1.00±0.23 | 3.21±0.92(#) | 0.88±0.23 | 5.34±1.22# | (C) | 1.00±0.18 | 1.55±0.20 | 0.97±0.39 | 1.30±0.16 |
| Chrebpb | S,C | 1.00±0.37 | 5.96±2.12 | 5.41±1.94* | 15.82±3.59# | C,× | 1.00±0.40 | 1.04±0.28 | 0.18±0.13 | 1.82±0.36# |

Gene expression was normalized to *B2m* and *Rn18s* expression and expressed relative to the vehicle-treated male mice. Sig. indicates significant effects ($P < 0.05$) analyzed with two-way ANOVA. Symbols in parentheses [*e.g.*, (C)] indicate a tendency to significance ($P < 0.10$). Abbreviations: C, corticosterone treatment; S, sex; ×, interaction of corticosterone treatment and sex.
* $P < 0.05$, (*) $P < 0.10$ (tendency to significance), for sex difference between mice with the same treatment; # $P < 0.05$, (#) $P < 0.10$ (tendency to significance), for effect of corticosterone treatment in mice of the same sex, by *post hoc* test.

**2**

## Sex-differential effects of corticosterone on adipokine secretion

Apart from energy storage as lipid droplets, adipose tissue depots secrete a number of adipokines into the circulation. Serum leptin concentrations were strongly elevated after corticosterone treatment in both male and female mice ($P_C < 0.001$; **Fig. 7A**). The serum concentrations of total adiponectin were in general higher in female mice than in male mice and were increased upon corticosterone treatment, especially in female mice ($P_{S \times C} = 0.005$; **Fig. 7B**). Serum concentrations of HMW adiponectin, the metabolically active adiponectin isoform, were also elevated by corticosterone treatment ($P_{S \times C} = 0.004$; **Fig. 7C**). The HMW/total adiponectin ratio did not differ between the sexes but was significantly higher after corticosterone treatment ($P_C < 0.001$; **Fig. 7D**). The adiponectin/leptin (A/L) ratio, a promising index for assessing insulin sensitivity (41), was higher in vehicle-treated female mice than in male mice, but this sex difference was attenuated and reduced to a similar low A/L ratio after corticosterone treatment ($P_{S \times C} = 0.007$; **Fig. 7E**). The HMW adiponectin/leptin ratio showed a similar pattern ($P_S < 0.001$, $P_C < 0.001$, $P_{S \times C} = 0.001$; data not shown).
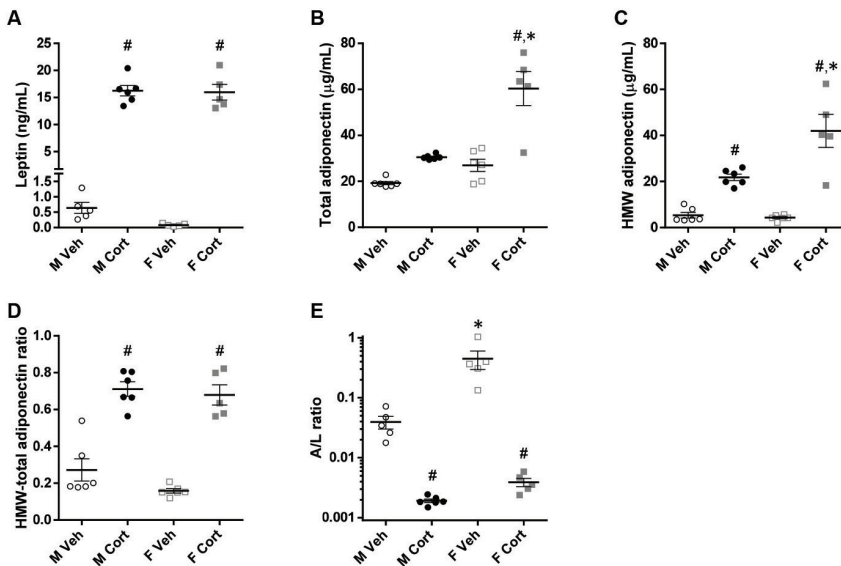


**Fig. 7** Serum adipokine levels

**(A)** Serum leptin levels and **(B** and **C)** serum total adiponectin and HMW isoform levels of the 2-wk vehicle- or corticosterone-treated mice (leptin, $P_S = 0.64$, $P_C < 0.001$, $P_{S \times C} = 0.89$; total adiponectin, $P_S < 0.001$, $P_C < 0.001$, $P_{S \times C} = 0.005$; HMW adiponectin, $P_S = 0.008$, $P_C < 0.001$, $P_{S \times C} = 0.004$). **(D)** Ratio of the HMW isoform to the total adiponectin levels ($P_S = 0.12$, $P_C < 0.001$, $P_{S \times C} = 0.37$). **(E)** Ratio of adiponectin to leptin levels, illustrated on a logarithmic scale ($P_S < 0.001$, $P_C < 0.001$, $P_{S \times C} = 0.007$). Statistical significance was determined by two-way ANOVA. * $P < 0.05$, for sex difference between mice with the same treatment; # $P < 0.05$, for effect of corticosterone treatment in mice of the same sex, by *post hoc* test.

**2**

The changes in leptin concentrations were also reflected by changes in gene expression. Corticosterone treatment induced *Lep* mRNA expression in gWAT and iWAT of both sexes, which was more pronounced in corticosterone-treated male mice than in female mice (**Table 2**). In contrast, corticosterone treatment reduced *Adipoq* mRNA expression in both depots of both sexes. Furthermore, female mice tended to have a higher *Adipoq* mRNA expression in iWAT than did male mice (**Table 2**). Note that *Lep* mRNA expression in gWAT was on average fivefold higher whereas *Adipoq* mRNA expression was 0.7-fold lower than in iWAT (data not shown).

### Corticosterone treatment reduces BAT activity in both male and female mice

In both male and female mice, corticosterone treatment increased BAT mass ($P_C < 0.001$; **Fig. 8A**) and induced lipid accumulation and unilocular rearrangement in BAT (**Fig. 8B**). The mRNA expression of *Ucp1*, a classical BAT thermogenic gene, was reduced by corticosterone treatment in both sexes (**Table 3**). Although corticosterone treatment tended to reduce mRNA expression of *Nr3c1* without a sex-dependent pattern in BAT, it significantly induced expression of the GR target genes *Fkbp5* and *Tsc22d3* in both sexes, albeit less pronounced in female mice than in male mice (**Table 3**). The mRNA expression of *Nr3c2* was lower in female mice than in male mice without an obvious effect by corticosterone treatment (**Table 3**).

*Lep* mRNA expression in BAT of female mice tended to be lower than that of male mice, and corticosterone treatment strongly induced the expression in both sexes by >35-fold (**Table 3**). However, *Adipoq* mRNA expression in BAT was not significantly affected by corticosterone treatment in both sexes (**Table 3**).

### Elevated concentrations of leptin and adiponectin are likely due to hyper-insulinemia, not a direct effect of corticosterone

To investigate whether the elevated serum leptin and adiponectin levels upon corticosterone treatment are caused directly by corticosterone or indirectly as a result of the compensatory hyperinsulinemia, *in vitro* studies using 3T3-L1 white adipocytes and T37i brown adipocytes were performed. In 3T3-L1 cells, corticosterone reduced whereas insulin induced *Lep* mRNA expression (**Table 4**). Leptin production and secretion by 3T3-L1 cells were also significantly stimulated by insulin treatment (**Table 4**). Although both insulin and corticosterone reduced *Adipoq* mRNA expression in 3T3-L1 cells, cotreatment of insulin and corticosterone attenuated the inhibitory effect of corticosterone on *Adipoq* mRNA expression (**Table 4**). In contrast, insulin significantly increased whereas corticosterone reduced the total adiponectin production in 3T3-L1 cells, and adiponectin secretion tended to be increased by corticosterone only (**Table 4**).
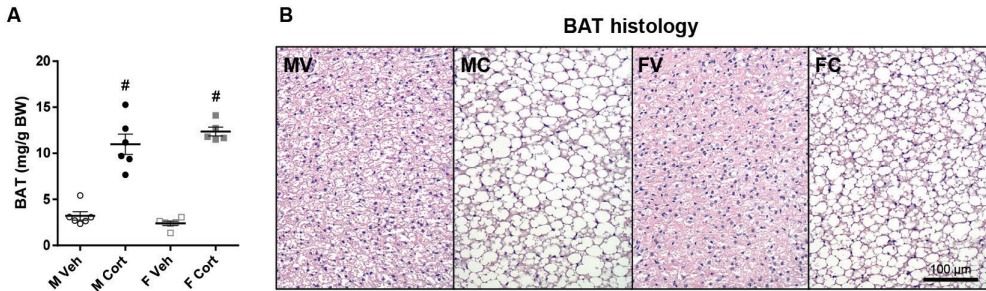
**Fig. 8** BAT mass and morphology upon corticosterone treatment

**(A)** BAT mass relative to BW of the 2-week vehicle- or corticosterone-treated mice ($P_S$ = 0.68, $P_C$ < 0.001, $P_{S\times C}$ = 0.12). **(B)** Hematoxylin and eosin–stained BAT. Experimental group abbreviations: FC, female corticosterone; FV, female vehicle; MC, male corticosterone; MV, male vehicle. Scale bar, 100 µm. Statistical significance was determined by two-way ANOVA. $^{\#}P$ < 0.05, for effect of corticosterone treatment in mice of the same sex, by *post hoc* test.

**Table 3** mRNA expression in BAT

| Genes | Sig. | M Veh | M Cort | F Veh | F Cort |
|---|---|---|---|---|---|
| Thermogenic gene | | | | | |
| Ucp1 | C,× | 1.00±0.16 | 0.80±0.21 | 1.61±0.25 | 0.50±0.15 $^{\#}$ |
| GR, MR, and GR-target genes | | | | | |
| Nr3c1 | (C) | 1.00±0.11 | 0.86±0.10 | 0.97±0.13 | 0.68±0.09 |
| Fkbp5 | S,C,× | 1.00±0.12 | 43.82±4.34 $^{\#}$ | 0.64±0.06 | 30.00±4.79 $^{\#,*}$ |
| Tsc22d3 | C,× | 1.00±0.08 | 5.05±0.35 $^{\#}$ | 1.36±0.13 | 3.89±0.41 $^{\#,*}$ |
| Nr3c2 | S | 1.00±0.07 | 0.89±0.11 | 0.59±0.12 $^{*}$ | 0.76±0.15 |
| Adipokine production | | | | | |
| Lep | (S),C | 1.00±0.36 | 38.56±7.49 $^{\#}$ | 0.12±0.03 | 23.54±4.55 $^{\#,(*)}$ |
| Adipoq | – | 1.00±0.10 | 0.98±0.14 | 1.23±0.15 | 0.82±0.09 |
| Glucose transport | | | | | |
| Irs1 | – | 1.00±0.21 | 1.19±0.11 | 2.10±0.78 | 1.12±0.21 |
| Slc2a1 | – | 1.00±0.15 | 1.23±0.19 | 0.74±0.09 | 1.00±0.15 |
| Slc2a4 | – | 1.00±0.17 | 1.00±0.13 | 0.84±0.08 | 1.10±0.10 |
| Chrebpb | × | 1.00±0.19 | 0.63±0.13 | 0.44±0.07 $^{(*)}$ | 0.92±0.18 |

Gene expression was normalized to *Actb* and *Rn18s* expression and expressed relative to the vehicle-treated male mice. Sig. indicates significant effects ($P$ < 0.05) analyzed with two-way ANOVA. Symbols in parentheses [*e.g.*, (C)] indicate a tendency to significance ($P$ < 0.10). Abbreviations: C, corticosterone treatment; S, sex; ×, interaction of corticosterone treatment and sex. $^{*}P$ < 0.05, $^{(*)}P$ < 0.10 (tendency to significance), for sex difference between mice with the same treatment; $^{\#}P$ < 0.05, for effect of corticosterone treatment in mice of the same sex, by *post hoc* test.

**2**

In T37i cells, corticosterone reduced whereas insulin strongly induced *Lep* mRNA expression (**Table 4**). Likewise, leptin production and secretion by T37i cells were stimulated by insulin treatment and cotreatment of corticosterone and insulin, while corticosterone treatment alone marginally reduced its production (**Table 4**). Although corticosterone reduced *Adipoq* and insulin did not alter *Adipoq* mRNA expression in T37i cells, cotreatment of insulin and corticosterone attenuated the inhibitory effect of corticosterone treatment (**Table 4**). Furthermore, whereas insulin treatment only increased intracellular adiponectin but did not affect the total production, corticosterone treatment reduced total adiponectin production but increased its secretion significantly (**Table 4**). Apart from adiponectin production in brown adipocytes, these data suggest that the elevated adipokine levels of corticosterone-treated mice were more likely caused by the high insulin level than by corticosterone treatment itself.

**Corticosterone treatment reduces insulin-stimulated Akt phosphorylation in WAT**

Insulin induces glucose uptake in WATs through Akt phosphorylation and subsequently GLUT4 translocation (42). To determine insulin signaling in WATs of vehicle- and corticosterone-treated mice, gWAT (a visceral depot) and iWAT (a subcutaneous depot) explants were stimulated with insulin and Akt phosphorylation was determined. Corticosterone treatment reduced baseline and insulin-stimulated Akt phosphorylation without a sex-dependent pattern in both gWAT and iWAT explants (repeated 3-way ANOVA: $P_{C\times I} < 0.05$ in both explants; **Fig. 9**).

**Corticosterone reduces whereas insulin induces glucose uptake, but both cause insulin resistance in WAT**

To address the effects of corticosterone treatment on adipose tissue glucose homeostasis, we assessed the adipose tissue mRNA expression of genes related to glucose transport. Corticosterone treatment did not affect mRNA expression of *Irs1*, the gene encoding the insulin receptor, in gWAT and BAT, but reduced its expression in iWAT (**Tables 2** and **3**). In gWAT, the mRNA expression of the glucose transporter 4 [*Slc2a4* (*Glut4*)], an insulin-dependent glucose transporter, and the glucose transporter 1 [*Slc2a1* (*Glut1*)], a basal glucose transporter, were in general increased by corticosterone treatment (**Table 2**). In iWAT, corticosterone treatment reduced *Slc2a1* expression but tended to increase *Slc2a4* expression (**Table 2**). In contrast, corticosterone treatment did not significantly affect *Slc2a1* and *Slc2a4* mRNA expression in BAT (**Table 3**). Finally, we analyzed the expression of *Mlxipl* variant β (or called *Chrebpb*), a gene whose transcription is regulated by the carbohydrate-responsive element-binding

**2**

**Table 4** Leptin and adiponectin gene expression and adipokine production in cultured adipocytes

| Adipokine | 3T3-L1 cells | | | | | T37i cells | | | | |
| --- | --- | --- | --- | --- | --- | --- | --- | --- | --- | --- |
| | Sig. | Control | CORT | INS | CORT+INS | Sig. | Control | CORT | INS | CORT+INS |
| *Lep* mRNA expression | C,I,× | 1.00±0.32 | 0.26±0.06# | 1.61±0.31 | 1.59±0.25* | C,I,× | 1.00±0.14 | 0.30±0.04# | 8.54±2.39* | 8.27±1.27* |
| Leptin (pg/g protein) | | | | | | | | | | |
| - in cell lysates | (I) | 40±7 | 43±9 | 59±4 | 52±4 | I | 285±52 | 259±59 | 181±20 | 178±23 |
| - in cultured media | I | 117±12 | 98±15 | 575±127* | 896±237* | C,I | 379±34 | 204±23# | 2851±539* | 2368±320* |
| - total production | I | 157±11 | 141±10 | 634±126* | 949±237* | (C),I | 664±43 | 463±55(#) | 3032±523* | 2546±304* |
| Leptin secretion (%) | I | 74.0±4.1 | 68.1±8.1 | 89.5±1.9(*) | 91.6±2.4* | I | 58.2±6.4 | 47.2±7.2 | 92.7±1.7 | 91.9±2.1* |
| *Adipoq* mRNA expression | C,× | 1.00±0.08 | 0.34±0.03# | 0.69±0.06* | 0.62±0.03* | C,I,× | 1.00±0.06 | 0.13±0.02# | 0.80±0.06 | 0.43±0.04#,* |
| Adiponectin (ng/g protein) | | | | | | | | | | |
| - in cell lysates | C,I | 2285±112 | 1810±219(#) | 2990±125* | 2524±137*(#) | C,I | 750±41 | 315±20# | 1139±94* | 733±75#,* |
| - in cultured media | I | 1437±103 | 1493±140 | 1801±164 | 1667±64 | C,I | 1061±91 | 775±88# | 766±31* | 520±29#,* |
| - total production | C,I | 3723±104 | 3303±262 | 4791±261* | 4192±144* | C | 1811±127 | 1090±87# | 1905±78 | 1253±89# |
| Adiponectin secretion (%) | (C) | 38.6±2.5 | 46.3±3.7(#) | 37.1±1.7 | 40.0±1.8 | C,I,× | 58.3±1.3 | 70.2±2.7# | 40.6±2.8* | 42.1±2.4* |

Gene expression was normalized to *Actb* and *B2m* expression and expressed relative to the control condition. Sig. indicates significant effects ($P < 0.05$) analyzed with two-way ANOVA. Symbols in parentheses [*e.g.*, (I)] indicate a tendency to significance ($P < 0.10$). Abbreviations: C, corticosterone; CORT, corticosterone treatment; CORT+INS, cotreatment with corticosterone and insulin; I, insulin; INS, insulin treatment; ×, interaction of corticosterone and insulin.
* $P < 0.05$, (*) $P < 0.10$ (tendency to significance), for effect of insulin within the same corticosterone treatment; # $P < 0.05$, (#) $P < 0.10$ (tendency to significance), for effect of corticosterone within the same insulin treatment, by *post hoc* test.

**2**

protein (ChREBP; also known as MLX interacting protein-like) because it can be considered a readout of intracellular glucose concentrations (43). Corticosterone treatment increased *Chrebpb* expression in gWAT and iWAT, but not in BAT, suggestive of an increased glucose uptake after corticosterone treatment in both WAT depots (**Tables 2** and **3**). Of note, *Chrebpb* expression in the iWAT depot was significantly induced by corticosterone treatment only in female mice due to the sex-differential baseline expression.

To determine whether the increased uptake of glucose in WAT upon corticosterone treatment is due to corticosterone *per se* and/or the high plasma insulin concentrations, we measured the insulin-stimulated glucose uptake in 3T3-L1 and T37i cells pretreated for 24 hours with corticosterone and/or insulin. In 3T3-L1 cells, pretreatment with corticosterone (PC) inhibited whereas pretreatment with insulin (PI) stimulated basal glucose uptake ($P_{PC\times PI}$ = 0.009; **Fig. 10A**). Note, however, that the co-pretreatment of corticosterone and insulin resulted in a 34% lower basal glucose uptake than did insulin pretreatment
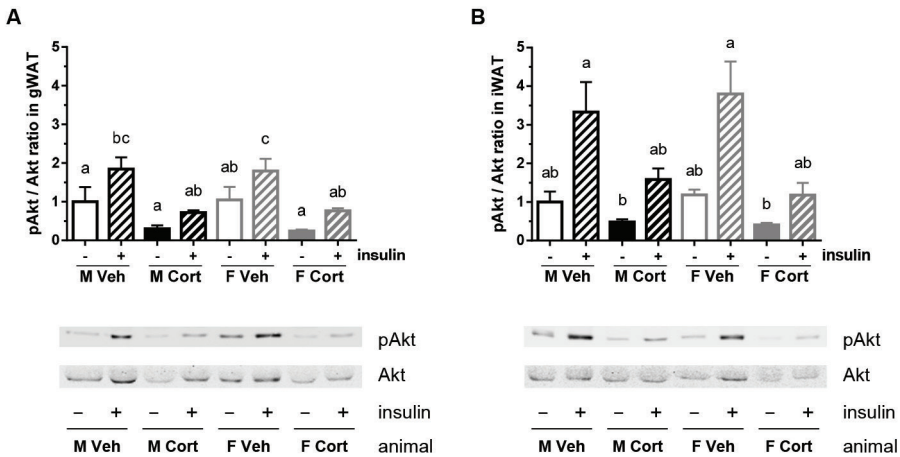


**Fig. 9** Insulin-stimulated Akt phosphorylation in WAT explants

**(A** and **B)** Akt phosphorylation level in **(A)** gWAT and **(B)** iWAT of the vehicle- or corticosterone-treated mice, *ex vivo* stimulated with insulin (gWAT, $P_S$ = 0.99, $P_C$ = 0.005, $P_I$ < 0.001, $P_{S\times C}$ = 0.99, $P_{S\times I}$ = 0.95, $P_{C\times I}$ = 0.02, $P_{S\times C\times I}$ = 0.39; iWAT, $P_S$ = 0.91, $P_C$ = 0.004, $P_I$ < 0.001, $P_{S\times C}$ = 0.45, $P_{S\times I}$ = 0.97, $P_{C\times I}$ = 0.02, $P_{S\times C\times I}$ = 0.57). Akt phosphorylation level was normalized to total Akt and expressed relative to the level of vehicle-treated male explants. A representative blot is shown of three biological samples per group. Statistical significance was determined by repeated three-way ANOVA with *post hoc* Tukey test: letters a,b, and c denote significant group differences (*P* < 0.05).

alone. The insulin-stimulated glucose uptake pattern was affected by pretreatment with corticosterone, pretreatment with insulin, and stimulatory insulin (SI) (repeated three-way ANOVA: $P_{PC \times PI \times SI} = 0.001$; **Fig. 10A**). Pretreatment with corticosterone and insulin alone or in combination significantly inhibited the insulin-induced glucose uptake (**Fig. 10A**).

For T37i cells, the basal glucose uptake was decreased by pretreatment with corticosterone but increased by pretreatment with insulin ($P_{PC} = 0.05$; $P_{PI} < 0.001$; **Fig. 10B**). The insulin-stimulated glucose uptake pattern was increased by stimulatory insulin, but it was not significantly altered by pretreatment with corticosterone or pretreatment with insulin, reflecting an insulin-sensitive state of the corticosterone- or insulin-pretreated T37i cells (repeated three-way ANOVA: $P_{SI} < 0.001$; **Fig. 10B**). These data suggest that corticosterone and high-dose insulin induce insulin resistance mainly in white adipocytes, but not in brown adipocytes.
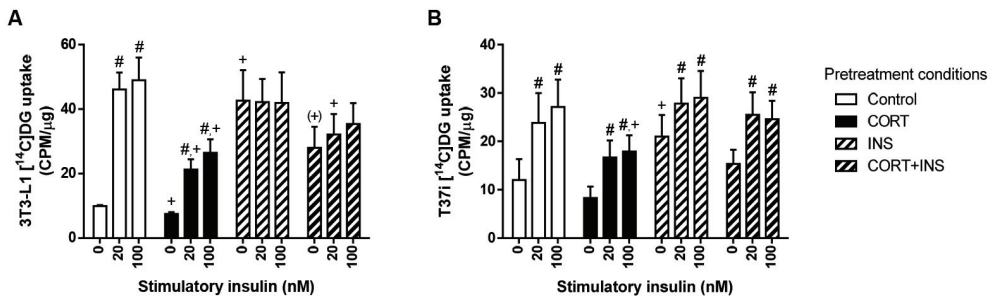


**Fig. 10** Insulin-stimulated radioactive glucose uptake in corticosterone- and/or insulin-treated 3T3-L1 and T37i adipocytes

**(A)** Differentiated 3T3-L1 white adipocytes and **(B)** differentiated T37i brown adipocytes pretreated with corticosterone (PC) and/or insulin (PI) for 24 h were stimulated with insulin (SI) at the indicated concentrations for 15 min and subsequently 2-[1-$^{14}$C]-deoxy-D-glucose was added to determine glucose uptake (3T3-L1, $P_{PC} = 0.03$, $P_{PI} = 0.09$, $P_{SI} < 0.001$, $P_{PC \times PI} = 0.60$, $P_{PC \times SI} = 0.08$, $P_{PI \times SI} < 0.001$, $P_{PC \times PI \times SI} = 0.001$; T37i, $P_C = 0.22$, $P_{PI} = 0.16$, $P_{SI} < 0.001$, $P_{PC \times PI} = 0.77$, $P_{PC \times SI} = 0.46$, $P_{PI \times SI} = 0.17$, $P_{PC \times PI \times SI} = 0.15$). Data from three independent experiment were plotted in counts per minute, relative to protein content (µg) of each sample. Pretreatment condition abbreviations: CORT, corticosterone; CORT+INS, cotreatment with corticosterone and insulin; INS, insulin. Statistical significance was determined by repeated three-way ANOVA. $^+ P < 0.05$, $^{(+)} P < 0.10$ (tendency to significance), for difference from baseline uptake of control condition; $^\# P < 0.05$, for effect of the stimulatory insulin from its baseline uptake, by *post hoc* Dunnett test.

**2**

### Effect of corticosterone treatment on gene expression in skeletal muscle

Not only adipose tissues, but also skeletal muscle is an important glucose-consuming organ that contributes to whole-body GCR, especially at the postprandial state, and GCs have been shown to reduce glucose uptake in the muscle by counteracting the effect of insulin (1,4). We therefore investigated whether corticosterone treatment affected the gene expression profile in skeletal muscle in a sex-dependent manner. The expressions of *Nr3c1* (GR) and *Nr3c2* (MR) were not significantly different between male and female mice and were not affected by corticosterone treatment (**Table 5**). Corticosterone treatment significantly increased the mRNA expression of the GR target genes *Fkpb5* and *Tsc22d3* in both sexes (**Table 5**).

Another hallmark of GC excess is GC-mediated muscle atrophy by reducing muscle protein synthesis and degrading muscle proteins. Corticosterone treatment strongly upregulated the mRNA expression of the muscle atrophy-related genes *Foxo1* and *Klf15* in both male and female mice (**Table 5**).

Vehicle-treated female mice had a higher *Irs1* mRNA expression than did vehicle-treated male mice, but corticosterone treatment reduced *Irs1* mRNA expression to a similar level in male and female mice (**Table 5**). Whereas the expression of *Slc2a1* and *Slc2a4* mRNA was not significantly affected by corticosterone treatment, *Chrebpb* mRNA expression was remarkably elevated by corticosterone treatment in both sexes (**Table 5**).

### Effect of corticosterone treatment on gene expression in liver

We also determined hepatic gene expressions of the vehicle- and corticosterone-treated mice because the liver is the central organ regulating whole-body glucose homeostasis, especially in the fasting state when hepatic gluconeogenesis is crucial to maintain euglycemia (1,4). *Nr3c1* mRNA expression tended to be higher in female mice than in male mice but was not significantly affected by corticosterone treatment (**Table 6**). However, corticosterone treatment clearly induced *Fkpb5* and *Tsc22d3* mRNA expression in both sexes (**Table 6**). Regarding transcriptional regulation of genes encoding gluconeogenic enzymes, corticosterone treatment upregulated the mRNA expression of *Pck1* (phosphoenolpyruvate carboxykinase 1, also known as PEPCK) and *Pcx* (pyruvate carboxylase) in a sex-independent manner (**Table 6**).

Whereas *Irs1* mRNA expression was not significantly affected by sex or corticosterone treatment, *Irs2* mRNA expression was higher in vehicle-treated female mice than in male mice and was reduced by corticosterone treatment to a comparable level in both sexes (**Table 6**). Corticosterone treatment induced transcription of *Slc2a2* (also known as *Glut2*), a major glucose transporter for hepatic glucose uptake, in male mice only (**Table 6**). Furthermore, corticosterone treatment increased *Chrebpb* mRNA expression in both sexes, but this increase tended to be higher in corticosterone-treated male mice than in female mice (**Table 6**).

**Table 5** mRNA expression in skeletal muscle

| Genes | Sig. | M Veh | M Cort | F Veh | F Cort |
|---|---|---|---|---|---|
| GR, MR, and GR-target genes | | | | | |
| *Nr3c1* | – | 1.00±0.17 | 0.90±0.06 | 0.88±0.20 | 0.91±0.15 |
| *Fkbp5* | S,C,× | 1.00±0.10 | 18.11±1.06[#] | 0.69±0.13 | 12.49±2.29[#,*] |
| *Tsc22d3* | C | 1.00±0.20 | 3.99±0.67[#] | 1.07±0.21 | 4.30±0.95[#] |
| *Nr3c2* | – | 1.00±0.10 | 1.36±0.29 | 1.22±0.34 | 1.21±0.13 |
| Muscle atrophy | | | | | |
| *Foxo1* | C | 1.00±0.13 | 12.80±2.11[#] | 1.30±0.30 | 14.25±3.46[#] |
| *Klf15* | C | 1.00±0.18 | 2.70±0.63[#] | 1.22±0.24 | 2.23±0.36 |
| Glucose transport | | | | | |
| *Irs1* | S,C,× | 1.00±0.17 | 0.66±0.10 | 2.24±0.45[*] | 0.61±0.19[#] |
| *Slc2a1* | – | 1.00±0.27 | 1.60±0.61 | 1.08±0.13 | 0.81±0.26 |
| *Slc2a4* | – | 1.00±0.08 | 1.04±0.09 | 1.01±0.16 | 1.24±0.12 |
| *Chrebpb* | C | 1.00±0.35 | 13.06±1.22[#] | 0.80±0.06 | 18.04±10.57[#] |

Gene expression was normalized to *Gapdh* and *Rn18s* expression and expressed relative to the vehicle-treated male mice. Sig. indicates significant effects ($P < 0.05$) analyzed with two-way ANOVA. Abbreviations: C, corticosterone treatment; S, sex; ×, interaction of corticosterone treatment and sex. [*] $P < 0.05$, for sex difference between mice with the same treatment; [#] $P < 0.05$, for effect of corticosterone treatment in mice of the same sex, by *post hoc* test.

## Discussion

This study demonstrates that a high-dose corticosterone treatment causes insulin resistance in both sexes of mice, but with a more severe phenotype in male than in female mice. Our results also show that corticosterone-treated female mice displayed a more protective feature in WAT expansion and adipokine secretion than did corticosterone-treated male mice.

The 2-week treatment with high-dose corticosterone induced an insulin-resistant state more potently in males than in females, which was confirmed by high FBI concentrations, and hence an increase in HOMA-IR levels. Moreover, in-depth analyses indicated that glucose metabolism was more disturbed in male mice than in female mice. First, the corticosterone-induced increase in FBI levels slightly decreased FBG levels only in female mice. Second, corticosterone treatment elevated NFBG levels in male mice but not in female mice, resembling the early pathognomonic postprandial hyperglycemia as a sign of GC-induced diabetes mellitus in humans (44). Third, the increases in glucose and insulin levels after an IPGTT were more severe in corticosterone-treated male mice than female mice.

**Table 6** mRNA expression in liver

| Genes | Sig. | M Veh | M Cort | F Veh | F Cort |
|---|---|---|---|---|---|
| GR, MR, and GR-target genes | | | | | |
| *Nr3c1* | (S) | 1.00±0.05 | 1.08±0.08 | 1.41±0.17 [(*)] | 1.20±0.22 |
| *Fkbp5* | C | 1.00±0.22 | 40.38±7.71 [#] | 4.09±0.68 | 31.63±6.59 [#] |
| *Tsc22d3* | C | 1.00±0.01 | 5.27±0.57 [#] | 1.55±0.25 | 4.50±0.51 [#] |
| *Nr3c2* | - | 1.00±0.09 | 1.00±0.16 | 1.15±0.13 | 1.22±0.31 |
| Gluconeogenesis | | | | | |
| *Pck1* | C | 1.00±0.13 | 2.30±0.33 [#] | 1.26±0.18 | 2.23±0.23 [#] |
| *Pcx* | (×),C | 1.00±0.05 | 1.92±0.25 [#] | 1.03±0.06 | 1.41±0.15 |
| Glucose transport | | | | | |
| *Irs1* | - | 1.00±0.15 | 0.70±0.11 | 0.99±0.09 | 1.02±0.10 |
| *Irs2* | ×,S,C | 1.00±0.09 | 0.55±0.02 [#] | 1.88±0.05 [*] | 0.74±0.07 [#] |
| *Slc2a2* | ×,C | 1.00±0.09 | 1.84±0.22 [#] | 1.43±0.17 | 1.43±0.19 |
| *Chrebpb* | (S),C | 1.00±0.11 | 1.69±0.10 [#] | 0.97±0.05 | 1.31±0.18 [(#,*)] |

Gene expression was normalized to *Actb* and *Rn18s* expression and expressed relative to the vehicle-treated male mice. Sig. indicates significant effects ($P < 0.05$) analyzed with two-way ANOVA. Symbols in parentheses [*e.g.*, (S)] indicate a tendency to significance ($P < 0.10$). Abbreviations: C, corticosterone treatment; S, sex; ×, interaction of corticosterone treatment and sex. * $P < 0.05$, [(*)] $P < 0.10$ (tendency to significance), for sex difference between mice with the same treatment; [#] $P < 0.05$, for effect of corticosterone treatment in mice of the same sex, by *post hoc* test.

To gain insight into the underlying mechanisms of the corticosterone-induced insulin resistance, especially the resemblance of a postprandial-like state, we determined EGP and GCR using an IPGTT enriched with a stable isotope tracer [U-$^{13}$C$_6$]-D-glucose. In contrast to the more severe whole-body insulin resistance in the corticosterone-treated male mice, the high blood insulin concentrations upon corticosterone treatment resulted in lower glucose production in male mice but not in female mice. Because GCs stimulate and insulin suppresses hepatic gluconeogenesis, it is hard to separate the contribution of these two factors in the control of EGP. Quinn *et al.* (45) have shown that female mice have a higher hepatic susceptibility to GCs. Thus, more pronounced actions of GCs in female mice might overrule the inhibitory effect of insulin on EGP or, alternatively, the FBG levels of corticosterone-treated mice were at their lowest limit which requires EGP to prevent symptomatic hypoglycemia. Corticosterone treatment had opposite effects on GCR in male and female mice. GCR tended to increase in female mice but tended to decrease in male mice. These findings confirm that peripheral insulin resistance was more severe in corticosterone-treated males than in corticosterone-treated females because the elevated insulin levels

by corticosterone treatment should have increased GCR substantially in both sexes. Altogether, our data show that the sex-differential effects of high-dose corticosterone treatment on insulin sensitivity were mainly driven by the more pronounced insulin resistance of peripheral tissues in male mice.

Remarkably, we observed that BW of corticosterone-treated female mice in this study increased much more than that of corticosterone-treated male mice. This seems in contrast to the more severe insulin resistance in corticosterone-treated male mice, as weight gain usually links with an increase in insulin resistance (46,47). The more pronounced increase in BW in female mice could be explained by the well-known effect of GC-induced muscle atrophy (48). Because lean mass of male C57BL/6J mice at this age is in general 6 g heavier than that of female mice (49), corticosterone treatment could lead to a substantial reduction in muscle mass in male mice and thereby masking an increase in fat mass resulting in an unchanged total BW. Nevertheless, we observed that the fold increase in WAT mass was greater upon corticosterone treatment in female mice than in male mice, suggesting a sex-dependent expansion rate of WAT to GCs.

WAT stores lipid and can expand by enlarging cell size (hypertrophy), increasing cell number (hyperplasia), or a combination of both (50,51). Hypertrophic expansion is considered more detrimental than hyperplasic expansion, as hypertrophy is associated with reduced insulin sensitivity (50). Adipose tissue expansion generally shows a depot-related pattern; that is, subcutaneous WAT is more hyperplastic than visceral WAT (51). Our finding that corticosterone-treated female mice tended to have larger WAT depots but smaller adipocytes, together with a lower mRNA expression of *Adamts1* and *Lep*, than do corticosterone-treated male mice suggests that female mice displayed more hyperplastic expansion in WATs than did male mice upon corticosterone treatment. This is in accordance with a previous study showing that corticosterone-induced adipocyte expansion was greater in ovariectomized female rats than in sham-operated female rats, which suggests a role for sex steroids in the sex difference in adipose depot expandability (52).

Besides its fundamental function as an energy reservoir, WAT secretes a number of adipokines that are essential mediators regulating systemic energy homeostasis and are also linked with the mode of expansion as previously discussed (50,53). We found that corticosterone treatment increased *Lep* expression in gWAT, iWAT, and BAT and increased circulating leptin levels in both sexes of mice, which was linked with an increased WAT mass and was in line with other studies (54). Moreover, the increased food intake after corticosterone treatment might indicate leptin resistance in the corticosterone-treated mice (53,54). Circulating levels of total and HMW adiponectin and A/L ratio are

**2**

considered reliable indicators for assessing adipocyte dysfunction and metabolic disorder because adiponectin levels decline in obesity and insulin resistance (41,50,55,56). Also in our study, both the A/L ratio and HMW adiponectin/ leptin ratio were reduced in the corticosterone-treated mice. Nevertheless, circulating levels of total adiponectin and HMW adiponectin were elevated upon corticosterone treatment, especially in female mice. In accordance with our data, a previous study in male mice showed that prednisolone treatment increased plasma adiponectin levels and the effect was more pronounced when administering prednisolone to the castrated mice (57). Expression of *Adipoq* in gWAT, iWAT, and BAT of corticosterone-treated mice, however, was lower or tended to be lower than that of the vehicle-treated mice. This contradictory effect on gene expression and total circulating protein level might be explained by the compensatory effect of insulin because our *in vitro* studies in cultured 3T3-L1 white adipocytes and T37i brown adipocytes revealed opposite effects of insulin and corticosterone on the production and secretion of adiponectin. More comprehensive *in vivo* studies are needed to elucidate this counterregulatory effect of insulin and corticosterone on adipocyte adaptations.

Note that our finding on *Adamts1* expression is different from a previous study that reported that dexamethasone-treated mice had a reduced ADAMTS1 abundance in WAT (40). However, another study demonstrated that cortisol treatment of cultured preadipocytes, obtained from WAT of healthy women who had undergone hysterectomy, upregulated *ADAMTS1* expression (58). These discrepancies may be caused by a different type, dosage, or duration of GC used among experiments. Unlike the endogenous GCs cortisol and corticosterone that can activate both GR and MR, dexamethasone is a potent GR activator with minimal mineralocorticoid effects (59), and *Adamts1* is reported to be an MR target gene, at least in cardiomyocytes (60).

Concerning the IPGTT data, an absence in spike of blood glucose levels in corticosterone-treated female mice is unlikely caused by a technical error since [U-$^{13}$C$_6$]-D-glucose can be detected in the blood of the mice and the IPGTT was performed simultaneously in all groups of mice. We speculate that this unique blood glucose pattern in the corticosterone-treated female mice reflects an effective β-cell response to secrete insulin for handling the injected glucose. This is in general confirmed by a recent study by Gasparini *et al.* (61) in which it was shown that only female mice remained insulin-sensitive after 4 weeks treatment with ~250 µg corticosterone per day in drinking water. Although insulin sensitivity was not assessed directly in our study, note that we found an increase in fasting insulin levels in both male and female mice whereas Gasparini *et al.* (61) found that corticosterone-treated female mice had an unchanged insulin concentration. This is likely due to a higher induction

of systemic corticosterone levels by the high-dose corticosterone treatment in our study. Further studies using hyperinsulinemic-euglycemic clamp, the gold standard method for assessing insulin sensitivity, are needed to elucidate the effect of chronic high-dose corticosterone treatment.

Another limitation of our study is the lack of data on energy expenditure of the animals, as we think that the increased food consumption can only partially explain the enhanced fat accumulation and weight gain of the corticosterone-treated mice. Thus, performing quantitative measurement of physical activity together with indirect calorimetry is needed in future studies on sex-dependent corticosterone effects.

A few studies have shown an apparent interaction of sex steroids with GC activity. For instance, estrogen depletion in female mice resulted in a GC-driven development of hepatic steatosis (45). The consequences of this on whole-body metabolism was not addressed in the aforementioned study, but another study revealed that corticosterone-induced metabolic derangements, such as BW gain and WAT expansion, were more severe in ovariectomized than in sham-operated female rats and were counteracted by estradiol supplementation (52). Recently, androgens were also reported to modulate GR activity in liver and adipose tissue of male mice (62). Although some signs/symptoms such as muscle wasting, osteoporosis, purple striae, and nephrolithiasis are more frequent in male patients with Cushing disease, the prevalence of metabolic derangements in Cushing syndrome, such as obesity and glucose abnormalities, does not differ between men and women (63-65). In contrast, metabolic derangements upon systemic or topical use of corticosteroids appeared slightly more frequent in women than in men (66). Thus, despite the irrefutable fact that GCs have more metabolically negative effects in male rodents, which can at least partly be attributed to differences in sex steroid, the clinical manifestation is unclear and requires more dedicated studies.

In conclusion, this study illustrates a sex-dependent insulin resistance caused by continuous treatment with high-dose corticosterone. Morphological changes upon metabolic challenges and adipokine secretions from adipose tissues indicate favorable protective mechanisms in female mice. This result warrants more careful evaluation of sex as a factor in the glucose monitoring strategy of patients receiving corticosteroid therapy.

## Acknowledgements

**2**

## Additional Information

### Disclosure Summary

The authors have nothing to disclose.

### Data Availability

The datasets generated during and/or analyzed during the current study are not publicly available but are available from the corresponding author on reasonable request.

## References and Notes

1. Kuo T, McQueen A, Chen TC, Wang JC. Regulation of Glucose Homeostasis by Glucocorticoids. *Adv Exp Med Biol*. 2015;**872**:99-126.
2. Ramamoorthy S, Cidlowski JA. Corticosteroids: Mechanisms of Action in Health and Disease. *Rheum Dis Clin North Am*. 2016;**42**(1):15-31, vii.
3. Juszczak A, Morris DG, Grossman AB, Nieman LK. Cushing's Syndrome. In: Jameson JL, De Groot LJ, de Kretser DM, Giudice LC, Grossman AB, Melmed S, Potts JT, Weir GC, eds. *Endocrinology: Adult and Pediatric*. Philadelphia: W.B. Saunders; 2016:227-255.e211.
4. Magomedova L, Cummins CL. Glucocorticoids and Metabolic Control. *Handb Exp Pharmacol*. 2016;**233**:73-93.
5. Nieman LK. Cushing's syndrome: update on signs, symptoms and biochemical screening. *Eur J Endocrinol*. 2015;**173**(4):M33-38.
6. Heck AL, Handa RJ. Sex differences in the hypothalamic-pituitary-adrenal axis' response to stress: an important role for gonadal hormones. *Neuropsychopharmacology*. 2019;**44**(1):45-58.
7. Oyola MG, Handa RJ. Hypothalamic-pituitary-adrenal and hypothalamic-pituitary-gonadal axes: sex differences in regulation of stress responsivity. *Stress*. 2017;**20**(5):476-494.
8. Meyer EJ, Nenke MA, Rankin W, Lewis JG, Torpy DJ. Corticosteroid-Binding Globulin: A Review of Basic and Clinical Advances. *Horm Metab Res*. 2016;**48**(6):359-371.
9. Mauvais-Jarvis F, Clegg DJ, Hevener AL. The role of estrogens in control of energy balance and glucose homeostasis. *Endocr Rev*. 2013;**34**(3):309-338.
10. Kautzky-Willer A, Harreiter J, Pacini G. Sex and Gender Differences in Risk, Pathophysiology and Complications of Type 2 Diabetes Mellitus. *Endocr Rev*. 2016;**37**(3):278-316.
11. Law J, Bloor I, Budge H, Symonds ME. The influence of sex steroids on adipose tissue growth and function. *Horm Mol Biol Clin Investig*. 2014;**19**(1):13-24.
12. Kim SN, Jung YS, Kwon HJ, Seong JK, Granneman JG, Lee YH. Sex differences in sympathetic innervation and browning of white adipose tissue of mice. *Biol Sex Differ*. 2016;**7**:67.
13. Macotela Y, Boucher J, Tran TT, Kahn CR. Sex and depot differences in adipocyte insulin sensitivity and glucose metabolism. *Diabetes*. 2009;**58**(4):803-812.
14. Michopoulos V. Stress-induced alterations in estradiol sensitivity increase risk for obesity in women. *Physiol Behav*. 2016;**166**:56-64.
15. Karatsoreos IN, Bhagat SM, Bowles NP, Weil ZM, Pfaff DW, McEwen BS. Endocrine and physiological changes in response to chronic corticosterone: a potential model of the metabolic syndrome in mouse. *Endocrinology*. 2010;**151**(5):2117-2127.
16. van den Beukel JC, Grefhorst A, Quarta C, Steenbergen J, Mastroberardino PG, Lombes M, Delhanty PJ, et al. Direct activating effects of adrenocorticotropic hormone (ACTH) on brown adipose tissue are attenuated by corticosterone. *FASEB J*. 2014;**28**(11):4857-4867.
17. Galarraga M, Campion J, Munoz-Barrutia A, Boque N, Moreno H, Martinez JA, Milagro F, Ortiz-de-Solorzano C. Adiposoft: automated software for the analysis of white adipose tissue cellularity in histological sections. *J Lipid Res*. 2012;**53**(12):2791-2796.
18. RRID:AB_2801466, https://scicrunch.org/resolver/AB_2801466.
19. RRID:AB_2801467, https://scicrunch.org/resolver/AB_2801467.

20. RRID:AB_2307314, https://scicrunch.org/resolver/AB_2307314.

21. Martin RM, Patel R, Zinovik A, Kramer MS, Oken E, Vilchuck K, Bogdanovich N, et al. Filter paper blood spot enzyme linked immunoassay for insulin and application in the evaluation of determinants of child insulin resistance. *PLoS One*. 2012;**7**(10):e46752.

22. RRID:AB_2801469, https://scicrunch.org/resolver/AB_2801469.

23. van Dijk TH, Boer TS, Havinga R, Stellaard F, Kuipers F, Reijngoud DJ. Quantification of hepatic carbohydrate metabolism in conscious mice using serial blood and urine spots. *Anal Biochem*. 2003;**322**(1):1-13.

24. Lee WN, Byerley LO, Bergner EA, Edmond J. Mass isotopomer analysis: theoretical and practical considerations. *Biol Mass Spectrom*. 1991;**20**(8):451-458.

25. Dalla Man C, Caumo A, Basu R, Rizza R, Toffolo G, Cobelli C. Measurement of selective effect of insulin on glucose disposal from labeled glucose oral test minimal model. *Am J Physiol Endocrinol Metab*. 2005;**289**(5):E909-914.

26. Bowe JE, Franklin ZJ, Hauge-Evans AC, King AJ, Persaud SJ, Jones PM. Metabolic phenotyping guidelines: assessing glucose homeostasis in rodent models. *J Endocrinol*. 2014;**222**(3):G13-25.

27. Alquier T, Poitout V. Considerations and guidelines for mouse metabolic phenotyping in diabetes research. *Diabetologia*. 2018;**61**(3):526-538.

28. Utzschneider KM, Prigeon RL, Tong J, Gerchman F, Carr DB, Zraika S, Udayasankar J, Montgomery B, Mari A, Kahn SE. Within-subject variability of measures of beta cell function derived from a 2 h OGTT: implications for research studies. *Diabetologia*. 2007;**50**(12):2516-2525.

29. Tissot S, Normand S, Guilluy R, Pachiaudi C, Beylot M, Laville M, Cohen R, Mornex R, Riou JP. Use of a new gas chromatograph isotope ratio mass spectrometer to trace exogenous 13C labelled glucose at a very low level of enrichment in man. *Diabetologia*. 1990;**33**(8):449-456.

30. Gastaldelli A, Coggan AR, Wolfe RR. Assessment of methods for improving tracer estimation of non-steady-state rate of appearance. *J Appl Physiol (1985)*. 1999;**87**(5):1813-1822.

31. Caumo A, Cobelli C. Hepatic glucose production during the labeled IVGTT: estimation by deconvolution with a new minimal model. *Am J Physiol*. 1993;**264**(5 Pt 1):E829-841.

32. Gottesman I, Mandarino L, Gerich J. Estimation and kinetic analysis of insulin-independent glucose uptake in human subjects. *Am J Physiol*. 1983;**244**(6):E632-635.

33. RRID:CVCL_0123, https://scicrunch.org/resolver/CVCL_0123.

34. RRID:CVCL_S893, https://scicrunch.org/resolver/CVCL_S893.

35. RRID:AB_915783, https://scicrunch.org/resolver/AB_915783.

36. RRID:AB_2315049, https://scicrunch.org/resolver/AB_2315049.

37. RRID:AB_621843, https://scicrunch.org/resolver/AB_621843.

38. Ayala JE, Samuel VT, Morton GJ, Obici S, Croniger CM, Shulman GI, Wasserman DH, McGuinness OP, Metabolic NM, Phenotyping Center Consortium. Standard operating procedures for describing and performing metabolic tests of glucose homeostasis in mice. *Dis Model Mech*. 2010;**3**(9-10):525-534.

39. van den Beukel JC, Boon MR, Steenbergen J, Rensen PC, Meijer OC, Themmen AP, Grefhorst A. Cold Exposure Partially Corrects Disturbances in Lipid Metabolism in a Male Mouse Model of Glucocorticoid Excess. *Endocrinology*. 2015;**156**(11):4115-4128.

40. Wong JC, Krueger KC, Costa MJ, Aggarwal A, Du H, McLaughlin TL, Feldman BJ. A glucocorticoid- and diet-responsive pathway toggles adipocyte precursor cell activity in vivo. *Sci Signal*. 2016;**9**(451):ra103.

41. Lopez-Jaramillo P, Gomez-Arbelaez D, Lopez-Lopez J, Lopez-Lopez C, Martinez-Ortega J, Gomez-Rodriguez A, Triana-Cubillos S. The role of leptin/adiponectin ratio in metabolic syndrome and diabetes. *Horm Mol Biol Clin Investig*. 2014;**18**(1):37-45.

42. Tsuchiya A, Kanno T, Nishizaki T. PI3 kinase directly phosphorylates Akt1/2 at Ser473/474 in the insulin signal transduction pathway. *J Endocrinol*. 2014;**220**(1):49-59.

43. Baraille F, Planchais J, Dentin R, Guilmeau S, Postic C. Integration of ChREBP-Mediated Glucose Sensing into Whole Body Metabolism. *Physiology (Bethesda)*. 2015;**30**(6):428-437.

44. Hwang JL, Weiss RE. Steroid-induced diabetes: a clinical and molecular approach to understanding and treatment. *Diabetes Metab Res Rev*. 2014;**30**(2):96-102.

45. Quinn MA, Xu X, Ronfani M, Cidlowski JA. Estrogen Deficiency Promotes Hepatic Steatosis via a Glucocorticoid Receptor-Dependent Mechanism in Mice. *Cell Rep*. 2018;**22**(10):2690-2701.

46. Paulson QX, Hong J, Holcomb VB, Nunez NP. Effects of body weight and alcohol consumption on insulin sensitivity. *Nutr J*. 2010;**9**:14.

**2**

**2**

47. Shoelson SE, Herrero L, Naaz A. Obesity, inflammation, and insulin resistance. *Gastroenterology.* 2007;**132**(6):2169-2180.

48. Schakman O, Kalista S, Barbe C, Loumaye A, Thissen JP. Glucocorticoid-induced skeletal muscle atrophy. *Int J Biochem Cell Biol.* 2013;**45**(10):2163-2172.

49. Yang Y, Kitten A, Griffey S, Chang F, Dixon K, Browne C, Clary D. Multi-system analysis of physiology on 7 inbred strains of mice. MPD:Jaxwest1. Mouse Phenome Database web resource (RRID:SCR_003212). The Jackson Laboratory; 2003. Accessed 31 December 2018. https:// phenome.jax.org/projects/Jaxwest1.

50. Choe SS, Huh JY, Hwang IJ, Kim JI, Kim JB. Adipose Tissue Remodeling: Its Role in Energy Metabolism and Metabolic Disorders. *Front Endocrinol (Lausanne).* 2016;**7**:30.

51. Lessard J, Tchernof A. Depot- and obesity-related differences in adipogenesis. *Clin Lipidol.* 2012;**7**(5):587-596.

52. de Souza CF, Stopa LRS, Santos GF, Takasumi LCN, Martins AB, Garnica-Siqueira MC, Ferreira RN, et al. Estradiol protects against ovariectomy-induced susceptibility to the anabolic effects of glucocorticoids in rats. *Life Sci.* 2019;**218**:185-196.

53. Stern JH, Rutkowski JM, Scherer PE. Adiponectin, Leptin, and Fatty Acids in the Maintenance of Metabolic Homeostasis through Adipose Tissue Crosstalk. *Cell Metab.* 2016;**23**(5):770-784.

54. Park HK, Ahima RS. Physiology of leptin: energy homeostasis, neuroendocrine function and metabolism. *Metabolism.* 2015;**64**(1):24-34.

55. Bahceci M, Gokalp D, Bahceci S, Tuzcu A, Atmaca S, Arikan S. The correlation between adiposity and adiponectin, tumor necrosis factor alpha, interleukin-6 and high sensitivity C-reactive protein levels. Is adipocyte size associated with inflammation in adults? *J Endocrinol Invest.* 2007;**30**(3):210-214.

56. Fruhbeck G, Catalan V, Rodriguez A, Gomez-Ambrosi J. Adiponectin-leptin ratio: A promising index to estimate adipose tissue dysfunction. Relation with obesity-associated cardiometabolic risk. *Adipocyte.* 2018;**7**(1):57-62.

57. Combs TP, Berg AH, Rajala MW, Klebanov S, Iyengar P, Jimenez-Chillaron JC, Patti ME, Klein SL, Weinstein RS, Scherer PE. Sexual differentiation, pregnancy, calorie restriction, and aging affect the adipocyte-specific secretory protein adiponectin. *Diabetes.* 2003;**52**(2):268-276.

58. Bujalska IJ, Quinkler M, Tomlinson JW, Montague CT, Smith DM, Stewart PM. Expression profiling of 11beta-hydroxysteroid dehydrogenase type-1 and glucocorticoid-target genes in subcutaneous and omental human preadipocytes. *J Mol Endocrinol.* 2006;**37**(2):327-340.

59. Arafah BM. Pharmacology of Glucocorticoids. In: Levine AC, ed. *Adrenal Disorders.* Cham: Springer International Publishing; 2018:67-81.

60. Fejes-Toth G, Naray-Fejes-Toth A. Early aldosterone-regulated genes in cardiomyocytes: clues to cardiac remodeling? *Endocrinology.* 2007;**148**(4):1502-1510.

61. Gasparini SJ, Swarbrick MM, Kim S, Thai LJ, Henneicke H, Cavanagh LL, Tu J, Weber MC, Zhou H, Seibel MJ. Androgens sensitise mice to glucocorticoid-induced insulin resistance and fat accumulation. *Diabetologia.* 2019;**62**(8):1463-1477.

62. Spaanderman DCE, Nixon M, Buurstede JC, Sips HC, Schilperoort M, Kuipers EN, Backer EA, et al. Androgens modulate glucocorticoid receptor activity in adipose tissue and liver. *J Endocrinol.* 2019;**240**(1):51-63.

63. Geer EB, Shen W, Strohmayer E, Post KD, Freda PU. Body composition and cardiovascular risk markers after remission of Cushing's disease: a prospective study using whole-body MRI. *J Clin Endocrinol Metab.* 2012;**97**(5):1702-1711.

64. Pecori Giraldi F, Moro M, Cavagnini F, Study Group on the Hypothalamo-Pituitary-Adrenal Axis of the Italian Society of E. Gender-related differences in the presentation and course of Cushing's disease. *J Clin Endocrinol Metab.* 2003;**88**(4):1554-1558.

65. Ferrau F, Korbonits M. Metabolic comorbidities in Cushing's syndrome. *Eur J Endocrinol.* 2015;**173**(4):M133-157.

66. Savas M, Muka T, Wester VL, van den Akker ELT, Visser JA, Braunstahl GJ, Slagter SN, Wolffenbuttel BHR, Franco OH, van Rossum EFC. Associations Between Systemic and Local Corticosteroid Use With Metabolic Syndrome and Body Mass Index. *J Clin Endocrinol Metab.* 2017;**102**(10):3765-3774.
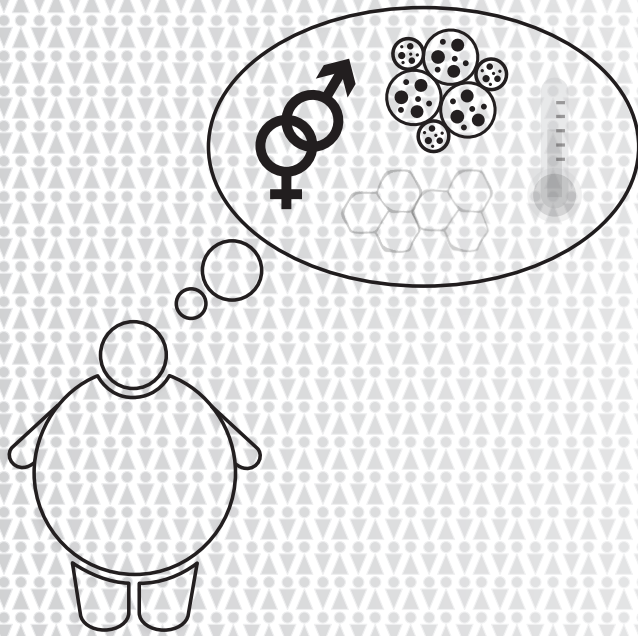
**2**

# Chapter 3

# Sex Difference in the Mouse BAT Transcriptome Reveals a Role of Progesterone in BAT Function

Kasiphak Kaikaew[1,2,*], Aldo Grefhorst[1,3,*], Jacobie Steenbergen[1], Sigrid M.A. Swagemakers[4], Anke McLuskey[1], Jenny A. Visser[1]

1  Department of Internal Medicine, Erasmus MC, University Medical Center Rotterdam, Rotterdam, the Netherlands

2  Department of Physiology, Faculty of Medicine, Chulalongkorn University, Bangkok, Thailand

3  Department of Experimental Vascular Medicine, Amsterdam University Medical Centers, Location AMC, Amsterdam, the Netherlands

4  Department of Pathology and Clinical Bioinformatics, Erasmus MC, University Medical Center Rotterdam, Rotterdam, the Netherlands

*  Shared first authorship

3

## Abstract

Brown adipose tissue (BAT) is a metabolically active organ that exhibits sex-differential features, i.e., being generally more abundant and active in females than in males. Although sex steroids, particularly estrogens, have been shown to regulate BAT thermogenic function, the underlying molecular mechanisms contributing to sexual dimorphism in basal BAT activity have not been elucidated. Therefore, we assessed the transcriptome of interscapular BAT of male and female C57BL/6J mice by RNA sequencing and identified 295 genes showing ≥2-fold differential expression (adjusted $P$<0.05). *In silico* functional annotation clustering suggested an enrichment of genes encoding proteins involved in cell-cell contact, interaction, and adhesion. Ovariectomy reduced the expression of these genes in female BAT towards a male pattern whereas orchiectomy had marginal effects on the transcriptional pattern, indicating a prominent role of female gonadal hormones in this sex-differential expression pattern. Progesterone was identified as a possible upstream regulator of the sex-differentially expressed genes. Studying direct effects of progesterone *in vitro* in primary adipocytes showed that progesterone significantly altered the transcription of several of the identified genes, likely via the glucocorticoid receptor. Moreover, several genes remained sex-differentially expressed under similar *in vitro* culture conditions, indicating intrinsic regulation by the sex origin of cells. In conclusion, this study reveals a sexually dimorphic transcription profile in murine BAT at general housing conditions and demonstrates a role for progesterone in the regulation of the interscapular BAT transcriptome.

## Introduction

A growing number of studies suggest that the prevalence of obesity and obesity-related diseases differs between women and men. Although the global prevalence of obesity is higher in women than in men (1), obese men are more prone to develop obesity-related conditions such as type 2 diabetes mellitus than obese women (2). This sex difference diminishes when women enter menopause, suggesting a prominent role for sex steroids, for instance in controlling adipose tissue function since disturbances in adipose tissue function lead to obesity and its associated metabolic diseases (3,4).

In general, two types of adipose tissue with a distinct physiological function can be recognized. White adipose tissue (WAT) serves as the largest energy-storing organ of the body, while brown adipose tissue (BAT) principally utilizes nutrient substrates for non-shivering thermogenesis, crucial for maintaining body temperature in small mammals and human infants (5). In BAT, thermogenesis is activated by the sympathetic nervous system that secretes norepinephrine (NE) upon stimuli such as cold exposure. Thermogenesis depends on uncoupling proton transport by the unique BAT mitochondrial protein, uncoupling protein 1 (UCP1) (6). BAT also plays a role in maintaining optimal energy balance, as illustrated by the development of obesity in UCP1-ablated mice housed at thermoneutral conditions (7). With the confirmation of the presence of active BAT in adults, BAT has been studied extensively because increasing energy expenditure through BAT activation is considered a potential therapeutic option for obesity (8).

While sex differences in WAT and the role of sex steroids herein have been addressed for many years by numerous excellent studies (9), studies on sex differences in BAT functioning and its role in sex-dependent protection against metabolic diseases is largely lacking, although some studies suggest that sex differences may exist in the presence and activity of BAT (10). It was observed that the prevalence of active BAT was about two-fold higher in women than in men (11). Also in rodents, female rats are reported to have higher relative BAT mass, higher BAT UCP1 protein levels, and greater sizes of mitochondria in BAT (12), Moreover, isolated brown adipocytes of female rats had a greater response to NE than those isolated from male rats (12). Circulating sex steroid concentrations are one of the major differences between males and females of reproductive age and therefore are obvious candidates regulating sex differences in BAT activity. Indeed, the roles of sex steroids in sex-differential energy homeostasis have been demonstrated at many levels (10,13). Especially the effects of estrogens on systemic energy balance and BAT activity have been studied in great detail (14,15). For example, ovariectomy in rodents led to an increase in food intake, weight gain, and lipid accumulation in WATs, but also resulted in

**3**

reduced thermogenic activity in BAT (16,17), suggesting a stimulating effect of ovarian hormones on BAT activity. In addition, central or peripheral injection of 17β-estradiol (E2) in ovariectomized mice resulted in induced BAT thermogenesis, showing a role for estrogens in stimulating BAT activation via the sympathetic nervous system (18). In contrast, orchiectomy led to increased *Ucp1* mRNA expression and UCP1-positive staining in BAT coinciding with elevated body temperature, revealing an inhibitory effect of male gonadal hormones on BAT thermogenesis (19). Treatment of cultured brown adipocytes with sex steroids confirmed that E2 facilitates while testosterone inhibits NE-induced lipolysis, an initial step of thermogenesis in BAT (20).

While sex steroids may control BAT thermogenic activity, the underlying molecular mechanisms contributing to the sex dimorphism in BAT function are still not fully elucidated. Therefore, in this study we have performed RNA-sequencing (RNA-seq) on the interscapular BAT of male and female mice to identify sex differences in the BAT transcriptome. Identified sex-differentially expressed genes were functionally clustered using available biological databases. We also performed gonadectomy (GDX) to study the roles of sex steroids on the expression of these identified genes. In addition, a possible upstream regulator of the sex-differentially expressed genes was studied in primary cultures of brown adipocytes isolated from male and female mice and in a brown adipocyte cell line.

## Materials and Methods

### Animals and housing conditions

All animal experiments were approved by the Animal Ethics Committee at Erasmus MC, Rotterdam, the Netherlands. For transcriptional analysis of BAT, 8-week-old male and female C57BL/6J mice were purchased from Charles River Laboratories (Maastricht, Netherlands). Upon arrival, mice were housed at ~22°C on a 12/12-h dark/light cycle with chow diets and water available *ad libitum*. After one-week acclimation, GDX or sham operation was performed as described previously (21). After the surgery, mice were housed at standard housing conditions for 45 days. After these 45 days, the mice were fasted for 4 h and were sacrificed by cardiac puncture under isoflurane anesthesia. BAT was snap-frozen in liquid nitrogen and stored at −80°C until RNA isolation.

For adipose-derived stromal vascular fraction (SVF) cell culture, male and female C57BL/6J mice were bred in the Erasmus MC animal facility and housed under similar conditions. At 20 weeks old, mice were sacrificed by cardiac puncture under isoflurane anesthesia. BAT was dissected and placed in ice-cold PBS (Gibco, Life Technologies Europe, Bleiswijk, Netherlands) containing 100 U/mL of penicillin, 100 μg/mL of streptomycin, and 0.25 μg/mL of Fungizone (Anti-Anti, Gibco) until SVF isolation.

**RNA isolation**

Total RNA was isolated from BAT using the TriPure isolation reagent (Roche Diagnostics, Mannheim, Germany) and contaminating genomic DNA was removed by the RQ1 RNase-free DNase (Promega Benelux, Leiden, Netherlands), according to the manufacturers' instructions. RNA was quantified with a NanoDrop 2000 spectrophotometer (Isogen Life Science, Utrecht, Netherlands).

**Library preparation, RNA sequencing, and expression analysis**

RNA quality was assessed by an Agilent 2100 Bioanalyzer (Agilent Technologies, Amstelveen, Netherlands). A TruSeq RNA Library Prep Kit v2 (Illumina, Eindhoven, Netherlands) was used for library preparation according to the manufacturer's instructions. Paired-end sequencing with 50 base pairs in length was performed using a HiSeq 2000 sequencer (Illumina). Adapter sequences were trimmed with Cutadapt (version 1.16 with Python 3.6.4) (22). The trimmed reads were aligned to the mouse reference genome mm10 by RNA STAR (Galaxy version 2.6.0b-2) (23). The number of reads per annotated gene was counted with featureCounts (Galaxy version 1.6.4) (24) using the genome annotation GRCm38 (release 97). The differential expression profile was analyzed in R with DESeq2 (package version 1.25.11) (25). Genes with very low expression (average read counts <3) were removed and genes with the Benjamini-Hochberg (BH)-adjusted *P* value <0.05 were considered sex-differentially expressed. The *rlog*-normalized counts of the differentially expressed genes were imported into OmniViz (version 6.1.13.0, Instem Scientific, Staffordshire, UK) and visualized with the OmniViz TreeScape (heat maps including dendrograms of the hierarchical clustering).

**Enrichment and pathway analysis**

Genes with a sex-differential expression ≥2-fold difference were uploaded in DAVID (Bioinformatics Resources, version 6.8; https://david.ncifcrf.gov/) (26). A default DAVID functional annotation (threshold count 2 and EASE 0.1) was performed for Gene Ontology (GO). Subsequently, default DAVID functional annotation tools (e.g. UniProtKB keywords, GO terms, KEGG Pathway, and BioCarta) were selected for functional annotation clustering with a default medium classification stringency (kappa similarity term overlap 3 and threshold 0.5; multiple linkage threshold 0.5; and EASE 0.1).

Next, the ≥2 folds differentially expressed genes together with their $\log_2$-transformed fold differences (female relative to male) were uploaded in Ingenuity Pathway Analysis (IPA, version 49309495; QIAGEN Inc., https://www. qiagenbioinformatics.com/products/ingenuity-pathway-analysis) (27) for expression

analysis using Ingenuity Knowledge Base (genes only) with a default setting (direct and indirect relationships; only experimentally observed confidence) to analyze the functional upstream regulators.

**Isolation of SVF cells, cell culture, and *in vitro* hormonal treatment**

BAT depots from 5–6 mice were pooled, minced in PBS containing 1% BSA (Sigma-Aldrich, Zwijndrecht, Netherlands) and Anti-Anti (Gibco), and centrifuged at 500 g for 6 min. Tissue suspensions were digested in 1 mg/mL collagenase (Sigma-Aldrich), 2.4 U/mL dispase II (Roche Diagnostics), and 0.5 mg/mL trypsin (Gibco) for 30 min at 37°C with gentle agitation. The digested BAT was filtered through a 100-µm mesh and centrifuged at 400 g for 8 min. Pellets were incubated with RBC lysis buffer (eBioscience, Life Technologies Europe) for 5 min, and then centrifuged at 500 g for 8 min. SVF pellets were resuspended in growth medium [DMEM (4.5 g/L glucose with sodium pyruvate and GlutaMAX) containing 10 mM HEPES, 10% fetal bovine serum (FBS), and Anti-Anti (all from Gibco)] and seeded with 200,000 cells/well in 12-wells plates. After a 24-h attachment period, differentiation was initiated by supplementing the growth medium with 4 nM insulin (Sigma-Aldrich), 1 µM rosiglitazone (Enzo Life Sciences, Brussels, Belgium), and 25 µg/mL L-ascorbic acid (Sigma-Aldrich). This differentiation medium was refreshed every 2–3 days for 13 days. For the female brown preadipocyte cell line T37i [(28); a gift provided by Dr. M. Lombès, Inserm U1185, France], cells were maintained and differentiated for 9 days as described previously (29).

Before progesterone stimulation, fully differentiated BAT SVF or T37i cells were steroid-starved for 3 h in starvation medium [original serum-free medium containing 0.2% dextran-coated charcoal-treated FBS (DCC-FBS), prepared as previously described (29)] after which the cells were pretreated for 60 min with 5 or 500 nM of RU486 (Sigma-Aldrich) or EtOH vehicle. Subsequently, cells were treated for 24 h with the indicated concentrations of progesterone (Steraloids, Newport, RI) or EtOH vehicle supplemented to the starvation medium.

To study the effect of progesterone on differentiation of T37i cells, cells were treated with the indicated concentrations of progesterone or EtOH vehicle supplemented to steroid-deprived T37i differentiation medium (similar to the normal T37i differentiation medium, except replacing 10% FBS with 9% DCC-FBS and 1% FBS). For NE stimulation on differentiated T37i cells, cells were starved for 3 h in 0.2% DCC-FCS starvation medium and subsequently stimulated for 24 h with 1 µM NE (Sigma-Aldrich) or HCl vehicle in the starvation medium.

### Glycerol measurement

Cultured media of the NE-stimulated T37i cells were collected, centrifuged for 10 min to remove debris, and used for determination of glycerol concentrations using the glycerol reagent set (INstruchemie, Delfzijl, Netherlands).

### Quantitative PCR

Reverse transcription was performed using the Transcriptor high-fidelity cDNA synthesis kit (Roche Diagnostics). Quantitative PCR (qPCR) was performed using the FastStart Universal SYBR Green Master (Rox) (Roche Diagnostics) with a QuantStudio 7 flex real-time PCR system (Applied Biosystems, Life Technologies, Carlsbad, CA). Gene expression was normalized to the indicated housekeeping genes using the $2^{-\Delta\Delta CT}$ method. Primer sequences of all tested genes are listed in **Table 1**.

## Results

### BAT transcriptional profile of male and female mice

RNA-seq analysis identified 17,798 transcripts in the interscapular BAT of mice, after filtering out transcripts with very low expression levels. Expression levels of these identified transcripts are visualized by the relative female-to-male fold changes in **Fig. 1A**. A total of 2,038 genes were identified being differentially regulated between the sexes (unadjusted $P<0.05$), but when accounting for a BH correction at FDR of 0.1 only 793 transcripts remained differentially expressed. Applying a more stringent BH-adjusted $P<0.05$, trimmed the number to 596 transcripts (**Fig. 1A** and **1B**). Of these 596 genes, 347 genes (58.2%) showed a female-biased expression and 249 genes (41.8%) showed a male-biased expression (**Fig. 1B**). Further trimming by applying a cut-off of two-fold difference resulted in 295 genes being significantly sex-differentially expressed, of which 242 genes (82.0%) showed higher expression and 53 genes (18.0%) showed lower expression in female BAT than in male BAT (**Fig. 1B**). Hierarchical clustering analysis of the 295 genes illustrates the differences in BAT transcriptional profile between male and female mice (**Fig. 1C**).

### Analysis of biological processes of the sex-differentially expressed genes

Of the 295 sex-differentially expressed genes, 291 genes were matched in the DAVID mouse data resources. Top GO annotation terms from enrichment analyses are presented in **Table 2** and top significant functional annotation clusters are presented in **Table 3**. In general, among the leading significant categories and clusters are genes that encode proteins involved in cellular structure and cell-cell contact, interaction, and adhesion.

**Table 1** Primer sequences

| Gene | Forward (5′→3′) | Reverse (5′→3′) |
|---|---|---|
| *Adipoq* | GCACTGGCAAGTTCTACTGCAA | GTAGGTGAAGAGAACGGCCTTGT |
| *Bax* | TGAAGACAGGGGCCTTTTTG | AATTCGCCGGAGACACTCG |
| *Bcl2* | GGACTTGAAGTGCCATTGGT | CATCACGATCTCCCGGTTAT |
| *Bmp8b* | CAACCACGCCACTATGCAG | CACTCAGCTCAGTAGGCACA |
| *C7* | CAACTGCAAGTGGGACTCCTA | CAGCAACTGAACGCCTTCG |
| *Cdh1* | AGACTTTGGTGTGGGTCAGG | ATCTGTGGCGATGATGAGAG |
| *Cfd* | CTACAAGCGATGGTATGATGTGC | GGACCCAACGAGGCATTCT |
| *Cldn3* | AGTGCTTTTCCTGTTGGCGGCTCT | ATCGCGGCGCAGAATAGAGGATCT |
| *Cldn4* | CAGTGCAAGATGTACGACTCGAT | TACCACTGAGAGAAGCATCCCC |
| *Cldn7* | AGGGTCTGCTCTGGTCCT | GTACGCAGCTTTGCTTTCA |
| *Cxcl13* | CATAGATCGGATTCAAGTTACGCC | TCTTGGTCCAGATCACAACTTCA |
| *Epcam* | GCGGCTCAGAGAGACTGTG | CCAAGCATTTAGACGCCAGTTT |
| *Esr1* | TGGGTCATGAGAGTCCTTTGAA | CCGGGATGGAAACTGAACTTT |
| *Fabp4* | GCGAGTAGAATGACAGCTCCTT | CTGTCGTCTGCGGTGATTT |
| *Fkbp5* | ATTTGATTGCCGAGATGTG | TCTTCACCAGGGCTTTGTC |
| *Irf4* | TGCAAGCTCTTTGACACACA | CAAAGCACAGAGTCACCTGG |
| *Krt5* | TCTGCCATCACCCCATCTGT | CCTCCGCCAGAACTGTAGGA |
| *Krt8* | CAAGGTGGAACTAGAGTCCCG | CTCGTACTGGGCACGAACTTC |
| *Krt14* | CCACCTTTCATCTTCCCAATTCTC | GTGCGGATCTGGCGGTTG |
| *Krt18* | CTGGAGGATGGAGAAGATTT | CTTTTATTGGTCCCTCAGTT |
| *Lcn2* | ACTTCCGGAGCGATCAGTT | CAGCTCCTTGGTTCTTCCAT |
| *Lep* | ACCCCATTCTGAGTTTGTCC | TCCAGGTCATTGGCTATCTG |
| *Mup** | CAAAACAGAAAAGGCTGGTGA | TTGTGCAAACCTTTCCTTGA |
| *Nr3c1* | CCGGGTCCCCAGGTAAAGA | TGTCCGGTAAAATAAGAGGCTTG |
| *Pgr* | GGGGTGGAGGTCGTACAAG | GCGAGTAGAATGACAGCTCCTT |
| *Pparg* | GAAAGACAACGGACAAATCACC | GGGGGTGATATGTTTGAACTTG |
| *Ppargc1a* | CCCTGCCATTGTTAAGACC | TGCTGCTGTTCCTGTTTTC |
| *Ptprf* | TGCTCTCGTGATGCTTGGTTT | ATCCACGTAATTCGAGGCTTG |
| *Scnn1b* | ACCCGGTGGTTCTCAATTTGT | AAGTTCCGCAAGGTACACACA |
| *Sdc1* | TGGAGAACAAGACTTCACCTTTG | CTCCCAGCACTTCCTTCCT |
| *St14* | TCATCGCCTACTACTGGTCAGAGT | TGGCGCGATCAACCTCTT |
| *Tsc22d3* | CAGCAGCCACTCAAACCAGC | ACCACATCCCCTCCAAGCAG |
| *Ucp1* | GGCCTCTACGACTCAGTCCA | TAAGCCGGCTGAGATCTTGT |
| *Wfdc2* | AACCAATTACGGACTGTGTGTT | TCGCTCGGTCCATTAGGCT |
| *Actb* | AAGGCCAACCGTGAAAAGAT | GTGGTACGACCAGAGGCATAC |
| *B2m* | ATCCAAATGCTGAAGAACGG | CAGTCTCAGTGGGGGTGAAT |
| *Hprt* | GCAGTACAGCCCCAAAATGG | AACAAAGTCTGGCCTGTATCCAA |
| *Rn18s* | GTAACCCGTTGAACCCCATT | CCATCCAATCGGTAGTAGCG |

\* The primers detect multiple genes of the MUP family due to its high similarity in mRNA sequences.

**3**
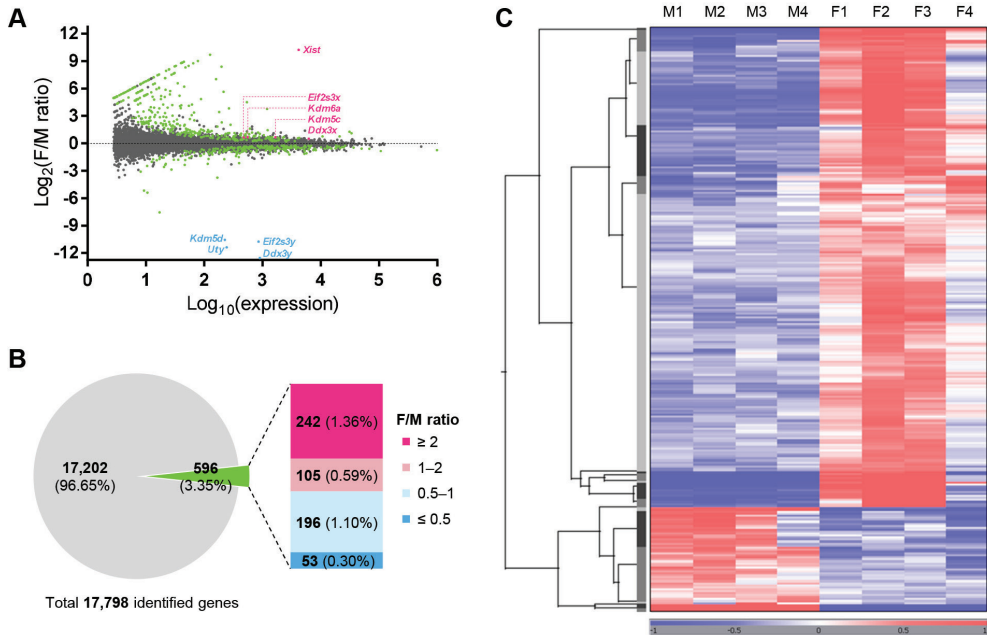
**Fig. 1** Sex difference in BAT RNA-seq profile

**(A)** Scatter plot demonstrating expression levels of all identified genes. Log-transformed average normalized counts of genes in BAT are presented on the X axis and log-transformed fold changes are presented on the Y axis, with positive values indicating female-biased expression and negative values indicating male-biased expression. Blue and pink dots represent known differentially expressed genes and serve as internal controls: blue indicates Y-chromosomal genes, whereas pink indicates X gametologs of the Y-chromosomal genes and the major X inactivation gene, *Xist*. Green dots indicate the significant sex-differentially expressed genes (BH-adjusted *P*<0.05). **(B)** Pie and bar chart demonstrating the number and percentage of identified genes. A two-fold cut-off was applied to select genes with a substantial sex-dependent expression. **(C)** Heat map and dendrogram presenting the expression of the 295 sex-differentially expressed genes (BH-adjusted *P*<0.05 and differential expression ≥2 folds) in BAT of 4 male (M1–M4) and 4 female (F1–F4) mice. Red indicates upregulation and blue indicates downregulation, compared to the geometric mean of the *rlog*-normalized expression levels of each gene, and the color intensity represents the magnitude of the difference.

**Table 2** Top GO terms in each annotation category by enrichment analysis in DAVID

| GO Term | Count | % | *P* value |
|---|---|---|---|
| **Biological process** | | | |
| Cell adhesion | 23 | 7.90 | 7.00E−7 |
| Mammary gland alveolus development | 5 | 1.72 | 1.05E−4 |
| Cellular response to platelet-derived growth factor stimulus | 5 | 1.72 | 2.30E−4 |
| Sodium ion transport | 9 | 3.09 | 2.73E−4 |
| Positive regulation of fat cell differentiation | 6 | 2.06 | 4.95E−4 |
| Canonical Wnt signaling pathway | 7 | 2.41 | 0.001 |
| **Cellular component** | | | |
| Extracellular exosome | 87 | 29.90 | 2.89E−16 |
| Extracellular region | 60 | 20.62 | 8.36E−12 |
| Proteinaceous extracellular matrix | 23 | 7.90 | 2.02E−10 |
| Extracellular space | 48 | 16.49 | 1.79E−8 |
| Apicolateral plasma membrane | 7 | 2.41 | 2.17E−7 |
| Cell junction | 29 | 9.97 | 2.68E−7 |
| **Molecular function** | | | |
| Structural molecule activity | 16 | 5.50 | 5.19E−7 |
| Symporter activity | 10 | 3.44 | 1.63E−5 |
| Cell adhesion molecule binding | 8 | 2.75 | 3.88E−5 |
| Protein binding | 78 | 26.80 | 2.43E−4 |
| Scaffold protein binding | 6 | 2.06 | 6.28E−4 |
| Transcriptional activator activity, RNA polymerase II core promoter proximal region sequence-specific binding | 12 | 4.12 | 8.79E−4 |

Count indicates the number of sex-differentially regulated genes in the GO term and % was calculated based on the total of 291 sex-differentially expressed genes uploaded in DAVID. *P* value indicates a modified Fisher exact test, the DAVID enrichment (EASE score) analysis.

**Table 3** Top functional annotation clusters by DAVID, presenting only GO terms

| Cluster 1 | Enrichment score 10.351 |
|---|---|
| GO terms | Extracellular region; Extracellular space |
| Genes | Acta2, Actg2, Adamts15, Adamts18, Alcam, Ano9, Anxa2, Apln, Aqp5, Areg, Atp4b, Bglap3, Bmp8b, Bnc2, Bsn, Btn1a1, C7, Ccdc3, Ccr3, Cdcp1, Cdh1, Cdh3, Cdh11, Cel, Cfd, Chil1, Clca3a2, Col4a6, Col9a2, Col12a1, Col17a1, Csn3, Ctse, Cxcl13, Cxcl15, Dkk11, Dmbt1, Dmkn, Dsg2, Epcam, Ephb3, Ezr, Faim2, Fam20c, Fbn2, Fcgbp, Fetub, Fgb, Flrt1, Frem1, Fxyd3, Galnt3, Gcnt4, Ggt1, Gldn, Glt1d1, Gpr156, Gpx3, Hc, Igfals, Il17b, Itgb3, Itih2, Krt8, Krt14, Krtdap, Lad1, Lama1, Lamc2, Large2, Lcn2, Lgals7, Ltf, Lvrn, Ly6d, Mfap2, Mfap4, Mfsd2a, Muc15, Mup1*, Myc, Ncan, Nectin4, Nipal2, Npr3, Nt5e, Olfm2, Oxtr, Pdgfd, Phyhip, Piezo2, Plb1, Plet1, Plod2, Plppr3, Prlr, Proc, Prom1, Prom2, Prtn3, Ptk7, Ptn, Ptprf, Ptprn2, R3hdml, S100a9, Scg3, Scnn1b, Sdc1, Serpinb5, Slc1a1, Slc5a1, Slc5a5, Slc5a7, Slc5a8, Slc5a9, Slc6a13, Slc12a2, Slc38a1, Slc44a4, Slco2a1, Slit2, Spint2, Spon1, St14, Sucnr1, Tacstd2, Thsd4, Tlr5, Tmem119, Tmprss2, Tmprss13, Tpbg, Tspan1, Upk3a, Vtcn1, Wfdc2, Wfdc18, Wisp2, Wnt7b |
| **Cluster 2** | Enrichment score 3.902 |
| GO terms | Membrane; Plasma membrane |
| Genes | Abcc8, Alcam, Ano9, Anxa2, Ap1m2, Aqp5, Areg, Atp4b, Atp6v1b1, Basp1, Bnc2, Btn1a1, Cacna1g, Cadps2, Ccr3, Cdcp1, Cdh1, Cdh3, Cdh11, Cldn3, Cldn4, Cldn7, Cldn8, Clic6, Col17a1, Ddx3y, Dmbt1, Dsg2, Dsp, Epcam, Ephb3, Esyt3, Ezr, Faim2, Fer114, Fermt1, Flrt1, Fxyd3, Galnt3, Gcnt4, Ggt1, Gldn, Gpr156, Hpd, Irf4, Irs1, Itgb3, Krt5, Krt19, Lamc2, Large2, Lvrn, Ly6d, Marveld3, Mfsd2a, Mmd2, Mrgprg, Mtmr7, Muc15, Ncan, Nectin4, Nipal2, Npr3, Nt5e, Olfm2, Oxtr, Pdgfd, Perp, Pgr, Piezo2, Pkp1, Plb1, Plch2, Plet1, Plod2, Plppr3, Pmepa1, Prlr, Prom1, Prom2, Prtn3, Ptk7, Ptn, Ptprf, Ptprn2, S100a14, S100a9, Scg3, Scnn1b, Sdc1, Slc1a1, Slc5a5, Slc5a7, Slc5a8, Slc5a9, Slc6a13, Slc12a2, Slc35f3, Slc38a1, Slc44a4, Slco2a1, Slit2, Smim3, Spint2, St14, Sucnr1, Syt14, Tacstd2, Tlr5, Tmem45b, Tmem56, Tmem119, Tmprss2, Tmprss13, Tpbg, Tspan1, Tusc5, Upk3a, Vtcn1, Wisp2, Wnt7b, Wwc1, 6430571L13Rik |
| **Cluster 3** | Enrichment score 3.542 |
| GO terms | Structural molecule activity; Cell periphery; Scaffold protein binding; Intermediate filament |
| Genes | Actg2, Cacna1g, Cdh1, Cgn, Cldn3, Cldn4, Cldn7, Cldn8, Col4a6, Dsp, Ezr, Fgb, Krt5, Krt8, Krt14, Krt15, Krt17, Krt18, Krt19, Lad1, Sprr1a |
| **Cluster 4** | Enrichment score 3.295 |
| GO terms | Symporter activity; Sodium ion transport; Transporter activity; Ion transport |
| Genes | Aqp5, Atp4b, Cacna1g, Clic6, Fxyd3, Kcng4, Lcn2, Ltf, Mfsd2a, Mup1*, Piezo2, Scnn1b, Slc1a1, Slc5a1, Slc5a5, Slc5a7, Slc5a8, Slc5a9, Slc6a13, Slc12a2, Slc38a1, Slco2a1 |
| **Cluster 5** | Enrichment score 3.022 |
| GO terms | Apicolateral plasma membrane; Bicellular tight junction; Calcium-independent cell-cell adhesion via plasma membrane cell-adhesion molecules |
| Genes | Alcam, Cdh1, Cdh3, Cgn, Cldn3, Cldn4, Cldn7, Cldn8, Epcam, Ezr, Krt8, Krt19, Mapk13, Marveld3, Perp, Pof1b, Ptprf, Rasgrf1, Sdc1, Vtcn1 |

\* Mup1 was entered in DAVID as a representative for Mup22 due to its highly similar protein sequences (https://www.uniprot.org/uniprot/Q4FZE8).

**3**

**3**

## Validation of the sex-differentially expressed genes by qPCR and influences of GDX
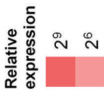
We selected a subset of genes, corresponding to the first five significant functional annotation clusters that showed a high sex-differential expression level in BAT according to the RNA-seq analysis. The summary of their known biological function is reported in the supplementary table, available in an online repository (30). Since sex steroids have been implicated to contribute to sex differences in BAT function (15), expression of these selected genes was validated in BAT of both sham-operated and gonadectomized mice by qPCR (**Fig. 2**). This analysis confirmed that sham-operated female mice had higher BAT mRNA expression of cell adhesion and structural molecules, e.g. epithelial cadherin (E-cadherin), claudins, epithelial cell adhesion molecule (EpCAM), keratins, and syndecan 1 than sham-operated male mice (**Fig. 2**). Removal of female sex steroids by GDX significantly reduced the expression of these genes, but GDX in males only had marginal effects. Hence, female gonadal factors are likely important regulators of the expression of cell adhesion and structural molecules in interscapular BAT of mice.

## Analysis of possible upstream regulators and its regulated genes

Next, we investigated possible regulators of the sex-differentially expressed genes in BAT by upstream regulator analysis in IPA. Top significant upstream regulators are presented in **Table 4**. In the gene, RNA, and protein category (**Table 4**), erb-b2 receptor tyrosine kinase 2 (ErbB2, also known as human epidermal growth factor receptor 2 [HER2]) and transforming growth factor (TGF)-β1 were identified as the top upstream regulators. The predicted state of ErbB2 on sex-differential (female over male) BAT transcriptome was an activation ($Z$=3.58), as well as that of TGF-β1, except that the prediction was less confident ($Z$=1.48). Interestingly, another top identified upstream regulator was the estrogen receptor which is in agreement with the finding that E2 was the top upstream regulator in the endogenous chemical category ($P$=2.45×10$^{-11}$; **Table 4**). The activation state of E2 on sex-differential (female over male) BAT transcriptome was predicted as an activation ($Z$=3.88). Another female sex steroid, progesterone, was predicted as the second upstream regulator in the endogenous chemical category ($P$=1.78×10$^{-7}$) and its activation state was possibly an activation ($Z$=1.35), albeit with less confidence than E2. Tretinoin (also known as all-trans retinoic acid) and dihydrotestosterone (DHT) were identified as additional upstream regulators ($P$=3.02×10$^{-7}$ and $P$=6.20×10$^{-5}$ respectively), but their activation states were uncertain.

The identification of E2 and estrogen receptor as upstream regulators is in line with previous studies implicating a role for E2 in the activation of BAT (15). However, involvement of progesterone in BAT function is less clear. In this study, we decided to further investigate effects of progesterone on BAT.

**3**

| Genes | RNA-seq F/M ratio, mean (95% CI) | qPCR relative expression level, mean±SEM | | | | |
|---|---|---|---|---|---|---|
| | | Male sham | Female sham | Male GDX | Female GDX | Sig. |
| *Epcam* | 520.3 (88.4–3060.7) | 1.00±0.37 | 698.2±247.9 $ | 0.27±0.07 | 19.00±11.01 $,# | ×,S,G |
| *Pgr*† | 439.9 (43.7–4433.0) | 1.00±0.49 | 1.80±0.38 | 0.42±0.25 | 0.15±0.08 # | G |
| *Wfdc2*† | 343.6 (69.3–1703.1) | 1.00±0.18 | 155.8±15.9 $ | 0.96±0.08 | 6.91±2.03 $,# | ×,S,G |
| *Krt8* | 332.5 (68.3–1619.0) | 1.00±0.22 | 2616.0±588.2 $ | 0.94±0.12 | 63.07±46.06 $,# | ×,S,G |
| *Cldn4*† | 315.0 (49.8–1992.2) | 1.00±0.07 | 1486.6±387.7 $ | 1.22±0.10 | 56.81±7.47 $,# | ×,S,G |
| *Krt14* | 243.6 (45.4–1308.0) | 1.00±0.41 | 172.8±48.8 $ | 0.39±0.06 | 5.55±3.08 ($),# | ×,S,G |
| *Krt5*† | 197.8 (38.5–1014.7) | 1.00±0.19 | 6.35±1.26 $ | 1.04±0.26 | 1.26±0.33 # | ×,S,G |
| *Krt18* | 129.5 (37.0–453.2) | 1.00±0.28 | 788.6±143.9 $ | 0.34±0.08 (#) | 20.91±7.82 $,# | ×,S,G |
| *Mup22* | 38.31 (7.08–207.4) | 1.00±0.20 | 17.17±6.73 $ | 0.92±0.29 | 1.46±0.65 # | ×,S,G |
| *Scnn1b*† | 25.90 (4.44–151.2) | 1.00±0.19 | 34.53±12.61 $ | 0.60±0.08 | 1.99±0.42 # | S,G |
| *Cldn3*† | 19.18 (7.50–49.06) | 1.00±0.21 | 103.6±33.1 $ | 1.59±0.49 | 6.26±1.29 $,# | ×,S,G |
| *Bmp8b* | 18.80 (9.08–38.92) | 1.00±0.57 | 28.46±12.26 $ | 0.29±0.06 | 1.71±0.19 $,# | (×),S,G |
| *Cdh1*† | 17.19 (7.98–37.02) | 1.00±0.04 | 26.86±7.88 $ | 0.69±0.23 | 2.12±0.45 $,# | ×,S,G |
| *Lcn2*† | 10.33 (5.75–18.56) | 1.00±0.62 | 4.98±2.14 $ | 0.77±0.39 | 0.32±0.13 # | (×),(G) |
| *St14* | 8.20 (3.88–17.35) | 1.00±0.28 | 11.90±3.05 $ | 0.67±0.19 | 2.84±0.65 $,# | S,G |
| *Cldn7* | 7.33 (2.69–19.97) | 1.00±0.18 | 25.20±6.40 $ | 0.60±0.11 | 2.95±0.84 $,# | ×,S,G |
| *Irf4* | 3.08 (2.15–4.41) | 1.00±0.29 | 3.23±0.41 $ | 2.34±0.56 (#) | 1.11±0.30 # | × |
| *Ptprf* | 2.53 (1.63–3.94) | 1.00±0.15 | 1.97±0.50 | 0.79±0.12 | 0.64±0.06 # | G |
| *Cfd*† | 2.41 (1.74–3.33) | 1.00±0.30 | 5.17±1.02 $ | 1.78±0.25 | 1.05±0.33 # | ×,(S) |
| *Sdc1* | 2.36 (1.70–3.26) | 1.00±0.11 | 1.77±0.31 $ | 0.96±0.09 | 0.75±0.14 # | ×,G |
| *Cxcl13* | 0.14 (0.08–0.25) | 1.00±0.29 | 0.39±0.09 | 2.95±1.32 | 0.22±0.10 $ | (×),S |
| *C7* | 0.07 (0.06–0.10) | 1.00±0.31 | 0.08±0.00 $ | 1.12±0.46 | 0.12±0.03 $ | S |

**Relative expression**

$2^9$ $2^6$ $2^3$ $2^0$ $2^{-3}$ $2^{-6}$ $2^{-9}$

**Fig. 2** Validation of gene expression by qPCR and influences of sex and GDX on sex-differential expression in BAT

The relative female/male (F/M) expression ratios by RNA-seq are shown in descending order in the left column. DESeq2-estimated $\log_2$-transformed fold changes (lfc) and the standard error of the lfc (lfcSE) were used to calculate the F/M ratio by $2^{lfc}$ and the 95% confidence interval by $2^{lfc-1.96(lfcSE)}$ and $2^{lfc+1.96(lfcSE)}$. † indicates genes that the Ingenuity database identified as progesterone-regulated molecules. The other columns present relative expression levels measured by qPCR. Expression levels were normalized to *B2m* and *Rn18s* and are shown relative to the sham-operated male mice. The Sig. column lists significant effects (*P*<0.05) analyzed from the log-transformed expression levels by two-way ANOVA. G for gonadal status (sham or GDX), S for sex, and × for an interaction between G and S. $ indicates a significant sex difference between mice with the same gonadal status and # indicates a significant effect of gonadal status within the same sex, by *post hoc* test (*P*<0.05). Symbol in parentheses indicates a tendency to significance (*P*<0.10). Color demonstrates $\log_2$-transformed relative expression levels. Abbreviation of operation: GDX, gonadectomy.

**Table 4** Upstream regulator analysis of sex-differential expression in BAT by IPA

| Upstream Regulator | Molecule Type | Activation $Z$ score | $P$ value of overlap |
|---|---|---|---|
| **Genes, RNAs, and Proteins** | | | |
| ERBB2 | kinase | 3.58 | 1.16E−15 |
| estrogen receptor | group | 1.43 | 2.43E−15 |
| TGFB1 | growth factor | 1.48 | 7.14E−13 |
| CAV1 | transmembrane receptor | | 1.53E−12 |
| KLF4 | transcription regulator | 3.55 | 1.51E−11 |
| CEBPA | transcription regulator | 0.22 | 5.91E−11 |
| TNF | cytokine | 1.15 | 4.68E−10 |
| CCN5 | growth factor | 1.27 | 6.00E−10 |
| SOX2 | transcription regulator | 0.58 | 9.36E−10 |
| EGF | growth factor | 1.23 | 1.07E−09 |
| **Endogenous Chemicals** | | | |
| 17β-estradiol | endogenous chemical | 3.88 | 2.45E−11 |
| progesterone | endogenous chemical | 1.35 | 1.78E−7 |
| tretinoin | endogenous chemical | −0.10 | 3.02E−7 |
| dihydrotestosterone | endogenous chemical | 0.53 | 6.20E−5 |

Activation $Z$ score identifies upstream regulators that can explain observed gene expression fold changes in the dataset and predicts the activation state of the possible upstream regulators based on the Ingenuity Knowledge Base. $Z>2$ indicates a significant prediction of an activated state whereas $Z<−2$ indicates a significant prediction of an inhibited state. $P$ value of overlap indicates enrichment of the database-known regulated genes in the dataset.

**Effects of progesterone on the RNA-seq–identified sex-differentially expressed genes in SVF-differentiated brown adipocytes**

Direct effects of progesterone on the gene transcription of the validated sex-differentially expressed genes reported in **Fig. 2** was assessed in SVF-differentiated primary brown adipocytes. Ingenuity database identified a total of 25 genes as progesterone-regulated molecules in our dataset, of which 9 genes (*Cdh1, Cfd, Cldn3, Cldn4, Krt5, Lcn2, Pgr, Scnn1b,* and *Wfdc2)* were among the qPCR-validated genes in BAT. We first determined whether these 9 IPA-identified progesterone-regulated genes were detectable in male and female SVF-differentiated brown adipocytes by qPCR. We could only detect mRNA expression of *Cfd, Lcn2,* and *Pgr* (**Fig. 3A**), of which the expression levels at basal conditions in primary brown adipocytes confirmed the higher expression levels in female than in male BAT. Progesterone stimulation for 24 hours revealed that progesterone dose-dependently reduced *Cfd* mRNA expression in differentiated

SVFs of both sexes (**Fig. 3B**), while it induced *Lcn2* (**Fig. 3C**) but reduced *Pgr* (**Fig. 3D**) mRNA expression more prominently in female adipocytes than in male adipocytes.

Apart from *Pgr*, which encodes the nuclear progesterone receptor (PR) and is a known progesterone-regulated gene, we also investigated the mRNA expression levels of other nuclear receptors to determine whether they may underlie the progesterone effects. Interestingly, progesterone dose-dependently reduced *Nr3c1* [encoding the glucocorticoid receptor (GR)] mRNA expression in adipocytes of both sexes (**Fig. 3E**). Moreover, mRNA expression of a GR-target gene *Tsc22d3* [also known as glucocorticoid-induced leucine zipper (*Gilz*)] was dose-dependently upregulated by progesterone treatment in adipocytes of both sexes (**Fig. 3F**), implicating involvement of GR signaling in the progesterone effects in these SVFs.

As RU486 is a PR- and GR-antagonist with a more PR-specific competitive antagonism at low concentrations (i.e. 5 nM) and a dual PR- and GR-antagonism at high concentrations (i.e. 500 nM) (31), we co-administrated progesterone with 5 or 500 nM of RU486 to study the contribution of PR and GR in the observed progesterone effects. Noticeably, the progesterone-induced upregulation of *Tsc22d3* mRNA expression remained unaffected upon 5 nM of RU486 co-administration, but was blocked in the presence of 500 nM of RU486 (**Fig. 3F**), confirming specificity of the selected RU486 doses. Similarly, we observed that progesterone influences on *Cfd*, *Lcn2*, and *Pgr* (**Fig. 3B–3D**) mRNA expression levels were marginally affected at 5 nM of RU486, but were completely blunted with 500 nM of RU486 cotreatment, suggesting GR-mediated responses of progesterone on these genes.

Next, we determined whether progesterone could affect the expression of the 13 qPCR-validated sex-differentially expressed genes not present in the IPA database of progesterone-regulated molecules (**Fig. 2**). By qPCR, only the mRNA expression of *C7*, *Ptprf*, *Scd1*, and *Krt14* was detectable in SVF-differentiated primary brown adipocytes (**Fig. 3G**). Unlike the expression pattern observed in the interscapular BAT, we found that mRNA expression levels of *C7* were higher in female- than in male-derived adipocytes and progesterone treatment of differentiated SVFs stimulated *C7* mRNA expression in adipocytes of both sexes (**Fig. 3H**). This stimulatory effect was abolished only by the 500 nM of RU486 but not by the 5 nM of RU486 cotreatment. Progesterone marginally inhibited *Ptprf* mRNA expression only in male-derived adipocytes (**Fig. 3I**) but did not affect *Sdc1* (**Fig. 3J**) and *Krt14* (data not shown) mRNA expression in cells of either sex. Of note, the finding that mRNA expression of only 7 out of 22 qPCR-validated sex-differentially expressed genes in the interscapular BAT were detectable in primary brown adipocytes (**Fig. 3A** and **3G**) suggests that these other 15 genes may be expressed by other cell types in the BAT depot.

**3**
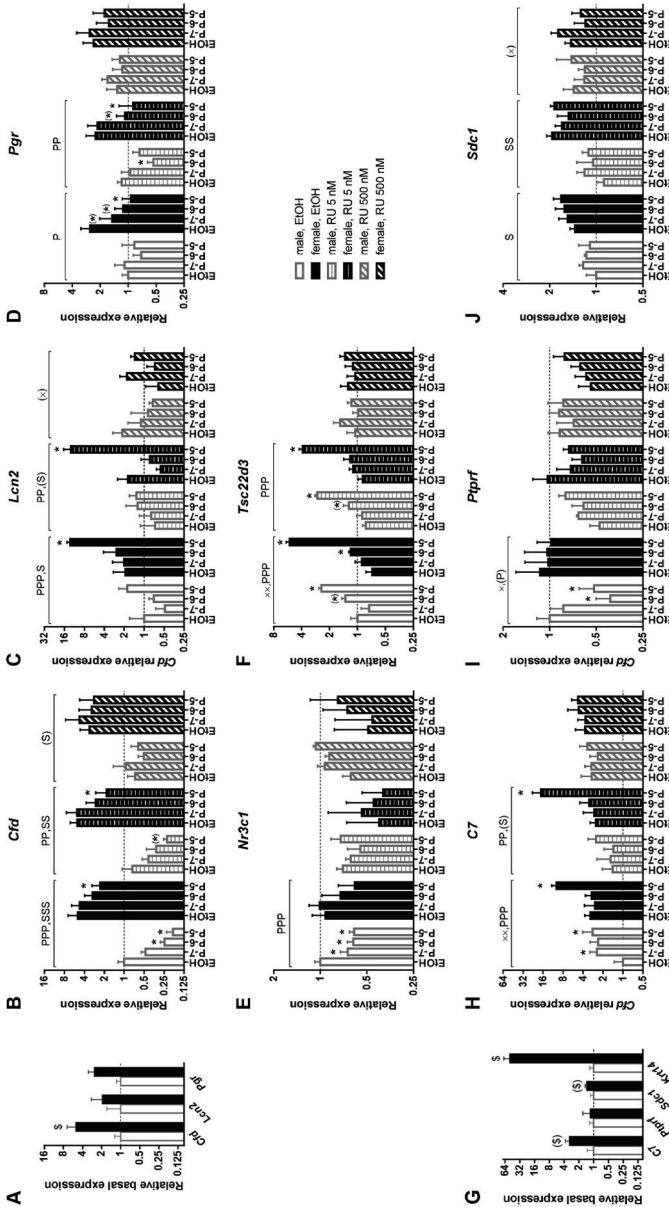


**Fig. 3** Effects of progesterone on the RNA-seq–identified sex-differentially expressed genes in SVF-differentiated brown adipocytes

SVF-derived primary cultures of brown adipocytes from male and female BAT were stimulated with progesterone at indicated concentrations: P-7 ($10^{-7}$ M), P-6 ($10^{-6}$ M), or P-5 ($10^{-5}$ M), together with RU486 (5 or 500 nM) or EtOH vehicle. Expression levels were normalized to *Actb* and *Hprt*, depicted relative to the level of EtOH-treated male adipocytes, and presented as mean±SEM. Data were log-transformed before statistical analyses. Basal mRNA expression levels of (**A**) the RNA-seq–identified sex-differentially expressed and IPA-identified progesterone-regulated genes and (**G**) the remaining RNA-seq–identified sex-differentially expressed genes. \$ indicates a significant sex difference [*P*<0.05] or a tendency to differ [P<0.10, (\$)] by unpaired *t* tests. (**B–F** and **H–J**) mRNA expression levels of the indicated genes. Two-way repeated measures ANOVA was performed to identify the effects of sex and progesterone in each RU486 condition. Significant effects are presented as follows: (S), $P_{sex}$ <0.10; S, $P_{sex}$ <0.05; SS, $P_{sex}$ <0.01; SSS, $P_{sex}$ <0.001; (P), $P_{progesterone}$ <0.10; P, $P_{progesterone}$ <0.05; PP, $P_{progesterone}$ <0.01; PPP, $P_{progesterone}$ <0.001; (×), $P_{sex×progesterone}$ <0.10; ×, $P_{sex×progesterone}$ <0.05; and ××, $P_{sex×progesterone}$ <0.01. Dunnett's *post hoc* tests were applied when appropriate. * indicates a significant difference [*P*<0.05] and (*) indicates a tendency to differ [*P*<0.10] from the EtOH control.
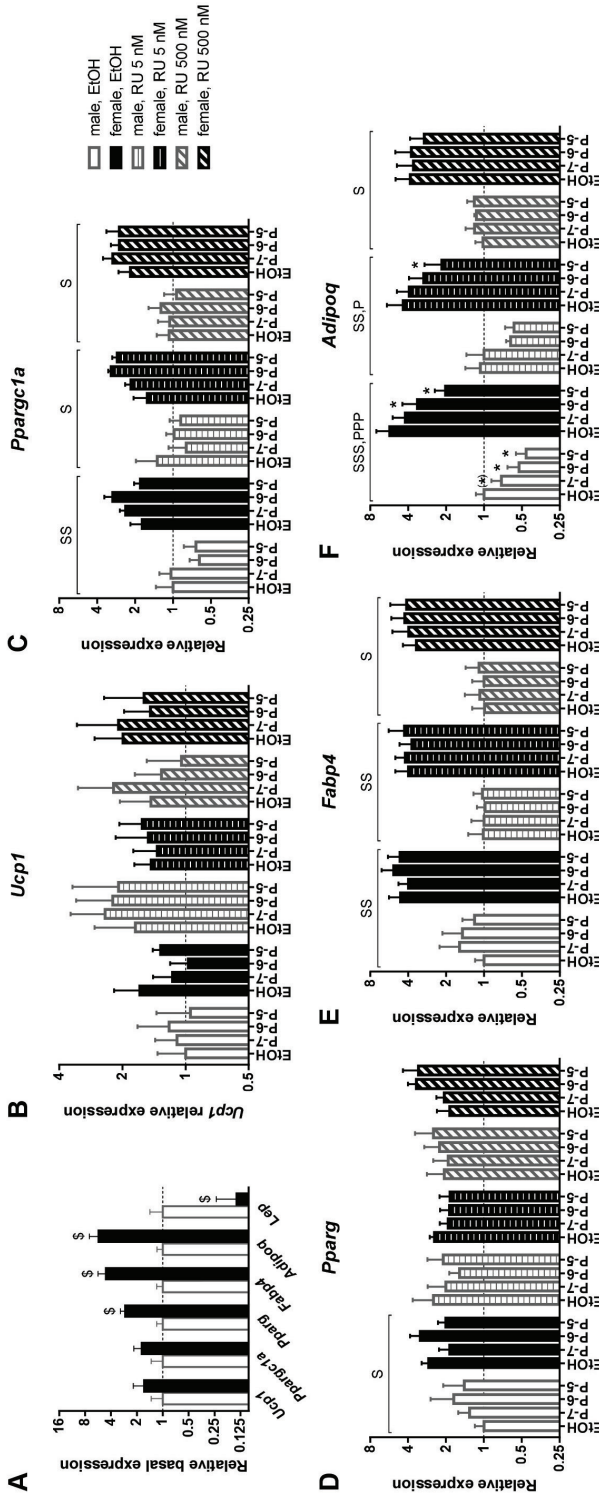
## Effects of progesterone on adipocyte markers in SVF-differentiated brown adipocytes

Since our results suggest that progesterone may regulate some of the sex-differentially expressed genes in BAT, we next determined whether progesterone affects adipocyte function by analyzing the expression of common adipocyte markers in differentiated SVFs. At basal conditions, mRNA expression of *Ucp1* and its transcription activator *Ppargc1a* were higher in female adipocytes than in male adipocytes, but both failed to reach significance ($P>0.10$; **Fig. 4A**). Female adipocytes had significantly higher expression levels of adipogenic differentiation and maturation genes *Pparg*, *Fabp4*, and *Adipoq* than male adipocytes (**Fig. 4A**). In addition, female adipocytes had a lower expression of the classical white adipocyte marker *Lep* than male adipocytes, suggesting a more metabolically active phenotype of female differentiated SVFs from BAT (**Fig. 4A**), although it should be noted that *Lep* mRNA expression was relatively low in these cells. Progesterone treatment did not significantly affect expression levels of *Ucp1* (**Fig. 4B**), *Ppargc1a* (**Fig. 4C**), *Pparg* (**Fig. 4D**), and *Fabp4* (**Fig. 4E**). Intriguingly, progesterone dose-dependently reduced *Adipoq* mRNA expression in adipocytes of both sexes (**Fig. 4F**), of which the inhibitory effect of progesterone was also likely driven by GR since the effect was marginally affected by 5 nM of RU486 cotreatment but was blunted by 500 nM of RU486 cotreatment.

## Effects of progesterone in a brown adipocyte cell line

To confirm the effects of progesterone on the expression of common brown adipocyte markers, we stimulated differentiated T37i, a female brown adipocyte cell line, with progesterone for 24 hours. High doses of progesterone significantly reduced *Ucp1* mRNA expression (**Fig. 5A)** but did not significantly influence mRNA expression of *Ppargc1a* (**Fig. 5B**). In contrast, *Pparg* mRNA expression was induced by high doses of progesterone (**Fig. 5C**). Interestingly, mRNA expression of *Fabp4* was induced by $10^{-6}$ and $10^{-5.5}$ M of progesterone stimulation, but tended to be reduced by $10^{-5}$ M of progesterone stimulation (**Fig. 5D**). Expression levels of both adipokines *Adipoq* and *Lep* were reduced by high-dose progesterone stimulation (**Fig. 5E** and **5F**).

Concerning the expression of receptors that can potentially mediate the effects of progesterone, we found that *Pgr* mRNA expression could not be detected in the T37i cells (data not shown) while *Nr3c1* mRNA expression was downregulated by progesterone stimulation, albeit only statistically significant at the highest tested concentration of $10^{-5}$ M (**Fig. 5G**). Transcription levels of the GR target genes *Tsc22d3* (**Fig. 5H)** and *Fkbp5* (data not shown) were dose-dependently upregulated, supporting an effect likely driven by the GR-signaling cascade.

**3**



**Fig. 4** Effects of progesterone on adipocyte markers in SVF-differentiated brown adipocytes

SVF-derived primary cultures of brown adipocytes from male and female BAT were stimulated with progesterone at indicated concentrations: P-7 ($10^{-7}$ M), P-6 ($10^{-6}$ M), or P-5 ($10^{-5}$ M), together with RU486 (5 or 500 nM), or EtOH vehicle. Expression levels were normalized to *Actb* and *Hprt*, depicted relative to the level of EtOH-treated male adipocytes, and presented as mean±SEM. Data were log-transformed before statistical analyses. **(A)** Basal mRNA expression levels of common adipocyte markers. $ indicates a significant sex difference [*P*<0.05] by unpaired *t* tests. **(B–F)** mRNA expression levels of the indicated genes. Two-way repeated measures ANOVA was performed to identify the effects of sex and progesterone in each RU486 condition. Significant effects are presented as follows: S, $P_{sex}$ <0.05; SS, $P_{sex}$ <0.01; SSS, $P_{sex}$ <0.001; P, $P_{progesterone}$ <0.05; PPP, $P_{progesterone}$ <0.001. Dunnett's *post hoc* tests were applied when appropriate. * indicates a significant difference [*P*<0.05] and (*) indicates a tendency to differ [*P*<0.10] from the EtOH control.
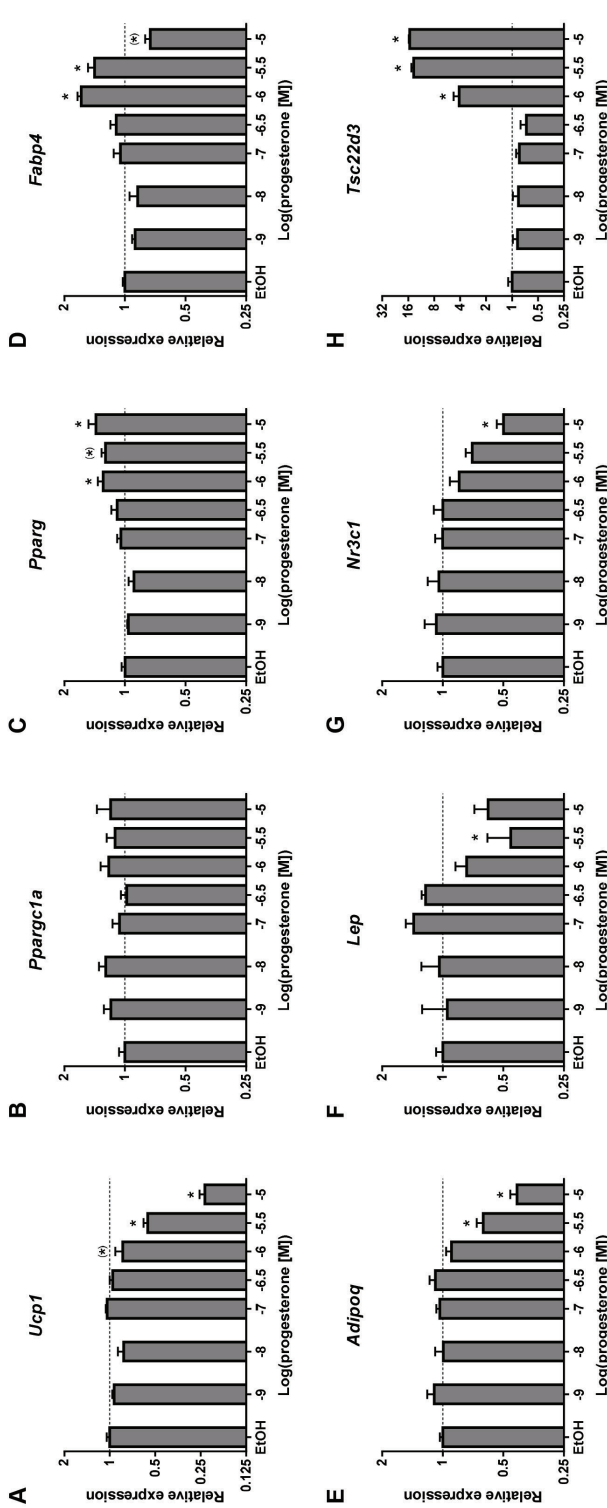
**Fig. 5** Effect of progesterone on differentiated T37i brown adipocytes

Differentiated T37i brown adipocytes were treated for 24 hours with progesterone at indicated concentrations. Expression levels were normalized to *Actb* and *B2m*, depicted relative to the EtOH vehicle-treated condition, and presented as mean±SEM. Data were log-transformed before statistical analyses with one-way ANOVA. * indicates a significant difference [*P*<0.05] and (*) indicates a tendency to differ from the EtOH-treated condition by Dunnett's *post hoc* tests.

**3**

Since progesterone affected the expression of *Pparg* (the master transcriptional activator of adipogenesis) and *Ucp1* expression in differentiated T37i cells, we next determined the impact of progesterone on T37i differentiation by adding progesterone to the differentiation cocktail. *Ucp1* and *Ppargc1a* (the transcriptional activator of mitochondrial biogenesis) mRNA expression levels were strongly upregulated during differentiation ($P_{day}$ <0.001), but were significantly inhibited in the presence of progesterone at the highest concentration (**Fig. 6A** and **6B**). In contrast, mRNA expression of *Pparg* was induced by co-stimulation with $10^{-6}$ M and $10^{-5}$ M of progesterone (**Fig. 6C**), while expression of the mature adipocyte marker *Fabp4* was not significantly regulated by progesterone (**Fig. 6D**). However, at the early differentiation phase (day 3), $10^{-7}$ M and $10^{-6}$ M of progesterone induced *Adipoq* mRNA expression, but this effect was absent at later stages when even a downregulation was seen at the highest concentration of $10^{-5}$ M after 9 days of differentiation (**Fig. 6E**). *Lep* mRNA expression was inhibited at the highest dose of progesterone treatment throughout differentiation (**Fig. 6F**). Of note, mRNA expression levels of a pro-apoptotic marker *Bax* and an anti-apoptotic marker *Bcl2* were not significantly affected by progesterone cotreatment (data not shown), suggesting that progesterone did not hamper cell survival. Subsequently, we tested the NE-induced thermogenic activity in differentiated T37i cells with/without progesterone treatment during differentiation. Cotreatment of high-dose progesterone during differentiation significantly inhibited baseline mRNA expression levels of *Ucp1* (**Fig. 6G**) and *Ppargc1a* (**Fig. 6H**). However, in the presence of progesterone the cells remained responsive to NE since NE stimulation induced the expression of these thermogenic genes in T37i cells, albeit that the NE-induced expression levels were reduced in cells treated with high concentrations of progesterone (**Fig. 6G** and **6H**). Furthermore, NE-induced glycerol release from T37i cells (a measure for thermogenic activity) was dose-dependently reduced by progesterone treatment during adipocyte differentiation (**Fig. 6I**).

## Discussion

To the best of our knowledge, this is the first study to investigate sex differences in the global transcriptional profile by RNA-seq in the interscapular BAT of mice at reproductive age and at basal housing conditions. Functional annotation and clustering showed enrichment of genes encoding proteins involved in cellular structure, cell-cell contact, and cell adhesion. Although female BAT was isolated randomly throughout the estrous cycle, the sex-differential expression remained apparent suggesting a robust sex-dependent regulation of transcription in BAT. In support, we confirmed our previous findings by this approach, showing that *Bmp8b* is sex-differentially expressed in BAT (32).
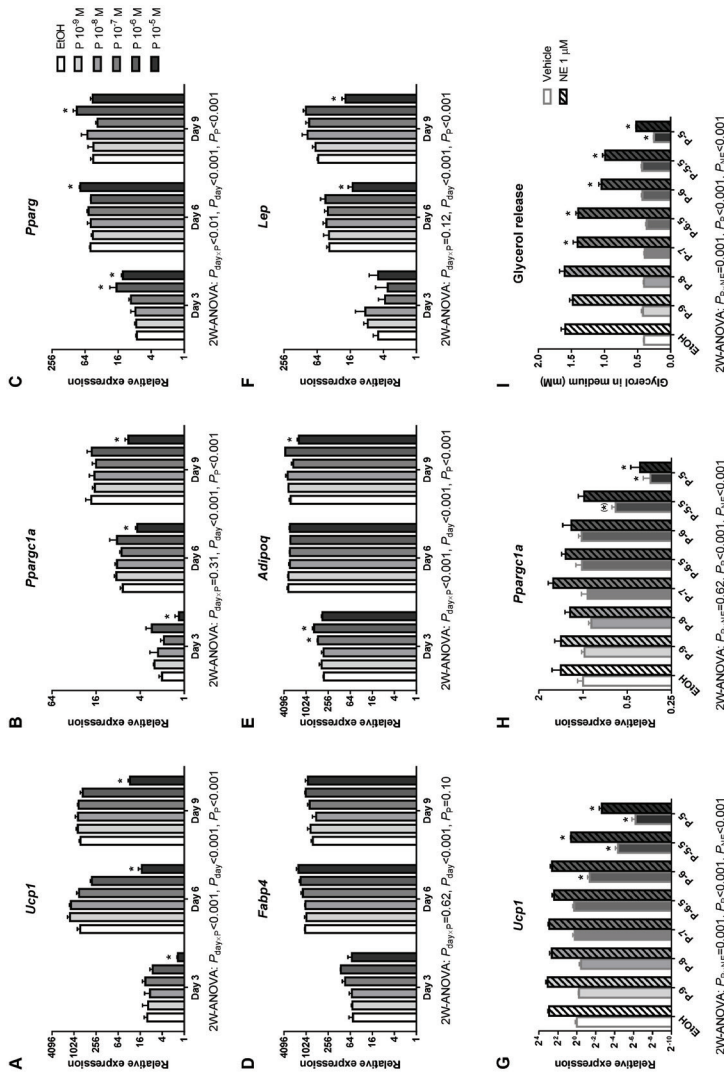
**Fig. 6** Effect of progesterone treatment during differentiation of T37i brown adipocytes

Progesterone (P) at indicated concentrations were treated during differentiation of T37i brown preadipocytes until full differentiation at day 9. Data are presented as mean±SEM. Gene expression data were log-transformed before statistical analyses with two-way ANOVA. * indicates a significant difference [$P$<0.05] and (*) indicates a tendency to differ from the EtOH-treated condition by Dunnett's *post hoc* tests. (**A–F**) Days after differentiation, when the differentiating cells were collected, are plotted on the X axis. Expression levels were normalized with *Actb* and *B2m* and depicted relative to the levels in undifferentiated cells (day 0). (**G–I**) Nine-day differentiated cells with/without progesterone during differentiation were stimulated for 24 hours with 1 μM of norepinephrine (NE) or vehicle and analyzed for mRNA expression or glycerol release in cultured media. Gene expression levels were normalized with *Actb* and *B2m* and depicted relative to levels of the EtOH-treated/vehicle-stimulated condition. Concentrations of progesterone treatment during differentiation are indicated on the X axis as follows: P-9 ($10^{-9}$ M), P-8 ($10^{-8}$ M), P-7 ($10^{-7}$ M), P-6.5 ($10^{-6.5}$ M), P-6 ($10^{-6}$ M), P-5.5 ($10^{-5.5}$ M), and P-5 ($10^{-5}$ M).

**3**

**3**

Cell adhesion is an essential process in maintaining tissue structure and cellular interaction with neighboring cells or with the extracellular matrix (ECM) (33). Structural and adhesion proteins, such as E-cadherin, claudins, and keratins, are well-known for their role in this process as well as in epithelial-to-mesenchymal transition, cancer progression, and tumor metastasis (34). However, their role in adipose tissues is less clear, although the microenvironment is shown to be important for visceral and subcutaneous WAT morphology and function, including the formation of new vessels to promote optimal tissue expansion (35,36). Upon high-fat diet (HFD) feeding, the murine male gonadal WAT showed a lack of angiogenesis whereas the murine female gonadal WAT had a high vascular density, together with an upregulation of the angiogenic factors, e.g. *Vegfa* and *Vegfr2* (37). The importance of the ECM is also illustrated by a study of Grandl *et al.* (38), showing that adipose progenitor cells isolated from gonadal WAT of male mice differentiated better when they were cultured in decellularized ECM of BAT or subcutaneous WAT than when they were cultured without ECM or in decellularized ECM of visceral WAT (38). In support of our findings in BAT, a study comparing obesity-prone and obesity-resistant rats in response to a HFD showed that genes encoding proteins involved in cell structure and motility constituted almost a quarter of the differentially expressed genes, with the lowest expression in the obesity-prone rats (39). However, no major overlap is observed between the genes detected in that study with our identified genes. Importantly, we observed that the expression of most of the identified structural and cell-adhesion genes was very low in our primary brown adipocyte cultures, despite having detectable expression in BAT itself. This might suggest that *in vivo* these genes are expressed by non-adipocyte cell types in BAT, such as endothelial cells and immune cells, and that these cell types play an essential role in maintaining an optimal microenvironment for BAT (35,40).

Upstream regulator analysis of the sex-differentially expressed genes identified ErbB2 and TGF-β1 as the most significant upstream regulators. ErbB2, a transmembrane tyrosine kinase receptor protein, is present in adipose-derived stem cells and is involved in adipogenic proliferation and differentiation (41). TGF-β1, a member of the TGF-β family of growth and differentiation factors, functions in adipose-derived stem cells to promote angiogenesis for optimal blood supply during adipose expansion (41). In mice, serum TGF-β1 levels correlate with obesity and blocking of its principal signal transducer Smad3 or treatment with a TGF-β neutralizing antibody resulted in browning of WAT and prevented development of obesity (42). Upstream regulator analysis also identified E2, progesterone, and DHT as endogenous hormones regulating the expression of the identified genes. Moreover, the fact that ovariectomy reduced the mRNA expression levels while orchiectomy almost had no significant

effect, strongly suggest a predominant role for female sex steroids in the sex-dimorphic expression pattern in BAT. Analysis of gene expression in primary brown adipocytes, isolated and differentiated from BAT SVF cells of male and female mice, showed that this sex-dependent expression pattern persisted under similar culture conditions. A similar pattern was observed for some of the common brown adipocyte markers, such as *Ppargc1a*, *Pparg*, *Fabp4*, and *Adipoq*. Combined, this suggests that the sex-dependent expression pattern is controlled by sex steroids but also partly by intrinsic factors such as the presence of X- and/or Y-chromosomes as well as epigenetic differences between the sexes. As discussed above, most of the identified structural and cell-adhesion genes are likely expressed by non-adipocytes cell types in BAT. Additional studies are, therefore, needed to determine which cell types express these genes in order to identify their role in BAT and to determine whether these genes are directly regulated by sex steroids. Based on literature, progesterone might be involved in the regulation of the expression of our identified genes, such as *Cdh1*, *Cfd*, and *Lcn2*, since these have been reported to show progesterone-dependent regulation in the endometrium, a tissue that also becomes highly vascularized during the preimplantation stage (43-46).

The role of progesterone in regulating BAT function has been studied in much less detail than the other female sex steroid E2, despite its elevated levels during the luteal phase and pregnancy. Furthermore, available data for progesterone effects on BAT activity are conflicting. Regarding the thermogenic function of BAT, progesterone treatment was found to induce NE-stimulated *Ucp1* mRNA expression in primary cultures of mouse brown adipocytes, but surprisingly only at the lowest stimulatory concentration of $10^{-9}$ M and not at higher stimulatory concentrations of $10^{-8}$ or $10^{-7}$ M (47). The ratio of $\alpha_{2A}/\beta_3$-AR receptors in primary brown adipocyte cultures was also reduced by progesterone treatment, reflecting induced thermogenic capacity, by all tested concentrations of $10^{-9}$, $10^{-8}$, and $10^{-7}$ M (20). In contrast, another recent study showed that the mRNA expression of *Ucp1* and other thermogenic genes in murine BAT was reduced during pregnancy as well as by *in vivo* progesterone treatment. Furthermore, treatment of primary brown adipocytes by $5\times10^{-7}$ M progesterone reduced NE-stimulated *Ucp1* mRNA expression (48). In our study, progesterone stimulation of primary cultures of brown adipocytes at a physiological concentration for female mice ($10^{-7}$ M) (49) or at supra-physiological concentrations ($10^{-6}$ and $10^{-5}$ M) did not affect *Ucp1* mRNA expression. However, in the T37i brown adipocyte cell line, progesterone treatment at high concentrations ($10^{-5.5}$ and $10^{-5}$ M) clearly inhibited *Ucp1* mRNA expression. Expression of common mature brown adipocyte markers such as *Ppargc1a*, *Pparg*, and *Fabp4* was not regulated by progesterone in primary cultures, although they showed a sex-

**3**

dependent expression being higher in female than in male adipocytes. Of note, concentrations of progesterone used in our study should be adequate to mediate progesterone effects because its equilibrium dissociation constant ($K_d$) has been reported to be 2–3 nM in various tissues (50). Further studies are required to investigate *in vivo* effects of progesterone on the BAT transcriptional profile and function to draw firm conclusions about the role of progesterone in the regulation of BAT and its importance for clinically relevant conditions.

Apart from its role in thermogenesis, BAT also serves as an endocrine organ, secreting several proteins including adiponectin and adipsin (also known as complement factor D) (51,52), of which the gene expression in primary brown adipocytes was dose-dependently reduced by progesterone. Adiponectin is a metabolic-favorable adipokine, having insulin-sensitizing and anti-inflammatory effects, of which the plasma concentrations are reduced in obesity (53,54). It has been reported that plasma adiponectin levels and adiponectin protein expressions in BAT and gonadal WAT are higher in female mice than in male mice, but no sex-dependent pattern was observed in mRNA expression levels (55). The fact that ovariectomy increased while pregnancy decreased plasma adiponectin levels suggest an inhibitory effect of progesterone (or other pregnancy-related hormones) on adiponectin secretion from adipocytes (55), which is in line with our *in vitro* results. However, another study in female rats found no significant effect of progesterone treatment on *Adipoq* mRNA expression in BAT but instead observed reduced *Adipoq* mRNA in inguinal WAT (56). Adipsin is necessary for initiation of the alternative complement pathway, an innate immune response for pathogen recognition and elimination (57) and plays a role in maintaining pancreatic β cell function (58). Adipsin also indirectly promotes adipogenesis and triglyceride storage in adipocytes via the product of its enzymatic action, the acylation-stimulating protein (ASP) (59,60). However, adipsin-deficient mice show a normal body weight (57), but reduced tissue inflammation, illustrated by reduced macrophages and crown-like structures in WAT, upon HFD treatment (58). Our results show that progesterone inhibited adipsin expression in primary brown adipocytes of murine origin. It remains to be determined how these results translate to human since serum adipsin levels were reduced during pregnancy but did not differ between the follicular and luteal phase in humans (61).

Studies have shown systemic metabolic effects of another adipokine lipocalin 2 although the findings are conflicting. Compared to lean controls, serum lipocalin 2 levels were higher in mouse models of obesity, such as *ob*/*ob* mice, *db*/*db* mice, and HFD feeding (62). Reduction of *Lcn2* expression in 3T3-L1 adipocytes by short-hairpin RNA resulted in improved insulin sensitivity (62). In contrast, lipocalin 2-deficient male mice were more obese and had more severe diet-induced insulin resistance as well as impaired thermogenic activity in BAT

upon cold exposure, compared to wild-type males (63). Lipocalin 2-deficient females were also more obese than wild-type females upon HFD feeding (64). Although lipocalin 2 was previously reported to be expressed in murine WAT but not in BAT depots (62), we could detect *Lcn2* mRNA expression in BAT depots and differentiated BAT SVFs, in which we found that female mice have a higher *Lcn2* expression which might be attributable to progesterone. More dedicated studies are required in order to draw firm conclusions on the regulation of lipocalin 2 in BAT.

Interestingly, using different concentrations of RU486 revealed that the progesterone-inhibiting effects on mRNA expression of various genes in brown adipocytes are likely driven by GR rather than PR because the inhibition was blunted when RU486 was applied at a GR- and PR- antagonistic concentration but not at a more PR-specific antagonistic concentration (31). Our findings are in agreement with previous studies, for instance, progesterone was reported to act via the GR to mediate regulatory T cells enrichment (65) and to repress *PTGS2* mRNA expression in myometrial cells (66). However, non-genomic actions of progesterone, e.g. through progesterone membrane receptors and the progesterone receptor membrane components, cannot be ruled out.

In summary, this study demonstrates a sex-dependent transcriptomic profile in BAT of mice at basal conditions and suggests a role for progesterone in the expression pattern of some of the identified sex differentially expressed genes. Furthermore, our results highlight a role for genes encoding proteins involved in cellular structure, cell-cell contact, and cell adhesion in the sex-differential function of BAT.

## Acknowledgements

We would like to thank Chen Hu for her valuable assistance during the experiment.

## Additional Information

### Disclosure Summary

The authors have nothing to disclose.

### Data availability

RNA-seq FASTQ files are available at ArrayExpress database of the EMBL's European Bioinformatics Institute (accession no. E-MTAB-8717). An Excel file summarizing the enrichment and pathway analyses in DAVID and IPA is available upon request to the corresponding author.

## References and Notes

1. GBD 2015 Obesity Collaborators, Afshin A, Forouzanfar MH, Reitsma MB, Sur P, Estep K, Lee A, et al. Health Effects of Overweight and Obesity in 195 Countries over 25 Years. *N Engl J Med.* 2017;**377**(1):13-27.

2. Logue J, Walker JJ, Colhoun HM, Leese GP, Lindsay RS, McKnight JA, Morris AD, et al. Do men develop type 2 diabetes at lower body mass indices than women? *Diabetologia.* 2011;**54**(12):3003-3006.

3. Longo M, Zatterale F, Naderi J, Parrillo L, Formisano P, Raciti GA, Beguinot F, Miele C. Adipose Tissue Dysfunction as Determinant of Obesity-Associated Metabolic Complications. *International journal of molecular sciences.* 2019;**20**(9).

4. Palmer BF, Clegg DJ. The sexual dimorphism of obesity. *Mol Cell Endocrinol.* 2015;**402**:113-119.

5. Townsend K, Tseng YH. Brown adipose tissue: Recent insights into development, metabolic function and therapeutic potential. *Adipocyte.* 2012;**1**(1):13-24.

6. Cannon B, Nedergaard J. Brown adipose tissue: function and physiological significance. *Physiol Rev.* 2004;**84**(1):277-359.

7. Feldmann HM, Golozoubova V, Cannon B, Nedergaard J. UCP1 ablation induces obesity and abolishes diet-induced thermogenesis in mice exempt from thermal stress by living at thermoneutrality. *Cell Metab.* 2009;**9**(2):203-209.

8. Moonen MPB, Nascimento EBM, van Marken Lichtenbelt WD. Human brown adipose tissue: Underestimated target in metabolic disease? *Biochim Biophys Acta Mol Cell Biol Lipids.* 2019;**1864**(1):104-112.

9. Newell-Fugate AE. The role of sex steroids in white adipose tissue adipocyte function. *Reproduction.* 2017;**153**(4):R133-R149.

10. Mauvais-Jarvis F. Sex differences in metabolic homeostasis, diabetes, and obesity. *Biol Sex Differ.* 2015;**6**:14.

11. Cypess AM, Lehman S, Williams G, Tal I, Rodman D, Goldfine AB, Kuo FC, et al. Identification and importance of brown adipose tissue in adult humans. *N Engl J Med.* 2009;**360**(15):1509-1517.

12. Rodriguez-Cuenca S, Pujol E, Justo R, Frontera M, Oliver J, Gianotti M, Roca P. Sex-dependent thermogenesis, differences in mitochondrial morphology and function, and adrenergic response in brown adipose tissue. *J Biol Chem.* 2002;**277**(45):42958-42963.

13. Geer EB, Shen W. Gender differences in insulin resistance, body composition, and energy balance. *Gend Med.* 2009;**6 Suppl 1**:60-75.

14. Mauvais-Jarvis F, Clegg DJ, Hevener AL. The role of estrogens in control of energy balance and glucose homeostasis. *Endocr Rev.* 2013;**34**(3):309-338.

15. Gonzalez-Garcia I, Tena-Sempere M, Lopez M. Estradiol Regulation of Brown Adipose Tissue Thermogenesis. *Adv Exp Med Biol.* 2017;**1043**:315-335.

16. Yoshioka K, Yoshida T, Wakabayashi Y, Nishioka H, Kondo M. Reduced brown adipose tissue thermogenesis of obese rats after ovariectomy. *Endocrinol Jpn.* 1988;**35**(4):537-543.

17. Rogers NH, Perfield JW, 2nd, Strissel KJ, Obin MS, Greenberg AS. Reduced energy expenditure and increased inflammation are early events in the development of ovariectomy-induced obesity. *Endocrinology.* 2009;**150**(5):2161-2168.

18. Martinez de Morentin PB, Gonzalez-Garcia I, Martins L, Lage R, Fernandez-Mallo D, Martinez-Sanchez N, Ruiz-Pino F, et al. Estradiol regulates brown adipose tissue thermogenesis via hypothalamic AMPK. *Cell Metab.* 2014;**20**(1):41-53.

19. Hashimoto O, Noda T, Morita A, Morita M, Ohtsuki H, Sugiyama M, Funaba M. Castration induced browning in subcutaneous white adipose tissue in male mice. *Biochem Biophys Res Commun.* 2016;**478**(4):1746-1750.

20. Monjo M, Rodriguez AM, Palou A, Roca P. Direct effects of testosterone, 17 beta-estradiol, and progesterone on adrenergic regulation in cultured brown adipocytes: potential mechanism for gender-dependent thermogenesis. *Endocrinology.* 2003;**144**(11):4923-4930.

21. Kaikaew K, Steenbergen J, Themmen APN, Visser JA, Grefhorst A. Sex difference in thermal preference of adult mice does not depend on presence of the gonads. *Biol Sex Differ.* 2017;**8**(1):24.

22. Martin M. Cutadapt removes adapter sequences from high-throughput sequencing reads. *EMBnet.journal.* 2011;**17**(1):3.

23. Dobin A, Davis CA, Schlesinger F, Drenkow J, Zaleski C, Jha S, Batut P, Chaisson M, Gingeras TR. STAR: ultrafast universal RNA-seq aligner. *Bioinformatics.* 2013;**29**(1):15-21.

24. Liao Y, Smyth GK, Shi W. featureCounts: an efficient general purpose program for assigning sequence reads to genomic features. *Bioinformatics*. 2014;**30**(7):923-930.

25. Love MI, Huber W, Anders S. Moderated estimation of fold change and dispersion for RNA-seq data with DESeq2. *Genome Biol*. 2014;**15**(12):550.

26. Huang da W, Sherman BT, Lempicki RA. Systematic and integrative analysis of large gene lists using DAVID bioinformatics resources. *Nat Protoc*. 2009;**4**(1):44-57.

27. Kramer A, Green J, Pollard J, Jr., Tugendreich S. Causal analysis approaches in Ingenuity Pathway Analysis. *Bioinformatics*. 2014;**30**(4):523-530.

28. RRID:CVCL_S893. https://scicrunch.org/resolver/CVCL_S893.

29. Kaikaew K, Steenbergen J, van Dijk TH, Grefhorst A, Visser JA. Sex Difference in Corticosterone-Induced Insulin Resistance in Mice. *Endocrinology*. 2019;**160**(10):2367-2387.

30. Kaikaew K, Grefhorst A, Steenbergen J, Swagemakers SMA, McLuskey A, Visser JA. Sex difference in the mouse BAT transcriptome reveals a role of progesterone in BAT function: Supplementary data. Mendeley Data 2020. Deposited 15 January 2020. https://data.mendeley.com/datasets/t3jc3k7dct/1.

31. Kroon J, Koorneef LL, van den Heuvel JK, Verzijl CRC, van de Velde NM, Mol IM, Sips HCM, Hunt H, Rensen PCN, Meijer OC. Selective Glucocorticoid Receptor Antagonist CORT125281 Activates Brown Adipose Tissue and Alters Lipid Distribution in Male Mice. *Endocrinology*. 2018;**159**(1):535-546.

32. Grefhorst A, van den Beukel JC, van Houten EL, Steenbergen J, Visser JA, Themmen AP. Estrogens increase expression of bone morphogenetic protein 8b in brown adipose tissue of mice. *Biol Sex Differ*. 2015;**6**:7.

33. Gumbiner BM. Cell adhesion: the molecular basis of tissue architecture and morphogenesis. *Cell*. 1996;**84**(3):345-357.

34. Basu S, Cheriyamundath S, Ben-Ze'ev A. Cell-cell adhesion: linking Wnt/beta-catenin signaling with partial EMT and stemness traits in tumorigenesis. *F1000Res*. 2018;**7**.

35. Pope BD, Warren CR, Parker KK, Cowan CA. Microenvironmental Control of Adipocyte Fate and Function. *Trends Cell Biol*. 2016;**26**(10):745-755.

36. Choe SS, Huh JY, Hwang IJ, Kim JI, Kim JB. Adipose Tissue Remodeling: Its Role in Energy Metabolism and Metabolic Disorders. *Front Endocrinol (Lausanne)*. 2016;**7**:30.

37. Rudnicki M, Abdifarkosh G, Rezvan O, Nwadozi E, Roudier E, Haas TL. Female Mice Have Higher Angiogenesis in Perigonadal Adipose Tissue Than Males in Response to High-Fat Diet. *Front Physiol*. 2018;**9**:1452.

38. Grandl G, Muller S, Moest H, Moser C, Wollscheid B, Wolfrum C. Depot specific differences in the adipogenic potential of precursors are mediated by collagenous extracellular matrix and Flotillin 2 dependent signaling. *Mol Metab*. 2016;**5**(10):937-947.

39. Joo JI, Yun JW. Gene expression profiling of adipose tissues in obesity susceptible and resistant rats under a high fat diet. *Cell Physiol Biochem*. 2011;**27**(3-4):327-340.

40. Panina YA, Yakimov AS, Komleva YK, Morgun AV, Lopatina OL, Malinovskaya NA, Shuvaev AN, Salmin VV, Taranushenko TE, Salmina AB. Plasticity of Adipose Tissue-Derived Stem Cells and Regulation of Angiogenesis. *Front Physiol*. 2018;**9**:1656.

41. Scioli MG, Bielli A, Gentile P, Mazzaglia D, Cervelli V, Orlandi A. The biomolecular basis of adipogenic differentiation of adipose-derived stem cells. *International journal of molecular sciences*. 2014;**15**(4):6517-6526.

42. Yadav H, Quijano C, Kamaraju AK, Gavrilova O, Malek R, Chen W, Zerfas P, et al. Protection from obesity and diabetes by blockade of TGF-beta/Smad3 signaling. *Cell Metab*. 2011;**14**(1):67-79.

43. Jha RK, Titus S, Saxena D, Kumar PG, Laloraya M. Profiling of E-cadherin, beta-catenin and Ca(2+) in embryo-uterine interactions at implantation. *FEBS Lett*. 2006;**580**(24):5653-5660.

44. Jeong JW, Lee KY, Kwak I, White LD, Hilsenbeck SG, Lydon JP, DeMayo FJ. Identification of murine uterine genes regulated in a ligand-dependent manner by the progesterone receptor. *Endocrinology*. 2005;**146**(8):3490-3505.

45. Yao MW, Lim H, Schust DJ, Choe SE, Farago A, Ding Y, Michaud S, Church GM, Maas RL. Gene expression profiling reveals progesterone-mediated cell cycle and immunoregulatory roles of Hoxa-10 in the preimplantation uterus. *Mol Endocrinol*. 2003;**17**(4):610-627.

46. Liu YF, Deng WB, Li SY, Yao MN, Liu J, Dou HT, Zhao ML, Yang ZM, Liang XH. Progesterone induces the expression of lipocalin-2 through Akt-c-Myc pathway during mouse decidualization. *FEBS Lett*. 2016;**590**(16):2594-2602.

**3**

47. Rodriguez AM, Monjo M, Roca P, Palou A. Opposite actions of testosterone and progesterone on UCP1 mRNA expression in cultured brown adipocytes. *Cell Mol Life Sci.* 2002;**59**(10):1714-1723.

48. McIlvride S, Mushtaq A, Papacleovoulou G, Hurling C, Steel J, Jansen E, Abu-Hayyeh S, Williamson C. A progesterone-brown fat axis is involved in regulating fetal growth. *Sci Rep.* 2017;**7**(1):10671.

49. Nilsson ME, Vandenput L, Tivesten A, Norlen AK, Lagerquist MK, Windahl SH, Borjesson AE, et al. Measurement of a Comprehensive Sex Steroid Profile in Rodent Serum by High-Sensitive Gas Chromatography-Tandem Mass Spectrometry. *Endocrinology.* 2015;**156**(7):2492-2502.

50. Jacobs BR, Smith RG. A comparison of progesterone and R5020 binding in endometrium, ovary, pituitary, and hypothalamus. *Fertil Steril.* 1981;**35**(4):438-441.

51. Ali Khan A, Hansson J, Weber P, Foehr S, Krijgsveld J, Herzig S, Scheideler M. Comparative Secretome Analyses of Primary Murine White and Brown Adipocytes Reveal Novel Adipokines. *Mol Cell Proteomics.* 2018;**17**(12):2358-2370.

52. Villarroya J, Cereijo R, Gavalda-Navarro A, Peyrou M, Giralt M, Villarroya F. New insights into the secretory functions of brown adipose tissue. *J Endocrinol.* 2019.

53. Stern JH, Rutkowski JM, Scherer PE. Adiponectin, Leptin, and Fatty Acids in the Maintenance of Metabolic Homeostasis through Adipose Tissue Crosstalk. *Cell Metab.* 2016;**23**(5):770-784.

54. Achari AE, Jain SK. Adiponectin, a Therapeutic Target for Obesity, Diabetes, and Endothelial Dysfunction. *International journal of molecular sciences.* 2017;**18**(6):E1321.

55. Combs TP, Berg AH, Rajala MW, Klebanov S, Iyengar P, Jimenez-Chillaron JC, Patti ME, Klein SL, Weinstein RS, Scherer PE. Sexual differentiation, pregnancy, calorie restriction, and aging affect the adipocyte-specific secretory protein adiponectin. *Diabetes.* 2003;**52**(2):268-276.

56. Stelmanska E, Kmiec Z, Swierczynski J. The gender- and fat depot-specific regulation of leptin, resistin and adiponectin genes expression by progesterone in rat. *J Steroid Biochem Mol Biol.* 2012;**132**(1-2):160-167.

57. Xu Y, Ma M, Ippolito GC, Schroeder HW, Jr., Carroll MC, Volanakis JE. Complement activation in factor D-deficient mice. *Proc Natl Acad Sci U S A.* 2001;**98**(25):14577-14582.

58. Lo JC, Ljubicic S, Leibiger B, Kern M, Leibiger IB, Moede T, Kelly ME, et al. Adipsin is an adipokine that improves beta cell function in diabetes. *Cell.* 2014;**158**(1):41-53.

59. Cianflone K, Xia Z, Chen LY. Critical review of acylation-stimulating protein physiology in humans and rodents. *Biochim Biophys Acta.* 2003;**1609**(2):127-143.

60. Song NJ, Kim S, Jang BH, Chang SH, Yun UJ, Park KM, Waki H, Li DY, Tontonoz P, Park KW. Small Molecule-Induced Complement Factor D (Adipsin) Promotes Lipid Accumulation and Adipocyte Differentiation. *PLoS One.* 2016;**11**(9):e0162228.

61. Poveda NE, Garces MF, Ruiz-Linares CE, Varon D, Valderrama S, Sanchez E, Castiblanco-Cortes A, et al. Serum Adipsin Levels throughout Normal Pregnancy and Preeclampsia. *Sci Rep.* 2016;**6**:20073.

62. Yan QW, Yang Q, Mody N, Graham TE, Hsu CH, Xu Z, Houstis NE, Kahn BB, Rosen ED. The adipokine lipocalin 2 is regulated by obesity and promotes insulin resistance. *Diabetes.* 2007;**56**(10):2533-2540.

63. Guo H, Jin D, Zhang Y, Wright W, Bazuine M, Brockman DA, Bernlohr DA, Chen X. Lipocalin-2 deficiency impairs thermogenesis and potentiates diet-induced insulin resistance in mice. *Diabetes.* 2010;**59**(6):1376-1385.

64. Guo H, Zhang Y, Brockman DA, Hahn W, Bernlohr DA, Chen X. Lipocalin 2 deficiency alters estradiol production and estrogen receptor signaling in female mice. *Endocrinology.* 2012;**153**(3):1183-1193.

65. Engler JB, Kursawe N, Solano ME, Patas K, Wehrmann S, Heckmann N, Luhder F, et al. Glucocorticoid receptor in T cells mediates protection from autoimmunity in pregnancy. *Proc Natl Acad Sci U S A.* 2017;**114**(2):E181-E190.

66. Lei K, Chen L, Georgiou EX, Sooranna SR, Khanjani S, Brosens JJ, Bennett PR, Johnson MR. Progesterone acts via the nuclear glucocorticoid receptor to suppress IL-1beta-induced COX-2 expression in human term myometrial cells. *PLoS One.* 2012;**7**(11):e50167.

**Supplementary table**  Selected genes from the significant functional annotation clusters and their functional description

| Gene | Full name | Description and biological function |
|---|---|---|
| Bmp8b | Bone morphogenetic protein 8b | This gene encodes a secreted ligand of the transforming growth factor (TGF)-β superfamily. These ligands bind various TGF-β receptors leading to recruitment and activation of SMAD family transcription factors that regulate gene expression. BMP8b may play a role in the generation of primordial germ cells and has been shown to stimulate thermogenesis in brown adipose tissue. Homozygous knockout mice of both sexes exhibit impaired thermogenesis and reduced metabolic rate, resulting in weight gain. |
| C7* | Complement component 7 | This gene encodes a serum glycoprotein that forms a membrane attack complex together with complement components C5b, C6, C8, and C9 as part of the terminal complement pathway of the innate immune system. The protein encoded by this gene contains a cholesterol-dependent cytolysin/membrane attack complex/perforin-like (CDC/MACPF) domain and belongs to a large family of structurally related molecules that form pores involved in host immunity and bacterial pathogenesis. This protein initiates membrane attack complex formation by binding to the C5b-C6 subcomplex and inserts into the phospholipid bilayer, serving as a membrane anchor. |
| Cdh1 | Cadherin 1 | This gene encodes E-cadherin, a calcium-dependent cell adhesion molecule that functions in the establishment and maintenance of epithelial cell morphology. |
| Cfd | Complement factor D (adipsin) | This gene encodes a serine protease that plays an important role in the alternative pathway of complement activation for pathogen recognition and elimination. The encoded preproprotein undergoes proteolytic processing to generate a mature, functional enzyme that in turn cleaves factor B in the complement pathway. This gene is expressed in adipocytes and the mature enzyme is secreted into the bloodstream. Mice lacking the encoded product cannot initiate the alternative pathway of complement activation. |
| Cldn3 | Claudin 3 | This gene encodes a member of the claudin family. Claudins are integral membrane proteins and components of tight junction strands. Tight junction strands serve as a physical barrier to prevent solutes and water from passing freely through the paracellular space between epithelial or endothelial cell sheets, and also play critical roles in maintaining cell polarity and signal transductions. CLDN3 is predominantly present in brain endothelial cells, where it plays a specific role in the establishment and maintenance of blood-brain barrier tight junction morphology. |
| Cldn4 | Claudin 4 | In addition to the general claudin family properties, CLDN4 augments alveolar epithelial barrier function and is induced in acute lung injury. |
| Cldn7 | Claudin 7 | In addition to the general claudin family properties, CLDN7 is expressed constitutively in the mammary epithelium throughout development and might be involved in vesicle trafficking to the basolateral membrane. CLDN7 is essential for NaCl homeostasis in distal nephrons. |
| Cxcl13* | Chemokine (C-X-C motif) ligand 13 | CXCL13 is a B lymphocyte chemoattractant strongly expressed in the follicles of the spleen, lymph nodes, and Peyer's patches. It preferentially promotes the migration of B lymphocytes (compared to T cells and macrophages), apparently by stimulating calcium influx into, and chemotaxis of, cells expressing Burkitt's lymphoma receptor 1 (BLR-1). |
| Epcam* | Epithelial cell adhesion molecule | This gene encodes a carcinoma-associated antigen and is a member of a family that includes at least two type I membrane proteins. This antigen is expressed on most normal epithelial cells and gastrointestinal carcinomas and functions as a homotypic calcium-independent cell adhesion molecule. |

**3**

| Gene | Full name | Description and biological function |
|---|---|---|
| Irf4* | Interferon regulatory factor 4 | This gene encodes a protein belonging to the IRF (interferon regulatory factor) family of transcription factors, characterized by a unique tryptophan pentad repeat DNA-binding domain. The IRFs are important in the regulation of interferons in response to infection by virus, and in the regulation of interferon-inducible genes. This family member negatively regulates Toll-like-receptor (TLR) signaling that is central to the activation of innate and adaptive immune systems. |
| Krt5* | Keratin 5 | This gene encodes a member of the keratin gene family. The type II cytokeratins consist of basic or neutral proteins which are arranged in pairs of heterotypic keratin chains coexpressed during differentiation of simple and stratified epithelial tissues. KRT5 is specifically expressed in the basal layer of the epidermis with family member KRT14. |
| Krt8* | Keratin 8 | This gene is a member of the type II keratin family. Type I and type II keratins heteropolymerize to form intermediate-sized filaments in the cytoplasm of epithelial cells. The product of this gene typically dimerizes with KRT18 to form an intermediate filament in simple single-layered epithelial cells. This protein plays a role in maintaining cellular structural integrity and also functions in signal transduction and cellular differentiation. |
| Krt14 | Keratin 14 | This gene encodes a member of the keratin family, the most diverse group of intermediate filaments. This gene product, a type I keratin, is usually found as a heterotetramer with two KRT5 molecules, a type II keratin. Together they form the cytoskeleton of epithelial cells. |
| Krt18* | Keratin 18 | This gene encodes the type I intermediate filament chain keratin 18. KRT18 and its filament partner KRT8 are perhaps the most commonly found members of the intermediate filament gene family. They are expressed in single layer epithelial tissues of the body. |
| Lcn2* | Lipocalin 2 | This gene encodes a protein that belongs to the lipocalin family. Members of this family transport small hydrophobic molecules such as lipids, steroid hormones and retinoids. The protein encoded by this gene is a neutrophil gelatinase-associated lipocalin and plays a role in innate immunity by limiting bacterial growth as a result of sequestering iron-containing siderophores. The presence of this protein in blood and urine is an early biomarker of acute kidney injury. This protein is thought to be involved in multiple cellular processes, including maintenance of skin homeostasis, and suppression of invasiveness and metastasis. Mice lacking this gene are more susceptible to bacterial infection than wild type mice. |
| Mup22# | Major urinary protein 22 | Major urinary proteins (MUPs) are members of the lipocalin family, which shares almost 99% sequence identity. Unlike lipocalin genes that are expressed in both humans and mice, MUP genes are only expressed in mice. MUPs are mainly expressed in the liver, secreted to the bloodstream, and excreted by the kidney. MUPs are involved in the communication in urine-derived scent marks and can also serve as pheromones. Circulating MUPs may also contribute to regulation of nutrient metabolism, possibly by suppressing hepatic gluconeogenesis and lipid metabolism. However, it remains unclear how MUPs regulate energy metabolism. |
| Pgr | Progesterone receptor | This gene encodes a member of the steroid receptor superfamily. The encoded protein mediates the physiological effects of progesterone, which plays a central role in reproductive events associated with the establishment and maintenance of pregnancy. |
| Ptprf* | Protein tyrosine phosphatase receptor type F | This gene encodes a protein in the protein tyrosine phosphatase (PTP) family. PTPs are known to be signaling molecules that regulate a variety of cellular processes including cell growth, differentiation, mitotic cycle, and oncogenic transformation. This PTP possesses an extracellular region, a single transmembrane region, and two tandem intracytoplasmic catalytic domains, and thus represents a receptor-type PTP. The extracellular region contains three Ig-like domains, and nine non-Ig-like domains similar to that of neural-cell adhesion molecule. This PTP was shown to function in the regulation of epithelial cell-cell contacts at adherents junctions, as well as in the control of beta-catenin signaling. |

| Gene | Full name | Description and biological function |
|------|-----------|-------------------------------------|
| Scnn1b* | Sodium channel epithelial 1 beta subunit | Nonvoltage-gated, amiloride-sensitive, sodium channels control fluid and electrolyte transport across epithelia in many organs. These channels are heteromeric complexes consisting of 3 subunits: alpha, beta, and gamma. This gene encodes the beta subunit, and mutations in this gene have been associated with pseudohypoaldosteronism type 1 (PHA1), and Liddle syndrome. |
| Sdc1* | Syndecan 1 | This gene encodes a transmembrane (type I) heparan sulfate proteoglycan which is a member of the syndecan proteoglycan family. The syndecans mediate cell binding, cell signaling, and cytoskeletal organization and syndecan receptors are required for internalization of the HIV-1 tat protein. The syndecan-1 protein functions as an integral membrane protein and participates in cell proliferation, cell migration and cell-matrix interactions via its receptor for extracellular matrix proteins. |
| St14* | Suppression of tumorigenicity 14 | This gene encodes an epithelial-derived, integral membrane serine protease. This protease forms a complex with the Kunitz-type serine protease inhibitor, HAI-1, and is found to be activated by sphingosine 1-phosphate. This protease has been shown to cleave and activate hepatocyte growth factor/scattering factor, and urokinase plasminogen activator, which suggests the function of this protease as an epithelial membrane activator for other proteases and latent growth factors. |
| Wfdc2* | WAP four-disulfide core domain 2 | This gene encodes a protein that is a member of the WFDC domain family. The WFDC domain, or WAP Signature motif, contains eight cysteines forming four disulfide bonds at the core of the protein, and functions as a protease inhibitor in many family members. This gene is expressed in pulmonary epithelial cells. The encoded protein is a small secretory protein, which may be involved in sperm maturation. |

Functional description was extracted from NCBI gene database (https://www.ncbi.nlm.nih.gov/gene).
* The mouse-specific description summary was not available and was obtained from its human ortholog.
# Information was based on general function of the MUP family, obtained from Charkoftaki G, Wang Y, McAndrews M, Bruford EA, Thompson DC, Vasiliou V, Nebert DW. Update on the human and mouse lipocalin (LCN) gene family, including evidence the mouse Mup cluster is the result of an "evolutionary bloom". *Hum Genomics*. 2019;**13**(1):11.

**3**
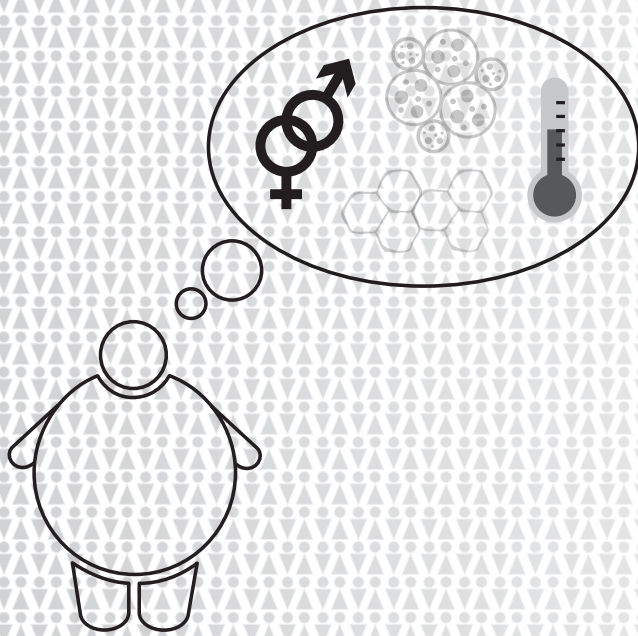
# Chapter 4

# Sex Difference in Thermal Preference of Adult Mice Does Not Depend on Presence of the Gonads

Kasiphak Kaikaew[1,2], Jacobie Steenbergen[1], Axel P.N. Themmen[1], Jenny A. Visser[1], Aldo Grefhorst[1]

1  Department of Internal Medicine, Erasmus MC, University Medical Center Rotterdam, Rotterdam, the Netherlands
2  Department of Physiology, Faculty of Medicine, Chulalongkorn University, Bangkok, Thailand

4

## Abstract

**BACKGROUND:** The thermoneutral zone (TNZ) is a species-specific range of ambient temperature ($T_a$), at which mammals can maintain a constant body temperature with the lowest metabolic rate. The TNZ for an adult mouse is between 26 and 34 °C. Interestingly, female mice prefer a higher $T_a$ than male mice although the underlying mechanism for this sex difference is unknown. Here, we tested whether gonadal hormones are dominant factors controlling temperature preference in male and female mice.

**METHODS:** We performed a temperature preference test in which 10-week-old gonadectomized and sham-operated male and female C57BL/6J mice were allowed to choose to reside at the thermoneutral cage of 29 °C or an experimental cage of 26, 29 or 32 °C.

**RESULTS:** All mice preferred a $T_a$ higher than 26 °C, especially in the inactive phase. Choosing between 29 °C and 32 °C, female mice resided more at 32 °C while male mice had no preference between the temperatures. Hence, the preferred $T_a$ for female mice was significantly higher (0.9±0.2 °C) than that of male mice. However, gonadectomy did not influence the $T_a$ preference.

**CONCLUSIONS:** Female mice prefer a warmer environment than male mice, a difference not affected by gonadectomy. This suggests that thermal sensing mechanisms may be influenced by sex-specific pathways other than gonadal factors or that the thermoregulatory set point has already been determined prior to puberty.

**4**

## Background

Mammals prefer ranges of ambient temperature ($T_a$) within their species-specific thermoneutral zone (TNZ) at which their metabolic rate is at its lowest and theoretically equal to their basal metabolic rate. To control the core body temperature ($T_c$) in TNZ, only dry heat loss, i.e., skin blood flow, is sufficient. However, metabolic heat production or evaporative heat loss is required to regulate $T_c$ at a $T_a$ outside the TNZ [1]. Disturbances in $T_a$ can alter normal physiological responses such as dietary requirement, cardiovascular functions, and reproduction capacity [2, 3]; thus, it is important to be aware of the changes of $T_a$. The TNZ for an adult mouse is considered to be broad and in between 26 and 34 °C, and mice therefore prefer a $T_a$ between 29 °C and 31 °C [4]. However, general animal facilities apply a $T_a$ for laboratory mice in the range of 20–24 °C [5], which matches a thermal comfort of husbandry staffs and handling procedures but poses a persistent moderate cold stress to mice [6] affecting their physiological processes [7].

Many factors contribute to distinct patterns of thermal preference among mice. For instance, since mice are nocturnal animals, their motor activity has a diurnal rhythm which peaks in the dark phase. An increase in heat production related to this physical activity during the active phase results in a preference for a lower $T_a$ to maintain $T_c$ at night [6]. In addition, a higher $T_a$ is required by neonatal mice due to limitations in their thermal regulatory mechanisms [8]. Elderly mice also require higher $T_a$ due to changes in total body surface area (BSA). Upon growth, the BSA to body mass ratio decreases resulting in less capacity to exchange heat with the environment [4, 9]. Finally, thermal differences in mice have a sex-dependent pattern: female mice prefer a slightly higher $T_a$ than male mice of the same age, especially in the inactive phase [10].

The mechanism(s) that underlie the differences in thermal regulation and preference between sexes are not clearly understood, but gonadal hormones such as the female sex hormones estradiol and progesterone and the male sex hormone testosterone might be considered dominant factors. The overall $T_c$ of post-pubertal female mice is 0.2–0.5 °C higher than that of male mice, especially when the levels of progesterone and, to a lesser extent, estradiol are elevated during the estrous cycle [11]. Of interest, this higher $T_c$ in female mice is not due to the difference in locomotor activity between male and female mice [11]. Progesterone shifts the thermoregulatory set point in the central nervous system resulting in an increase of basal $T_c$ in the luteal phase of the human ovarian cycle [12]. Since the mouse estrous cycle lasts only 4–5 days and does not include a true luteal phase, major and prolonged elevations of progesterone are only seen during (pseudo)pregnancy [13]. Estradiol influences energy balance by increasing the energy expenditure through modulation of central

neuronal circuits [14], which includes the production of heat by brown adipose tissue (BAT) [15]. BAT is an important source of heat production in rodents, especially in the inactive phase. Interestingly, both estradiol and progesterone also directly stimulate biogenesis of brown adipocytes while testosterone inhibits differentiation of brown adipocytes [16, 17]. However, the effects of gonadal hormones on the thermal preferences in mammals are not clearly studied.

To elucidate the effects of gonadal hormones on thermal preference, we performed temperature preference tests (TPTs) in adult mice of both sexes, in a range of $T_a$ close to their TNZ. The results of the TPTs will reveal whether removal of gonadal hormones by gonadectomy (GDX) affects temperature preference.

## Methods

### Animals and housing conditions

Six-week-old C57BL/6J mice (16 male and 16 female mice) were obtained from Charles River Laboratories (Maastricht, the Netherlands). Upon arrival, the mice were housed for 1 week in groups of three animals in standard laboratory cages (Sealsafe 1145T, Tecniplast, Buguggiate, Italy; 36.9 cm $L$ × 15.6 cm $W$ × 13.2 cm $H$) with bedding material (Lignocel BK 8/15, J. Rettenmaier & Söhne GmbH, Rosenberg, Germany) and nesting material (facial tissue paper, Tork, SCA Hygiene Products, Zeist, the Netherlands) on a 12:12-h light-dark cycle (lights on at 8 a.m.), at temperatures of 21–23 °C with 40–70% relative humidity. Chow food pellets (801722 CRM (P), Special Diets Services, Essex, UK) and water were available *ad libitum*. After the 1-week acclimatization, the mice were housed individually in a cage of the same setting for 3 days before the first series of TPTs was started. Thus, the mice were about 8 weeks old when enrolled in the experimental setups. All experimental procedures were performed with the approval of the Animal Ethics Committee at Erasmus MC, Rotterdam, the Netherlands.

### Temperature preference test setup

For the TPT, a setup was designed based on the thermal preference apparatus by Gaskill et al. [18]. To connect two cages, an opening was drilled in one wall of each cage (4 cm diameter at the position of 7.5 cm from the cage floor) and a black corrugated connecting tube was placed, as shown in **Fig. 1A,B**. Water baths, in which electric submersible aquarium heaters and water pumps (Superfish Combi Heater and Aqua-Flow, Aquadistri, Cambridgeshire, UK) were installed, were used to maintain a constant $T_a$ in the cages. The water bath was filled with water to the level of 7.5 cm depth, and the cages were fastened by fabric straps to ensure that the water level was 5 cm from the cage bottom. At

this water level, the $T_a$ inside the cage (measured at the floor) was less than 0.5 °C different from the temperature in the water bath. Each cage contained a bottle of water, food pellets, nesting material (one sheet of the facial tissue paper, two layers per sheet, size 20 cm × 21 cm, weight 1.3 g), and bedding material (0.5 cm depth of Lignocel BK 8/15 woodchips). The mice were allowed to freely explore both cages. To prevent position bias from adjacent cages, opaque plastic sheets were placed as visual barriers between the cages. In total, the setup consisted of six TPT sets (**Fig. 1B**) for studying six mice simultaneously.

## Experimental design

The total experimental procedure had a duration of 6 weeks, consisting of weeks 1 and 2 for adaptation to the TPT setup, week 3 for surgical procedure and recovery, and weeks 4 to 6 for behavioral observation (**Fig. 1C**). In the adaptation period (weeks 1 and 2) and the experimental period (weeks 4, 5, and 6), we performed the TPT in a total of 96 h after which the mice returned to their individual cage for the weekends. On Mondays, the temperature of the outer cages (the experimental cages) was set at 23 °C to mimic the general animal facility environment, while the temperature of the middle cages (the thermoneutral (TMN) cages) was set at 29 °C. The routine care was performed daily between 1 and 2 p.m. including replacing of bedding and nesting material, weighing mice and food, and adjusting the temperature of the experimental cages to 26, 29, and 32 °C on Tuesday, Wednesday, and Thursday, respectively. The temperature of the TMN cages was kept at 29 °C throughout the week. After the daily routine, the mouse was put back in its experimental cage. The cages and water baths were cleaned thoroughly at the end of every week. For the surgical week (experimental week 3), the mice were randomized to undergo GDX or sham operation on Monday. After the surgery, the mice were allowed to recover for 7 days in their individual cage. To reduce the effect of position bias, the mice were relocated to an adjacent TPT set in the following week.

## Gonadectomy

GDX was operated under isoflurane (Isofluraan, Teva Pharmachemie, Haarlem, the Netherlands) anesthesia and carprofen (Rimadyl Cattle, Pfizer, Capelle a/d IJssel, the Netherlands) analgesia. For the GDX of female mice, small incisions were made in both flanks to remove the ovaries. In the male mice, small incisions were made in the lower abdomen through which the testes were removed. Sham-operated animals underwent the same procedures without removal of ovaries or testes. Bleeding was verified and stopped and then the muscle layer and skin were sutured.

**4**
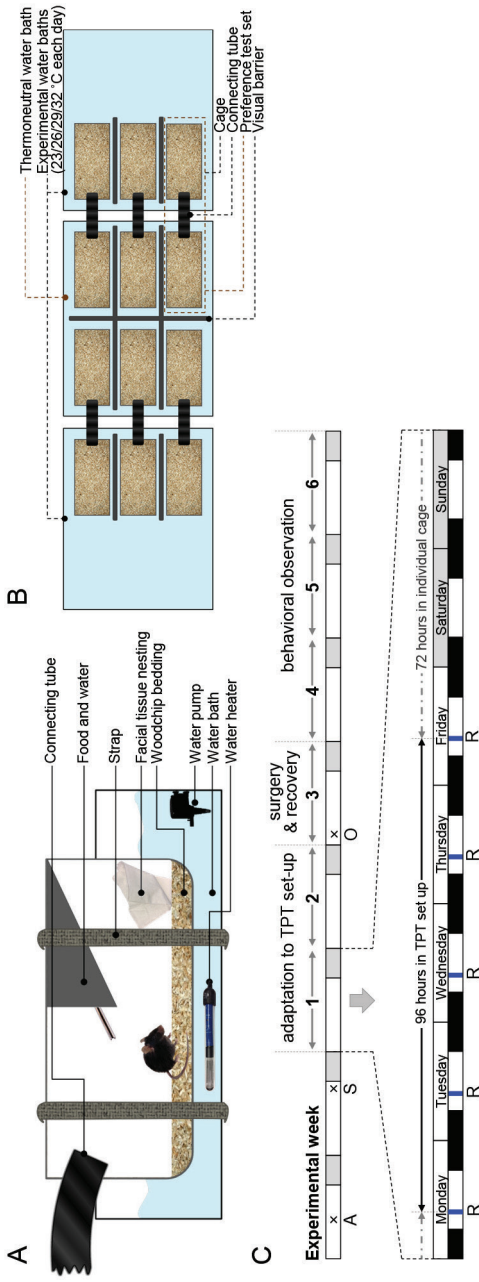


**Fig. 1** Experimental design

(**A**) Side view of each experimental cage showing cage enrichments provided for each mouse. (**B**) Top view of six temperature preference sets of which the two outer water baths were set at a different experimental temperature each day, while the middle water bath was kept constant at 29 °C. (**C**) Experimental scheme. Abbreviations: A arrival of mice, S separation to individual cage, O surgical operation, R daily routine care

## Termination of mice

In the week after the last TPT, the mice were euthanized by cardiac puncture under isoflurane anesthesia. For the female mice, the uterus was dissected and weighed to verify if the ovariectomy was successful.

## Behavioral observation, data collection, and analysis

The thermal preference of each mouse was recorded by webcams (Exis, Trust, Dordrecht, the Netherlands) with the time-lapse function of Netcam Studio software (Moonware Studios) resulting in pictures with a 5-min interval that were collected for 23 h, excluding the hour of the daily routine period. In the dark period, the photographs were taken under red lights. After a pilot study (results not shown), the periods of 9–12 p.m. and 9–12 a.m. (starting 1 hour after light off and on, respectively) were selected for the study. Data from the mice that failed to explore both the experimental and the TMN cage for the whole experimental period were excluded from data analysis.

After weighing the mice and the food in all cages during the routine care, the bedding and nesting materials were gathered for further processing. Feces were sorted out from the woodchip bedding and weighed. The nesting material was unfolded, put on a black board, and photographed for analysis by three assessors. The "paperwork score," modified from Kalueff et al. [19], was assessed to quantify how active a mouse was in biting and shredding the paper. This score ranges from 1 to 4: 1—without or little paper damage (<5% of destruction compared to the total area of the nest), 2—mild paper damage (5–25%), 3—moderate paper damage (25–50%), and 4—severe paper damage (>50%), as shown in **Fig. S1**. An average overall agreement of the paperwork score by three blinded assessors equaled to 84.7% ($\kappa = 0.79$), without any more-than-1 ordinal score discrepancy. Since the nesting material can be transferred from one cage to the other, we also assessed the "nest score" for each cage. This score is calculated as follows:

Nest score = ((paperwork score)/4) × (relative amount of nest in the cage).

In this, the relative amount of nest is a proportion of nest weight in that cage to the total weight of the nesting material provided to the animal, ranging from 0 to 1. For comparison between the experimental and the TMN cage of each mouse, the higher paperwork score and the higher nest score were used for data analysis.

The BSA of the mice was calculated by Meeh's formula with the C57BL/6J specific constant as described by Cheung et al. [20]:

BSA = $9.822 \times BW^{0.667}$.

In this, BW is the body weight in gram and BSA is the surface in square centimeter ($cm^2$).

Baseline characteristics of mice taken during the adaptation weeks are provided in **Table S1**.

## Statistical analysis

The statistical tests were performed using IBM SPSS Statistics for Windows, version 21 (IBM Corp.) with $p < .05$ considered statistically significant. Unless otherwise stated, the effects of experimental $T_a$, sex of mice, and gonadal status were analyzed by repeated three-way ANOVA, and then, the post hoc tests were evaluated by two-way ANOVA for the effects of sex and gonadal status in each $T_a$ and Tukey tests to determine differences among groups. The $p$ values of $T_a$, sex, and gonadal status are indicated by $p_T$, $p_S$ and $p_G$, respectively. The proportion of time that a mouse spent in each cage was arcsine transformed. The preference to either the TMN cage or the experimental cage in each $T_a$ was analyzed by one-sample $t$ test. Correlations between the time-weighted average $T_a$ and other factors were calculated by Pearson's correlation coefficient. All data are presented as mean ± SD unless otherwise indicated.

## Results

### Gonadectomy affected the energy balance pattern mainly in female mice

GDX differentially affected body weight (BW) in male and female mice. While ovariectomy increased BW of female mice, orchiectomy did not affect BW of male mice during the study period. As a result, the BW of gonadectomized female mice was higher than the sham-operated female mice in the last experimental week (two-way ANOVA: $p_S < .001$, $p_G = .011$, $p_{S \times G} = .014$; **Fig. 2A**). In addition, the ratio of BSA to BW at the start of the last experimental week depended significantly on both sex and gonadal status (female sham $3.57 \pm 0.03$ $cm^2$/g, female GDX $3.43 \pm 0.09$ $cm^2$/g, male sham $3.32 \pm 0.04$ $cm^2$/g, and male GDX $3.33 \pm 0.07$ $cm^2$/g; two-way ANOVA: $p_S < .001$, $p_G = .013$, $p_{S \times G} = .006$; Tukey post hoc test revealed $p < .05$ for all pairs except sham-operated male vs gonadectomized male mice).

In general, the experimental $T_a$ influenced the relative daily food intake ($p_T = .003$) and female mice ate relatively more than male mice without an effect of gonadal status ($p_S < .001$; **Fig. 2B**). However, the negative correlation of $T_a$ on daily food intake was only significant for sham-operated male mice ($r = -.54$, $p = .011$). In line with the food intake, the experimental $T_a$ was related to the relative fecal production ($p_T = .018$). Moreover, the fecal production of female

mice was higher than that of male mice, with a significant interaction between sex and gonadal status ($p_S < .001$, $p_{S \times G} = .049$; **Fig. 2C**). Although the general trend of daily food intake (energy input) was negatively correlated with the experimental $T_a$, the daily BW change of mice tended to positively correlate with the experimental $T_a$ without a significant effect of sex or gonadal status but with a significant interaction between $T_a$, sex, and gonadal status ($p_T = .002$, $p_{T \times S \times G} = .002$; **Fig. 2D**). The positive correlations between $T_a$ and daily BW change were significant in sham-operated female mice ($r = .62$, $p = .003$) and gonadectomized male mice ($r = .54$, $p = .007$).
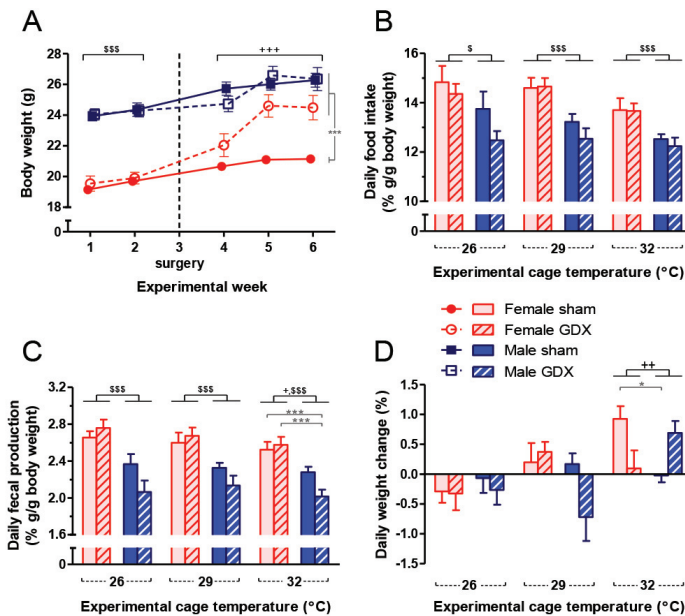
**Fig. 2** Gonadectomy affected the energy balance pattern mainly in female mice

**(A)** Gonadectomy increased body weight only in female mice. Weights of mice measured at the first day of each experimental week are plotted. **(B)** Daily food intake and **(C)** fecal production were higher in female mice with negative correlations with the experimental $T_a$. **(D)** Body weight was unchanged during the 24-h period in the experimental setup when the experimental $T_a$ was set at 26 and 29 °C, but some groups of mice gained weight when the experimental $T_a$ was set at 32 °C. Two-way ANOVA: $ $p_S < .05$, $$ $p_S < .001$, + $p_{S \times G} < .05$, ++ $p_{S \times G} < .01$, +++ $p_{S \times G} < .001$, and Tukey test: * $p < 0.05$, *** $p < 0.001$. *Error bar* indicates SEM, n = 7–8 per group

**Female mice preferred a higher ambient temperature, especially in the inactive phase**

The time mice spent in the TMN cage was influenced by experimental $T_a$, sex, and the interaction between these factors, but was not altered by gonadal status ($p_T < .001$, $p_S < .001$, $p_{T \times S} = .002$, $p_{T \times S \times G} = .004$; **Fig. 3A**). When the $T_a$ of the experimental cages was set at 26 °C, all groups of mice preferred to reside in the TMN cages rather than the experimental cages ($p_S = .038$, $p_{S \times G} = .026$; **Fig. 3A**). Calculated from the cage preference data, the time-weighted average $T_a$ the mice were exposed to was slightly higher for male than for female mice, with a significant interaction between sex and gonadal status (female sham $28.3 \pm 0.3$ °C, female GDX $28.1 \pm 0.2$ °C, male sham $28.3 \pm 0.3$ °C, and male GDX $28.5 \pm 0.3$ °C; $p_S = .044$, $p_{S \times G} = .030$; **Fig. 3B**). When the $T_a$ of the experimental cages was set the same as of the TMN cages at 29 °C, male mice (both sham-operated and gonadectomized) resided more in the TMN cages while female mice had no preference to either cage ($p_S < .001$, $p_{S \times G} = .033$; **Fig. 3A**). When the $T_a$ of the experimental cages was set at 32 °C, female mice (both sham-operated and gonadectomized) spent more time in the experimental cage than in the TMN cage, while sham-operated male mice preferred the TMN cage and gonadectomized male mice had no preference for either the TMN or the 32 °C cage ($p_S < .001$; **Fig. 3A**). Calculated from the cage preference data, the time-weighted average $T_a$ the mice were exposed to when able to choose between 29 and 32 °C was significantly higher for female mice than male mice, without an effect of gonadal status (female sham $31.2 \pm 0.2$ °C, female GDX $31.1 \pm 0.4$ °C, male sham $30.2 \pm 0.2$ °C, and male GDX $30.4 \pm 0.3$ °C; $p_S < .001$; **Fig. 3B**). Thus, in general, the female mice preferred a higher $T_a$ than male mice, a difference that was not affected by presence of the gonads.

Next, we determined whether $T_a$ preference between the sexes was different in the active or inactive phase and found that the sex of mice influenced the thermal demand differently between the dark (active) phase ($p_T < .001$, $p_{T \times S \times G} = .002$; **Fig. 3C**) and the light (inactive) phase ($p_T < .001$, $p_S < .001$, $p_{T \times S} = .002$, $p_{T \times G} = .013$; **Fig. 3E**). When the experimental $T_a$ was set at 26 °C, sham-operated female, gonadectomized female, and gonadectomized male mice preferred to stay in the TMN cage in the dark phase, while sham-operated male mice had no preference to either cage in the dark phase. In the light phase, all groups preferred the TMN cage over the experimental 26 °C cage with a more prominent preference in male mice, without an effect of gonadal status. When the experimental $T_a$ was set at 32 °C, all groups equally resided in both the 32 °C and the TMN cages in the dark phase. In the light phase, sham-operated and gonadectomized female mice preferred the 32 °C cage over the TMN cage, whereas gonadectomized male mice preferred the TMN cage and sham-operated male mice showed no preference to either cage.

**Fig. 3** Female mice preferred a higher ambient temperature, especially in the inactive phase

(A) Both male and female mice preferred the TMN over the lower $T_a$ (26 °C) while female but not male mice preferred the higher $T_a$ (32 °C) over TMN. The thermal preference in the (C) dark (active) phase and (E) light (inactive) phase showed distinct patterns. The percentage of time that mice spent in each cage is represented on the *y*-axis as an angular transformed scale. Zero means the mice equally spent time in both cages. A positive value means preference to the TMN cage while a negative value means a preference to the experimental cage, of which the temperature is indicated on the *x*-axis. (B, D, F) *Box-and-whiskers plots* (box indicates interquartile range and whisker is plotted using Tukey method) show the time-weighted average $T_a$ that the mice were exposed to. The *gray area* indicates a temperature range of 28.5–29.5 °C. Two-way ANOVA: $ p_S < .05, $$$ p_S < .001, # p_G < .05, $$$ p_S < .05, + p_G < .05, ++ p_{S \times G} < .05, *** p < .05, ** p < .01, *** p < .001. *Error bar* indicates SEM, n = 7–8 per group
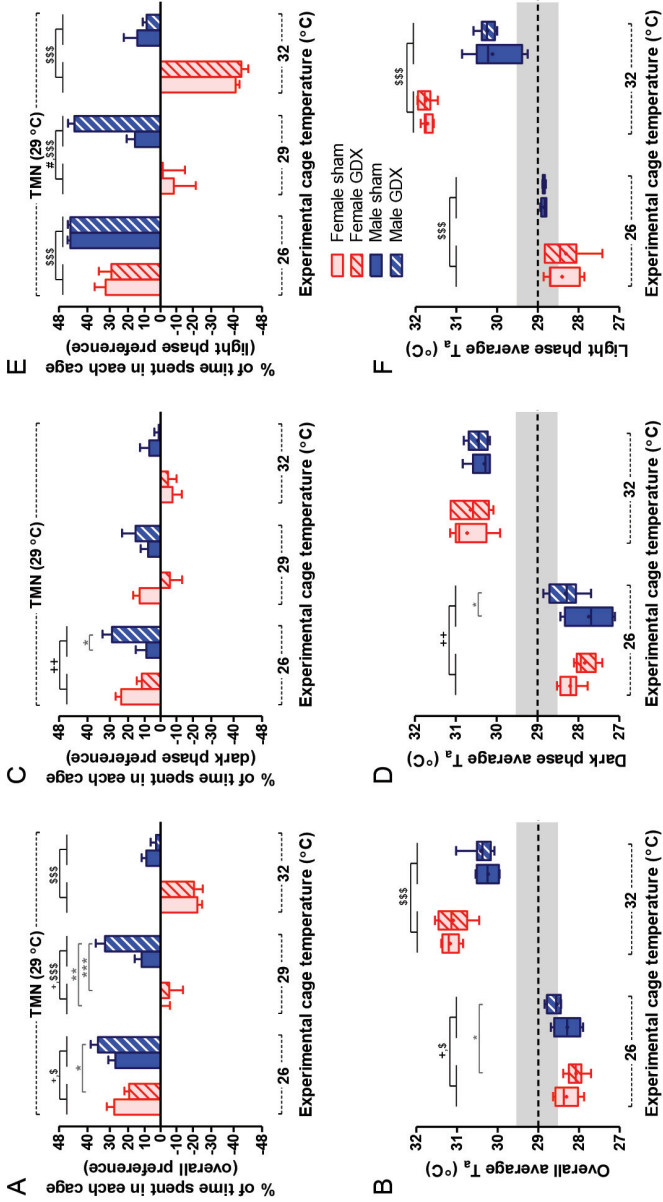
4

141

It is thus evident that GDX did not alter the sex-dependent thermal preferences when analyzing the active and inactive phase independently, except only for the male mice in the dark phase at experimental $T_a$ of 26 °C ($p$ = .030). In addition, the time-weighted average $T_a$, calculated from the location where the mice resided, was different between the active and inactive phases (**Fig. 3D,F**, respectively). The difference between male and female mice was the most obvious when they were able to choose between 29 and 32 °C in the inactive phase: female mice preferred higher $T_a$ than male mice without an effect of gonadal status (female sham 31.7 ± 0.1 °C, female GDX 31.8 ± 0.2 °C, male sham 30.1 ± 0.6 °C, and male GDX 30.2 ± 0.2 °C; $p_S$ < .001; **Fig. 3F**).

## The location of activities was affected mainly by ambient temperature and partially by orchiectomy

The experimental $T_a$ and sex influenced the transfer of nesting material by the mice ($p_T$ < .001, $p_S$ < .001, $p_{T\times S}$ = .013, $p_{T\times G}$ = .021; **Fig. 4A**). When the experimental $T_a$ was at 26 °C, all mice preferred to transfer the nesting material to the TMN cage. When the experimental $T_a$ was at 32 °C, female mice transferred the nesting material to this warmer cage while male mice did not transfer the nesting material at all. This trend of nest transfer to a warmer cage was similar to the temperature preference shown in **Fig. 3A** and was not affected by gonadal status. The "paperwork score," reflecting nest destructions, was only affected by the experimental $T_a$ without an effect of sex or gonadal status ($p_T$ < .001; **Fig. 4B**). The "nest score," which also takes the relative nest amount into account, was solely influenced by the experimental $T_a$ ($p_T$ < .001; **Fig. 4C**). Generally, the "nest score" negatively correlated with the experimental $T_a$, but the correlations were only significant for sham-operated female mice ($r$ = −.47, $p$ = .030) and gonadectomized male mice ($r$ = −.48, $p$ = .016).

The preference to consume food in the TMN or the experimental cage was not affected by experimental $T_a$, sex, or gonadal status, but there was a significant interaction between sex and gonadal status ($p_{S\times G}$ = .042; **Fig. 4D**). All mice generally consumed the food equally from both cages except at the experimental temperature of 26 °C when sham-operated male mice preferred food from the 26 °C experimental cage while the gonadectomized male mice preferred food from the TMN cage. The position where mice preferred to defecate was dependent on the experimental $T_a$ and the interactions between gonadal status and the other factors ($p_T$ < .001, $p_{T\times G}$ < .001, $p_{S\times G}$ = .002; **Fig. 4E**). When the experimental $T_a$ was set at 26 °C, most mice predominantly defecated in the 26 °C cage, except gonadectomized male mice that had no preference to defecate in either cage. When the $T_a$ was equal in both cages at 29 °C, only sham-operated male mice preferred the experimental cage while the others defecated equally

in both cages. When the experimental $T_a$ was at 32 °C, sham-operated female mice defecated more in the TMN cage, while mice of the other groups showed no preference. Interestingly, when correlating the nest-building pattern (the cage with a higher nest score) with the defecating pattern, it was evident that while all other mice defecated in the cage without the nest, gonadectomized male mice defecated more in the cage where they had built their nest.
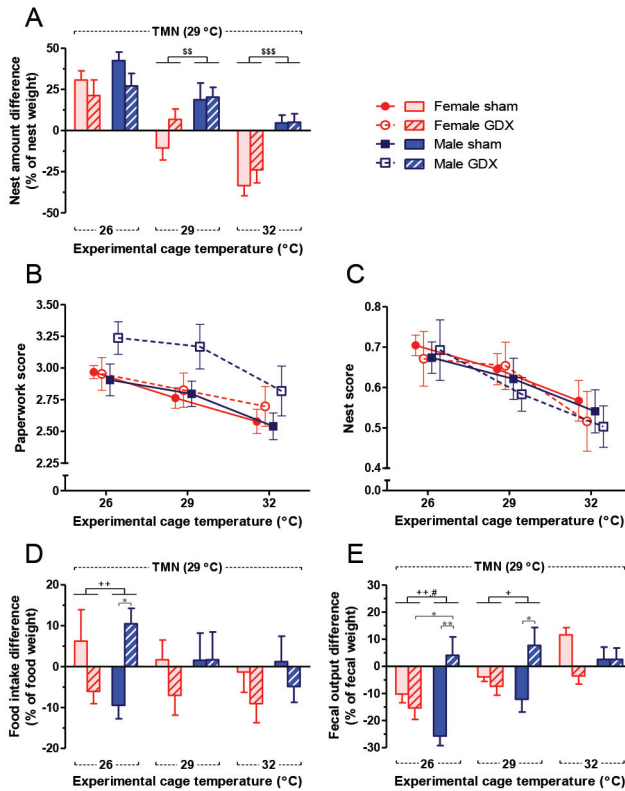


**Fig. 4** The location of activities was affected mainly by ambient temperature and partially by orchiectomy

**(A)** At the experimental $T_a$ of 26 °C all groups transferred the nest to the TMN cage, whereas at the experimental $T_a$ of 32 °C only female mice transferred the nest to the experimental cage. The difference of nest amount found in each cage is represented on the *y*-axis. Zero means the mice did not transfer the nesting material. A positive value means transfer of nesting material to the TMN cage while a negative value means transfer to the experimental cage, of which the $T_a$ is indicated on the *x*-axis. Nest-relating activities revealed negative correlations of $T_a$ to the **(B)** paperwork score and **(C)** nest score without an effect of sex or gonadal status. The experimental $T_a$, sex, or gonadal status did not affect **(D)** the preferred cage for food consumption, but orchiectomy and the experimental $T_a$ altered **(E)** the preferred cage for defecation. Two-way ANOVA: \$\$ $p_S < .01$, \$\$\$ $p_S < .001$, # $p_G < .05$, + $p_{S \times G} < .05$, ++ $p_{S \times G} < .01$, and Tukey test: * $p < .05$, ** $p < .01$. *Error bar* indicates SEM, n = 7–8 per group

## Discussion

The data presented in this paper demonstrate that female mice prefer a warmer environment than male mice, in agreement with previous studies [10, 21]. This article is the first to show that this sex difference in thermal preference in adult mice is not altered by GDX, suggesting that gonadal hormones are not the main driver of this sex difference in adult mice.

The preference to a higher $T_a$ of female mice could be explained by many other mechanisms involving a complex circuit that controls whole body thermal and energy homeostasis. The differences in body compositions may affect thermal preferences. We found that female C57BL/6J mice had a higher BSA to body mass ratio than male mice of the same age. Therefore, the female mice likely had a higher heat dissipation rate from the skin to the environment and consequently a higher energy demand than male mice which may have resulted in the preference to reside at a higher $T_a$. Moreover, this may have resulted in a higher relative daily food intake to match the higher passive heat loss. The higher food consumption of female mice was also noted in a previous study [22].

The body composition of C57BL/6J mice is sexually dimorphic: male mice have a higher lean body mass [23] with relatively more skeletal muscle mass [24] than female mice. Because heat is a byproduct of muscular activities, the higher muscle mass in male mice could explain why male mice have generally less thermal demand compared to female mice. Paul et al. [24] found that GDX abolished the sex-specific pattern of muscle mass leading to a reduction in muscle mass in castrated male mice to a comparable amount as found in ovariectomized and sham-operated female mice. This effect of castration could also explain the higher thermal demand of castrated male mice compared to sham-operated male mice in our study, while ovariectomy did not alter the thermal preference of female mice in the active phase at $T_a$ of 26 °C.

Control of $T_c$ is regulated by the brain. The preoptic area of the anterior hypothalamus (POAH) is the primary site that integrates afferent signals from peripheral thermoreceptors to control the physiological responses through projections to other hypothalamic areas that modulate non-shivering thermogenesis of BAT to match the overall thermal demand [25–27]. The female gonadal steroids estradiol and progesterone differently modulate the thermo-regulatory set point during the estrous cycle of mammals. A decline of $T_c$ in the pre-ovulatory phase is related to estrogen secretion in that phase while progesterone secretion at the luteal phase increases $T_c$ [11, 28]. Furthermore, there is evidence that estradiol and testosterone differentially affect steroid-sensitive neurons in the POAH of rats [29] and the central set point of temperature in different groups of hypothalamic neurons [12, 26]. We found that when the mice

were allowed to choose between 32 and 29 °C, the overall average preferred $T_a$ was higher for female mice than for male mice in the inactive phase, suggesting a sex-dependent regulation of the temperature set point in the mouse brain. However, since our study revealed that the removal of gonadal hormones by GDX did not affect the thermal preference of both male and female mice, we cannot conclude that the sex-dependent regulation of the temperature set point in the POAH depends on the different gonadal hormones. Nevertheless, effects of gonadal hormones outside the brain might be involved. For instance, estradiol, progesterone or testosterone differentially stimulated or inhibited the peripheral thermoreceptors [30], and estradiol and progesterone induce while testosterone reduces the thermogenesis of BAT [31, 32].

It is highly unlikely that the lack of an effect of GDX on thermal preference found in our studies is due to the sustained presence of sex hormones after GDX. Steroid hormones, including sex hormones, generally have half-lives of 4–170 min [33]. In C57BL/6 mice, the half-lives of 17β-estradiol and testosterone are less than 1 h [34, 35]. Moreover, locomotor activities and circadian rhythms have been shown to be altered as soon as 1 week after GDX [36].

Since we did not find an effect of post-pubertal GDX on thermal preference in adult mice, it is plausible that the mechanisms underlying the sex difference in thermal preference were generated prior to puberty. Sex hormones have permanent organizational effects on brain development during two sensitive periods [37]. Perinatally, testosterone secreted from the testes masculinizes the neural circuit in male mice while androgen absence in female rodents feminizes the nervous system. During puberty, elevations of gonadal hormones due to maturation of the hypothalamic-pituitary-gonadal axis strengthen the sex-dependent behaviors. In addition, it is reported that the POAH is a sexually dimorphic region in which morphological changes develop during puberty and that exposure to estrogenic compounds at puberty disturbs the development of neuronal circuits [38, 39].

## Conclusions

In summary, we found that adult female mice preferred a warmer environment than male mice of the same age, a difference that was especially apparent in the inactive phase. However, this sex difference did not depend on the presence of gonads. The sex difference in thermal preference in adult mice might be influenced by other sex-specific pathways rather than the gonadal factors or the central set point that controls the thermal balance has already been established at pre-pubertal stages.

## Abbreviations

BAT: brown adipose tissue; BSA: body surface area; BW: body weight; GDX: gonadectomy; POAH: preoptic area of the anterior hypothalamus; $T_a$: ambient temperature; $T_c$: core body temperature; TMN: thermoneutral; TNZ: thermoneutral zone; TPT: temperature preference test

## Acknowledgements

## Funding

## Availability of data and materials

The datasets generated and/or analyzed during the current study are available from the corresponding author on reasonable request.

## Authors' contributions

AG and APNT conceived the study. KK, AG and JS designed and performed the experiments and collected the data. KK, AG and JAV analyzed the data. KK wrote the paper. All authors provided valuable feedback on the manuscript and approved the final manuscript.

## Ethics approval

All experimental procedures were performed with the approval of the Animal Ethics Committee at Erasmus MC, Rotterdam, the Netherlands.

## Consent for publication

Not applicable

## Competing interests

The authors declare that they have no competing interests.

# References

1. IUPS Thermal Commission. Glossary of terms for thermal physiology. Jpn J Physiol. 2001;51:245-80.
2. Swoap SJ, Li C, Wess J, Parsons AD, Williams TD, Overton JM. Vagal tone dominates autonomic control of mouse heart rate at thermoneutrality. Am J Physiol Heart Circ Physiol. 2008;294:H1581-8.
3. Yamauchi C, Fujita S, Obara T, Ueda T. Effects of room temperature on reproduction, body and organ weights, food and water intakes, and hematology in mice. Exp Anim. 1983;32:1-11.
4. Gordon CJ. Temperature regulation in laboratory rodents. Cambridge: Cambridge University Press; 1993.
5. Havenaar R, Meijer JC, Morton DB, Ritskes-Hoitinga J, Zwart P. Biology and husbandry of laboratory animals. In: Van Zutphen LFM, Baumans V, Beynen AC, editors. Principles of Laboratory Animal Science. Second ed. Amsterdam: Elsevier; 2001: p. 19-76.
6. Gordon CJ, Becker P, Ali JS. Behavioral thermoregulatory responses of single- and group-housed mice. Physiol Behav. 1998;65:255-62.
7. Maloney SK, Fuller A, Mitchell D, Gordon C, Overton JM. Translating animal model research: does it matter that our rodents are cold? Physiology (Bethesda). 2014; 29:413-20.
8. Cannon B, Nedergaard J. Nonshivering thermogenesis and its adequate measurement in metabolic studies. J Exp Biol. 2011;214:242-53.
9. Schmidt-Nielsen K. Warm-blooded vertebrates: What do metabolic regression equations mean? In: Scaling: Why is Animal Size so Important? Cambridge: Cambridge University Press; 1984: p. 75-89.
10. Gaskill BN, Rohr SA, Pajor EA, Lucas JR, Garner JP. Some like it hot: Mouse temperature preferences in laboratory housing. Appl Anim Behav Sci. 2009;116:279-85.
11. Sanchez-Alavez M, Alboni S, Conti B. Sex- and age-specific differences in core body temperature of C57Bl/6 mice. Age (Dordr). 2011;33:89-99.
12. Charkoudian N, Stachenfeld N. Sex hormone effects on autonomic mechanisms of thermoregulation in humans. Auton Neurosci. 2016;196:75-80.
13. Stouffer RL, Hennebold JD. Structure, function, and regulation of the corpus luteum. In: Plant TM, Zeleznik AJ, editors. Knobil and Neill's Physiology of Reproduction. Fourth Edition). San Diego: Academic; 2015: p. 1023-76.
14. Sinchak K, Wagner EJ. Estradiol signaling in the regulation of reproduction and energy balance. Front Neuroendocrinol. 2012;33:342-63.
15. Martínez de Morentin Pablo B, González-García I, Martins L, Lage R, Fernández-Mallo D, Martínez-Sánchez N, et al. Estradiol regulates brown adipose tissue thermogenesis via hypothalamic AMPK. Cell Metab. 2014;20:41-53.
16. Rodriguez AM, Monjo M, Roca P, Palou A. Opposite actions of testosterone and progesterone on UCP1 mRNA expression in cultured brown adipocytes. Cell Mol Life Sci. 2002;59:1714-23.
17. Rodriguez-Cuenca S, Monjo M, Gianotti M, Proenza AM, Roca P. Expression of mitochondrial biogenesis-signaling factors in brown adipocytes is influenced specifically by 17beta-estradiol, testosterone, and progesterone. Am J Physiol Endocrinol Metab. 2007;292:E340-6.
18. Gaskill BN, Gordon CJ, Pajor EA, Lucas JR, Davis JK, Garner JP. Heat or insulation: behavioral titration of mouse preference for warmth or access to a nest. PLoS One. 2012;7:e32799.
19. Kalueff AV, Keisala T, Minasyan A, Kuuslahti M, Miettinen S, Tuohimaa P. Behavioural anomalies in mice evoked by "Tokyo" disruption of the Vitamin D receptor gene. Neurosci Res. 2006;54:254-60.
20. Cheung MC, Spalding PB, Gutierrez JC, Balkan W, Namias N, Koniaris LG, Zimmers TA. Body surface area prediction in normal, hypermuscular, and obese mice. J Surg Res. 2009;153:326-31.
21. Gaskill BN, Rohr SA, Pajor EA, Lucas JR, Garner JP. Working with what you've got: changes in thermal preference and behavior in mice with or without nesting material. J Therm Biol. 2011;36:193-9.
22. Comprehensive metabolic survey of 16 inbred strains of mice. MPD:9233. Mouse Phenome Database website. Seburn KL. 2001. http://phenome.jax.org. Accessed 30 Nov 2016.
23. Densitometric survey of 11 strains of mice. MPD:Jaxpheno1. Mouse Phenome Database website. The Jackson Laboratory. 2006. http://phenome.jax.org. Accessed 30 Nov 2016

24. Paul R, McMahon C, Elston M, Conaglen J. Regulation of murine skeletal muscle mass by testosterone and 17β-oestradiol. In *17th European Congress of Endocrinology; 16-20 May 2015; Dublin, Ireland*. Edited by Arlt W, Visser J, Beuschlein F. *Endocrine Abstracts*; 2015: GP.05.1

25. Boulant JA. Neuronal basis of Hammel's model for set-point thermoregulation. J Appl Physiol. 2006;100:1347-54.

26. Boulant JA. Hypothalamic neurons regulating body temperature. In: Comprehensive Physiology. Hoboken: Wiley; 2010: p. 105-26.

27. Saper CB, Lowell BB. The hypothalamus. Curr Biol. 2014;24:R1111-6.

28. Kaciuba-Uscilko H, Grucza R. Gender differences in thermoregulation. Curr Opin Clin Nutr Metab Care. 2001;4:533-6.

29. Silva NL, Boulant JA. Effects of testosterone, estradiol, and temperature on neurons in preoptic tissue slices. Am J Physiol. 1986;250:R625-32.

30. Kondrats'kyi AP, Kondrats'ka KO, Skryma R, Prevars'ka N, Shuba Ia M. Gender differences in cold sensitivity: role of hormonal regulation of TRPM8 channel [abstract]. Fiziol Zh. 2009;55:91-9.

31. Quarta C, Mazza R, Pasquali R, Pagotto U. Role of sex hormones in modulation of brown adipose tissue activity. J Mol Endocrinol. 2012;49:R1-7.

32. Law J, Bloor I, Budge H, Symonds ME. The influence of sex steroids on adipose tissue growth and function. Horm Mol Biol Clin Investig. 2014;19:13-24.

33. Molina PE. Chapter 1. General principles of endocrine physiology. In: Endocrine Physiology, 4e. New York: The McGraw-Hill Companies; 2013.

34. Laurent MR, Hammond GL, Blokland M, Jardi F, Antonio L, Dubois V, et al. Sex hormone-binding globulin regulation of androgen bioactivity in vivo: validation of the free hormone hypothesis. Sci Rep. 2016;6:35539.

35. Deshpande D, Kethireddy S, Gattacceca F, Amiji M. Comparative pharmacokinetics and tissue distribution analysis of systemically administered 17-β-estradiol and its metabolites in vivo delivered using a cationic nanoemulsion or a peptide-modified nanoemulsion system for targeting atherosclerosis. J Control Release. 2014;180:117-24.

36. Iwahana E, Karatsoreos I, Shibata S, Silver R. Gonadectomy reveals sex differences in circadian rhythms and suprachiasmatic nucleus androgen receptors in mice. Eur J Neurosci. 2008;27:432-43.

37. Sisk CL, Zehr JL. Pubertal hormones organize the adolescent brain and behavior. Front Neuroendocrinol. 2005;26:163-74.

38. Ceccarelli I, Della Seta D, Fiorenzani P, Farabollini F, Aloisi AM. Estrogenic chemicals at puberty change ERα in the hypothalamus of male and female rats. Neurotoxicol Teratol. 2007;29:108-15.

39. Tabarean I, Morrison B, Marcondes MC, Bartfai T, Conti B. Hypothalamic and dietary control of temperature-mediated longevity. Ageing Res Rev. 2010;9:41.

**4**

## Supplementary data



**score 1 :** < 5% damage

**score 2 :** 5-25% damage

**score 3 :** 25-50% damage

**score 4 :** > 50% damage
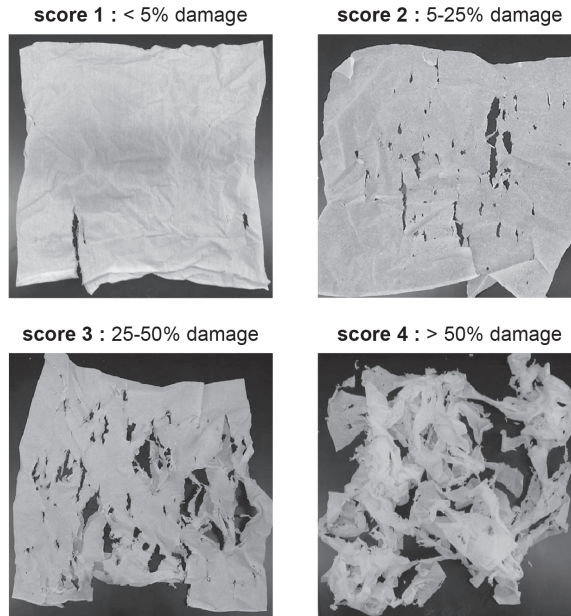
**Fig. S1**  Paperwork score

**Table S1**  Baseline characteristics

| Characteristic | Female sham before surgery (n=7) | Female GDX before surgery (n=7) | Male sham before surgery (n=7) | Male GDX before surgery (n=8) |
|---|---|---|---|---|
| Initial body weight (g) | 19.1 ± 0.7 | 19.5 ± 1.3 | 23.9 ± 0.8 | 24.0 ± 1.0 |
| Daily body weight gain (g) | 0.12 ± 0.13 | 0.08 ± 0.05 | 0.13 ± 0.05 | 0.19 ± 0.07 |
| Daily food intake (g) | 3.26 ± 0.44 | 3.10 ± 0.47 | 3.57 ± 0.63 | 3.48 ± 0.43 |
| Food intake in TMN cage (%) | 45.7 ± 9.7 | 47.2 ± 10.5 | 42.9 ± 6.9 | 46.8 ± 16.8 |
| Daily fecal production (mg) | 558 ± 56 | 576 ± 77 | 618 ± 86 | 593 ± 38 |
| Fecal weight in TMN cage (%) | 47.4 ± 10.8 | 44.6 ± 8.5 | 38.2 ± 9.0 | 30.9 ± 10.6 |
| Total time in TMN cage (%) | | | | |
|   29 °C *vs* 26 °C day | 79.1 ± 9.7 | 79.0 ± 9.9 | 70.9 ± 5.1 | 76.6 ± 11.1 |
|   29 °C *vs* 29 °C day | 55.2 ± 26.4 | 61.3 ± 25.7 | 64.3 ± 16.5 | 78.6 ± 17.0 |
|   29 °C *vs* 32 °C day | 46.3 ± 13.9 | 43.8 ± 20.6 | 54.9 ± 15.2 | 53.1 ± 22.7 |
| Preferred temperature (°C) | | | | |
|   29 °C *vs* 26 °C day | 28.37 ± 0.29 | 28.37 ± 0.30 | 28.13 ± 0.15 | 28.30 ± 0.33 |
|   29 °C *vs* 32 °C day | 30.61 ± 0.42 | 30.68 ± 0.62 | 30.35 ± 0.46 | 30.41 ± 0.68 |

All variables are described by the mean ± SD. No difference between sham and GDX groups of the same sex. (All *p* values > .05, unpaired *t* tests).
Abbreviations: TMN = Thermoneutral (29 °C), GDX = Gonadectomy
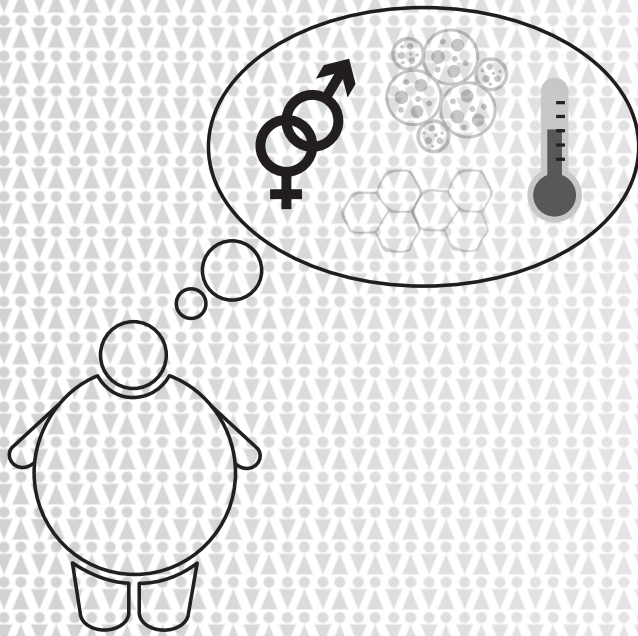
# Chapter 5

# Sex Difference in Cold Perception and Shivering Onset upon Gradual Cold Exposure

Kasiphak Kaikaew[1,2], Johanna C. van den Beukel[1], Sebastian J.C.M.M. Neggers[1], Axel P.N. Themmen[1], Jenny A. Visser[1], Aldo Grefhorst[1]

1  Department of Internal Medicine, Erasmus MC, University Medical Center Rotterdam, Rotterdam, the Netherlands
2  Department of Physiology, Faculty of Medicine, Chulalongkorn University, Bangkok, Thailand

5

## Abstract

To maintain a thermal balance when experiencing cold, humans reduce heat loss and enhance heat production. A potent and rapid mechanism for heat generation is shivering. Research has shown that women prefer a warmer environment and feel less comfortable than men in the same thermal condition. Using the Blanketrol® III, a temperature management device commonly used to study brown adipose tissue activity, we tested whether the experimental temperature ($T_E$) at which men and women start to shiver differs. Twenty male and 23 female volunteers underwent a cooling protocol, starting at 24 °C and gradually decreasing by 1–2 °C every 5 min until an electromyogram detected the shivering or the temperature reached 9 °C. Women started shivering at a higher $T_E$ than men (11.3 ± 1.8 °C for women *vs* 9.6 ± 1.8 °C for men, $P = 0.003$). In addition, women felt cool, scored by a visual analogue scale, at a higher $T_E$ than men (18.3 ± 3.0 °C for women *vs* 14.6 ± 2.6 °C for men, $P < 0.001$). This study demonstrates a sex difference in response to cold exposure: women require shivering as a source of heat production earlier than men. This difference could be important and sex should be considered when using cooling protocols in physiological studies.

**5**

## Highlights

- Women start shivering at a higher experimental temperature than men.
- Women feel colder and less comfortable than men during the same cooling protocol.
- Thermal perception at room temperature and sex are determinants of shivering onset.
- Sex of a participant should be considered for thermoregulation studies.

## Introduction

Humans tightly control their core body temperature ($T_c$) by balancing heat loss and heat production (Costanzo, 2017). When exposed to mild cold, humans first reduce heat loss by energy-inexpensive mechanisms such as the constriction of blood vessels supplying the peripheral tissues. This peripheral vasoconstriction not only reduces the heat transfer from the isothermal core to the non-isothermal shell, but also increases the insulating capacity of the skin and subcutaneous tissues. The shift of blood from superficial layers to deeper vessels results in an increased total body insulation since the bloodless layer, where the convective heat loss substantially diminishes, becomes thicker (Anderson, 1999). However, if the thermal balance cannot be accomplished by a reduction in heat loss, heat production is required (Tansey and Johnson, 2015).

Heat production can be achieved by many mechanisms (Castellani and Young, 2016; Hall, 2015). Exposure to cold activates the sympathetic nervous system (SNS), immediately increasing the metabolic rates of all cells in the body that consequently generate heat as a by-product of metabolism. The direct stimulation of β-adrenergic receptors by the SNS also activates brown adipose tissue (BAT), a specialized metabolic tissue that can convert energy into heat (Lee et al., 2013). When the metabolic heat production (non-shivering thermogenesis) together with the cutaneous vasoconstriction is not sufficient to maintain the optimal $T_c$, shivering begins.

Shivering, which is the involuntary rhythmic contraction of skeletal muscles, is the most potent and rapid mechanism to generate heat in response to cold stress. When the skin senses cold via the transient receptor potential cation channel subfamily M member 8 (TRPM8) on the sensory nerves (Voets et al., 2004), it signals to the temperature center in the hypothalamus. The primary motor center for shivering in the posterior hypothalamus is then activated and transmits signals to the skeletal muscles to initiate shivering throughout the body (Hall, 2015). At the maximum intensity of shivering, metabolic heat production can rise to five times of the resting levels (Eyolfson et al., 2001).

Various cooling techniques have been used to study the physiological responses to cold environment, especially after the rediscovery of BAT in adult humans in the last decade (Nedergaard et al., 2007) because cold is a well-known stimulant for the thermogenic function of BAT. The cooling methods include cold-water immersion, cold-air exposure, cold-air exposure combined with localized cooling e.g. feet cooling in ice water, and water-filled cooling blankets or suits (Castellani and Young, 2016; van der Lans et al., 2014). The cooling blanket with temperature of the filling water set at 1–2°C above the shivering point (also known as a personalized cooling protocol) is likely the method that maximally

activates BAT (Bahler et al., 2017). Using this cooling method, conduction will be the mode of heat transfer at those body areas that are covered and in direct contact with the cooling blankets whereas convection will occur at areas without direct contact with the blankets. One of the frequently used cooling blankets is the Blanketrol® III, a temperature management device that can control the temperature of the circulating water in a range from 4 °C to 42 °C.

Research has shown that sex is one of the important factors that influence thermal perception and physiological responses to cold. Karjalainen (2007) demonstrated that women prefer a higher ambient temperature and feel less comfortable than men in the same thermal environment, especially during the winter season. Furthermore, Kingma and van Marken Lichtenbelt (2015) showed that women require more heat production than men in the standard indoor climate setting that was mainly based on male metabolic rates. Castellani and Young (2016) revealed that the primary source of the variable capability to maintain a normal $T_c$ between men and women during whole-body cold exposure is body anthropometric and body composition characteristics. At the same body mass and surface area, women generally have a higher subcutaneous fat content than men that enhances insulation (Anderson, 1999; Castellani and Young, 2016; Kuk et al., 2005). On the other hand, when the subcutaneous fat thickness is equal between a man and a woman, the latter in general will have a larger body surface area (BSA) and a smaller body mass contributing to a greater total heat loss and a lower heat-production capacity during resting cold exposure (Castellani and Young, 2016; Graham, 1988).

Understanding sex differences in thermal regulation and cold-induced physiological responses is beneficial in many aspects. For instance, Iyoho et al. (2017) proposed a sex-specific modification of the thermoregulation model for predicting thermal response in a wide range of the operational conditions for military relevant tasks, especially in the cold-stress responses. Chaudhuri et al. (2018) showed that different physiological parameters from male and female occupants were needed to accurately predict the thermal comfort status in a range of the general indoor climate setting. Graham (1988) demonstrated that men and women respond differently in many physiological parameters when exercising or resting in either a cold room or cold water, which frequently could not be explained solely by sex-specific morphological differences. A review of chamber experiments and field studies to identify the factors influencing individual differences on thermal comfort by Wang et al. (2018) revealed that women are more critical about indoor thermal settings and more sensitive to deviations of thermal environment than men, but a consistent conclusion on sex differences in thermal comfort could not be drawn. Moreover, it has not been addressed whether men and women differ in the shivering onset after a gradually

cold exposure using the Blanketrol® III, a common method for studying BAT activation. To test this, we exposed healthy volunteers to cold progressively and determined the experimental temperature ($T_E$) at which the volunteers started to shiver. This study demonstrates sex differences in the physiological responses to a gradual cold exposure.

## Methods

### Participants

We recruited 43 participants (20 men and 23 women) who met the inclusion criteria: age 16–35 years; being physically healthy; Caucasian ethnicity; body mass index (BMI) 18.5–29.9 kg/m$^2$ for participants aged more than 20 years old, or BMI standard deviation score (BMI-SDS) between −2 and +2 for participants aged 16–19 years old. The following exclusion criteria were used: diabetes mellitus, thyroid disorders, substance use disorders, pregnancy, breastfeeding, and using β-adrenergic blocking medication. Participants were requested to eat, drink, and sleep as their usual routines, and requested not to smoke, eat, or drink any caffeinated or alcohol beverage within one hour before an appointment.

Since female sex hormones fluctuate during the reproductive cycle and could potentially influence the thermal balance (Charkoudian and Stachenfeld, 2014), female participants were included as follows. When a female participant was using contraceptive pills, she could only participate on a day she was taking a hormone-containing pill. When the female participant was not using contraceptive pills, she could not participate in the early follicular phase of her menstrual cycle, i.e. her menstruation period. In addition, we asked the female participants about their menstrual history to identify the phase of reproductive cycle at the day of experiment.

The experiment was performed after the participants had signed the written informed consent. The study was conducted according to the principles of the Declaration of Helsinki (version 19 October 2013). The procedures had been approved by the IRB of Erasmus MC, University Medical Center Rotterdam, the Netherlands.

### Study design

To limit the influence of the environmental temperature on thermal perception (Makinen et al., 2004), the experiment was performed during the summer (July–September 2017). Daily mean temperatures of Rotterdam, the city where the experiment was performed, were obtained from the Royal Dutch

Meteorological Institute (KNMI) via a publicly accessible database (KNMI, 2017). For further analysis, the outside temperature for each individual was calculated from three-day daily-mean-temperatures (2 days before and the day of the experiment).

The experiment was performed in the same laboratory with a standard heating, ventilation and air-conditioning system at a spot without direct air flow. The overall experimental design is illustrated in **Fig. 1**. Room temperature was recorded to verify the thermal condition. After arriving at the laboratory, participants acclimatized to the thermal setting of the room for at least 30 min. During the acclimatization period, participants changed their clothing to shorts and a T-shirt, filled in a questionnaire (**Fig. 2A**), rated their thermal perception, and were measured for anthropometric characteristics.

**5**

### Pre-experiment

**Possibly contributing factor assessment**

- Anthropometric measurement
- Behavioral data (questionnaire)
- Record ambient temperature

### Experiment: Cooling protocol

**Physiological monitoring**

- Surface electromyography for identifying shivering $T_E$
- Skin temperature
  - Supraclavicular area
  - Midsternal area
  - Dorsum of hand

**Subjective measurement**

- Thermal sensation
- Thermal comfort
- Shivering intensity

### Post-experiment: Data analysis

**Male *vs* Female comparison**

- Unpaired *t* test
- RM-ANOVA

**Predictor identification**

- Stepwise linear regression

**Fig. 1** Overall experimental procedure

The primary outcome is to identify a shivering $T_E$: the experimental temperature at which shivering started.

To assess the thermal perception, we used the visual analogue scales (VAS; **Fig. 2B**) for thermal sensation ($VAS_{sensation}$) and thermal comfort ($VAS_{comfort}$), adapted from Zhang and Zhao (2008). $VAS_{sensation}$ is reported on ASHRAE 7-point scales: hot (+3), warm (+2), slightly warm (+1), neutral (0), slightly cool (−1), cool (−2), and cold (−3). $VAS_{comfort}$ includes 6-point scales: very comfortable (+3), comfortable (+2), just comfortable (+1), just uncomfortable (−1), uncomfortable (−2), and very uncomfortable (−3). Of note, the $VAS_{comfort}$ score does not contain 'neutral', to make a clear determination to either the 'comfortable' or 'uncomfortable' category.

We followed the American College of Sports Medicine (ACSM)'s Guidelines For Exercise Testing and Prescription (ACSM, 2013) for anthropometric measurement. In brief, body mass was measured with a 0.5-kg based scale, and body height was measured with a 0.5-cm based stadiometer. Waist circumference was measured at the height of the iliac crest, and hip circumference was measured at the maximal circumference of buttocks with the subject standing upright. BSA was calculated by the formula (Reading and Freeman, 2005):

$$BSA = 1/6 \cdot (W \cdot H)^{0.5}.$$

In this formula, BSA is in $m^2$, W is weight in kg, and H is height in m. Skinfold thickness was measured in mm at three sites, depending on the sex of the participant (Nieman, 2011). For men, skinfolds were measured at the chest (diagonal fold, halfway between the anterior axillary line and the nipple), the abdomen (vertical fold, 2 cm to the right side of the umbilicus), and the thigh (vertical fold, on the anterior midline, halfway between the proximal border of the patella and the inguinal crest). For women, skinfolds were measured at the triceps (vertical fold, halfway between the acromion and olecranon processes, with the arm held freely to the side of the body), the suprailiac site (diagonal fold, at the anterior axillary line immediately superior to the iliac crest), and the abdomen (as described above). Body density (BD) and body fat percentage (%BF) were calculated by the following formulas (ACSM, 2013).

$BD_{men}$ = 1.10938 − 0.0008267·(sum of skinfolds) + 0.0000016·(sum of skinfolds)$^2$ − 0.0002574·age

$BD_{women}$ = 1.089733 − 0.0009245·(sum of skinfolds) + 0.0000025·(sum of skinfolds)$^2$ − 0.0000979·age

%BF = (457/BD) − 414.2

For the mentioned formulas, sum of skinfolds is in mm, and age is in years.

After the acclimatization period, two surface electromyography (EMG) electrodes (Nutrode Mini-P10MO, O&R Medical) for monitoring the electrical activity of the rectus femoris muscle were placed at anterior mid-thigh with an

**5**

**5**

**A**

1. Do you smoke? If yes, how many cigarettes per day?
   ☐ Never
   ☐ Rarely / Sometimes
   ☐ 1–10 cigarettes per day
   ☐ > 10 cigarettes per day

2. Do you drink alcoholic beverages? If yes, how many drinks per day?
   ☐ Never
   ☐ Rarely / Sometimes
   ☐ 1 drink per day
   ☐ 2–3 drinks per day
   ☐ ≥ 4 drinks per day

3. Do you drink caffeinated beverages (e.g. coffee, cola, energy drink)? If yes, how many cups/cans per day?
   ☐ Never
   ☐ Rarely / Sometimes
   ☐ 1 cup/can per day
   ☐ 2–3 cups/cans per day
   ☐ ≥ 4 cups/cans per day

4. How often do you do physical exercises / sports?
   ☐ Never
   ☐ Rarely / Sometimes
   ☐ Once per week
   ☐ 2–3 days per week
   ☐ ≥ 4 days per week

5. Do you have any problems or feel uncomfortable with thermal conditions at home or workplace?

**B**

How do you feel?

├ Hot
├ Warm
├ Slightly warm
├ Neutral
├ Slightly cool
├ Cool
├ Cold

How comfortable are you?

├ Very comfortable
├ Comfortable
├ Just comfortable
├ Just uncomfortable
├ Uncomfortable
├ Very uncomfortable

**C**

| Time (minute) | $T_E$ (°C) |
|---|---|
| 0 | 24 |
| 5 | 22 |
| 10 | 20 |
| 15 | 18 |
| 20 | 16 |
| 25 | 14 |
| 30 | 12 |
| 35 | 11 |
| 40 | 10 |
| 45 | 9 |
| 50 or at shivering | 30 |

**Fig. 2** Tools for evaluating thermal perception

(**A**) A questionnaire for evaluating the possible factors that may influence thermal perception. (**B**) Visual analogue scales (VAS) for assessing thermal perception: $VAS_{sensation}$ and $VAS_{comfort}$. (**C**) A cooling protocol showing the experimental temperature ($T_E$) setup of the Blanketrol at each indicated time.

inter-electrode center-to-center distance of 4 cm. The rectus femoris muscle was chosen for monitoring since it is one of the muscle groups recruited at onset of the shivering (Blondin et al., 2011; Tikuisis et al., 1991) and the movement artefact of the leg is easily detected by an investigator. The other electrode was placed on an ankle as a ground. EMG signals were transmitted using the Bio Amp Cable (model MLA2540, ADInstruments) to the PowerLab 26T (model ML856, ADInstruments). The signals were monitored on LabChart software (version 7, ADInstruments) with a sampling rate of 1,000 Hz, band-pass filters of 10 Hz and 500 Hz, a notch filter of 50 Hz, and an amplification range between ±1 mV to ±5 mV depending on the resting activity of each individual [modified from Blondin et al. (2011)]. Next, three Thermochron iButton® digital thermometers (model DS1921H, Maxim Integrated) were applied at the supraclavicular area, the midsternal area, and the dorsum of the hand with medical adhesive tapes (Micropore, 3M) for continuous measuring of skin temperature ($T_{sk}$) with a one-minute interval. Then, the cooling protocol started.

## Cooling protocol

The Blanketrol® III Hyper-Hypothermia System (model 233, Cincinnati Sub-Zero), the Maxi-Therm® Lite Patient Vest (model 800, Cincinnati Sub-Zero), and the Maxi-Therm® Lite Blanket (model 876, Cincinnati Sub-Zero) were used as a temperature management system. The Blanketrol regulates the temperature of the water that circulates through the Vest and the Blanket. The Vest covered shoulders, chest, abdomen, and back of the participant who was lying supine on a bed. The Blanket covered hip, groin, buttock, and anterior and posterior of thighs. Calculated with the Lund and Browder chart that is normally used to estimate the burn areas in patients (Hettiaratchy and Papini, 2004), the Vest and Blanket covered more than 50% of total BSA.

The cooling protocol started with the Blanketrol set at 24 °C after which the $T_E$ was reduced by 1–2 °C every 5 min (a detailed setting is shown in **Fig. 2C**). During the cooling protocol, a participant was requested to lie still without any leg movement. When the EMG detected an onset of shivering burst (EMG amplitudes exceeded the resting values with a duration of > 0.2 s and an interburst interval of > 0.75 s; without any active movement of the leg observed by an investigator), the cooling protocol was terminated and the temperature of the Blanketrol was recorded as the shivering $T_E$. However, if the participant did not shiver after 50 min of the cooling protocol (at 9 °C), the experiment was also stopped and the shivering $T_E$ of that participant was assumed to be 8 °C. Subsequently, the Blanketrol was set at 30 °C to warm up a participant for at least 10 min or until the participant was satisfied with the thermal comfort.

During the cooling protocol, a participant rated the $VAS_{sensation}$ score every 5 min before the next-step $T_E$ setting and rated the $VAS_{comfort}$ score every 15 min at the $5^{th}$, $20^{th}$, $35^{th}$, and $50^{th}$ minutes. At the end of the cooling protocol, we asked a participant to rate his or her shivering intensity as either no shivering, minimal shivering, moderate shivering, or profound shivering.

**Data analysis & Statistics**

The statistical tests were performed using IBM SPSS Statistics for Windows (version 24, IBM Corp.) and GraphPad Prism for Windows (version 6, GraphPad Software Inc.). A difference between groups was analyzed by an unpaired *t* test or a Mann–Whitney *U* test when the data were not normally distributed. For categorical data, a difference between groups was analyzed with a Fisher's exact test. The effects of sex and $T_E$ on $VAS_{sensation}$ score, $VAS_{comfort}$ score, and $T_{sk}$ were analyzed using 2-way repeated measures analysis of variance (RM-ANOVA) with a Bonferroni's multiple comparisons test when appropriate. Stepwise linear regression was used to identify factors influencing the shivering $T_E$. Statistical significance is considered when $P < 0.05$. Unless otherwise indicated, data are presented as mean ± SD.

**Results**

The characteristics and the anthropometric data of the recruited participants are shown in **Table 1**. The age was not different between the sexes ($P = 0.67$). Men were taller and heavier than women ($P < 0.001$ for both height and weight). When calculating BMI and categorizing to normal or overweight subgroups, there was no difference between the sexes ($P = 0.90$ for BMI and $P = 1.00$ for BMI category). Men had a larger BSA than women ($P < 0.001$) while women had a higher BSA-to-mass ratio than men ($P < 0.001$). Men had a larger waist circumference than women ($P < 0.001$) but they had equal hip circumferences ($P = 0.96$); hence, waist-to-hip ratio is higher for men than for women ($P < 0.001$). Women tended to have a greater sum of skinfold thickness (P = 0.08) and had a significantly higher body fat percentage than men ($P < 0.001$). Concerning the five behavioral data collected from the questionnaire (**Fig. 2A**), four of them revealed no significant difference between men and women, except that women reported more discomforts than men at their home or workplace thermal condition ($P = 0.01$). The outside temperature when the experiment was performed was slightly higher for women than for men ($P = 0.04$; **Table 1**). However, the room temperature at which all participants acclimatized before the cooling protocol was not different between men and women ($P = 0.09$).

**Table 1** Characteristics of participants and ambient temperatures

| Parameters | Men (n = 20) | Women (n = 23) |
|---|---|---|
| Age (year) | 23.5 (8.8) | 22.0 (9.0) |
| Height (cm) * | 184.4 (6.9) | 170.9 (4.8) |
| Weight (kg) * | 76.0 (9.8) | 64.8 (9.0) |
| BMI (kg/m$^2$) | 22.4 (2.7) | 22.2 (3.4) |
| Normal | 16 (80%) | 19 (83%) |
| Overweight | 4 (20%) | 4 (17%) |
| BSA (m$^2$) * | 1.97 (0.14) | 1.75 (0.12) |
| BSA-to-mass ratio (×10$^{-2}$ m$^2$/kg) * | 2.61 (0.15) | 2.72 (0.18) |
| Waist circumference (cm) * | 83.7 (7.7) | 74.7 (6.3) |
| Hip circumference (cm) | 100.9 (4.5) | 100.8 (7.0) |
| Waist-to-hip ratio * | 0.83 (0.06) | 0.74 (0.04) |
| Sum of skinfolds (cm) | 46.0 (20.3) | 56.9 (18.9) |
| Body fat percentage (%) * | 13.1 (5.6) | 23.6 (4.8) |
| Smoking history | | |
| Never | 16 (80%) | 22 (96%) |
| Rarely/sometimes | 3 (15%) | – |
| 1–10 cigarettes per day | – | 1 (4%) |
| > 10 cigarettes per day | 1 (5%) | – |
| Alcohol consumption | | |
| Never | 4 (20%) | 4 (17%) |
| Rarely/sometimes | 13 (65%) | 16 (70%) |
| One drink per day | 3 (15%) | 3 (13%) |
| Caffeine consumption | | |
| Never | 2 (10%) | – |
| Rarely/sometimes | 6 (30%) | 10 (43%) |
| One cup per day | 3 (15%) | 7 (30%) |
| 2–3 cups per day | 5 (25%) | 6 (26%) |
| ≥ 4 cups per day | 4 (20%) | – |
| Exercise/sports frequency | | |
| Never | 2 (10%) | – |
| Rarely/sometimes | 6 (30%) | 8 (35%) |
| once per week | 8 (40%) | 11 (48%) |
| 2–3 days per week | 4 (20%) | 4 (17%) |
| Thermal complaint/discomfort * | | |
| No | 20 (100%) | 16 (70%) |
| Sometimes | – | 5 (22%) |
| Often | – | 2 (9%) |
| Outside temperature (°C) * | 16.3 (4.7) | 18.0 (1.8) |
| Room temperature (°C) | 23.7 (0.7) | 24.0 (0.7) |

For BMI category, normal indicates BMI 18.5–24.9 kg/m$^2$ for adult (≥ 20 years) and BMI-SDS from −2 to 1 for adolescent (16–19 years); overweight indicates BMI 25.0–29.9 kg/m$^2$ for adult and BMI-SDS 1–2 for adolescent.

Data are shown as mean (SD), except age and outside temperature are shown as median (IQR), and BMI category and behavioral data are shown as n (%).

* indicates a statistically significant difference between male and female participants.

Experiencing the identical cooling protocol, women started shivering at a higher $T_E$ than men (shivering $T_E$: 11.3 ± 1.8 °C for women *vs* 9.6 ± 1.8 °C for men, $P = 0.003$; **Fig. 3A**). At the average shivering $T_E$ for women, 65% (15/23) of women shivered while only 25% (5/20) of men started shivering ($P = 0.014$). Throughout the cooling protocol, all participants felt colder when the $T_E$ declined with women perceiving the $T_E$ colder (lower $VAS_{sensation}$ score) than men ($P_{Sex×Temp}$ < 0.001, $P_{Sex}$ = 0.004, $P_{Temp}$ < 0.001; **Fig. 3B**). Remarkably, the difference in $VAS_{sensation}$ score between men and women was statistically significant when the $T_E$ was between 14 °C and 20 °C. Furthermore, women felt more uncomfortable (lower $VAS_{comfort}$ score) than men during the experiment, and both groups felt more uncomfortable when the $T_E$ declined ($P_{Sex×Temp}$ = 0.006, $P_{Sex}$ = 0.01, $P_{Temp}$ < 0.001; **Fig. 3C**).

Concerning thermal sensation and thermal comfort at room temperature before the cooling protocol started, female and male participants did not differ in both $VAS_{sensation}$ score ($P = 0.98$) and $VAS_{comfort}$ score ($P = 0.61$). Interestingly, women started to feel 'colder than neutral' ($VAS_{sensation}$ score < 0) at a higher $T_E$ than men (22.1 ± 1.9 °C for women *vs* 20.3 ± 3.5 °C for men, $P = 0.04$; **Fig. 3D**). Women also started to feel 'cool' ($VAS_{sensation}$ score ≤ −2) at a higher $T_E$ than men (18.3 ± 3.0 °C for women *vs* 14.6 ± 2.6 °C for men, $P < 0.001$; **Fig. 3E**). At the average 'cool' $T_E$ for women, 65% (15/23) of women felt cool whereas only 20% (4/20) of men did ($P = 0.005$). At the end of the cooling protocol, when shivering was detected or $T_E$ reached 9 °C, women felt colder than men ($VAS_{sensation}$ score −3 ± 0 for women *vs* −3 ± 1 for men [median ± IQR], $P = 0.03$), but both sexes perceived the thermal discomfort equally ($VAS_{comfort}$ score −2 ± 1 for women *vs* −2 ± 1.25 for men [median ± IQR], $P = 0.29$). Women, moreover, perceived the shivering more intense than men at the end of cooling protocol ($P = 0.009$; **Fig. 3F**).

Factors that could possibly influence the shivering $T_E$ are listed in **Table 2**. Only sex of the participants, $VAS_{comfort}$ score at room temperature, and $VAS_{sensation}$ score at room temperature were statistically significant predictors of the shivering $T_E$ (stepwise linear regression: $F(3,39) = 9.352$, $P < 0.001$, $R^2$ = 0.418). Interestingly, when sex of the participants was removed from the analysis, the statistically significant predictors of the shivering $T_E$ consisted of BSA-to-mass ratio, $VAS_{comfort}$ score at room temperature, and an amount of caffeine consumption (stepwise linear regression: $F(3,39) = 7.026$, $P = 0.001$, $R^2$ = 0.351).

Since body composition was different between men and women, we performed a subgroup analysis of 19 men and 16 women by using the lowest BSA-to-mass ratio of the female participants as a minimal cut-off value and the highest BSA-to-mass ratio of the male participants as a maximal cut-off value
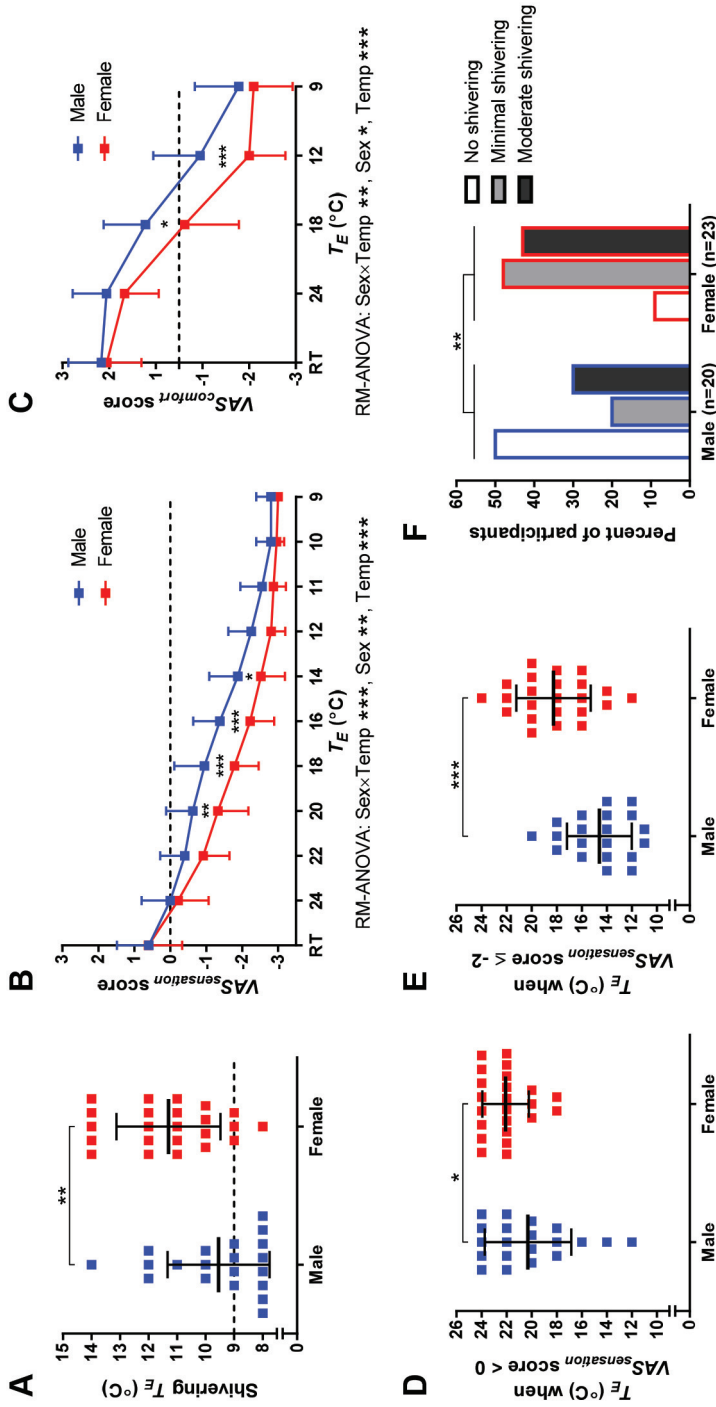
**Fig. 3** Women shivered and perceived cold earlier than men.

**(A)** Women started shivering at a higher experimental temperature ($T_E$) than men. The dotted line indicates the lowest experimental temperature. For those participants not shivering at 9 °C, the shivering temperature was set at 8 °C. **(B–C)** Women felt colder (lower $VAS_{sensation}$ score) and more uncomfortable (lower $VAS_{comfort}$ score) than men during the cooling protocol. Dotted lines indicate 'neutral' perception. **(D–E)** Women started to feel 'colder than neutral' ($VAS_{sensation}$ score < 0) and 'cool' ($VAS_{sensation}$ score ≤ −2) at higher temperatures than men. **(F)** Women perceived the shivering more intense than men. Statistical significance indicates by $P$ values: $P < 0.05$ (*), $P < 0.01$ (**), and $P < 0.001$ (***). Error bar indicates SD.

**5**

(BSA-to-mass ratio 0.0263 ± 0.0014 m²/kg for men *vs* 0.0264 ± 0.0016 m²/kg for women, $P = 0.70$). The results showed the same pattern that women started shivering at a higher $T_E$ than men (11.1 ± 1.9 °C for women *vs* 9.6 ± 1.8 °C for men, $P = 0.03$). Women also started to feel 'cool' ($VAS_{sensation}$ score ≤ −2) at a higher $T_E$ than men (17.6 ± 2.7 °C for women *vs* 14.6 ± 2.7 °C for men, $P = 0.002$) whereas the $T_E$ at which a participant started to feel 'colder than neutral' ($VAS_{sensation}$ score < 0) was not statistically significant (21.8 ± 1.9 °C for women *vs* 20.4 ± 3.5 °C for men, $P = 0.18$).

**Table 2** Factors that could influence the shivering $T_E$

| Factors | All factors | | | Excluding Sex | | |
|---|---|---|---|---|---|---|
| | Beta | Sig. | | Beta | Sig. | |
| Sex | 0.444 | 0.001 | ** | — | | |
| Age (year) | 0.049 | 0.71 | ns | 0.154 | 0.44 | ns |
| BSA-to-mass ratio (m²/kg) | 0.148 | 0.31 | ns | 0.480 | 0.002 | ** |
| Body fat percentage (%) | −0.325 | 0.08 | ns | 0.231 | 0.08 | ns |
| Sum of skinfolds (cm) | −0.239 | 0.07 | ns | 0.101 | 0.52 | ns |
| Abdominal skinfold (cm) | −0.230 | 0.08 | ns | −0.100 | 0.55 | ns |
| Smoking | −0.072 | 0.57 | ns | −0.212 | 0.15 | ns |
| Alcohol consumption | 0.156 | 0.21 | ns | 0.189 | 0.17 | ns |
| Caffeine consumption | 0.238 | 0.06 | ns | 0.299 | 0.04 | * |
| Exercise frequency | 0.056 | 0.66 | ns | 0.011 | 0.93 | ns |
| Thermal complaint | 0.240 | 0.07 | ns | 0.253 | 0.08 | ns |
| $VAS_{sensation}$ score at room temperature | −0.282 | 0.03 | * | −0.171 | 0.23 | ns |
| $VAS_{comfort}$ score at room temperature | −0.339 | 0.009 | ** | −0.284 | 0.04 | * |
| Baseline 3-site average $T_{sk}$ | 0.092 | 0.49 | ns | −0.177 | 0.19 | ns |
| Outside temperature (°C) | −0.087 | 0.53 | ns | 0.120 | 0.42 | ns |
| Room temperature (°C) | −0.161 | 0.21 | ns | −0.086 | 0.52 | ns |
| Time of experiment | 0.206 | 0.10 | ns | 0.239 | 0.08 | ns |

Stepwise linear regression was analyzed to predict the shivering $T_E$ from indicated factors. Time of experiment indicates the period of the day when the experiment was performed, dividing into 3 periods: 09:00–11:59, 12:00–14:59, and 15:00–17:59. Sig. (statistical significance) indicates by *P* values: *P* > 0.05 (ns), *P* < 0.05 (*), and *P* < 0.01 (**).

Throughout the cooling experiment, $T_{sk}$ was monitored at 3 areas of the body. The $T_{sk}$ at the supraclavicular area decreased with the declining $T_E$ without a statistically significant difference between men and women ($P_{Sex \times Temp}$ = 1.00, $P_{Sex}$ = 0.14, $P_{Temp}$ < 0.001; **Fig. 4A**). The $T_{sk}$ at the midsternal area was not different between men and women; however, it was statistically significantly increased during the first few minutes of the cooling protocol, and remained stable until the end of the protocol ($P_{Sex \times Temp}$ = 0.64, $P_{Sex}$ = 0.65, $P_{Temp}$ < 0.001; **Fig. 4B**). The $T_{sk}$ at the dorsum of the hand decreased with the declining $T_E$ and, interestingly, male participants had higher hand temperatures than female participants during the cooling protocol ($P_{Sex \times Temp}$ < 0.001, $P_{Sex}$ = 0.02, $P_{Temp}$ < 0.001; **Fig. 4C**).

Concerning the 5-min average $T_{sk}$ at each stage of the cooling protocol, women tended to have a lower baseline $T_{sk}$ at the dorsum of the hand and supraclavicular area than men while the $T_{sk}$ at the midsternal area was similar in both sexes (**Table 3** and **Fig. 4**). The average $T_{sk}$ from the 3 sites at baseline was significantly lower in women than in men. However, when the baseline 3-site average $T_{sk}$ was added into the stepwise linear regression analysis, it was not a significant predictor for the shivering $T_E$ (**Table 2**). When participants started to feel 'colder than neutral' ($VAS_{sensation}$ score < 0) or 'cool' ($VAS_{sensation}$ score ≤ −2), all of the measured $T_{sk}$'s and the declines of $T_{sk}$'s from the baseline values ($\Delta T_{sk}$) were not different between the sexes (**Table 3**). At the end of the cooling protocol (shivering started or $T_E$ reached 9 °C), women had a significantly lower hand $T_{sk}$ than men while the supraclavicular and midsternal $T_{sk}$'s were not different between the sexes. The 3-site average $T_{sk}$ at the end of cooling protocol was also significantly lower in women than in men; however, the decline in average $T_{sk}$ ($\Delta T_{sk}$) at the end of the cooling protocol was similar in both sexes. Interestingly, the midsternal $T_{sk}$ did not differ between the sexes and remained unchanged during the cooling stages. As a result, the difference between the midsternal $T_{sk}$ and the hand $T_{sk}$ was greater after cold exposure and tended to be higher in women than in men (midsternal $T_{sk}$ − hand $T_{sk}$: 4.5 ± 2.0 °C for women at baseline, 3.4 ± 2.6 °C for men at baseline, 6.0 ± 1.4 °C for women at shivering, and 4.6 ± 2.1 °C for men at shivering; $P_{Cold \times Sex}$ = 0.42, $P_{Cold}$ < 0.001, $P_{Sex}$ = 0.07).

## Discussion

This study revealed that women and men respond differently when experiencing cold. Female participants felt cold at a higher $T_E$ and started shivering at a higher $T_E$ than male participants upon the gradually cold exposure using the water-filled cooling blanket, a commonly used device to study the BAT activity in humans.
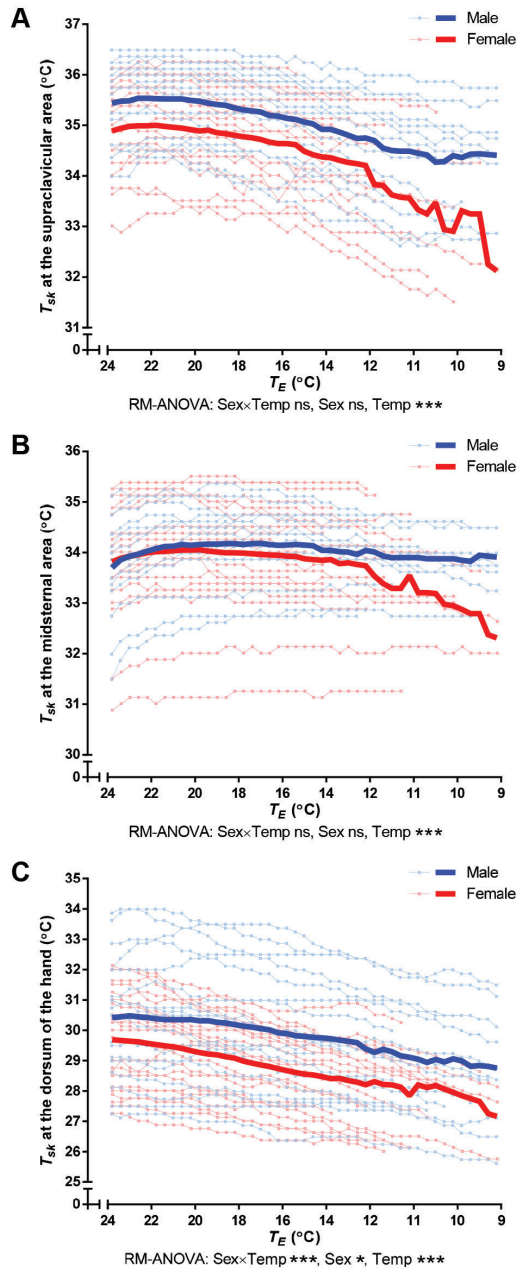
**Fig. 4** Skin temperatures during the cooling protocol

Skin temperatures ($T_{sk}$) measured by the iButton digital thermometers at **(A)** the supraclavicular area, **(B)** the midsternal area, and **(C)** the dorsum of the hand. Statistical significance indicates by $P$ values: $P < 0.05$ (*), $P < 0.01$ (**), and $P < 0.001$ (***). Thin lines show the data of individual participants, and thick lines indicate the mean. The deviation in mean $T_{sk}$ between men and women at $T_E$ lower than 14 °C is mainly driven by the decreasing number of female participants that started shivering beyond this $T_E$.

**Table 3** Skin temperatures measured at three sites during the cooling protocol

| Site and condition of measurement | $T_{sk}$ (°C) | | | $\Delta T_{sk}$ (°C) | | |
|---|---|---|---|---|---|---|
| | **Men** | **Women** | **P** | **Men** | **Women** | **P** |
| **Supraclavicular area** | | | | | | |
| Baseline | 35.4 ± 0.7 | 34.9 ± 1.1 | 0.08 | – | – | – |
| At $VAS_{sensation}$ score < 0 | 35.3 ± 0.9 | 34.8 ± 1.1 | 0.16 | −0.1 ± 0.3 | −0.0 ± 0.1 | 0.44 |
| At $VAS_{sensation}$ score ≤ −2 | 35.0 ± 1.0 | 34.7 ± 1.1 | 0.51 | −0.4 ± 0.4 | −0.2 ± 0.3 | 0.08 |
| End of cooling protocol | 34.5 ± 1.0 | 34.3 ± 1.2 | 0.48 | −0.9 ± 0.5 | −0.6 ± 0.9 | 0.25 |
| **Midsternal area** | | | | | | |
| Baseline | 34.0 ± 0.8 | 34.0 ± 1.1 | 0.97 | – | – | – |
| At $VAS_{sensation}$ score < 0 | 34.0 ± 0.7 | 33.9 ± 1.1 | 0.89 | −0.1 ± 0.2 | −0.0 ± 0.2 | 0.27 |
| At $VAS_{sensation}$ score ≤ −2 | 33.8 ± 0.9 | 34.0 ± 1.0 | 0.56 | −0.1 ± 0.7 | 0.0 ± 0.2 | 0.33 |
| End of cooling protocol | 34.0 ± 0.6 | 33.9 ± 1.0 | 0.62 | 0.0 ± 0.6 | −0.1 ± 0.4 | 0.38 |
| **Dorsum of hand** | | | | | | |
| Baseline | 30.5 ± 2.0 | 29.6 ± 1.5 | 0.12 | – | – | – |
| At $VAS_{sensation}$ score < 0 | 30.3 ± 2.0 | 29.6 ± 1.5 | 0.19 | −0.1 ± 0.3 | −0.0 ± 0.2 | 0.16 |
| At $VAS_{sensation}$ score ≤ −2 | 29.8 ± 1.8 | 29.0 ± 1.3 | 0.12 | −0.7 ± 0.7 | −0.6 ± 0.4 | 0.68 |
| End of cooling protocol | 29.0 ± 1.8 | 27.9 ± 1.2 | **0.02** | −1.5 ± 1.1 | −1.7 ± 1.0 | 0.47 |
| **Average 3-site $T_{sk}$** | | | | | | |
| Baseline | 33.3 ± 0.6 | 32.8 ± 0.7 | **0.02** | – | – | – |
| At $VAS_{sensation}$ score < 0 | 33.1 ± 0.6 | 32.8 ± 0.7 | 0.12 | −0.1 ± 0.3 | −0.0 ± 0.1 | 0.18 |
| At $VAS_{sensation}$ score ≤ −2 | 32.8 ± 0.7 | 32.6 ± 0.8 | 0.24 | −0.4 ± 0.5 | −0.2 ± 0.2 | 0.17 |
| End of cooling protocol | 32.5 ± 0.6 | 32.0 ± 0.6 | **0.02** | −0.8 ± 0.5 | −0.8 ± 0.6 | 0.99 |

$\Delta T_{sk}$ demonstrates the change in $T_{sk}$ at each condition relative to baseline value. $T_{sk}$ at the end of the cooling protocol was measured when shivering started or $T_E$ reached 9 °C. Data are shown as mean ± SD. Statistically significant difference between men and women is marked in bold.

**5**

Shivering can be considered an indicator of cold stress since it is activated only if energy-inexpensive mechanisms are not sufficient to maintain a constant $T_c$ (Daanen and Van Marken Lichtenbelt, 2016). The stimulus for shivering is not only a drop in $T_c$, but also a cold stimulus that contacts the skin. The decrease in $T_{sk}$ is transmitted as a cold signal by TRPM8, a temperature-sensitive receptor that can be activated when an ambient temperature is lower than 25 °C (Patapoutian et al., 2003). In mice, Caudle et al. (2017) found that TRPM8 receptors in females had a higher sensitivity to low temperatures than receptors in males. Our finding that women perceived the same cooling protocol colder than men might therefore partly be explained by a different sensitivity of the TRPM8 receptors.

Anderson et al. (1995) demonstrated that there was not a significant difference between men and women in the shivering threshold, which was defined by the deviation of the esophageal $T_c$ from an individual baseline value when resting after exercise in 28 °C water. We could not address the shivering threshold in terms of the change of $T_c$ because a lack of $T_c$ monitoring is a limitation of our study. A study by Boon et al. (2014), which used the same cooling method as in this study to study the BAT activation, showed that $T_c$ was unchanged after the 2-hour cooling protocol. Moreover, Xu et al. (2013) showed that the $T_{sk}$ measured from the sternum are best correlated with the $T_c$. Thus, it is likely that the $T_c$ of the participants in this study was not remarkably affected since the midsternal $T_{sk}$ remained unchanged during the cooling protocol. Interestingly, Boon et al. (2014) also found that the gradient between the proximal and the distal $T_{sk}$ was greater after cold exposure, which was confirmed in our study. A decline in distal $T_{sk}$ together with a greater gradient between the proximal and the distal $T_{sk}$ reflects the vasoconstriction capacity of the peripheral tissues to conserve heat during an exposure to cold. Overall, our results suggest that women approach the maximal capacity of vasoconstriction earlier, and thus need shivering as a source of heat production sooner than men.

The BSA-to-mass ratio is an important factor explaining differences in the net heat transfer in cold conditions (Castellani and Young, 2016; Parsons, 2014). An increase in BSA results in a higher heat loss from the body to the environment. On the other hand, an increase in total body mass contributes to a higher heat production capacity (Arciero et al., 1993). A combination of high BSA and low body mass causes a low capability to maintain a proper thermal balance for a constant $T_c$ during cold stress. In general, the body composition of adult men and women shows a sexually dimorphic pattern (Kuk et al., 2005; Wells, 2007), which is the same pattern observed in this study cohort. Female participants in our study cohort had a slightly higher BSA-to-mass ratio than male participants and the BSA-to-mass ratio was a statistically significant

determinant for the shivering $T_E$. Hence, the BSA-to-mass ratio is likely a principal factor determining this sex difference (Castellani and Young, 2016; Tikuisis et al., 2000). However, this anthropometric characteristic is not the only factor underlying the sex difference in our cohort since the subgroup analysis of an equivalent BSA-to-mass ratio between the sexes still showed the sex-dependent pattern. Further research is needed to identify why women need shivering as a source of heat production earlier than men to maintain their thermal balance when experiencing the same cold stress.

Concerning the thermal sensation and thermal comfort over the whole cooling period as a subjective method to evaluate cold perception, we found that women did feel colder and less comfortable than men. Intriguingly, the $T_E$'s at which the participants started to feel 'colder than neutral' ($VAS_{sensation}$ score < 0) and 'cool' ($VAS_{sensation}$ score ≤ −2) were both higher for women than for men. Karjalainen (2012) and Wang et al. (2018) illustrated that women feel colder and are less comfortable than men in a standard indoor climate setting. Our results, however, did not find a difference in thermal sensation or thermal comfort between men and women at the acclimatization period before the cooling protocol started. We previously performed a behavioral mouse study to identify sex differences in thermal preference of adult mice (Kaikaew et al., 2017) and found that female mice preferred to reside at a higher ambient temperature than male mice. Overall, our data of both the previous mouse study and this current human study confirmed the sex difference in thermal perception.

Since our institutionally approved cooling protocol allowed us to study the effect of cold exposure in a healthy individual up to a minimum $T_E$ of 9 °C only, we assumed a shivering $T_E$ of 8 °C in those participants that failed to shiver at this minimum $T_E$. Using this assumption, we found that male participants started shivering at a statistically lower $T_E$ than female participants. It is very unlikely that this assumption led to a false conclusion since 89% (8 out of 9) of the participants with undetectable shivering at 9 °C were male participants. Thus, this assumption may even underestimate the effect size in the difference in shivering $T_E$ between the sexes. Although this conclusion is based on a rather small cohort (20 men and 23 women), our power analysis to determine a potential sex difference in shivering $T_E$ indicated that this sample size is sufficient as a minimum of 16 participants per sex was needed.

Cold-induced activation of BAT, the thermogenic organ that utilizes energy to generate heat, can be detected in many regions of the body, including the supraclavicular area (van der Lans et al., 2014). The current 'gold standard' method to study the activity of human BAT is the ^{18}F-fluorodeoxyglucose (^{18}F-FDG) positron emission tomography integrated with computed tomography (PET/CT) imaging (Blondin and Carpentier, 2016). ^{18}F-FDG uptake in BAT was

**5**

detected in only ~6% of individuals when the PET/CT scan was performed in unstimulated conditions, with a significantly higher prevalence in women than in men (Cypess et al., 2009; Ouellet et al., 2011). Nevertheless, when participants were exposed to 19 °C for 2 hours before the scan, ^{18}F-FDG uptake in BAT was observed in 52% of young participants (aged 23–35 years), without an apparent sex difference (Saito et al., 2009). Thus, an individualized cooling protocol could be beneficial for studying BAT activity.

^{18}F-FDG-PET/CT imaging has limitations such as underestimating a weakly activated BAT in normal physiological conditions, requiring expensive equipment, and exposing a subject to ionizing radiation (Cypess et al., 2014). A proposed non-invasive method to determine the activity of BAT is measurement of the $T_{sk}$ at the supraclavicular area. Unlike previous reports that cold exposure enhanced the supraclavicular $T_{sk}$ suggesting activation of BAT (Boon et al., 2014; van der Lans et al., 2016), our cooling protocol did not increase the supraclavicular $T_{sk}$. This conflicting result is likely explained by the shorter duration of cold exposure in our protocol compared to those published previously, which is possibly not potent enough to stimulate BAT to a detectable level.

## Conclusions

This study demonstrates that women and men respond differently to low temperatures. Women not only started shivering at a higher $T_E$ than men, they also felt colder and less comfortable than men throughout the same cooling protocol using the Blanketrol® III. These sex differences could be important for studying the physiological responses at temperatures lower than the thermo-neutral zone, such as those using cooling protocols for radiologic diagnostic imaging in patients or those studying BAT activity in the general population.

## Acknowledgements

## Author contributions

## Declarations of interest

## Funding

## References

ACSM, 2013. Body composition. In: Pescatello, L.S. (Ed.), ACSM's Guidelines for Exercise Testing and Prescription, 9th ed. Wolters Kluwer Health, Baltimore, MD, pp. 62-72.

Anderson, G.S., 1999. Human morphology and temperature regulation. Int J Biometeorol 43, 99-109.

Anderson, G.S., Ward, R., Mekjavic, I.B., 1995. Gender differences in physiological reactions to thermal stress. Eur J Appl Physiol Occup Physiol 71, 95-101.

Arciero, P.J., Goran, M.I., Poehlman, E.T., 1993. Resting metabolic rate is lower in women than in men. J Appl Physiol (1985) 75, 2514-2520.

Bahler, L., Holleman, F., Booij, J., Hoekstra, J.B., Verberne, H.J., 2017. Hot heads & cool bodies: The conundrums of human brown adipose tissue (BAT) activity research. European Journal of Internal Medicine 40, 26-29.

Blondin, D.P., Carpentier, A.C., 2016. The role of BAT in cardiometabolic disorders and aging. Best Pract Res Clin Endocrinol Metab 30, 497-513.

Blondin, D.P., Maneshi, A., Imbeault, M.A., Haman, F., 2011. Effects of the menstrual cycle on muscle recruitment and oxidative fuel selection during cold exposure. J Appl Physiol (1985) 111, 1014-1020.

Boon, M.R., Bakker, L.E., van der Linden, R.A., Pereira Arias-Bouda, L., Smit, F., Verberne, H.J., van Marken Lichtenbelt, W.D., Jazet, I.M., Rensen, P.C., 2014. Supraclavicular skin temperature as a measure of $^{18}$F-FDG uptake by BAT in human subjects. PLoS One 9, e98822.

Castellani, J.W., Young, A.J., 2016. Human physiological responses to cold exposure: Acute responses and acclimatization to prolonged exposure. Auton Neurosci 196, 63-74.

Caudle, R.M., Caudle, S.L., Jenkins, A.C., Ahn, A.H., Neubert, J.K., 2017. Sex differences in mouse Transient Receptor Potential Cation Channel, Subfamily M, Member 8 expressing trigeminal ganglion neurons. PLoS One 12, e0176753.

Charkoudian, N., Stachenfeld, N.S., 2014. Reproductive hormone influences on thermoregulation in women. Compr Physiol 4, 793-804.

Chaudhuri, T., Zhai, D., Soh, Y.C., Li, H., Xie, L., 2018. Random forest based thermal comfort prediction from gender-specific physiological parameters using wearable sensing technology. Energy and Buildings 166, 391-406.

Costanzo, L.S., 2017. Temperature Regulation. Physiology, 6th ed. Elsevier, Philadephia, PA, pp. 177-178.

**5**

Cypess, A.M., Haft, C.R., Laughlin, M.R., Hu, H.H., 2014. Brown Fat in Humans: Consensus Points and Experimental Guidelines. Cell Metab 20, 408-415.

Cypess, A.M., Lehman, S., Williams, G., Tal, I., Rodman, D., Goldfine, A.B., Kuo, F.C., Palmer, E.L., Tseng, Y.-H., Doria, A., Kolodny, G.M., Kahn, C.R., 2009. Identification and Importance of Brown Adipose Tissue in Adult Humans. N Engl J Med 360, 1509-1517.

Daanen, H.A., Van Marken Lichtenbelt, W.D., 2016. Human whole body cold adaptation. Temperature (Austin) 3, 104-118.

Eyolfson, D.A., Tikuisis, P., Xu, X., Weseen, G., Giesbrecht, G.G., 2001. Measurement and prediction of peak shivering intensity in humans. Eur J Appl Physiol 84, 100-106.

Graham, T.E., 1988. Thermal, metabolic, and cardiovascular changes in men and women during cold stress. Med Sci Sports Exerc 20, S185-192.

Hall, J.E., 2015. Body Temperature Regulation and Fever. Guyton and Hall Textbook of Medical Physiology, 13th ed. Elsevier, Philadelphia, PA, pp. 911-922.

Hettiaratchy, S., Papini, R., 2004. Initial management of a major burn: II—assessment and resuscitation. BMJ : British Medical Journal 329, 101-103.

Iyoho, A.E., Ng, L.J., MacFadden, L., 2017. Modeling of Gender Differences in Thermoregulation. Mil Med 182, 295-303.

Kaikaew, K., Steenbergen, J., Themmen, A.P.N., Visser, J.A., Grefhorst, A., 2017. Sex difference in thermal preference of adult mice does not depend on presence of the gonads. Biol Sex Differ 8, 24.

Karjalainen, S., 2007. Gender differences in thermal comfort and use of thermostats in everyday thermal environments. Build Environ 42, 1594-1603.

Karjalainen, S., 2012. Thermal comfort and gender: a literature review. Indoor Air 22, 96-109.

Kingma, B., van Marken Lichtenbelt, W., 2015. Energy consumption in buildings and female thermal demand. Nat Clim Change 5, 1054-1056.

KNMI, 2017. Climatology - Daily weather data for the Netherlands. http://www.sciamachy-validation.org/climatology/daily_data/selection.cgi (Accessed 6 October 2017).

Kuk, J.L., Lee, S., Heymsfield, S.B., Ross, R., 2005. Waist circumference and abdominal adipose tissue distribution: influence of age and sex. Am J Clin Nutr 81, 1330-1334.

Lee, P., Swarbrick, M.M., Ho, K.K., 2013. Brown adipose tissue in adult humans: a metabolic renaissance. Endocr Rev 34, 413-438.

Makinen, T.M., Paakkonen, T., Palinkas, L.A., Rintamaki, H., Leppaluoto, J., Hassi, J., 2004. Seasonal changes in thermal responses of urban residents to cold exposure. Comp Biochem Physiol A Mol Integr Physiol 139, 229-238.

Nedergaard, J., Bengtsson, T., Cannon, B., 2007. Unexpected evidence for active brown adipose tissue in adult humans. Am J Physiol Endocrinol Metab 293, E444-452.

Nieman, D.C., 2011. Body Composition. Exercise Testing and Prescription : a health-related approach, 7th ed. McGraw-Hill, New York, NY, pp. 87-132.

Ouellet, V., Routhier-Labadie, A., Bellemare, W., Lakhal-Chaieb, L., Turcotte, E., Carpentier, A.C., Richard, D., 2011. Outdoor Temperature, Age, Sex, Body Mass Index, and Diabetic Status Determine the Prevalence, Mass, and Glucose-Uptake Activity of 18F-FDG-Detected BAT in Humans. J Clin Endocrinol Metab 96, 192-199.

Parsons, K., 2014. Human Thermal Environments. Human Thermal Environments: The Effects of Hot, Moderate, and Cold Environments on Human Health, Comfort, and Performance, 3rd ed. CRC Press, Boca Raton, FL, pp. 1-32.

Patapoutian, A., Peier, A.M., Story, G.M., Viswanath, V., 2003. ThermoTRP channels and beyond: mechanisms of temperature sensation. Nature Rev Neurosci 4, 529.

Reading, B.D., Freeman, B., 2005. Simple formula for the surface area of the body and a simple model for anthropometry. Clin Anat 18, 126-130.

Saito, M., Okamatsu-Ogura, Y., Matsushita, M., Watanabe, K., Yoneshiro, T., Nio-Kobayashi, J., Iwanaga, T., Miyagawa, M., Kameya, T., Nakada, K., Kawai, Y., Tsujisaki, M., 2009. High incidence of metabolically active brown adipose tissue in healthy adult humans: effects of cold exposure and adiposity. Diabetes 58, 1526-1531.

Tansey, E.A., Johnson, C.D., 2015. Recent advances in thermoregulation. Adv Physiol Educ 39, 139-148.

Tikuisis, P., Bell, D.G., Jacobs, I., 1991. Shivering onset, metabolic response, and convective heat transfer during cold air exposure. J Appl Physiol (1985) 70, 1996-2002.

**5**

Tikuisis, P., Jacobs, I., Moroz, D., Vallerand, A.L., Martineau, L., 2000. Comparison of thermoregulatory responses between men and women immersed in cold water. J Appl Physiol (1985) 89, 1403-1411.

van der Lans, A.A., Vosselman, M.J., Hanssen, M.J., Brans, B., van Marken Lichtenbelt, W.D., 2016. Supraclavicular skin temperature and BAT activity in lean healthy adults. J Physiol Sci 66, 77-83.

van der Lans, A.A., Wierts, R., Vosselman, M.J., Schrauwen, P., Brans, B., van Marken Lichtenbelt, W.D., 2014. Cold-activated brown adipose tissue in human adults: methodological issues. Am J Physiol Regul Integr Comp Physiol 307, R103-113.

Voets, T., Droogmans, G., Wissenbach, U., Janssens, A., Flockerzi, V., Nilius, B., 2004. The principle of temperature-dependent gating in cold- and heat-sensitive TRP channels. Nature 430, 748-754.

Wang, Z., de Dear, R., Luo, M., Lin, B., He, Y., Ghahramani, A., Zhu, Y., 2018. Individual difference in thermal comfort: A literature review. Build Environ 138, 181-193.

Wells, J.C.K., 2007. Sexual dimorphism of body composition. Best Pract Res Clin Endocrinol Metab 21, 415-430.

Xu, X., Karis, A.J., Buller, M.J., Santee, W.R., 2013. Relationship between core temperature, skin temperature, and heat flux during exercise in heat. Eur J Appl Physiol 113, 2381-2389.

Zhang, Y., Zhao, R., 2008. Overall thermal sensation, acceptability and comfort. Build Environ 43, 44-50.

**5**

# Chapter 6

General Discussion

6

## Overview

Adipose tissue is a multifunctional organ essential for maintaining whole-body energy homeostasis. The first known function of adipose tissue is an energy reservoir for the body by storing excess energy as triglycerides in intracellular lipid droplets which can be supplied in energy-deprived conditions. Second, adipose tissue acts as an endocrine organ since it secretes a variety of adipokines that systematically reflect the metabolic status. Apart from the classical type of adipose tissue [white adipose tissue (WAT)] which serves the above-mentioned functions, brown adipose tissue (BAT) is another specialized adipose tissue that can utilize energy substrates for non-shivering thermogenesis. In this latter process, the uncoupling protein 1 (UCP1) plays a crucial role (1). Currently, increasing energy expenditure by BAT activation or by "browning" of WAT is considered a promising tool for the treatment of obesity and metabolic diseases (2).

Despite being relatively overlooked, studies in rodents and humans have shown that males and females display many sex-dependent characteristics in WAT and BAT (3). Although the precise mechanisms underlying these sex differences are still not completely understood, studies have revealed crucial roles for sex hormones, particularly estrogens and androgens herein. This thesis broadens the understanding of sex differences in adipose tissue function upon modulation by corticosterone [an endogenous rodent glucocorticoid (GC)] or progesterone [a circulating female sex steroid that has been limitedly investigated]. Furthermore, this thesis also demonstrates sex differences in thermal perception, the sensory signal for whole-body thermoregulatory system, in which activation of BAT thermogenesis is its major autonomic response.

## Factors affecting sex differences in WAT

The most prominent characteristic of sex differences in WAT is sexual dimorphism in fat distribution. Men and male rodents are prone to accumulate fat in visceral depots, known as the apple-shaped or android fat distribution which correlates to worsened metabolic health, whereas women and female rodents store fat in subcutaneous depots, known as the pear-shaped or gynoid fat distribution which is relatively protective against metabolic diseases (4). The sex-differential fat distribution is principally driven by sex steroids because it becomes apparent during puberty and reverses at menopause when women gain more visceral fat (4-6).

WAT expansion is a coordinated response by multiple cells in the adipose tissue, namely adipocytes, endothelial cells, fibroblasts, and immune cells (7). A healthy adipose tissue expansion is accomplished by four reciprocal steps:

1) transient hypoxic stress caused by a limitation in oxygen diffusion of enlarged adipocytes, 2) sufficient angiogenesis induced by local hypoxia and upregulations of angiogenic factors, such as vascular endothelial growth factors, 3) formation of new adipocytes through recruitment and differentiation of the perivascular adipose progenitors, and 4) remodeling of the extracellular matrix to promote further expansion (7,8). Studies in rodents have shown that female WAT depots exhibit a higher angiogenic induction, a greater differentiation capacity of adipose progenitor cells, and more optimal remodeling in extracellular matrix proteins than male WAT depots (9,10).

Endogenous GCs are adrenal hormones crucial for diverse physiological processes, including regulation of glucose homeostasis. Exogenous GCs are widely used due to their anti-inflammatory properties. Elevated endogenous or chronic exposure to exogenous GCs can cause many adverse effects in a variety of organ systems leading to Cushing syndrome that includes weight gain, fat redistribution towards truncal obesity (Cushingoid appearance), increased insulin resistance, and worsening of glycemic control or new-onset diabetes mellitus (11,12). GC-induced diabetes or insulin resistance predominantly presents with postprandial hyperglycemia through increased hepatic gluconeogenesis and reduced glucose uptake in skeletal muscle and adipose tissue (13). Although male sex has been suggested to be a risk factor to develop GC-induced diabetes (14), other studies have reported that the GC-induced insulin resistance was not sexually dimorphic (12,15,16). The study in **Chapter 2**, therefore, investigated the glucometabolic effects of a high dose of corticosterone in male and female mice. The results of this study demonstrate that corticosterone induces nonfasting hyperglycemia only in male mice but the compensatory hyperinsulinemia is profound in both sexes. Upon corticosterone treatment, serum total adiponectin and high-molecular-weight adiponectin levels, which are tightly correlated with improved insulin sensitivity (17), were higher in female mice than in male mice. In addition, the hyperplastic expansion of adipose tissue, which is associated with better insulin sensitivity compared with the hypertrophic expansion (8), was more evident in female adipocytes than in male adipocytes. Altogether, **Chapter 2** suggests a more beneficial adaptation in WAT depots of female mice upon GC administration than that of male mice.

## Factors affecting sex differences in BAT and browning of WAT

GCs are known to suppress BAT thermogenesis, likely through the glucocorticoid receptor (GR) (18,19), but interestingly most studies have only been performed in males. Whether GCs affect BAT in a sex-dependent manner has not been extensively studied. The study in **Chapter 2** also demonstrates that treatment with a supraphysiological dose of corticosterone reduced *Ucp1*

mRNA expression and induced lipid accumulation in BAT in a sex-independent manner. In contrast, Gasparini *et al.* (20) found that corticosterone treatment induced lipid accumulation (whitening) in BAT only in male mice, not in female mice, but corticosterone treatment marginally reduced the amount of UCP1 in BAT. The discrepancy between findings in this thesis and the study of Gasparini *et al.* (20) is likely due to a higher dose of administered corticosterone and higher circulating corticosterone levels after treatment in our study, suggesting a sex difference in dose-sensitivity. Nevertheless, a recent study in mice with BAT-specific GR knockdown presented contradictory findings, i.e., GR signaling for BAT thermogenesis and metabolic activity was negligible upon cold exposure or high-fat diet–induced obesity (21). This observation could suggest that the deleterious effect of systemic GC administration on BAT *in vivo* is an indirect consequence of systemic metabolic disturbances via modulation of efferent signals from the central nervous system to BAT, or that the direct effect of GCs on BAT is signaled through other receptors or modulated by the interaction of GR and those receptors. Hence, the GC-GR-BAT axis still requires further validation.

A major plausible explanation for sexual dimorphism in BAT activity is likely a difference in circulating sex hormones. Detection of active BAT in adults by the positron emission tomography/computed tomography (PET/CT) imaging suggests that BAT is more prevalent in women than in men and that its presence is inversely correlated with outdoor temperatures, underscoring its thermogenic function (22). Another PET/CT study under thermoneutral conditions confirmed that women have higher BAT activity and BAT mass than men (23). This study also reported that BAT activity declines with age, which might be due to a decline in sex hormones (23). A similar sex difference is found in rodents: female rats have a larger BAT depot, a higher *Ucp1* mRNA expression in BAT, as well as greater lipolytic and thermogenic activation by $\beta_3$-adrenergic receptor ($\beta_3$-ADR) agonists than male rats (24). An *in vitro* study in primary brown adipocytes isolated from adult mice also supported direct effects of sex steroids on brown adipocytes. Testosterone dose-dependently inhibited norepinephrine-induced *Ucp1* mRNA expression, while 17β-estradiol (E2) and progesterone had no significant effects or slightly upregulated *Ucp1* mRNA expression (25). Moreover, E2 and progesterone were shown to reduce the $\alpha_{2A}/\beta_3$-ADR protein ratio in primary brown adipocytes, reflecting a greater thermogenic and lipolytic capacity, whereas testosterone did not alter the $\alpha_{2A}/\beta_3$-ADR ratio (26). Concerning the browning of WAT to reach a maximal thermogenic capacity, female sex hormones are important factors to induce WAT browning since CL316,243 (a $\beta_3$-ADR agonist) stimulation was able to induce browning of gonadal WAT only in female but not male C57BL/6J mice (27). This is remarkable since this depot is considered the most refractory WAT depot for browning in this mouse strain (28,29). Moreover,

the CL316,243-induced gonadal WAT browning was abolished when female mice had chemically induced ovarian failure (27), suggesting an interaction with female gonadal factors.

To uncover more sex-specific features in BAT, gene expression profiling was performed on BAT of male and female mice of which the data are described in **Chapter 3**. This study reveals that BAT gene expression profiles of male and female mice were indeed different, especially for genes encoding proteins involved in cellular structure, cell-cell contact, and cell adhesion. As expected, E2, progesterone, and dihydrotestosterone (DHT; a potent and active form of testosterone) were identified as possible upstream regulators for the sex-differential expression profile. Although expression of thermogenic markers *Ucp1* and *Ppargc1a* (the transcription factor of *Ucp1*) in BAT and primary brown adipocytes were not significantly sex-dependent, they show a tendency to be higher in female brown adipocytes.

In literature, the effects of progesterone on BAT activities are conflicting. Some studies have shown a stimulatory effect of progesterone on brown adipocytes (25,26), whereas *in vivo* observations show that BAT becomes inactive and atrophied during pregnancy (when progesterone concentrations are high), likely to conserve maternal energy for fetal growth (1). BAT of pregnant mice showed whitening morphological changes (enlarging intracellular lipid droplets) with decreased expression of thermogenic genes and increased expression of WAT markers (30). In **Chapter 3**, high concentrations of progesterone inhibited basal and norepinephrine-stimulated *Ucp1* and *Ppargc1a* mRNA expression in T37i cells, a female brown adipocyte cell line, in accordance with the findings of McIlvride *et al.* (30). The studies described in **Chapter 3** also test the effects of progesterone on primary brown adipocytes differentiated from stromal vascular fraction cells in BAT of male and female mice. In contrast to data in T37i cells, progesterone stimulation did not significantly affect *Ucp1* and *Ppargc1a* mRNA expression in primary brown adipocytes, but it dose-dependently reduced mRNA expression of *Adipoq*, the gene encoding the metabolically favorable adipokine adiponectin. Interestingly, the inhibitory effect of progesterone was likely due to the enhanced GR signaling. This suggests an interesting interaction between sex steroid and glucocorticoid signaling that requires further research to unravel the full physiological consequences. In addition, female primary brown adipocytes tended to express thermogenic genes and some cell-cell contact or structural genes at higher levels than male adipocytes although the cells were maintained in similar culture conditions, including sex steroid concentrations. This suggests intrinsic roles for the sex origin of the cells, driven by epigenetic programming or sex chromosomes. This finding stresses the need for stable cell lines generated from BAT of both male and female mice, which are currently lacking, in order

**6**

to understand these additional mechanisms beyond or in interaction with sex steroids.

At 22 °C (a usual temperature for housing conditions of laboratory animals), female rats have been reported to have higher *Ucp1* mRNA expression levels and higher mitochondrial activity in BAT than male rats (31). Surprisingly, this sex difference disappeared when the thermogenic capacity of BAT was maximally stimulated by exposing animals to cold (4 °C) since *Ucp1* mRNA expression was upregulated to a similar level in both sexes (31). These data suggest that a sex difference in thermal perception at 22 °C might result in sexually dimorphic BAT activity, a plausible explanation that will be discussed in the following section.

## Factors affecting sex differences in thermal perception

Males and females pose many differences in the thermoregulatory system to achieve optimal thermal homeostasis. The major contributing factors are sexual dimorphisms in body composition and anthropometric characteristics implicating that women (or female rodents) generally have larger body surface area (BSA)-to-mass ratios, which result in greater net heat loss to the surroundings, than men (or male rodents) (32,33). Since mice are >3,000-fold smaller in body mass and have a larger BSA-to-mass ratio than humans, mice present some unique characteristics in thermoregulation. Compared to humans, mice prefer higher ambient temperatures ($T_a$) with a thermoneutral zone (TNZ) around 30–32 °C and mice have a lower vasomotor dependency, higher metabolic rates, larger BAT relative to body mass, and more diurnal variations in the core body temperature ($T_c$) (34,35).

Thermal perception is a broader term than thermal sensation since it incorporates thermal sensation (neural thermal reception), individual interpretation of thermal sensation (e.g. cold, cool, neutral, warm, or hot), and thermal comfort or satisfaction (comfortable vs. uncomfortable or satisfied vs. dissatisfied) (36). Many experimental and field studies indicate that women are more sensitive to deviations from a preferred $T_a$ and women experience more dissatisfaction in a similar thermal environment than men (37,38). Some studies demonstrate that women prefer a higher $T_a$ than men to achieve their thermal comfort (39); however, this observation is not always consistent since some studies show no sex-dependency in thermal preference (37,38).

To study thermal perception in animals, temperature preference tests, i.e. behavioral observations to study where animals prefer to reside among a range of $T_a$'s, are usually performed. That is because behavioral thermoregulatory responses, i.e. movement to a preferred $T_a$, are energy-inexpensive mechanisms that animals use to optimize thermal needs (34). The temperature preference test

in adult mice presented in **Chapter 4** shows that female mice spend more time in cages with a higher $T_a$ than male mice, especially during the light (inactive) phase, which is in line with a previous study (40). More specifically, the study in **Chapter 4** is the first to demonstrate that females prefer a $T_a$ close to an upper limit of TNZ (32 °C) whereas male mice show no preference to either an upper limit (32 °C) or lower limit (29 °C) of TNZ.

The cool-sensitive thermoreceptor TRPM8 of females has been reported to be more sensitive than that of males and the *ex vivo* study in isolated dorsal root ganglion neurons showed that this difference was depended on the presence of E2 and testosterone (41). Surprisingly, the study in **Chapter 4** reveals that gonadectomy in adult mice does not affect the sex-specific thermal preference. This might suggest that an effect of gonadal hormones on thermal sensory inputs alone cannot explain the sex difference in thermal preference of adult mice and/or that sex hormones may have influenced the thermal neural circuits during earlier stages of life, such as the two most critical periods of brain development: pubertal and neonatal stages (42). In literature, it has been demonstrated that the preoptic area (POA) of the anterior hypothalamus (the thermoregulatory integration area) is responsive to gonadal hormones during development and shows striking sexual dimorphism in both molecular and morphological components, and hence causes several sex-specific behaviors in adults (42). Hence, it would be of interest to repeat this study using mice at prepubertal age.

The study in male and female volunteers in **Chapter 5** supports the findings in mice. Experiencing a gradually cooling protocol using a temperature-controlled water-perfused blanket, women start shivering at a higher temperature (a quantitative outcome for cold sensation) and sense/perceive a similar temperature colder and less comfortable than men. A subgroup analysis that matches the BSA-to-mass ratio between men and women does not change the sex-dependent outcomes, suggesting that body composition is not the only factor for the sex difference in thermal demand and that thermal preference has been determined in a sex-specific fashion. Hence, further (animal) studies investigating the roles of sex hormones before puberty are needed to obtain further insight into the underlying mechanism of the sex-dimorphic thermal preference.

**6**

## Future perspectives for studies of sex difference in adipose tissue function

Apart from sex hormones, sex chromosomes are likely independent factors regulating adiposity (43). The four core genotypes (FCG) mouse model in which the testis-determining gene *Sry* is relocated from the Y chromosome to an autosome, has been used to investigate the segregation of the effects of the

gonadal sex and gonad-secreting factors from the sex chromosome complement (44). Comparing mice with a similar gonadal type in early adulthood, mice with XX chromosomes were slightly but significantly heavier than those with XY chromosomes (45). When gonadectomy was performed to remove acute effects of sex hormones, the XX mice had a substantial increase in total fat mass and plasma leptin levels, compared to XY mice, regardless of their original gonads (45). This suggests that the sex chromosomes themselves have effects on adipose tissue function. Indeed, an increase in adiposity by the number of X chromosomes was also observed in the XY* mouse model in which the paternal unusual Y* chromosome produces offspring equivalent to XO, XX, XY, and XXY genotypes (44,45). Metabolic challenges with a high-fat diet revealed sex-chromosomal effects on fat distribution: XX mice had a larger inguinal WAT depot whereas XY mice had a larger gonadal WAT depot, independent of gonads (45). All these studies were performed with mice of the C57BL/6J strain, but similar genetic models in mice of the MF1 strain confirmed a role of the total number of sex chromosomes on adiposity and metabolism (46), but showed no differential effects whether these were X or Y chromosomes. Thus, animal studies indicate that the number of the sex chromosome is an independent factor for body fat accumulation. In humans, men with Klinefelter syndrome (47,XXY) and women with Turner syndrome (e.g. 45,X) have increased risks of abdominal obesity and metabolic diseases relative to their normal karyotype controls (47,48). Because patients with Klinefelter and Turner syndromes also suffer from hypogonadism, effects of sex chromosomes and sex hormones on adiposity in humans cannot be individually evaluated.

The effect of sex chromosomes on BAT function has not been studied in detail. Thus far, there has been only one study investigating BAT of the FCG mice, in which no effect of sex chromosomes on *Ucp1* and *Ppargc1a* mRNA expression in BAT at 4 weeks or 10 months after gonadectomy was described (45). Interestingly, in a similar sex-chromosomal status at 4 weeks after gonadectomy, orchiectomized gonadal male mice had a slightly higher *Ucp1* mRNA expression level in BAT than ovariectomized gonadal female mice (45), stating a role of gonadal hormones rather than sex chromosome complements. Nevertheless, since the study in **Chapter 3** reveals sex-dependent gene expression patterns in primary brown adipocytes independent of sex steroids, further analysis of the role of sex chromosomes and their interaction with sex steroids, particularly in pathological conditions in which cells are exposed to sex steroids opposite to their sex-chromosomal status, is warranted.

Genome-wide association studies (GWAS) of genetic variants, such as single-nucleotide polymorphisms (SNPs) and short deletions or insertions, revealed many genetic loci associated with body mass index (BMI; a surrogate

for obesity) and waist-to-hip ratio adjusted for BMI (WHR$_{adjBMI}$; an index for abdominal obesity) (49). A study in 339,224 individuals identified 97 autosomal genetic loci associated with BMI of which only 2 loci were marginally sex-dependent (50). Another study in 224,459 individuals identified 49 loci associated with WHR$_{adjBMI}$ of which 20 loci were sex-dependent (51). Interestingly, there was no overlap in the identified loci for general and abdominal obesity [see a comprehensive list in (49)]. A subsequent study in 320,485 individuals revealed that 15 BMI-associated loci showed age-specific effects and 44 WHR$_{adjBMI}$-associated loci showed sex-specific effects, but interestingly there was neither a sex-specific effect on BMI-associated loci nor an age-specific effect on WHR$_{adjBMI}$-associated loci (52). Therefore, these GWAS data suggest that genetic variants in autosomal DNA might contribute to sex dimorphisms in the fat distribution pattern, but not for general obesity. Of note, variants in sex chromosomes were excluded from these GWAS due to technical reasons.

Epigenetic modifications, such as DNA methylation, histone modifications, and environmental factors, have been shown to play an important role in WAT programming (53), which includes some sex-differential features. For example, a single injection of testosterone in female mice and rats during the early postnatal period resulted in obesity, increased visceral fat accumulation, and insulin resistance at adult age (54,55). These phenotypes likely resulted from imprinting or epigenetic programming due to neonatal testosterone exposure. The epigenetic effect of androgens is supported by a study in women with polycystic ovary syndrome (PCOS) whose classical manifestations include hyperandrogenism (56). Several DNA methyltransferases (*DNMT*s; major enzymes that maintain methylation patterns upon DNA replication) were differentially methylated and *DMAP1* (DNMT1 associated protein 1; a protein involved in DNA methylation and obesity-related inflammation) was differentially expressed in abdominal subcutaneous WAT of women with PCOS compared to those of healthy controls. In addition, 30 differentially expressed genes were identified with changes in DNA methylation sites (56), suggesting the potential influence of DNA methylation on corresponding gene expression.

Epigenetic regulation is also important for BAT function at many levels (57). For example, a retrospective study found that individuals with active BAT in PET/CT imaging were more likely to have been conceived in the colder period of the year (October–February) than in the warmer period (April–September) (58). Studies in mice showed that paternal cold exposure before mating led to upregulated basal and cold-stimulated UCP1 protein levels in BAT and inguinal WAT in the offspring of both sexes, which is likely due to a differential methylation status in the sperm of the cold-exposed males compared to control fathers (58). Some histone deacetylases (HDACs), which remove acetyl groups from histones,

compact the chromatin structure, and generally suppress gene transcription, are recognized as negative regulators for BAT thermogenesis (57). For instance, acute cold exposure or an injection of CL316,243 in mice downregulated *Hdac1* mRNA expression in BAT and inhibitions of HDAC1 upregulated *Ucp1* mRNA and UCP1 protein levels in cultured brown adipocytes (59). Another relevant observation is that a single injection of testosterone during the neonatal period in female mice increased lipid accumulation and reduced mRNA expression of *Ucp1* and other BAT-specific genes in BAT in later life (55), suggesting lifelong epigenetic modulation by postnatal sex steroid exposure. However, our preliminary unpublished study observed no apparent sex difference in the global methylation pattern in BAT of adult male and female mice housed at normal housing conditions. Hence, whether sex-dependent epigenetic programming in BAT at physiological conditions exists and whether it affects sex differences in BAT function warrants further studies.

Concerning the secretory function of adipose tissue apart from conventional adipokines, WAT and BAT produce and secrete exosomes containing microRNAs (miRNAs) which are 19–22-nucleotide long non-coding RNAs that regulate gene expression and translation in other tissues, such as liver (60). A study in the FCG mice revealed that sex differences in miRNA expression levels in gonadal WAT were mainly driven by the gonadal type, thus likely by sex hormones (61). When gonadectomy was performed to eliminate the acute effects of sex hormones, sex chromosome complements were also found to play a role in miRNA profiles, but to a lower extent than sex hormones (61). To the best of my knowledge, sex differences in miRNA expression levels in BAT have not been investigated. It is worth mentioning that circulating levels of exosomal miRNAs, such as miR-34c, miR-92a, and miR-122, are possibly a non-invasive biomarker to reflect *in vivo* BAT activity in mice or humans (62-64). However, our preliminary unpublished data and a subsequent study by Okamatsu-Ogura *et al.* (64) could not confirm a correlation of miR-92a levels and BAT activity. It would, therefore, be of interest to study the circulating concentrations of miRNAs in males and females with an emphasis on the role of sex steroids in the circulating miRNA levels.

As mentioned earlier, effects of sex steroids or other factors could differ depending on the sex origin of the cells. The human-induced pluripotent stem cell (hiPSC) is a promising tool to produce an *in vitro* functional white or brown adipocyte model that is most analogous to *in vivo* adipocytes to study sex-dimorphic features. Somatic cells, such as skin fibroblasts, can be used to generate iPSCs (65). Since iPSCs are capable of long-term self-renewal and can be expanded into large numbers, many biological or translational tests can be performed. In addition, obtaining iPSCs is more feasible than obtaining other

primary human cells, namely human embryonic stem cells (which raises ethical issues) or adipose-derived stromal vascular cells (which have limited proliferative potential and may quickly lose differentiation capacities) (66,67). However, one might argue that the traditional cell culture in which cells are maintained in monolayer cultures is not an ideal model for adipose tissue structure. To mimic the natural structure, three-dimensional cultures may be preferred and this would also allow studying interactions with additional cell types such as endothelial cells and immune cells. Protein scaffolds of biomaterials, e.g. silk or elastin-like polypeptides conjugated to polyelectrolytes, have been shown to enhance long-term tissue sustainability, structural organization, and functional activities (68,69). Three-dimensional cultures may facilitate the understanding if sex difference in adipose tissue structure persists *ex vivo* and whether this leads to the functional discrepancy.

WAT shows many sex- and depot-specific morphology and composition in its microenvironment, an aspect that has been limitedly studied in BAT. Our transcriptional data in **Chapter 3** suggest that the microenvironment also plays an important role in regulation of sex-specific BAT function. Our data furthermore implicates that interactions of brown adipocytes with various cells present in the BAT depot contribute to sex-specific BAT function. Compared to WAT, BAT has a higher number of endothelial cells and denser vasculature in the tissue (70,71), as well as a higher norepinephrine turnover rate per depot, which indicates a dense innervation of sympathetic nerves (72,73). These features of BAT facilitate its thermogenic function in both mice and humans, as blood flow to BAT, uptake of glucose or fatty acids in BAT, and skin temperature overlaying BAT depots are markedly increased by norepinephrine injection or cold exposure (71,74,75). Female BAT is more responsive to adrenergic stimulation than male BAT (24), but whether the adrenergic innervation or the blood supply to BAT is sexually dimorphic has not been studied. Our data showing sex-dimorphic expression of structural genes in BAT, not being expressed in primary adipocytes, suggest that these additional features may be interesting targets to activate BAT.

Steroid hormone receptors such as the GR, mineralocorticoid receptor (MR), estrogen receptor (ER), progesterone receptor (PR), and androgen receptor (AR) are members of the nuclear receptor superfamily 3 and they therefore share several molecular and functional characteristics. Upon ligand binding, the ligand-receptor complex is translocated from the cytoplasm to the nucleus, binds to the response elements and/or interacts with coregulatory proteins, and hence activates or inhibits transcription of target genes (76,77). The coregulatory proteins, e.g. the steroid receptor coactivator (SRC) family, also known as the nuclear receptor coactivator (NCoA), have been shown to regulate adipocyte differentiation and energy expenditure (78). However, whether coregulatory

**6**

proteins influence sex-dependent transcriptional profile in adipose tissue has not been systematically evaluated. Since studies in **Chapters 2–3** suggest interactions of sex hormones and GR signaling on adipose tissue functional activities, nuclear receptor coregulatory complexes, as well as crosstalk among sex hormones and nuclear receptors, should be investigated. The most relevant study of hormonal crosstalk described so far in literature was performed only in male mice. Upon corticosterone treatment, DHT cotreatment potentiated transcription of GR-target genes in WAT and BAT, and cotreatment with the AR antagonist enzalutamide attenuated the GR signaling in WAT (79). The GR-inhibiting effect of enzalutamide in WAT is likely driven by reduced activity of the enzyme 11β-hydroxysteroid dehydrogenase type 1 (11β-HSD1; an intra-tissue GC reactivating enzyme) (79).

## Summary

Altogether, this thesis has broadened our understanding of sex differences in control of WAT and BAT function in various aspects, namely sex-dependent adaptation of WAT upon corticosterone exposure, sex-specific transcriptional profile in BAT at basal conditions, and sex-biased thermal perception (the afferent signals essential for BAT activation and WAT browning). These findings generally support that inclusion of sex should be considered as an independent risk factor when considering individualized treatment options for patients with obesity. However, more studies are warranted to fully understand this complex picture of sexual dimorphisms in adipose tissue biology.

**6**
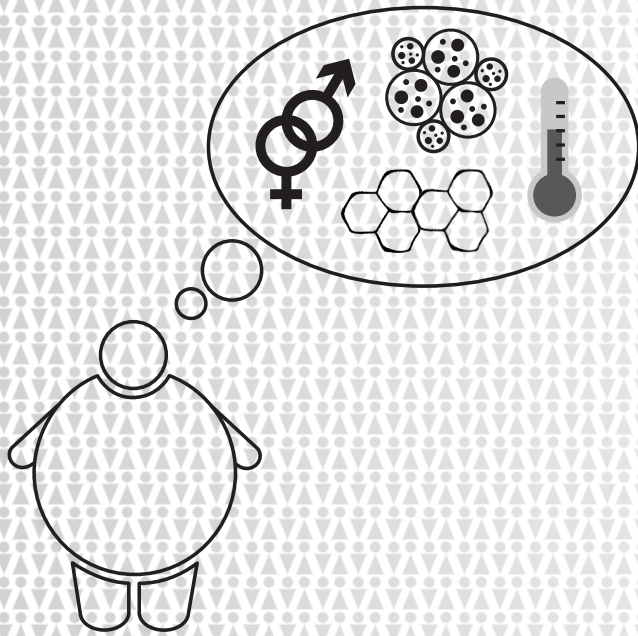
## References

1. Cannon B, Nedergaard J. Brown adipose tissue: function and physiological significance. *Physiol Rev.* 2004;**84**(1):277-359.
2. Loh RKC, Kingwell BA, Carey AL. Human brown adipose tissue as a target for obesity management; beyond cold-induced thermogenesis. *Obes Rev.* 2017;**18**(11):1227-1242.
3. Valencak TG, Osterrieder A, Schulz TJ. Sex matters: The effects of biological sex on adipose tissue biology and energy metabolism. *Redox Biol.* 2017;**12**:806-813.
4. Karastergiou K, Smith SR, Greenberg AS, Fried SK. Sex differences in human adipose tissues - the biology of pear shape. *Biol Sex Differ.* 2012;**3**(1):13.
5. Wells JC. Sexual dimorphism of body composition. *Best Pract Res Clin Endocrinol Metab.* 2007;**21**(3):415-430.
6. Lovejoy JC, Champagne CM, de Jonge L, Xie H, Smith SR. Increased visceral fat and decreased energy expenditure during the menopausal transition. *Int J Obes (Lond).* 2008;**32**(6):949-958.
7. Crewe C, An YA, Scherer PE. The ominous triad of adipose tissue dysfunction: inflammation, fibrosis, and impaired angiogenesis. *J Clin Invest.* 2017;**127**(1):74-82.
8. Choe SS, Huh JY, Hwang IJ, Kim JI, Kim JB. Adipose Tissue Remodeling: Its Role in Energy Metabolism and Metabolic Disorders. *Front Endocrinol (Lausanne).* 2016;**7**:30.
9. Rudnicki M, Abdifarkosh G, Rezvan O, Nwadozi E, Roudier E, Haas TL. Female Mice Have Higher Angiogenesis in Perigonadal Adipose Tissue Than Males in Response to High-Fat Diet. *Front Physiol.* 2018;**9**:1452.
10. Wu Y, Lee MJ, Ido Y, Fried SK. High-fat diet-induced obesity regulates MMP3 to modulate

depot- and sex-dependent adipose expansion in C57BL/6J mice. *Am J Physiol Endocrinol Metab*. 2017;**312**(1):E58-E71.

11. Liu D, Ahmet A, Ward L, Krishnamoorthy P, Mandelcorn ED, Leigh R, Brown JP, Cohen A, Kim H. A practical guide to the monitoring and management of the complications of systemic corticosteroid therapy. *Allergy Asthma Clin Immunol*. 2013;**9**(1):30.

12. Pivonello R, Isidori AM, De Martino MC, Newell-Price J, Biller BM, Colao A. Complications of Cushing's syndrome: state of the art. *Lancet Diabetes Endocrinol*. 2016;**4**(7):611-629.

13. Perez A, Jansen-Chaparro S, Saigi I, Bernal-Lopez MR, Minambres I, Gomez-Huelgas R. Glucocorticoid-induced hyperglycemia. *J Diabetes*. 2014;**6**(1):9-20.

14. Bonaventura A, Montecucco F. Steroid-induced hyperglycemia: An underdiagnosed problem or clinical inertia? A narrative review. *Diabetes Res Clin Pract*. 2018;**139**:203-220.

15. Binnert C, Ruchat S, Nicod N, Tappy L. Dexamethasone-induced insulin resistance shows no gender difference in healthy humans. *Diabetes Metab*. 2004;**30**(4):321-326.

16. Katsuyama T, Sada KE, Namba S, Watanabe H, Katsuyama E, Yamanari T, Wada J, Makino H. Risk factors for the development of glucocorticoid-induced diabetes mellitus. *Diabetes Res Clin Pract*. 2015;**108**(2):273-279.

17. Geer EB, Islam J, Buettner C. Mechanisms of glucocorticoid-induced insulin resistance: focus on adipose tissue function and lipid metabolism. *Endocrinol Metab Clin North Am*. 2014;**43**(1):75-102.

18. Kroon J, Koorneef LL, van den Heuvel JK, Verzijl CRC, van de Velde NM, Mol IM, Sips HCM, Hunt H, Rensen PCN, Meijer OC. Selective Glucocorticoid Receptor Antagonist CORT125281 Activates Brown Adipose Tissue and Alters Lipid Distribution in Male Mice. *Endocrinology*. 2018;**159**(1):535-546.

19. Moriscot A, Rabelo R, Bianco AC. Corticosterone inhibits uncoupling protein gene expression in brown adipose tissue. *Am J Physiol*. 1993;**265**(1 Pt 1):E81-87.

20. Gasparini SJ, Swarbrick MM, Kim S, Thai LJ, Henneicke H, Cavanagh LL, Tu J, Weber MC, Zhou H, Seibel MJ. Androgens sensitise mice to glucocorticoid-induced insulin resistance and fat accumulation. *Diabetologia*. 2019;**62**(8):1463-1477.

21. Glantschnig C, Mattijssen F, Vogl ES, Ali Khan A, Rios Garcia M, Fischer K, Muller T, et al. The glucocorticoid receptor in brown adipocytes is dispensable for control of energy homeostasis. *EMBO Rep*. 2019;**20**(11):e48552.

22. Cypess AM, Lehman S, Williams G, Tal I, Rodman D, Goldfine AB, Kuo FC, et al. Identification and importance of brown adipose tissue in adult humans. *N Engl J Med*. 2009;**360**(15):1509-1517.

23. Pfannenberg C, Werner MK, Ripkens S, Stef I, Deckert A, Schmadl M, Reimold M, Haring HU, Claussen CD, Stefan N. Impact of age on the relationships of brown adipose tissue with sex and adiposity in humans. *Diabetes*. 2010;**59**(7):1789-1793.

24. Rodriguez-Cuenca S, Pujol E, Justo R, Frontera M, Oliver J, Gianotti M, Roca P. Sex-dependent thermogenesis, differences in mitochondrial morphology and function, and adrenergic response in brown adipose tissue. *J Biol Chem*. 2002;**277**(45):42958-42963.

25. Rodriguez AM, Monjo M, Roca P, Palou A. Opposite actions of testosterone and progesterone on UCP1 mRNA expression in cultured brown adipocytes. *Cell Mol Life Sci*. 2002;**59**(10):1714-1723.

26. Monjo M, Rodriguez AM, Palou A, Roca P. Direct effects of testosterone, 17 beta-estradiol, and progesterone on adrenergic regulation in cultured brown adipocytes: potential mechanism for gender-dependent thermogenesis. *Endocrinology*. 2003;**144**(11):4923-4930.

27. Kim SN, Jung YS, Kwon HJ, Seong JK, Granneman JG, Lee YH. Sex differences in sympathetic innervation and browning of white adipose tissue of mice. *Biol Sex Differ*. 2016;**7**:67.

28. Guerra C, Koza RA, Yamashita H, Walsh K, Kozak LP. Emergence of brown adipocytes in white fat in mice is under genetic control. Effects on body weight and adiposity. *J Clin Invest*. 1998;**102**(2):412-420.

29. de Jong JM, Larsson O, Cannon B, Nedergaard J. A stringent validation of mouse adipose tissue identity markers. *Am J Physiol Endocrinol Metab*. 2015;**308**(12):E1085-1105.

30. McIlvride S, Mushtaq A, Papacleovoulou G, Hurling C, Steel J, Jansen E, Abu-Hayyeh S, Williamson C. A progesterone-brown fat axis is involved in regulating fetal growth. *Sci Rep*. 2017;**7**(1):10671.

31. Quevedo S, Roca P, Pico C, Palou A. Sex-associated differences in cold-induced UCP1 synthesis in rodent brown adipose tissue. *Pflugers Arch*. 1998;**436**(5):689-695.

32. Castellani JW, Young AJ. Human physiological responses to cold exposure: Acute responses and acclimatization to prolonged exposure. *Auton Neurosci*. 2016;**196**:63-74.

**6**

33. Schile A, Denegre J. Growth curve analysis of 10 strains of mice. MPD:Jaxpheno5. Mouse Phenome Database web resource (RRID:SCR_003212). The Jackson Laboratory; 2014. Accessed 11 November 2019. https://phenome.jax.org/projects/Jaxpheno5.

34. Gordon CJ. The mouse thermoregulatory system: Its impact on translating biomedical data to humans. *Physiol Behav.* 2017;**179**:55-66.

35. Taylor NAS, Gordon CJ. The origin, significance and plasticity of the thermoeffector thresholds: Extrapolation between humans and laboratory rodents. *J Therm Biol.* 2019;**85**:102397.

36. Schweiker M, Huebner GM, Kingma BRM, Kramer R, Pallubinsky H. Drivers of diversity in human thermal perception - A review for holistic comfort models. *Temperature (Austin).* 2018;**5**(4):308-342.

37. Karjalainen S. Thermal comfort and gender: a literature review. *Indoor Air.* 2012;**22**(2):96-109.

38. Wang Z, de Dear R, Luo M, Lin B, He Y, Ghahramani A, Zhu Y. Individual difference in thermal comfort: A literature review. *Build Environ.* 2018;**138**:181-193.

39. Maykot JK, Rupp RF, Ghisi E. A field study about gender and thermal comfort temperatures in office buildings. *Energy Build.* 2018;**178**:254-264.

40. Gaskill BN, Rohr SA, Pajor EA, Lucas JR, Garner JP. Some like it hot: Mouse temperature preferences in laboratory housing. *Appl Anim Behav Sci.* 2009;**116**(2-4):279-285.

41. Kondrats'kyi AP, Kondrats'ka KO, Skryma R, Prevars'ka N, Shuba Ia M. [Gender differences in cold sensitivity: role of hormonal regulation of TRPM8 channel]. *Fiziol Zh.* 2009;**55**(4):91-99.

42. Lenz KM, Nugent BM, McCarthy MM. Sexual differentiation of the rodent brain: dogma and beyond. *Front Neurosci.* 2012;**6**:26.

43. Zore T, Palafox M, Reue K. Sex differences in obesity, lipid metabolism, and inflammation-A role for the sex chromosomes? *Mol Metab.* 2018;**15**:35-44.

44. Mauvais-Jarvis F, Arnold AP, Reue K. A Guide for the Design of Pre-clinical Studies on Sex Differences in Metabolism. *Cell Metab.* 2017;**25**(6):1216-1230.

45. Chen X, McClusky R, Chen J, Beaven SW, Tontonoz P, Arnold AP, Reue K. The number of x chromosomes causes sex differences in adiposity in mice. *PLoS Genet.* 2012;**8**(5):e1002709.

46. Chen X, McClusky R, Itoh Y, Reue K, Arnold AP. X and Y chromosome complement influence adiposity and metabolism in mice. *Endocrinology.* 2013;**154**(3):1092-1104.

47. Gravholt CH, Jensen AS, Host C, Bojesen A. Body composition, metabolic syndrome and type 2 diabetes in Klinefelter syndrome. *Acta Paediatr.* 2011;**100**(6):871-877.

48. Ros C, Castelo-Branco C. Management of Turner's syndrome in adult life: case-series and systematic review. *Gynecol Endocrinol.* 2012;**28**(9):726-732.

49. Fall T, Mendelson M, Speliotes EK. Recent Advances in Human Genetics and Epigenetics of Adiposity: Pathway to Precision Medicine? *Gastroenterology.* 2017;**152**(7):1695-1706.

50. Locke AE, Kahali B, Berndt SI, Justice AE, Pers TH, Day FR, Powell C, et al. Genetic studies of body mass index yield new insights for obesity biology. *Nature.* 2015;**518**(7538):197-206.

51. Shungin D, Winkler TW, Croteau-Chonka DC, Ferreira T, Locke AE, Magi R, Strawbridge RJ, et al. New genetic loci link adipose and insulin biology to body fat distribution. *Nature.* 2015;**518**(7538):187-196.

52. Winkler TW, Justice AE, Graff M, Barata L, Feitosa MF, Chu S, Czajkowski J, et al. The Influence of Age and Sex on Genetic Associations with Adult Body Size and Shape: A Large-Scale Genome-Wide Interaction Study. *PLoS Genet.* 2015;**11**(10):e1005378.

53. Seki Y, Williams L, Vuguin PM, Charron MJ. Minireview: Epigenetic programming of diabetes and obesity: animal models. *Endocrinology.* 2012;**153**(3):1031-1038.

54. Nilsson C, Niklasson M, Eriksson E, Bjorntorp P, Holmang A. Imprinting of female offspring with testosterone results in insulin resistance and changes in body fat distribution at adult age in rats. *J Clin Invest.* 1998;**101**(1):74-78.

55. Jang H, Bhasin S, Guarneri T, Serra C, Schneider M, Lee MJ, Guo W, Fried SK, Pencina K, Jasuja R. The Effects of a Single Developmentally Entrained Pulse of Testosterone in Female Neonatal Mice on Reproductive and Metabolic Functions in Adult Life. *Endocrinology.* 2015;**156**(10):3737-3746.

56. Kokosar M, Benrick A, Perfilyev A, Fornes R, Nilsson E, Maliqueo M, Behre CJ, et al. Epigenetic and Transcriptional Alterations in Human Adipose Tissue of Polycystic Ovary Syndrome. *Sci Rep.* 2016;**6**:22883.

57. Sambeat A, Gulyaeva O, Dempersmier J, Sul HS. Epigenetic Regulation of the Thermogenic Adipose Program. *Trends Endocrinol Metab.* 2017;**28**(1):19-31.

58. Sun W, Dong H, Becker AS, Dapito DH, Modica S, Grandl G, Opitz L, et al. Cold-induced

epigenetic programming of the sperm enhances brown adipose tissue activity in the offspring. *Nat Med.* 2018;**24**(9):1372-1383.

59. Li F, Wu R, Cui X, Zha L, Yu L, Shi H, Xue B. Histone Deacetylase 1 (HDAC1) Negatively Regulates Thermogenic Program in Brown Adipocytes via Coordinated Regulation of Histone H3 Lysine 27 (H3K27) Deacetylation and Methylation. *J Biol Chem.* 2016;**291**(9):4523-4536.

60. Thomou T, Mori MA, Dreyfuss JM, Konishi M, Sakaguchi M, Wolfrum C, Rao TN, et al. Adipose-derived circulating miRNAs regulate gene expression in other tissues. *Nature.* 2017;**542**(7642):450-455.

61. Link JC, Hasin-Brumshtein Y, Cantor RM, Chen X, Arnold AP, Lusis AJ, Reue K. Diet, gonadal sex, and sex chromosome complement influence white adipose tissue miRNA expression. *BMC Genomics.* 2017;**18**(1):89.

62. Goody D, Pfeifer A. BAT Exosomes: Metabolic Crosstalk with Other Organs and Biomarkers for BAT Activity. *Handb Exp Pharmacol.* 2019;**251**:337-346.

63. Chen Y, Buyel JJ, Hanssen MJ, Siegel F, Pan R, Naumann J, Schell M, et al. Exosomal microRNA miR-92a concentration in serum reflects human brown fat activity. *Nat Commun.* 2016;**7**:11420.

64. Okamatsu-Ogura Y, Matsushita M, Bariuan JV, Nagaya K, Tsubota A, Saito M. Association of circulating exosomal miR-122 levels with BAT activity in healthy humans. *Sci Rep.* 2019;**9**(1):13243.

65. Yao X, Salingova B, Dani C. Brown-Like Adipocyte Progenitors Derived from Human iPS Cells: A New Tool for Anti-obesity Drug Discovery and Cell-Based Therapy? *Handb Exp Pharmacol.* 2019;**251**:97-105.

66. Singh AM, Dalton S. What Can 'Brown-ing' Do For You? *Trends Endocrinol Metab.* 2018;**29**(5):349-359.

67. Volarevic V, Markovic BS, Gazdic M, Volarevic A, Jovicic N, Arsenijevic N, Armstrong L, Djonov V, Lako M, Stojkovic M. Ethical and Safety Issues of Stem Cell-Based Therapy. *Int J Med Sci.* 2018;**15**(1):36-45.

68. Abbott RD, Kimmerling EP, Cairns DM, Kaplan DL. Silk as a Biomaterial to Support Long-Term Three-Dimensional Tissue Cultures. *ACS applied materials & interfaces.* 2016;**8**(34):21861-21868.

69. Turner PA, Tang Y, Weiss SJ, Janorkar AV. Three-dimensional spheroid cell model of in vitro adipocyte inflammation. *Tissue engineering. Part A.* 2015;**21**(11-12):1837-1847.

70. Grandl G, Muller S, Moest H, Moser C, Wollscheid B, Wolfrum C. Depot specific differences in the adipogenic potential of precursors are mediated by collagenous extracellular matrix and Flotillin 2 dependent signaling. *Mol Metab.* 2016;**5**(10):937-947.

71. Orava J, Nuutila P, Lidell ME, Oikonen V, Noponen T, Viljanen T, Scheinin M, et al. Different metabolic responses of human brown adipose tissue to activation by cold and insulin. *Cell Metab.* 2011;**14**(2):272-279.

72. Bartness TJ, Vaughan CH, Song CK. Sympathetic and sensory innervation of brown adipose tissue. *Int J Obes (Lond).* 2010;**34 Suppl 1**:S36-42.

73. Brito MN, Brito NA, Baro DJ, Song CK, Bartness TJ. Differential activation of the sympathetic innervation of adipose tissues by melanocortin receptor stimulation. *Endocrinology.* 2007;**148**(11):5339-5347.

74. Cannon B, Nedergaard J. Nonshivering thermogenesis and its adequate measurement in metabolic studies. *J Exp Biol.* 2011;**214**(Pt 2):242-253.

75. van der Lans AA, Wierts R, Vosselman MJ, Schrauwen P, Brans B, van Marken Lichtenbelt WD. Cold-activated brown adipose tissue in human adults: methodological issues. *Am J Physiol Regul Integr Comp Physiol.* 2014;**307**(2):R103-113.

76. Alexander SP, Cidlowski JA, Kelly E, Marrion NV, Peters JA, Faccenda E, Harding SD, et al. THE CONCISE GUIDE TO PHARMACOLOGY 2017/18: Nuclear hormone receptors. *Br J Pharmacol.* 2017;**174 Suppl 1**:S208-S224.

77. Lu NZ, Wardell SE, Burnstein KL, Defranco D, Fuller PJ, Giguere V, Hochberg RB, et al. International Union of Pharmacology. LXV. The pharmacology and classification of the nuclear receptor superfamily: glucocorticoid, mineralocorticoid, progesterone, and androgen receptors. *Pharmacol Rev.* 2006;**58**(4):782-797.

78. Lonard DM, O'Malley BW. Nuclear receptor coregulators: modulators of pathology and therapeutic targets. *Nat Rev Endocrinol.* 2012;**8**(10):598-604.

79. Spaanderman DCE, Nixon M, Buurstede JC, Sips HC, Schilperoort M, Kuipers EN, Backer EA, et al. Androgens modulate glucocorticoid receptor activity in adipose tissue and liver. *J Endocrinol.* 2019;**240**(1):51-63.

**6**

# Chapter 7

Summary / Samenvatting

7

**7**

## Summary

Obesity and overweight are both conditions of excessive/abnormal fat accumulation and are leading risk factors for many metabolic diseases, such as insulin resistance and type 2 diabetes mellitus. The principal site of fat accumulation in the body is adipose tissue, the organ traditionally defined as a quiescent energy reservoir. Nowadays, adipose tissue has gained interests as an endocrine organ since its secretory function reflects adaptability to an altered systemic metabolic status. In addition to white adipose tissue (WAT), brown adipose tissue (BAT) is another specialized adipose tissue that, in contrast to WAT, utilizes energy substrates for metabolic heat production, a crucial cold-defense mechanism to maintain body temperature in neonates and small mammals. After the rediscovery of active BAT in adult humans, activation of BAT is considered one of the promising therapeutic targets to increase energy expenditure for combating the global obesity pandemic.

Fat distribution physiologically shows a sexually dimorphic pattern: men store fat predominantly in visceral (intra-abdominal) WAT depots, resulting in an apple-shaped body, whereas women accumulate fat principally in subcutaneous WAT depots, e.g. gluteofemoral region, resulting in a pear-shaped body contour. In addition, women of reproductive age have a lower incidence of metabolic diseases than age-matched men. However, after menopause, women are more susceptible to visceral obesity (the male pattern of fat accumulation), which is linked to an increased incidence of metabolic diseases. Sex differences in BAT abundance and function are also reported. In general, women and female rodents have a higher BAT mass and/or greater BAT activity than men and male rodents. Altogether, human and rodent studies pinpoint protective effects of estrogens on energy balance and metabolic risk factors, while androgens in general have a negative effect on metabolic risk factors.

Apart from sex steroids, glucocorticoids (GCs; cortisol for humans and corticosterone for rodents), which are adrenal steroid hormones principally secreted in response to stress, have also been implicated in the control of energy metabolism and hence metabolic risk factors. The main function of endogenous GCs is to supply glucose for vital organs through many mechanisms, including inhibition of glucose uptake by WAT. Sustained elevated GC levels or chronic exposure to exogenous GCs, such as synthetic corticosteroids, result in many metabolic adverse effects, including weight gain, truncal obesity, insulin resistance, and poor glycemic control. However, whether the adverse effects of GCs are expressed in a sex-dependent manner is unclear. The general aim of this thesis therefore is to broaden our understanding of sex differences in adipose tissue function.

**7**

**Chapter 1** is a general introduction of this thesis and describes 1) basic knowledge of adipose tissue biology, including adipogenic programming, lipid metabolism in adipocytes, secretory function of WAT, and thermogenic function of BAT; 2) roles of sex and stress steroids on the distribution and function of adipose tissue; and 3) a general concept of body thermoregulation which is important for an understanding of BAT thermogenesis.

In **Chapter 2**, the effects of a high dose of corticosterone on systemic glucose homeostasis and adipose tissue adaptation were studied in male and female mice. Upon corticosterone treatment, male mice had nonfasting hyperglycemia, which resembles the pathognomonic sign of steroid-induced diabetes in humans. Female mice, in contrast, remained normoglycemic throughout the two weeks of treatment. However, both sexes showed normal fasting glucose levels and profoundly elevated fasting insulin levels, indicative of insulin resistance. Stable isotope-labeled glucose techniques were utilized during the glucose tolerance test and confirmed that female mice had a higher basal glucose clearance rate than male mice upon corticosterone treatment. WAT and BAT depots were enlarged by corticosterone treatment in both sexes, but female mice manifested more metabolically protective adaptations than males, i.e., more hyperplastic WAT morphology and higher serum adiponectin levels. *In vitro* studies in white and brown adipocyte cell lines suggested that the increased adiponectin level in female mice was likely driven by an elevated insulin level rather than a direct effect of corticosterone treatment.

Sex differences in BAT prevalence and activity are reported to be likely caused by a stimulatory effect of estrogens and/or an inhibitory effect of androgens on BAT, or a stimulatory effect of estrogens on the central nervous system that regulates BAT thermogenesis. To uncover if molecular mechanisms contribute to the sexual dimorphism in BAT function, RNA-sequencing was performed to identify sex differences in the murine BAT transcriptome. The data presented in **Chapter 3** show that sex differences in BAT gene expression were evident for genes encoding proteins involved in cellular structure, cell-cell contact, and cell adhesion. Interestingly, ovariectomy significantly affected while orchiectomy marginally influenced expression levels of the identified genes. Moreover, *in silico* upstream regulator analysis supported that 17β-estradiol (E2), progesterone, and dihydrotestosterone were among the top significant upstream regulators for these sex-differentially expressed genes. Direct effects of progesterone were further tested in primary cultures of brown adipocytes and it was found that progesterone inhibited expression of some identified genes, as well as common brown adipocyte markers. This inhibitory effect of progesterone is likely mediated by the glucocorticoid receptor rather than the progesterone receptor. Furthermore, although primary brown adipocytes were maintained in a

**7**

similar sex steroid milieu, basal expression of many sex-differentially expressed genes remained higher in female adipocytes than in male adipocytes, suggesting intrinsic roles of sex origin of the cells.

When housed under general laboratory conditions, female rodents have a higher thermogenic capacity in BAT than their male counterparts. However, this difference is diminished upon cold exposure in which BAT thermogenesis is maximally activated. This finding indicates that a difference in thermal perception might underlie the sex-dependent thermogenic responses, which we studied subsequently in both mouse and human. **Chapter 4** describes that female mice prefer a higher ambient temperature than male mice, especially when physical activities are generally low. Of interest, gonadectomy in adult mice did not alter this sex-specific thermal preference, indicating that the neural control of thermal sensation is sex-dependently regulated by factors other than gonadal factors or that the neural circuit has been determined prior to puberty.

It is documented that males and females pose many differences in the thermoregulatory system. One of the principal determining factors is sexual dimorphism in body composition. Women (or female rodents) have a larger body-surface-area/mass ratio than men (or male rodents) that hence leads to a higher rate of net heat loss and greater thermal demand in females. Apart from the sex-dependent physical property, women also perceive a temperature lower than the thermoneutral zone colder and less comfortable than men, as is shown by the study in **Chapter 5**. This study shows that women start shivering at a higher temperature (a quantitative measure for cold sensation) than men during a gradually cold exposure protocol by a temperature-controlled water-perfused blanket. Interestingly, subgroup analysis which matches the body-surface-area/ mass ratio between men and women did not alter the sex-dependent shivering temperature, suggesting that body composition is not the sole factor for sex differences in thermoregulation.

Finally, **Chapter 6** discusses the findings in this thesis that broaden our understanding of sex differences in the control of adipose tissue function. However, further studies are required to complete this complex picture of sexual dimorphisms in adipose tissue biology and energy metabolism in general.

**7**

## Samenvatting

Een toegenomen opslag van vetten in vetweefsel leidt tot overgewicht of, in meer extreme mate, obesitas. Overgewicht is een risicofactor voor metabole ziekten zoals insuline resistentie en diabetes mellitus type 2. Tot voor kort werd aangenomen dat het vetweefsel een relatief passief orgaan is met als enige functie de opslag van vet. We weten nu echter dat vetweefsel één van de meest actieve endocriene organen is, het scheidt namelijk diverse factoren uit en reflecteert daarmee veranderingen in de metabole status van het lichaam. Naast het bekende wit vetweefsel, bestaat er ook bruin vetweefsel. Waar wit vetweefsel voornamelijk een grote rol speelt in de opslag van vetten, is bruin vetweefsel gespecialiseerd in het verbranden van vetten om warmte te produceren. Dit proces wordt thermogenese genoemd en is cruciaal bij neonaten en kleine zoogdieren om de lichaamstemperatuur op peil te houden. Nog niet zo lang geleden is aangetoond dat ook volwassenen bruin vetweefsel hebben en sindsdien wordt activering van bruin vetweefsel beschouwd als een veelbelovende methode in de strijd tegen overgewicht.

De vetverdeling verschilt tussen mannen en vrouwen: mannen hebben over het algemeen meer buikvet terwijl vrouwen meer onderhuids vet hebben. Een toename in lichaamsgewicht resulteert daarom bij mannen in een zogenaamde 'appelvorm' en bij vrouwen in een 'peervorm'. Dit verschil in vetverdeling verklaart ook voor een deel waarom vrouwen voor de menopauze, de periode waarin er een groot verschil is tussen mannen en vrouwen in de hoeveelheid en type geslachtshormonen, beschermd zijn tegen metabole ziekten. Echter na de menopauze neemt bij vrouwen de hoeveelheid buikvet over het algemeen toe, een effect dat correleert met een toename in de incidentie van metabole ziekten.

Naast een verschil in de verdeling van wit vetweefsel tussen mannen en vrouwen is er ook een verschil in bruin vetweefsel tussen de geslachten. Vrouwen en vrouwelijke ratten en muizen - dieren die veelvuldig voor metabool onderzoek worden gebruikt - hebben over het algemeen meer en actiever bruin vetweefsel dan mannen en mannelijke ratten en muizen. Diverse studies hebben aangetoond dat oestrogenen (vrouwelijke geslachtshormonen) een positief effect en androgenen (mannelijke geslachtshormonen) een negatief effect hebben op de vet- en energiehuishouding.

Niet alleen geslachtshormonen, ook glucocorticosteroïden hebben een effect op de vet- en energiehuishouding. Glucocorticosteroïden zijn hormonen die onder invloed van stress door de bijnieren worden afgescheiden opdat vitale weefsels voldoende glucose krijgen, onder andere door de glucose opname door wit vetweefsel te remmen. Langdurig verhoogde glucocorticosteroïd concentraties zorgen voor diverse metabool ongewenste effecten zoals gewichtstoename,

**7**

toename van de hoeveelheid buikvet en insuline resistentie. Het is niet bekend of mannen en vrouwen verschillend reageren op deze effecten van glucocorticosteroïden.

Het overkoepelende doel van dit proefschrift is om meer inzicht te krijgen in de geslachtsgebonden verschillen in de functionaliteit van het vetweefsel. **Hoofdstuk 1** is een algemene introductie en geeft een overzicht van de basale kennis van wit en bruin vetweefsel en -cellen. Daarnaast behandelt dit hoofdstuk de effecten van geslachtshormonen en glucocorticosteroïden op de vetverdeling en de functies van vetcellen. Dit hoofdstuk geeft eveneens een beschrijving van de processen die betrokken zijn bij de regulatie van de lichaamstemperatuur, hetgeen belangrijk is om de thermogene activiteit van bruin vetweefsel te begrijpen.

De geslachtsgebonden effecten van glucocorticosteroïden op het vetweefsel en de glucosehuishouding worden beschreven in **hoofdstuk 2**. Mannelijke en vrouwelijke muizen werden gedurende twee weken behandeld met een hoge dosis van het knaagdier-specifieke glucocorticosteroïd corticosteron. De mannelijke muizen kregen onder invloed van corticosteron in de niet gevaste toestand een verhoogde bloedsuikerwaarde, maar opmerkelijk genoeg werd dit niet waargenomen in de vrouwelijk muizen. In gevaste toestand hadden zowel de mannelijke als de vrouwelijke muizen na corticosteron behandeling een normale bloedsuikerwaarde met een verhoogde plasma insuline concentratie: een indicatie dat corticosteron in beide geslachten insuline resistentie induceert. Met behulp van stabiele isotopen van glucose werd vervolgens aangetoond dat de glucose klaring na corticosteron behandeling hoger is in vrouwelijke dan in mannelijke muizen. In beide geslachten resulteerde corticosteron behandeling in een toename van wit en bruin vetweefsel. In vrouwelijk muizen ging deze toename gepaard met metabool relatief gunstige modificaties zoals een verhoogde plasma adiponectine concentratie. *In vitro* experimenten toonden vervolgens aan dat de verhoogde adiponectine concentratie waarschijnlijk het gevolg is van de hoge insuline spiegels en niet zozeer een direct effect is van corticosteron.

Geslachtsgebonden verschillen in bruin vetweefsel worden waarschijnlijk veroorzaakt door een stimulerend effect van oestrogenen en/of een remmend effect van androgenen op de activiteit van dit vetweefsel. Het is bijvoorbeeld bekend dat oestrogenen de thermogenese stimuleert via een effect op het centrale zenuwstelsel. Om de moleculaire mechanismen te achterhalen die betrokken zijn bij de geslachtsgebonden verschillen in bruin vetweefsel is de gen expressie van dit vetweefsel van mannelijke en vrouwelijke muizen onderzocht met behulp van RNA sequencing. De data die in **hoofdstuk 3** worden gepresenteerd laten zien dat genen die coderen voor eiwitten betrokken bij de cellulaire structuur, cel-cel contacten en de celadhesie meer tot expressie komen in bruin vetweefsel van

**7**

vrouwelijk muizen dan in dat van mannelijke muizen. Het verwijderen van de ovaria had een sterk effect op de expressie van deze genen, maar het verwijderen van de testes had geen of slechts marginaal invloed. In silico analyses toonden aan dat de expressie van de gevonden genen onder andere wordt gereguleerd door het oestrogeen 17β-estradiol en het androgeen dihydrotestosteron, maar dat tevens progesteron een rol speelt. De effecten van het vrouwelijk geslachtshormoon progesteron op vetweefsel en vetcellen zijn slechts in beperkte mate onderzocht. Daarom werd besloten om het effect van progesteron in meer detail te onderzoeken. Celkweek experimenten met primaire bruine vetcellen geïsoleerde uit muizen toonden aan dat progesteron de expressie van enkele van de geïdentificeerde genen onderdrukt. Daarnaast onderdrukt progesteron ook enkele klassieke markers van bruin vetweefsel, een effect dat zeer waarschijnlijk wordt bewerkstelligd door de glucocorticosteroïd receptor en slechts in mindere mate door de progesteron receptor. Opvallend was dat bruine vetcellen geïsoleerd uit vrouwelijke muizen nog steeds een ander expressie patroon lieten zien dan de cellen uit mannelijke muizen, ondanks dat ze dagenlang in hetzelfde medium werden gekweekt. Dit suggereert dat niet alleen geslachtshormonen, maar ook het geslacht zelf een rol speelt in de geslachtsgebonden verschillen van bruin vetweefsel.

Het is gebruikelijk om laboratorium muizen bij circa 22 °C te huisvesten. Bij deze temperatuur heeft bruin vetweefsel van vrouwelijke muizen een hogere thermogene activiteit dan bruin vetweefsel van mannelijke muizen. Dit verschil verdwijnt echter wanneer de muizen worden blootgesteld aan een lage temperatuur zoals 4 °C, wat een gebruikelijke methode is om de thermogene activiteit van bruin vetweefsel te verhogen. Blijkbaar zorgt een verschil in perceptie van temperatuur voor een verschil in de thermogene activiteit van bruin vetweefsel van mannelijke en vrouwelijke muizen. Het is te verwachten dat een dergelijk verschil ook tussen mannen en vrouwen bestaat. Dit proefschrift bevat een tweetal studies waarin dit verschil werd bestudeerd. **Hoofdstuk 4** beschrijft een studie waarin werd gevonden dat vrouwelijk muizen een hogere omgevingstemperatuur prefereren dan mannelijke muizen, met name gedurende de inactieve fase. Gonadectomie (het verwijderen van de ovaria bij vrouwelijke muizen en de testes bij mannelijke muizen) had hierop geen effect, wat suggereert dat verschillen in neuronale netwerken die de gevoeligheid voor temperatuur reguleren niet afhankelijk zijn van geslachtshormonen. Het is echter ook mogelijk dat het verschil tussen de geslachten al is aangelegd voordat de pubertijd begint. Het onderzoek in **hoofdstuk 5** werd uitgevoerd met gezonde vrijwilligers die door middel van een koelvest werden blootgesteld aan een geleidelijke verlaging van de omgevingstemperatuur. Deze studie toont aan dat vrouwen een bepaalde temperatuur over het algemeen als kouder en minder

comfortabel beschouwen dan mannen. Eén van de factoren die betrokken zou kunnen zijn bij dit verschil tussen mannen en vrouwen is de lichaamscompositie. In vergelijking met mannen hebben vrouwen relatief meer lichaamsoppervlakte per lichaamsgewicht wat resulteert in netto meer verlies van warmte. Een verschil in lichaamsoppervlakte verklaarde echter niet de waargenomen verschillen tussen mannen en vrouwen. Het kan daarom geconcludeerd worden dat de lichaamscompositie niet de enige factor is die het verschil in temperatuur gevoeligheid tussen mannen en vrouwen verklaart.

Tot slot worden in **hoofdstuk 6** de resultaten en conclusies uit dit proefschrift besproken. Alhoewel de studies uit dit proefschrift opheldering hebben gegeven omtrent geslachtsgebonden verschillen in de functionaliteit van het vetweefsel en vetcellen, is het ook duidelijk dat er nog verder onderzoek nodig is om meer inzicht te krijgen waarom het vetweefsel, de vetcellen en de energiehuishouding verschilt tussen mannen en vrouwen.

**7**
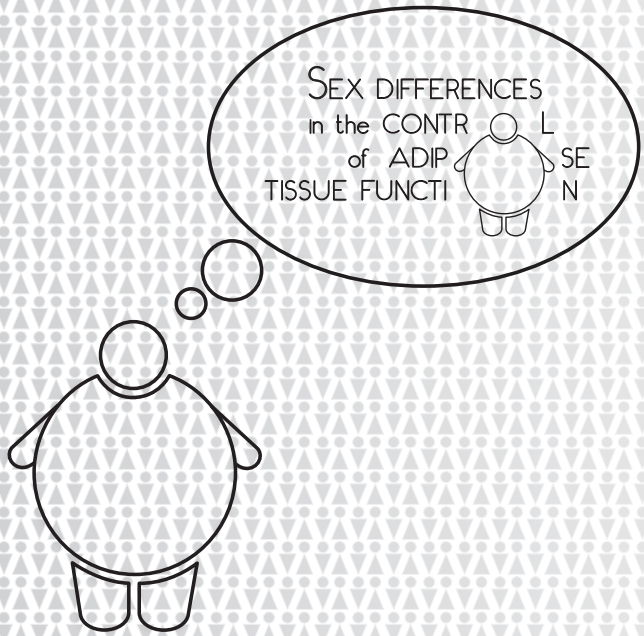
Sex differences in the CONTROL of ADIPOSE TISSUE FUNCTION

# Chapter 8

## Appendix

- Authors' affiliations
- List of publications
- PhD portfolio
- Acknowledgement
- About the author

8

8

## Authors' Affiliations

Department of Internal Medicine, Erasmus MC, University Medical Center Rotterdam, Rotterdam, the Netherlands

  Johanna C. van den Beukel
  Aldo Grefhorst
  Kasiphak Kaikaew
  Aart J. van der Lelij
  Anke McLuskey
  Sebastian J.C.M.M. Neggers
  Jacobie Steenbergen
  Axel P.N. Themmen
  Jenny A. Visser

Department of Pathology and Clinical Bioinformatics, Erasmus MC, University Medical Center Rotterdam, Rotterdam, the Netherlands

  Sigrid M.A. Swagemakers

Department of Experimental Laboratory Medicine, Amsterdam University Medical Centers, Location AMC, Amsterdam, the Netherlands

  Aldo Grefhorst

Department of Laboratory Medicine, University Medical Center Groningen, Groningen, the Netherlands

  Theo H. van Dijk

Department of Physiology, Faculty of Medicine, Chulalongkorn University, Bangkok, Thailand

  Kasiphak Kaikaew

8

8

## Publications in this Thesis

**Kaikaew K**, Steenbergen J, Themmen APN, Visser JA, Grefhorst A. Sex difference in thermal preference of adult mice does not depend on presence of the gonads. *Biol Sex Differ*. 2017;**8**(1):24.

**Kaikaew K**, van den Beukel JC, Neggers S, Themmen APN, Visser JA, Grefhorst A. Sex difference in cold perception and shivering onset upon gradual cold exposure. *J Therm Biol*. 2018;**77**:137–144.

**Kaikaew K**, Steenbergen J, van Dijk TH, Grefhorst A, Visser JA. Sex Difference in Corticosterone-Induced Insulin Resistance in Mice. *Endocrinology*. 2019;**160**(10):2367–2387.

## Manuscripts in this Thesis

**Kaikaew K**, Grefhorst A, Steenbergen J, Swagemakers SMA, McLuskey A, Visser JA. Sex Difference in the Mouse BAT Transcriptome Reveals a Role of Progesterone in BAT Function. *Submitted*

**Kaikaew K**, Grefhorst A, van der Lelij AJ, Visser JA. Sex Difference in Adipose Tissue Biology: Gonadal and Adrenal Steroid Perspectives. *Manuscript in preparation*

## Publications not in this Thesis

**Kaikaew K**. Paracetamol Poisoning: Review of Pathophysiology and Management. *Thai J Gastroenterol*. 2014;**15**(2):110–113.

Tasing P, Kulaputana O, Sanguanrungsirikul S, **Kaikaew K**. Effects of Precooling with Cold Water Ingestion on Thermoregulatory Response of Obese Men during Moderate Intensity Exercise in Hot and Humid Environment. *J Med Assoc Thai*. 2016;**99**(2):197–205.

**8**

8

## PhD Portfolio

PhD student:                         Kasiphak Kaikaew

Erasmus MC department:   Internal Medicine

Research school:                  Molecular Medicine

PhD period:                          April 2015 – January 2020

Promotor:                            Prof. dr. Aart J. van der Lelij

Co-promotors:                     Dr. ir. Jenny A. Visser
                                            Dr. Aldo Grefhorst

| Training / Activities | Year | Workload (ECTS) |
|---|---|---|
| **Courses and Workshops** | | |
| Laboratory Animal Science (Utrecht University) | 2015 | 3.0 |
| Introduction in GraphPad Prism | 2015 | 0.3 |
| Annual Course on Molecular Medicine | 2016 | 0.7 |
| Biostatistical Methods I: Basic Principles Part A (NIHES, CC02A) | 2016 | 2.0 |
| 6th Course and Workshop Basic and Translational Endocrinology | 2016 | 1.0 |
| Biomedical Research Techniques XV | 2016 | 1.5 |
| Research Integrity | 2017 | 0.3 |
| Biomedical English Writing and Communication | 2017 | 3.0 |
| Course on R | 2017 | 1.8 |
| Microscopic Image Analysis from Theory to Practice | 2018 | 0.8 |
| Ensembl Browser Workshop | 2018 | 0.6 |
| Workshop on NCBI, PubMed & other open source software | 2018 | 1.0 |
| **Conferences (Presentations and Participation)** | | |
| Endo Retreat (Newark/Athens/Rotterdam/Copenhagen/Paris) 2015, Rotterdam, Netherlands (attending) | 2015 | 1.0 |
| Chulalongkorn/Erasmus International Symposium 2015: Nephrology, Dermatology, Endocrinology and Immunology, Bangkok, Thailand (attending) | 2015 | 1.0 |
| Wetenschapsdagen (Science Days) 2016, Antwerp, Belgium *Corticosterone reduces glucose uptake in brown adipose tissue via GLUT4 expression and translocation* (oral presentation) | 2016 | 1.0 |
| Dutch Endocrine Meeting 2016, Noordwijkerhout, the Netherlands *Corticosterone disturbs glucose uptake in brown adipose tissue via GLUT4 translocation* (oral presentation) | 2016 | 1.0 |
| 20th Molecular Medicine Day 2016, Rotterdam, the Netherlands *Corticosterone disturbs glucose uptake in brown adipose tissue via GLUT4 translocation* (poster presentation) | 2016 | 0.3 |
| 3rd JNVE conference, Leiden, the Netherlands *Sex difference in thermal preference in adult mice is not affected by gonadectomy* (oral presentation) | 2016 | 1.0 |

**8**

| Training / Activities | Year | Workload (ECTS) |
|---|---|---|
| Wetenschapsdagen (Science Days) 2017, Antwerp, Belgium<br>*Sex difference in thermal preference in adult mice is not affected by gonadectomy* (poster presentation) | 2017 | 1.0 |
| Dutch Endocrine Meeting 2017, Noordwijkerhout, the Netherlands<br>*Tissue-specific effects of corticosterone on glucose homeostasis in male mice* (oral presentation) | 2017 | 1.0 |
| Adipocyte-Brain Crosstalk Symposium, Lübeck, Germany<br>*Sex difference in thermal preference in adult mice is not affected by gonadectomy* (poster presentation) | 2017 | 1.0 |
| Sex and Gender Factors Affecting Metabolic Homeostasis, Diabetes and Obesity (Keystone Symposium), Tahoe City, California, USA<br>*Sex difference in thermal preference in adult mice is not affected by gonadectomy* (poster presentation) | 2017 | 1.0 |
| ENDO 2017, Orlando, Florida, USA<br>*Tissue-specific effects of corticosterone on glucose homeostasis in male mice* (poster and short oral presentation) | 2017 | 1.0 |
| 4th JNVE conference, Leiden, the Netherlands<br>*While women feel cold, men may not* (oral presentation) | 2017 | 1.0 |
| 10th NRRN (Nuclear Receptor Research Network) meeting, Leuven, Belgium (attending) | 2017 | 1.0 |
| Wetenschapsdagen (Science Days) 2018, Antwerp, Belgium<br>*While women feel cold, men may not* (oral presentation) | 2018 | 1.0 |
| Dutch Endocrine Meeting 2018, Noordwijkerhout, the Netherlands<br>*While women feel cold, men may not* (oral presentation) | 2018 | 1.0 |
| Erasmus/Ohio Collaborative Activities in Endocrinology, Rotterdam, the Netherlands (attending) | 2018 | 0.3 |
| 22nd Molecular Medicine Day 2018, Rotterdam, the Netherlands<br>*While women feel cold, men may not* (poster presentation) | 2018 | 0.3 |
| 20th European Congress of Endocrinology (ECE) 2018, Barcelona, Spain<br>*Sex differences in glucocorticoid-induced metabolic disturbances in mice* (poster presentation) | 2018 | 1.0 |
| Wetenschapsdagen (Science Days) 2019, Sint-Michielsgestel, the Netherlands<br>*Dose-dependent effect of progesterone on T37i brown adipocyte differentiation* (poster presentation) | 2019 | 1.0 |
| Dutch Endocrine Meeting 2019, Noordwijkerhout, the Netherlands<br>*Dose-dependent effect of progesterone on T37i brown adipocyte differentiation* (oral presentation) | 2019 | 1.0 |
| 23rd Molecular Medicine Day 2019, Rotterdam, the Netherlands<br>*Dose-dependent effect of progesterone on T37i brown adipocyte differentiation* (poster presentation) | 2019 | 0.3 |
| Early Career Forum and ENDO 2019, New Orleans, Louisiana, USA<br>*Dose-dependent effect of progesterone on T37i brown adipocyte differentiation* (poster presentation) | 2019 | 1.0 |
| Wetenschapsdagen (Science Days) 2020, Sint-Michielsgestel, the Netherlands (attending) | 2020 | 1.0 |

8

| Training / Activities | Year | Workload (ECTS) |
|---|---|---|
| **Seminars and Work Discussion** | | |
| Sex and Gender Differences in Metabolism (COEUR) | 2015 | 0.2 |
| Internal Medicine Research Symposium (June, September) | 2016 | 0.4 |
| Internal Medicine Research Symposium (April, June, September) | 2017 | 0.6 |
| Internal Medicine Research Symposium (April, June, September) | 2018 | 0.6 |
| Internal Medicine Research Symposium (April, June) | 2019 | 0.4 |
| Lecture Series on Endocrinology | 2015–2019 | 1.6 |
| Endocrinology & Internal Medicine Work Discussion | 2015–2019 | 3.6 |
| Centrum Gezond Gewicht (Obesity Clinic CGG) lab meeting | 2016–2019 | 1.7 |
| **Teaching and Supervision** | | |
| Supervision Junior Med School (JMS) students 2015 | 2015 | 2.0 |
| Supervision Junior Med School (JMS) students 2016 | 2016 | 2.0 |
| Supervision Junior Med School (JMS) students 2017 | 2017 | 2.0 |
| **Grants and Awards** | | |
| Erasmus Trustfonds for ENDO 2017 | 2017 | |
| ESE Basic Science Meeting Grant (The European Society of Endocrinology) | 2018 | |
| EndoCareers Travel Awards (The Endocrine Society) | 2019 | |
| Erasmus Trustfonds for ENDO 2019 | 2019 | |

8

8

## Acknowledgement

Performing PhD research is challenging, but also sometimes very tough. Without these supports, I could not have accomplished this long PhD journey. Thereby, I would like to express my gratitude to all supporters.

Looking back to 2014 when I was searching for an international PhD position, I got many supports and advice from **Prof.dr. A.J. van der Lelij, Prof.dr. A.P.N. Themmen**, **Prof.dr. P.M. van Hagen**, and **Prof.dr. Nattiya Hirankarn**. Dear AJ, you are the first person from the Endocrinology Section of Erasmus MC whom I met at Chulalongkorn University in Bangkok in 2014. During my PhD, you always give me wonderful feedback and brilliant ideas, especially in the translational and clinical endocrinologist's aspects. I am grateful that you are finally my promotor. Dear Axel, thank you for accepting me as your PhD student and letting me start my PhD journey in the lab Metabolism and Reproduction in 2014. I am grateful for your hospitality during my first year and also thank for accepting to be one of the PhD promotion committees. Dear Martin and ajahn Ple, thanks for your support and guidance to an available PhD project at Erasmus MC, which I finally find the most suitable research position for me. And I would like to thank Martin for the assessment of this thesis.

I would like to express my gratitude to my first co-promotor and daily supervisor, **Dr. J.A. Visser**. Dear Jenny, I could not have been writing this acknowledgement if you are not my supervisor. I am very grateful that I can always interrupt you at any time (even in the evenings or the weekends) if I have any questions or problems, and you will find the solutions for any issues mostly immediately. You always believe in my lab skills and results, find a way to interpret and present the data in a scientifically sound concept, and guide me to proceed on with the next step. Not only work-related aspects, you did also support me in my personal issues, e.g. the accommodation problems that I faced in my first year. Also, thanks to John for helping me with this issue as well.

My PhD research might have not been able to start without the support of my second co-promotor and daily supervisor, **Dr. A. Grefhorst**. Dear Aldo, I am very glad that you have been my supervisor since the beginning. You are my first hands-on teacher and a great role model of basic science researchers. You always help me tackle all lab-related problems, are optimistic for my results, and finally come up with new creative ideas for following experiments. When you sat next to me in the office, I could turn around at any time to ask any simple or complicated questions and you were always happy to answer. Although you are my remote mentor for the last two years, you still reply to my emails super quickly, mostly in minutes or hours, and are willing to come to Rotterdam whenever we need you. I really appreciate that.

**8**

I appreciate the PhD promotion committee for accepting our invitation to be assessors for my thesis, especially the other two reading committees: **Prof. dr. O.C. Meijer** and **Prof.dr. E.F.C. van Rossum**. Dear Onno, thank you for your valuable feedback on my thesis and your inputs for my corticosterone work during my PhD period. It was my honor to collaborate with you during my PhD. Dear Liesbeth, thank you for assessing my thesis and also your feedback and ideas on my projects during the fruitful CGG meetings.

I would like to express my gratitude to all collaborators and coauthors of my PhD projects: **Dr. S.J.C.M.M. Neggers**, **Dr. J.C. van den Beukel**, **Dr. T.H. van Dijk**, **Dr. J. Kroon**, and **S.M.A. Swagemakers**. Dear Sebastian, thanks for your valuable feedback during our Monday meetings and for your contribution to the shivering experiment. Dear Anneke, thanks for your contribution to the BAT project line, which really facilitates my PhD researches. Dear Theo, I appreciate your contribution and inputs on the glucose tracer measurement and analysis. Without your valuable technique and knowledge, my corticosterone project could not have been completed. Dear Jan, thanks for all our productive meetings on the corticosterone project. It was very nice to collaborate with you. Dear Sigrid, thanks for your assistance in analyzing the RNA-sequencing data and your rapid responses to my naïve questions.

I appreciate the financial support for my PhD program from the Faculty of Medicine, Chulalongkorn University, Bangkok, Thailand. I would like to also thank all my colleagues in the Department of Physiology, in particular the heads of the department, **Prof. Duangporn Werawatganon** and **Dr. Pasakorn Watanatada**, who support me to gain my research experiences abroad. I promise to dedicate myself to MDCU after my graduation.

Dear **Cobie**, how can I survive in the lab without your support? Thank you so much for all your technical and mental supports during these five years. You are so kind to allow me to change your working schedules if I need an extra hand. Doing all lab works with you (e.g. cell culture, mouse experiments, Western blot, 3D staining and scanning, etc.) was always relaxing and productive. I appreciate that you accept to be my paranymph without any hesitation and thank for helping me organizing the coming ceremony day. Hope to see you again in Thailand soon!

Of course, there are also many PhD companions during my journey, **Margreet**, **Gido**, **Loes**, and **Karina**, who are all great officemates and friends. I will remember all wonderful and happy dinners and trips that we spent together. Dear Margreet, you are my first wonderful PhD buddy. Thanks for being very supportive during the time of our journey. I really enjoyed the time we spent in the lab and at our first-time-US congresses. Please don't forget the campaign Thailand 2020s. Dear Gido, you are a super supportive colleague and friend.

8

Thanks for always sharing fancy gadgets and funny clips with me. I hope you will hit your PhD goal in a real soon. Dear Loes, thanks for being such a good colleague and friend and accepting to be my paranymph. You are always super helpful to me in many ways, namely Dutch phone calls and bike issues. I must admit that you should be called a terrific toddler, who makes many of my working days more cheerful. I wish you a very successful PhD journey. Dear Karina, you are a very energetic and creative PhD friend of mine. Sitting next to you in the office is an enjoyable relaxing spot. Also, I wish you a successful PhD trajectory.

My lab work has also been assisted by all the Met&Repro lab members: **Patric**, **Anke**, **Bas**, **Martin**, **Rosinda**, **Piet**, and **Melitza**. Dear Patric, I am grateful for your valuable feedback and inputs for my research, and thanks for all the nice time at national and international congresses. Dear Anke, I really appreciate all your help, such as cell culture, mouse experiment, and finding information and quotations of all chemicals. And thanks for your frequent joyful laughs in the lab. Dear Bas, thanks for your assistance in the histological work. I will miss chatting with you in the evening before going back home. Dear Martin, thanks for your assistance in the flow cytometry and Victor-related issues, and nice discussions about movies and Thai foods. Dear Rosinda, thanks for your assistance during my last months, and for the cookies and fun moments during coffee breaks.

The Met&Repro lab could not be completed without the clinical people who join the productive meetings on Mondays: **Hans**, **Laura**, **Mark**, **Ammar**, **Eva**, and **Selvetta**. Thanks for your feedback on my work and fun time we had together during many scientific conferences.

I would like to thank many collaborators and colleagues, namely Dr. Johan Pel, Dr. Gert van Cappellen, Prof.dr. Freek Hoebeek, Prof.dr. Joost Gribnau, Prof.dr. Patrick Rensen, Dr. Jelmer Alsma, Dr. Anton Roks, Dr. Youri Hoogstrate, Dr. Wouter Zandee, Dr. Chiara Milanese, Ruben Boers, Jeroen van Rooij, Marcel van Riel, Chen Hu, and JMS students (Eva, Esmée, Emma, Anouk, and Annemarie), for their direct and indirect assistance and valuable feedback and inputs for my research. Also, thanks to **all Ee-5 colleagues** who all make a nice working environment (I am avoiding to list all the names here because I will definitely miss some) and thanks for all nice work discussions at the **CGG** meeting.

I must say that I could not have survived abroad, >9,000 km from home, without these wonderful supports of Thai friends, the 'Hello Kariang' group. Dear **Dew⁺**, how can I thank you enough for your invaluable support since the med-school time? I truly appreciate it! My life in Rotterdam would not be pleasant without your presence. I am looking forward to continuing working with you at MDCU and you will always be one of my best friends. And special

**8**

thanks for the cover design of this thesis, as well as many artworks you did for me, they are all brilliant! Dear **P'Karn**, thank you so much for being a superb companion along my PhD (and Disneyland) journey. You know that you are the most funny person, even though you try to admit you aren't. Having you working on the same floor is so brilliant, especially for the time I need to speak Thai to someone during working hours. It was also my honor to be your paranymph. I hope we will meet again in Bangkok or Chiang Mai frequently for fun activities. Dear **P'Utt** & **Nook** (also **Yi Chien**), thanks for all great times that we shared, especially yummy weekly dinners, relaxing lunches, and wonderful trips. I wish your PhD trajectories (and work) will be very smooth and you will hit all your goals soon. Dear **Kib**, **P'Ply**, **Jan**, **P'Aung**, **P'Ann**, **P'Prayer**, **P'Ball**, **P'Joyce**, and also many Thai friends who came to visit me in the Netherlands, you all have shared memorable moments with me in Rotterdam and please know that you all did make me feel Rotterdam more like home. I am also very glad that many friends in Thailand were always available and willing to listen to my unique basic science journey during my short breaks between this PhD journey. And special thanks to **Waen**, who is planning to visit Rotterdam just for my thesis defense.

I would also like to thank my international friends who spent many fantastic days and evenings with me. Dear **Monique** & **Marthijs**, thanks for taking me to the Architect day tour and inviting me to many wonderful Thai dinners. Dear **Zhongli**, thanks for being very good friends and sharing lots of happy moments with me, including those wonderful New Year celebrations. Dear **Do**, thanks for all fun conversations that we had together during our Asian times.

Last but most importantly, I would like to express my deepest gratitude to my family, particularly **dad**, **mom**, and **P'Champ**, who always support me whatever happens. Your unconditional loves do push me forward and make me who I am. Your supports are the most important part of my achievement.

**8**

## About the Author

Kasiphak Kaikaew was born on 19 February 1988 in Kanchanaburi, Thailand. In 2006, he graduated from Triam Udom Suksa School in Bangkok and started his medical training at the Faculty of Medicine, Chulalongkorn University, Bangkok, Thailand. During his medical study in 2010, he was elected a president of the Student Union of the Faculty of Medicine, Chulalongkorn University and obtained the award of Excellence in intellect, manner, extracurricular activity dedication, and collaboration to the university. He obtained the Doctor of Medicine Degree (2nd Class Honours) from Chulalongkorn University and the Thai Medical License in 2012. After graduation, he finished the one-year clinical internship at Hua Hin Hospital and Thap Sakae Hospital in Prachuap Khiri Khan and started working as an academic teaching assistant at the Department of Physiology, Faculty of Medicine, Chulalongkorn University and as a general practitioner at King Chulalongkorn Memorial Hospital in Bangkok. Since 2014, he has become an academic lecturer at Department of Physiology, Faculty of Medicine, Chulalongkorn University. In 2015, he obtained a doctoral scholarship from the Faculty of Medicine, Chulalongkorn University to start his PhD project entitled "Control of brown adipose tissue function by brain, temperature, and sexes" at the Laboratory Metabolism and Reproduction, Section of Endocrinology, Department of Internal Medicine, Erasmus MC, under supervision of Prof.dr.ir. A.P.N. Themmen (initially), Dr.ir. J.A. Visser, Dr. Aldo Grefhorst, and Prof.dr. A.J. van der Lelij. The results of his research are presented in this thesis entitled "Sex Differences in the Control of Adipose Tissue Function". After graduation, he is going to continue his carreer as an academic lecturer and researcher at the Department of Physiology, Faculty of Medicine, Chulalongkorn University.

8